ISSN 0021-9673

VOL. 479 NO. 2 OCTOBER 6, 1989

THIS ISSUE COMPLETES VOL. 479

JOURNAL OF CHROMATOGRAPHY

INTERNATIONAL JOURNAL ON CHROMATOGRAPHY, ELECTROPHORESIS AND RELATED METHODS

ELSEVIER

JOURNAL OF CHROMATOGRAPHY

Scope. The *Journal of Chromatography* publishes papers on all aspects of chromatography, electrophoresis and related methods. Contributions consist mainly of research papers dealing with chromatographic theory, instrumental development and their applications. The section *Biomedical Applications*, which is under separate editorship, deals with the following aspects: developments in and applications of chromatographic and electrophoretic techniques related to clinical diagnosis or alterations during medical treatment; screening and profiling of body fluids or tissues with special reference to metabolic disorders; results from basic medical research with direct consequences in clinical practice; drug level monitoring and pharmacokinetic studies; clinical toxicology; analytical studies in occupational medicine.

Submission of Papers. Papers in English, French and German may be submitted, in three copies. Manuscripts should be submitted to: The Editor of *Journal of Chromatography*, P.O. Box 681, 1000 AR Amsterdam, The Netherlands, or to: The Editor of *Journal of Chromatography, Biomedical Applications*, P.O. Box 681, 1000 AR Amsterdam, The Netherlands. Review articles are invited or proposed by letter to the Editors. An outline of the proposed review should first be forwarded to the Editors for preliminary discussion prior to preparation. Submission of an article is understood to imply that the article is original and unpublished and is not being considered for publication elsewhere. For copyright regulations, see below.

Subscription Orders. Subscription orders should be sent to: Elsevier Science Publishers B.V., P.O. Box 211, 1000 AE Amsterdam, The Netherlands, Tel. 5803 911, Telex 18582 ESPA NL. The *Journal of Chromatography* and the *Biomedical Applications* section can be subscribed to separately.

Publication. The *Journal of Chromatography* (incl. *Biomedical Applications*) has 37 volumes in 1989. The subscription prices for 1989 are:

J. Chromatogr. + *Biomed. Appl.* (Vols. 461–497):
Dfl. 6475.00 plus Dfl. 999.00 (p.p.h.) (total *ca.* US$ 3428.50)

J. Chromatogr. only (Vols. 461–486):
Dfl. 5200.00 plus Dfl. 702.00 (p.p.h.) (total *ca.* US$ 2707.25)

Biomed. Appl. only (Vols. 487–497):
Dfl. 2200.00 plus Dfl. 297.00 (p.p.h.) (total *ca.* US$ 1145.50).

Our p.p.h. (postage, package and handling) charge includes surface delivery of all issues, except to subscribers in Argentina, Australia, Brasil, Canada, China, Hong Kong, India, Israel, Malaysia, Mexico, New Zealand, Pakistan, Singapore, South Africa, South Korea, Taiwan, Thailand and the U.S.A. who receive all issues by air delivery (S.A.L. — Surface Air Lifted) at no extra cost. For Japan, air delivery requires 50% additional charge; for all other countries airmail and S.A.L. charges are available upon request. Back volumes of the *Journal of Chromatography* (Vols. 1–460)are available at Dfl. 195.00 (plus postage). Claims for missing issues will be honoured, free of charge, within three months after publication of the issue. Customers in the U.S.A. and Canada wishing information on this and other Elsevier journals, please contact Journal Information Center, Elsevier Science Publishing Co. Inc., 655 Avenue of the Americas, New York, NY 10010. Tel. (212) 633-3750.

Abstracts/Contents Lists published in Analytical Abstracts, ASCA, Biochemical Abstracts, Biological Abstracts, Chemical Abstracts, Chemical Titles, Chromatography Abstracts, Clinical Chemistry Lookout, Current Contents/Physical, Chemical & Earth Sciences, Current Contents/Life Sciences, Deep-Sea Research/Part B: Oceanographic Literature Review, Excerpta Medica, Index Medicus, Mass Spectrometry Bulletin, PASCAL-CNRS, Pharmaceutical Abstracts, Referativnyi Zhurnal, Science Citation Index and Trends in Biotechnology.

See inside back cover for Publication Schedule, Information for Authors and information on Advertisements.

0021-9673/89/$03.50

Printed in The Netherlands

CONTENTS

(Abstracts/Contents Lists published in Analytical Abstracts, ASCA, Biochemical Abstracts, Biological Abstracts, Chemical Abstracts, Chemical Titles, Chromatography Abstracts, Current Contents/Physical, Chemical & Earth Sciences, Current Contents/Life Sciences, Deep-Sea Research/Part B: Oceanographic Literature Review, Excerpta Medica, Index Medicus, Mass Spectrometry Bulletin, PASCAL-CNRS, Referativnyi Zhurnal and Science Citation Index)

(Continued overleaf)

In articles with more than one author, the name of the author to whom correspondence should be addressed is indicated in the article heading by a 6-pointed asterisk (*)

Journal of Chromatography, 479 (1989) 221–231
Elsevier Science Publishers B.V., Amsterdam — Printed in The Netherlands

CHROM. 21 745

EVALUATION OF DIRECT AXIAL SAMPLE INTRODUCTION FOR ION MOBILITY DETECTION AFTER CAPILLARY GAS CHROMATOGRAPHY

R. H. St. LOUIS, W. F. SIEMS and H. H. HILL, Jr.*
Department of Chemistry, Washington State University, Pullman, WA 99164-4630 (U.S.A.)
(First received November 24th, 1988; revised manuscript received June 20th, 1989)

SUMMARY

An ion mobility detector has been designed and constructed for direct axial interfacing with capillary gas chromatography. The principle advantages of this detector were the following: (1) Direct concentric introduction of the capillary column into the ionization region, eliminating peak broadening in the transfer line and improving the efficiency with which neutral molecules were swept from the detector. (2) A variable capillary insertion distance, providing a sensitivity/resolution interplay that could be modified in response to the needs of the assay. (3) An inert gas flow external to the drift cylinder, preventing atmospheric impurities from infiltrating the ultratrace detector. Qualitative and quantitative capabilities of the detector were evaluated using standard preparations of *n*-hexyl ether.

INTRODUCTION

Ion mobility spectrometry (IMS), an atmospheric pressure technique for trace organic analysis, was first introduced in 1970 by Cohen and Karasek[1]. In IMS, organic molecules are ionized by any of several methods, including ^{63}Ni β ionization[1], photoionization[2,3], laser ionization[4], resonance enhanced two-photon ionization[5], coronaspray ionization[6], or via use of a high temperature ceramic alkali bead[7]. These ions are then driven by an electric field against a counterflowing neutral drift gas, achieving an average velocity dependent on the ion charge, mass, and collision cross sectional area. Ions can be thus distinguished by their arrival time at a downfield collector[8,9].

Due to the high sensitivity of the technique, particularly with ^{63}Ni β ionization, IMS has continued to be suggested as a tuneable selective detector for gas chromatography (GC). Several researchers have used GC–IMS[10–14], but its efficient utilization has only recently been realized. With the introduction of low bleed, bonded fused-silica capillary columns and a detector design which introduced a unidirectional gas flow, an enclosed drift tube, and a reduced ionization cell volume[15], IMS has become a reliable method of detection after high-resolution GC. The detector to be described within this paper, maintains the resolution enhancing characteristics of the previous detector, while introducing additional modifications directed towards improved chro-

0021-9673/89/$03.50

matographic efficiency and stability. General reviews of modes of operation and capabilities of ion mobility detection (IMD) for capillary GC have been published recently[16–18].

The purpose of this work was to design an ion mobility detector that could be interfaced directly to a capillary gas chromatograph. Initial experiments with the new design addressed spectral stability and detector residence times when measuring trace quantities of *n*-hexyl ether.

EXPERIMENTAL

Detector design and ancillary instrumentation

The ion mobility detector designed for direct interfacing to capillary GC is illustrated in Fig. 1. A stainless-steel detector base, with 1/16-in. stainless-steel tubing welded through its center and extending 1/16 in. above and 2.25 in. below the base, was connected to a 1 × 1 5/16″ × 3/4 in. heating block (not shown in schematic) by a swagelock fitting. The heating block temperature was controlled to within 1°C by the detector temperature controls of the HP 5890 GC system. The capillary column was inserted into 1/16-in. stainless-steel tubing, directing it through the heating block, detector base and macor insulator into the ionization region of the detector. This insertion distance was variable and the consequent trade-off between chromatographic peak areas and peak widths will be discussed in the results and discussion section.

The 1½-in. diameter by 7/16-in. round macor insulator electrically isolated the gas chromatograph from the high voltages applied to the drift tube. The ionizer was a 1½-in. diameter by ½-in. stainless-steel disc with a 1-cm diameter by 1-cm ionizing cell in its center (cell volume, 0.8 cm^3). Lining the ionizing cell was a 3.1 cm × 0.8 cm × 0.002 mm nickel foil electroplated on one side with 11.78 mCi/mg ^{63}Ni (E.I. du Pont de Nemours, Billerica, MA, U.S.A.). Total activity was 15 mCi β radiation with a

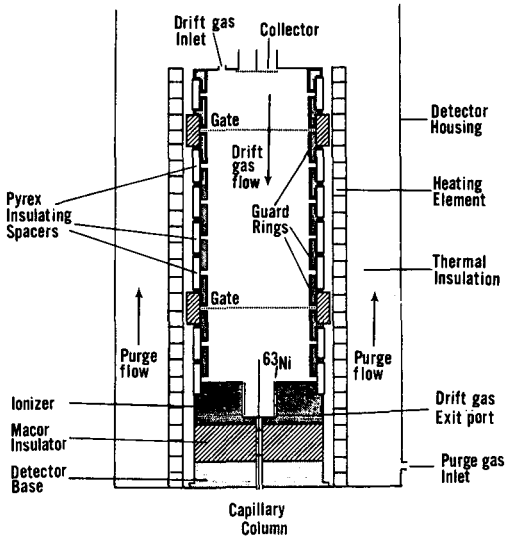

Fig. 1. Schematic of the ion mobility detector.

maximum beta energy of 67 keV. Four 1/16-in. openings at the base of the ionizer functioned as exit ports for the neutral drift gas and unionized chromatographic effluent molecules. The efficiency with which neutral molecules are swept through these ports determines the ultimate detector contribution to peak broadening.

The electric field was created and maintained by a high voltage applied directly to the ionizer block, from a ±5000 V voltage supply (Bertan Assoc., Syosset, NY, U.S.A.). This voltage was then dropped to ground via a series of 1-MΩ resistors connected to successive guard rings. Guard rings were stainless-steel of 3.15 cm I.D. and 3.6 cm O.D. Their depth on the inner surface was 0.90 cm, a 0.1 × 0.1 cm ledge extended from the outer surface of the ring. The gates and insulating spacers were designed to fit over the ring and rest on the 0.1-cm outside ledge, providing a snug but not hermetically sealed fit. The electrical insulating spacers were pyrex rings of 3.7 cm I.D., 4.1 cm O.D., and 0.90 cm depth.

The gates were composed of parallel 0.003-in. nichrome wire (California Fine Wire, Grover City, CA, U.S.A.) separated by approximately 1 mm. The wires were sandwiched between two 3.7 cm I.D., 4.5 cm O.D., 0.45 cm depth macor rings with zirconia base 940 ceramic adhesive (Cotronics, Brooklyn, NY, U.S.A.). Alternate wires were biased +25 V and −25 V relative to the appropriate voltage based on the gates location in the electric field. With voltage applied to the wires, an approximately 500-V/cm field is generated orthogonal to the drift field (generally 150–350 V/cm). Drifting ions are thus neutralized on the gate wires.

The ion collector was a stainless-steel wire mesh spot welded into a 0.020 in. macor ring. Current was sent to a Keithley Model 427 current amplifier (Keithley Instruments, Cleveland, OH, U.S.A.) modified to provide a 2.1-s rise time for chromatography. The amplified signal proceeded to an HP 3392A integrator (Hewlett-Packard, Avondale, PA, U.S.A.) for chromatographic detection and integration or to an IBM XT personal computer for ion mobility spectral collection and processing by either signal averaging or fourier transform[19] methodology. Preceeding the collector was an aperture grid (not shown in schematic) also made of 0.003-in. parallel nichrome wires, separated from the collector by approximately 1 mm and biased at approximately 30 V. This grid capacitively decouples the collector from the approaching ion, providing improved resolution in signal averaging spectral collection.

Preheated drift gas entered through a 1/8-in. inlet in the top of the detector. The drift gas was preheated to the drift tube temperature by its entrance through 1/8-in. stainless-steel tubing that quadruply encircled the detector heating block and was then carried to the top of the drift tube within a insulating cylinder. Temperature control to the drift tube was provided by heavy insulated Samox heating tape, maximum temperature 760°C, (Thermolyne, Dubuque, IA, U.S.A.) wound around a 13 cm × 4.8 cm I.D., 5.1 cm O.D. Pyrex cylinder and held in place by high-temperature aluminum tape, maximum temperature 315°C (3M, St. Paul, MN, U.S.A.). The pyrex cylinder was insulated externally with moldable ceramic felt (Cotronics, Brooklyn, NY, U.S.A.) and held within an aluminum cylinder 19 × 9.5 I.D. The heating tape temperature was maintained with a Digisense Model 2168-70 temperature controller (Cole Parmer, Chicago, IL, U.S.A.), accurate to 0.4°C. The insulating cylinder was swept during operation with approximately 1 l/min of nitrogen gas to prevent infiltration of ambient impurities into the drift tube of the detector. Drift gas and external purifying gas were either prepure nitrogen or industrial grade compressed air (Liquid

Air, San Francisco, CA, U.S.A.), dried with 5Å molecular sieve (Linde Division, Union Carbide, South Plainfield, NJ, U.S.A.).

Capillary insertion distance studies

Injections of 2.0 μl of 68.0 ng/μl and 6.80 ng/μl standard solutions of tributylamine in hexane were made, producing 1.36 ng and 136 pg of tributylamine on column after the 100:1 split ratio. The average of duplicate measurements of each concentration at each insertion distance were used for graphical presentation. Peak areas and area/height measurements were made by an HP 3392A integrator. Deviation of duplicate points varied from 1 to 8% for peak areas, but was generally around 2%. The maximum deviation of duplicate peak width measurements was 6%, generally being <2%. Operational parameters are listed in Table I.

TABLE I

EXPERIMENTAL CONDITIONS OF THE INSERTION DISTANCE STUDY

Ion mobility detection	
Drift length	5.0 cm
Temperature	200°C
Drift gas flow-rate	1400 ml/min air
Electric field	285 V/cm
Gate voltage	± 25 V
Pressure	690 Torr
Chromatography	
Column	DB-5, 22 m × 0.25 mm I.D., 0.25 μm film
Split ratio	100:1
Flow-rate	0.9 ml/min helium
Injector temperature	200°C
Oven temperature	130°C
Drift times monitored	4.9–8.7 ms
Duty cycle (% of collection time entrance gate is open)	16%

Ether studies

Di-*n*-hexyl ether was first chromatographed under non-selective conditions[16], in which all product ion peaks were monitored. Retention time of the di-*n*-hexyl ether was determined to be 3.34 min using the chromatographic conditions listed in Table II. Spectral collection was triggered at 3.31 min, so as to capture the maximum intensity of the chromatographic peak.

From the spectra, the product ion drift time was determined to be 5.1 ms ($K_0 = 1.70\,cm^2\,V^{-1}\,s^{-1}$). A calibration curve was then obtained by selective monitoring of product ion drift times between 4.6 and 5.6 ms, with maximal collection centered at 5.1 ms. Spectral and chromatographic conditions for the ether studies are listed in Table II.

TABLE II

EXPERIMENTAL CONDITIONS OF THE ETHER STUDIES

Ion mobility detection	
Temperature	200°C
Drift gas flow-rate	1400 ml/min nitrogen
Electric field	310 V/cm
Entrance gate voltage	±32.5 V
Exit gate voltage	±15 V
Pressure	695 Torr
Chromatography	
Column	DB-5, 22 m × 0.25 mm I.D., 0.25 μm film
Flow-rate	0.7 ml/min helium
Split ratio	285:1
Injector temperature	250°C
Capillary insertion distance	1.3 cm
Oven temperature	150°C
Drift times monitored	4.6–5.6 ms
Duty cycle	5%
Spectroscopy, signal averaging	
Drift length	7.73 cm
Entrance pulse width	0.20 ms
Spectral collection time	25.6 ms
No. averaged	64
Total time	1.64 s
Spectroscopy, Fourier transform	
Drift length	6.0 cm
Frequency range	20–10 020 Hz
No averaged	1
Total time	2.05 s

RESULTS AND DISCUSSION

Design modifications

Salient modifications to earlier designs include firstly, the direct concentric introduction of the capillary column into the center of the ionizer. Our earlier design[15] introduced the chromatographic effluent laterally after traversing some 3 ft. of heated transfer line. The design reported in this paper eliminated the extracolumn addition to peak broadening while introducing the effluent in a more defined zone than is obtained with lateral introduction into a flowing drift gas. The resolution capabilities of the system are qualitatively demonstrated in Fig. 2, a gas chromatogram of light petroleum (90–110°C). Several additional chromatograms of complex samples are illustrated in a recent review of IMD[16].

A second unique characteristic of this detector was the ability to vary the distance that the column was inserted into the ionizer. The effect that varying this distance has on chromatographic peaks is illustrated in Fig. 3. It can be seen in the upper graph, that peak areas increased approximately 8 × when the insertion distance was varied from 0.4 to 1.8 cm. These areas were reasonably stable from 1.8 to 2.4 cm.

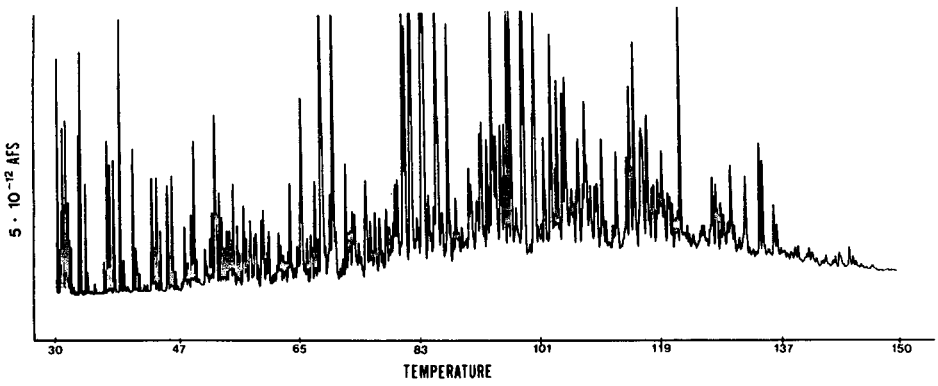

Fig. 2. Chromatogram of light petroleum using ion mobility detection. Column: DB-5, 22 m × 0.259 mm I.D., 0.25 μm film. Flow-rate, 1.3 ml/min hydrogen. Split ratio, 100:1. Injector temperature, 225°C. Temperature program: 30°C, 1 min; 0.6°C/min; 150°C, 5 min. Insertion distance, 1.9 cm. Detector temperature, 200°C. Drift gas flow-rate, 1400 ml/min air. Electric field, 340 V/cm. Gate voltage, 50 V. Drift length, 5.0 cm. Drift times monitored, 4.1–9.9 ms. Duty cycle, 5%.

The lower graph illustrates the effect on peak base widths of varying the insertion distance. Little peak broadening was observed as the insertion distance was increased. Insertion distance can thus be varied to maximize sensitivity without significantly sacrificing the resolving power of the chromatographic system.

The third major modification was the addition of a sheath of flowing gas between the drift tube and the insulating cylinder. This external flow functioned to eliminate infiltration of the detector by ambient impurities in the laboratory air. Impurities have been seen previously, in moderate cases as baseline instabilities or in extreme cases as complete depletion of the reactant ions[20]. With the design described here, no baseline instabilities were detected while exposing the detector to acetone vapors from a 250-ml beaker at a distance of approximately 4 in. Without the sheath gas flow, these acetone vapors completely depleted the reactant ions and produced a dominant acetone product ion.

Two additional modifications included firstly, the elimination of PTFE as an insulator in the detector which removed a previous limitation to high-temperature work. Secondly, the ionizing cell volume was reduced to 0.8 cm^3 from the previous 1.0 cm^3. No direct evidence links this cell reduction with the consequent increase in total ion current from 1.0 to 2.5 nA. However, based on these data, the increased speed with which a reduced cell volume can be swept, and the earlier work of Aue and Kapila[21] which proposes that the center of ionization occurs within 2 mm of a ^{63}Ni foil; the potential chromatographic benefits in resolution, sensitivity, and linear range from further cell size reductions deserves investigation.

Selective chromatographic detection of di-n-hexyl ether

In 1973, ion mobility spectrometry was evaluated as a separator/identifier and as a detector to be used in conjunction with chromatography[22]. Neat ethers were injected directly into the ionization region of a bidirectional flow ion mobility spectrometer. Ion mobility spectra revealed instabilities in product ion position and in-

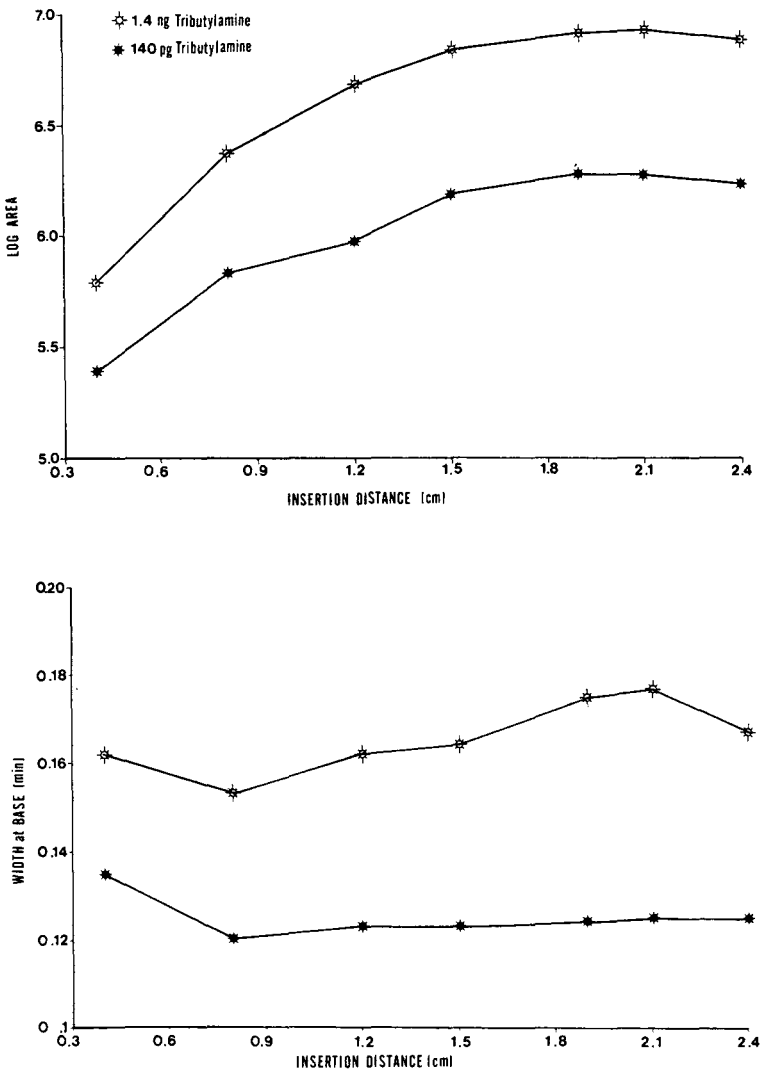

Fig. 3. (a) Chromatographic peak area *vs.* distance capillary column inserted into ionizer. 1 Area count = $6.25 \cdot 10^{-19}$ C. (b) Chromatographic peak widths at base *vs.* distance capillary column inserted into ionizer. Conditions as in Table I.

tensity with detector clearance times exceeding 1.7 h. These instabilities were probably due to complex ion–molecule reactions occurring at high concentrations and the presence of trace contaminants in the ethers. The experiments discussed below were designed to evaluate spectral stability and detector clearance times when introducing trace quantities of chromatographically purified ethers into the unidirectional flow ion mobility detector described in this paper.

Fig. 4a shows the background reactant ions obtained with a signal averaged

spectral collection method when only helium carrier gas was eluting from the capillary column. Fig. 4b is a signal averaged spectra collected as 27 ng of di-*n*-butyl ether was introduced. The product ion was seen as a shoulder on the second reactant ion. Comparison to the earlier work[22], revealed similarities between these spectra and those taken 1.7 h after the injection of more then 100 μg into an ion mobility spectrometer. This indicates that only after this time period were concentrations reduced to a level where stable product ion species were formed.

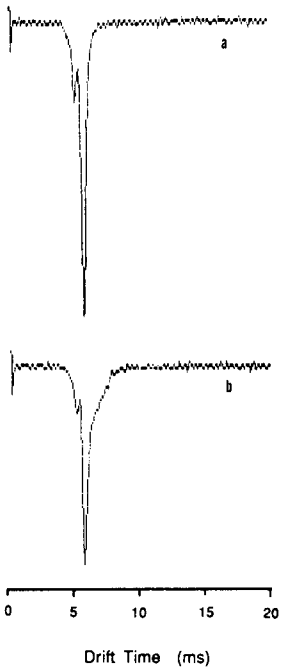

Fig. 4. (a) Background reactant ions, signal averaged spectral collection. (b) IMS Spectra of 27 ng di-*n*-butyl ether. Conditions as in Table II.

Using a Fourier transform method of spectral collection[19] and the slightly larger and thus slower drifting di-*n*-hexyl ether, we were able to baseline resolve the product ion from the reactant ions, as seen in Fig. 5. Fig. 5a displays the background reactant ions and Fig. 5b–d displays spectra obtained when increasing quantities of ether were injected into the GC system. Spectra varied as expected, reactant ions being depleted as product ions increase. The product ion drift time remains constant at 5.1 ms throughout, and no additional product ions were observed.

More sensitive and precise quantitative measurements can be obtained using the GC selective mobility monitoring mode[16]. By narrowing the entrance and exit gates, and using controlled timing, selective detection of ions drifting in 5.1 ms was obtained. Fig. 6 displays a calibration curve obtained under selective monitoring conditions. A well behaved response profile was evident from approximately 0.03 to 30.0 ng, indicating the stability of the product ions drift times in those ranges. Linear

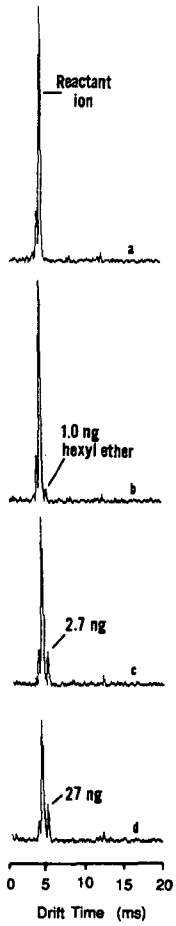

Fig. 5. (a) Background reactant ions, Fourier transform spectral collection. (b) 1 ng di-*n*-hexyl ether. (c) 2.7 ng di-*n*-hexyl ether. (d) 27 ng di-*n*-hexyl ether. Conditions as in Table II.

regression of the data points in Fig. 6 (excluding the point at 27 ng) produces a line of the following equation:

$$Y = 3.17 + 0.621X \quad \text{variance} = 5.15 \cdot 0^{-3}$$

Based on the calibration curve and examination of Fig. 5d and 4b of 27-ng samples, it can be stated that over three orders of magnitude extending from 28 pg to 27 ng, no spectral instabilities were observed.

Fig. 7a and b shows examples of two of the chromatograms used in the di-*n*-hexyl ether calibration curve. Peak base widths are on the order of 6 s, indicative of efficient clearance times from the ion mobility detector.

Based on these data, we conclude that the ion mobility detector herein described is suitable for sensitive and selective detection of ethers. With concentric,

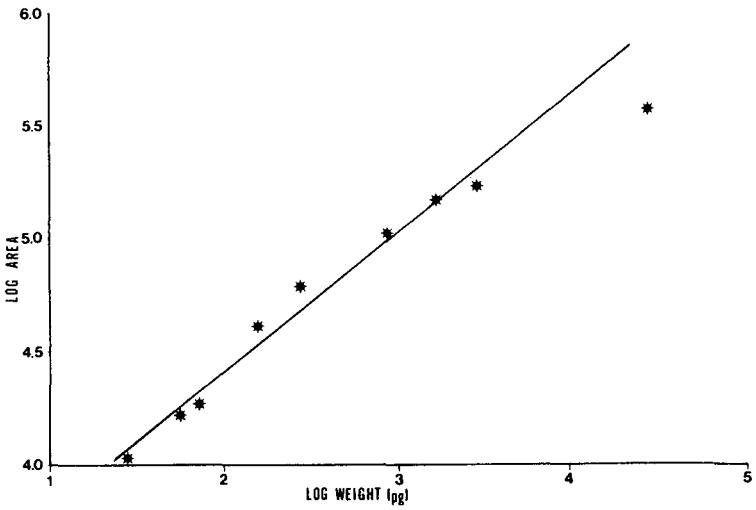

Fig. 6. Calibration curve of di-*n*-hexyl ether. Selective monitoring, 4.6–5.6 ms. Conditions as in Table II.

capillary introduction and unidirectional gas flow, clearance time of the detector ionization region is on the order of 1 s (the *entire* detector volume of 69.2 cm^3 being swept in 3 s by drift gas at a flow-rate of 1400 ml/min). With the introduction of chromatographically purified components at non-saturating concentrations, *i.e.*, reactant ions still visible in the spectra, only single product ion drift times were observ-

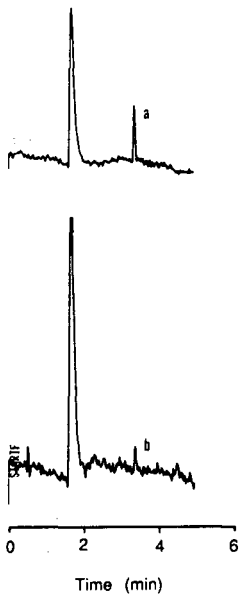

Fig. 7. Di-*n*-hexyl ether chromatograms. (a) 150 pg di-*n*-hexyl ether on column. (b) 28 pg di-*n*-hexyl ether on column. Conditions as in Table II.

ed. These drift times reflecting the charge, reduced mass and collision cross section of the product ion and consequently providing qualitatively useful information. While complex ion–molecule reactions at high concentrations restricts certain analytical applications of IMS, they do not diminish the usefullness of IMS as a chromatographic detection method for the determination of trace amounts of compounds.

ACKNOWLEDGEMENT

This research was supported in part by grant No. GM29523 from the Public Health Service.

REFERENCES

1 M. J. Cohen and F. W. Karasek, *J. Chromatogr. Sci.*, 8 (1970) 330.
2 M. A. Baim, R. L. Eatherton and H. H. Hill, Jr., *Anal. Chem.*, 55 (1983) 1761.
3 C. S. Leasure, M. E. Fleischer, G. K. Anderson and G. A. Eiceman, *Anal. Chem.*, 58 (1986) 2142.
4 D. M. Lubman and M. N. Kronick, *Anal. Chem.*, 54 (1982) 1546.
5 D. M. Lubman and M. N. Kronick, *Anal. Chem.*, 55 (1983) 1486.
6 C. Shumate and H. H. Hill, Jr., *Anal. Chem.*, 61 (1989) 601.
7 H. Wohltjen, *U.S. Pat. Appl.*, US 581 398 (1984); Avail. NTIS Order No. Pat.-Appl.-6-581 398.
8 H. E. Revercomb and E. A. Mason, *Anal. Chem.*, 47 (1975) 970.
9 C. Shumate, R. H. St. Louis and H. H. Hill, Jr., *J. Chromatogr.*, 373 (1986) 141.
10 F. W. Karasek and R. A. Keller, *J. Chromatogr. Sci.*, 10 (1972) 626.
11 S. P. Cram and S. N. Chesler, *J. Chromatogr. Sci.*, 11 (1973) 391.
12 F. W. Karasek, H. H. Hill, Jr., S. H. Kim and S. Rokushika, *J. Chromatogr.*, 135 (1977) 329.
13 Y. Ramstad, T. J. Nestrick and J. C. Tou, *J. Chromatogr. Sci.*, 16 (1978) 240.
14 D. S. Ithakissios, *J. Chromatogr. Sci.*, 18 (1980) 88.
15 M. A. Baim and H. H. Hill, Jr., *Anal. Chem.*, 54 (1982) 38.
16 R. H. St. Louis, W. F. Siems and H. H. Hill, Jr., *LC · GC, Mag. Liq. Gas Chromatogr.*, 6 (1988) 810.
17 M. Dressler, *Selective Gas Chromatographic Detectors (Journal of Chromatography Library*, Vol 36), Elsevier, Amsterdam, 1986, p. 275.
18 H. H. Hill, Jr. and M. A. Baim, in T. W. Carr (Editor), *Plasma Chromatography*, Plenum Press, New York, 1984, p. 144.
19 F. J. Knorr, R. L. Eatherton, W. F. Siems and H. H. Hill, Jr., *Anal. Chem.*, 57 (1985) 402.
20 G. A. Eiceman, C. S. Leasure, V. J. Vandiver and G. Rico, *Anal. Chim. Acta*, 175 (1985) 135.
21 W. A. Aue and S. Kapila, *J. Chromatogr.*, 188 (1980) 1.
22 M. M. Metro and R. A. Keller, *J. Chromatogr. Sci.*, 11 (1973) 520.

Journal of Chromatography, 479 (1989) 233–242
Elsevier Science Publishers B.V., Amsterdam — Printed in The Netherlands

CHROM. 21 749

SCREENING OF STEROIDS IN HORSE URINE AND PLASMA BY USING ELECTRON IMPACT AND CHEMICAL IONIZATION GAS CHROMATOGRAPHY–MASS SPECTROMETRY

ASHOK K. SINGH*

Minnesota Racing Laboratory, Department of Veterinary Diagnostic Laboratory, College of Veterinary Medicine, University of Minnesota, St. Paul, MN 55108 (U.S.A.)

B. GORDON

Large Animal Clinical Sciences, College of Veterinary Medicine, University of Minnesota, St. Paul, MN 55108 (U.S.A.)

and

D. HEWETSON, K. GRANLEY, M. ASHRAF, U. MISHRA and D. DOMBROVSKIS

Minnesota Racing Laboratory, Department of Veterinary Diagnostic Laboratory, College of Veterinary Medicine, University of Minnesota, St. Paul, MN 55108 (U.S.A.)

(First received February 28th, 1989; revised manuscript received June 27th, 1989)

SUMMARY

Gas chromatography with chemical ionization mass spectrometry and selected-ion monitoring provided a sensitive method for the screening and confirmation of steroids in horse urine and plasma. Chemical ionization mass spectrometry was more sensitive than the electron impact ionization mass spectrometry for most of the steroids except for testosterone, prednisone-metabolite-2 and prednisolone-metabolite-2. The chromatographic conditions used in this study provided clean separation of different natural and synthetic steroids. Approximately 75–85% of the steroids added to plasma and approximately 65–70% of the steroids added to urine were recovered by the extraction procedure used in this study.

INTRODUCTION

Corticosteroids play an important role in glucose and electrolyte metabolism[1,2], and produce strong anti-inflammatory effects[3,4]. Hydrocortisone (cortisol) is the major natural anti-inflammatory corticosteroid present in horse plasma and urine[5]. By selective modifications of the natural steroids, several synthetic steroids have been designed which are more potent anti-inflammatory drugs than cortisol[6]. Prednisone and prednisolone are important synthetic corticosteroids which are extensively used in horses for therapeutic purposes and for improving the performance of the racing horse[7]. Previously reported analytical procedures used for the detection of corticosteroids include radioimmuno assay (RIA), receptor binding assay (RBA) and gas chromatographic assay (GC)[8–11]. The RIA and RBA methods are sensitive but the antibodies partially crossreact with the naturally occurring corticosteroids[12]. The

0021-9673/89/$03.50

GC method lacks sensitivity and cannot be used for the detection of trace levels of compounds[11]. Gustafson and Sjovall[13] and Houghton[14] described the use of gas chromatography–mass spectrometry (GC–MS) in the ~~electron impact (EI)~~ ionization mode for the analysis of steroids in urine and feces. Although the method detected various steroids and their metabolites, EI ionization produced smaller and diagnostically insignificant ions which were not suitable for analyzing steroids in the selective-ion monitoring (SIM) mode. The SIM analysis has been reported to be several times more sensitive than the conventional MS[15]. Recently Matin and Amos[16] described a specific and sensitive method for the screening of prednisolone and prednisone by using GC–MS and chemical ionization (CI). They observed that CI of prednisolone and prednisone provided diagnostically significant ions at high m/z values. The objective of this investigation was to compare the EI and CI mass fragmentation patterns of various natural and synthetic steroids, and to develop a sensitive procedure for the simultaneous screening of synthetic and natural steroids and their metabolites in plasma and urine.

MATERIALS AND METHODS

Reagents

Methoxyamine hydrochloride, pyridine and N,O-bis(trimethylsilyl)trifluoroacetamide (BSTFA) were obtained from the Aldrich. Various steroid standards and other reagents were obtained from the Sigma (St. Louis, MO, U.S.A.).

Instrument

The GC–MS system used was an HP 5980 equipped with electron impact and chemical ionization sources. Methane gas was used as the reagent gas (20 ml/min).

Synthesis of prednisone and prednisolone metabolites

Prednisone metabolite-1 (M_1) (pregna-1,4-dien-17α,20β,21-triol-3,11 dione) and prednisolone metabolite-1 (M_1) (pregna-1,4-dien-11β,17α,20β,21-tetrol-3-one) were synthesized as described by Gray *et al*[17]. Prednisolone or prednisone (100 mg) was mixed with sodium borohydride in methanol and incubated for 30 min at 0°C. After incubation, the mixture was acidified and dried at 45°C under reduced pressure. The dried residue was redissolved in 100 μl of methanol, spotted on a thin-layer chromatography (TLC) plate and developed in ethyl acetate–methanol–ammonium hydroxide (85:10:5) for 5 cm. The metabolite spot, which appeared below the parent spot, was scraped and the compound was eluted from silica with methanol as described previously[17]. Prednisone metabolite-2 (M_2) (androsta-1,4-dien-11β-ol-3,17-trione) and prednisolone metabolite-2 (M_2) (androsta-1,4-dien-11β-ol-3,17-dione) were synthesized by oxidizing the drugs as described previously[17]. 6 mg of prednisone or prednisolone solution in 3 ml of 15% acetic acid was mixed with 200 mg of sodium bismuthate and the mixture was rotoracked for 1.0 h. Thereafter, the mixture was centrifuged at 1500 g for 20 min, supernatant was transferred into a small flask and dried at 45°C under reduced pressure. The dried residue was redissolved in 100 μl of methanol, spotted on a TLC plate and developed in ethyl acetate–methanol–ammonium hydroxide (85:10:5) for 5 cm. The M_2 spot, which appeared above the parent spot,

was scraped and eluted with methanol. The methanol extract was further purified by alumina chromatography as described previously[17].

Collection of urine and plasma samples from horses

Urine samples from control (undrugged) horses were collected before they were treated with steroids. The urine sample was mixed with prednisolone, prednisone and their metabolites before analysis. After the collection of a control urine sample, horses were treated with testosterone (25 μg/kg), prednisolone (1.0 mg/kg), or prednisone (1.0 mg/kg) by intramuscular injections. Blood samples were collected from the testosterone injected horse at 0.5, 1, 2, 4, 10, 24 and 48 h after injection. Urine samples were collected from all the drugged horses at 12 h after the drug injection.

Processing of the urine samples for analysis

Urine samples of 5 ml obtained from the drug-injected horses or from the control horses were mixed with glucuronidase and incubated for 2 h at 60°C as described by Singh *et al.*[18]. After incubation, the urine sample was mixed with saturated sodium borate solution (1.0 ml) and the mixture was extracted with ethyl acetate (5 ml). The ethyl acetate layer was collected and washed with 1.0 ml of 15% sodium sulfate in 1.0 *M* sodium hydroxide (w/v). The ethyl acetate layer was collected and dried at 60°C in nitrogen and mixed with 50 μl of methoxyamine (prepared by dissolving 600 mg of methoxyamine hydrochloride in 10 ml of pyridine). The mixture was heated at 110°C for 45 min, thereafter 50 μl of BSTFA was added to each sample and the sample was reheated at 120°C for 30 min. A 1-μl volume of this derivative was injected into the GC–MS system.

Processing of plasma samples for GC–MS analysis

A 2-ml volume of plasma was mixed with 5 ml of light petroleum (b.p. 34.4°C) and the mixture was shaken for 5 min. After centrifugation (1500 *g*), the organic layer was separated and dried at 60°C under nitrogen. The dried residue was derivatized as described for the urine sample. A 1-μl sample was injected into the GC–MS. For quantitative analysis cloprednol was used as an internal standard as described previously[19]. The level of testosterone in plasma was also determined by a radioimmuno assay (RIA) procedure. A 10-μl volume of plasma was incubated with [^{3}H]testosterone and the antibody obtained from the Diagnostic Products Corporation. Unbound tracer was removed from the sample by using dextran coated charcoal. The bound radioactivity was counted in a scintillation counter and the levels of testosterone were determined by using the RIA programs built into the scintillation counter.

GC–MS analysis

The following GC–MS conditions were used in this study: column used, fused-silica capillary (25 M) DB5; inlet temperature, 200°C; initial oven temperature, 150°C; rate, 15°C/min; final oven temperature, 280°C; run time, 30 min. For EI ionization, the source temperature was 200°C, the electron energy was 70 eV, and the mass spectrometer source pressure was $2.0 \cdot 10^{-4}$ Torr. For CI ionization, the ionization gas was methane, the source temperature was 150°C, and the electron energy was 200 eV.

Clean-up of urine extract by TLC

If large volume of urine sample is extracted and pooled for screening, it may be necessary to clean the extract by using TLC before GC–MS analysis. The R_F values of various steroids and their metabolites were determined in different solvents (Table III). A volume of 20–40 ml of urine sample (obtained from the prednisolone or prednisone treated horse) was extracted by using the extraction procedure described earlier. The extract was dried at 50°C under nitrogen and the dried residue was redissolved in 100 μl of ethyl acetate and spotted on a preparative TLC plate as described previously[8]. The plate was developed in ethyl acetate–methanol–ammonium hydroxide (85:10:5) solvent for 5 cm. The standards and part of the sample spot was sprayed with sulfuric acid–ethanol and the sprayed portion was heated at 60°C until the standards turned brown. Silica gel from the unsprayed sample corresponding to the standard spot(s) were scraped and transferred into another tube. Steroids were eluted from silica gel with methanol and the methanol layer was dried. The dried residue was derivatized and injected into the GC–MS system as described previously.

Recovery of steroids from urine and plasma

The extraction efficiency for different steroids were determined by adding known amounts of compounds in urine and determining the amount recovered. The concentration of each steroid was determined by both the CI and EI methods. Cloprednol was used as an internal standard for the quantitation of steroids as described previously[19].

RESULTS AND DISCUSSION

Mass fragmentation of steroids

The major ions produced by the CI or EI of steroids is listed in Table I. Similar to previous EI ionization studies, this study also indicated that ion at *m/z* 73 was the predominant ion produced by most of the steroids. Testosterone produced the ion at *m/z* 129 in highest abundance. Prednisolone-M_2 exhibited base ion at *m/z* 120 and another significant ion at *m/z* 327 (70% abundance). The testosterone metabolites 1 and 2 exhibited significant ions at *m/z* 180 and 309, respectively. These observations indicated that the steroid metabolites were more stable to EI fragmentation than their parent drugs. Unlike the EI fragmentation, the CI fragmentation produced larger ions at high abundances and the molecular (M^+) ions were also present in high abundance for most of the steroids (Table I). However, the CI and EI fragmentations were similar for prednisone-M_2 or prednisolone-M_2.

Selection of ions for the analysis of steroids

The ions selected for the qualitative and quantitative analysis of steroids are shown in Table II. The criterion used for the selection of ions for selected-ion monitoring (SIM) has been described by Singh *et al.*[20].

Chromatography

The capillary column and the chromatography conditions used in this study provided a clear separation of prednisone, prednisolone, their metabolites and several other natural steroids (Fig. 1). Unlike the observations of Matin and Amos[16], a clear

TABLE I

MASS FRAGMENTATION AND ABUNDANCES OF INDIVIDUAL IONS FOR VARIOUS STEROIDS SUBJECTED TO CI OR EI

	CI [m/z (abundance)]	*EI [m/z (abundance)]*
Prednisolone	635(100)[a], 636(30), 603(30)	73(100), 103(10), 149(10), 262(10)
Prednisolone-M_1	606(100), 516(80)	73(100), 205(75), 147(70)
Prednisolone-M_2	357(100), 325(25)	356(100), 91(80), 174(75)
Prednisone	561(100)[a], 589(30), 602(10)	73(100), 215(25), 309(10), 561(1), 103(10)
Prednisone-M_1	320(100), 410(90), 681(30)	73(100), 147(20), 205(10)
Prednisone-M_2	359(100), 327(90), 387(20)	120(100), 73(90), 149(70), 327(70)
Testosterone	563(100)[a], 368(50)	129(100), 73(80), 329(50), 368(30)
Testosterone-M_1	–	180(100), 73(80)
Testosterone-M_2	–	73(100), 309(70)
Hydrocortisone	141(100), 476(90), 637(80)[a], 605(50)	73(100), 103(15), 147(10), 605(1)
Tetrahydro-cortisone	520(100), 594(90), 639(10)[a]	73(100), 103(20), 147(15), 488(5)
11-β-Hydroxy-etiocholanone	464(100)[a], 300(80), 268(75), 480(50)	73(100), 448(70), 268(50), 479(2), 129(80)
α-Cortol	141(100), 459(50), 714(50)	73(100), 147(30), 253(20), 343(15)
β-Cortol	141(100), 459(50), 714(50)	73(100), 147(30), 253(15), 343(10)
α-Cortolone	475(100), 639(50), 565(30)	73(100), 147(20), 359(10), 449(10)
β-Cortolone	475(100), 639(80), 565(50)	73(100), 147(20), 243(20), 359(1), 445(5)
5-β-Pregan-3α, 11β,-17α,21-tetrol	523(100), 668(80)[a], 504(50)	73(100), 103(10), 147(15) 652(15), 653(5)

[a] M + 1 ions, M_1 and M_2: metabolites 1 and 2.

TABLE II

IONS (*m/z*) SELECTED FOR THE MONITORING OF VARIOUS STEROIDS

	CI (m/z)	*EI (m/z)*
5-β-Pregan-3α,-11β, 17α,21-tetrol	523, 668	147, 652
Prednisolone	635	149, 262
Prednisolone-M_1	606, 516	205, 147
Prednisolone-M_2	357	356, 91
Prednisone	561	215, 309
Prednisone-M_1	320, 410	147, 205
Prednisone-M_2	359, 327	149, 327
Testosterone	563	129, 329
Testosterone-M_1	–	180
Testosterone-M_2	–	309
Hydrocortisone	476, 637	103, 147
Tetrahydrocortisone	520, 594	103, 147

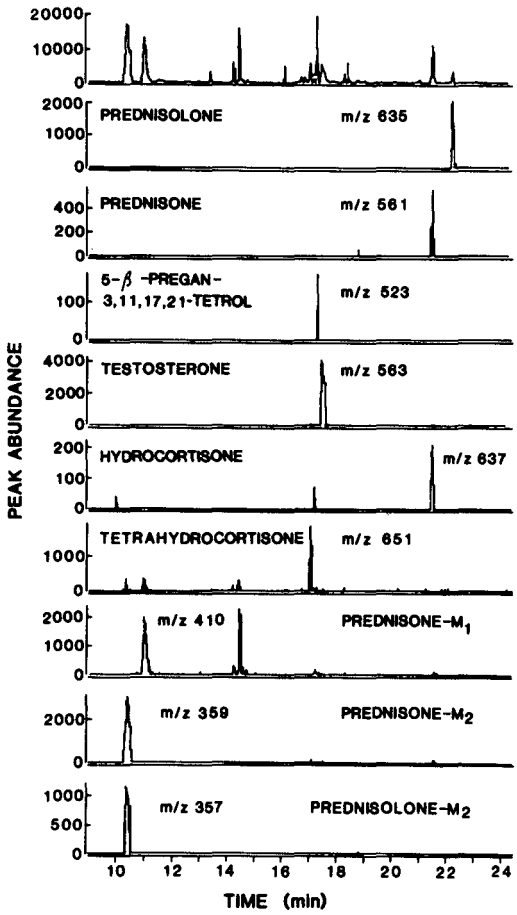

Fig. 1. Selected-ion chromatogram for various steroids present in horse urine which was analyzed by CI-GC–MS.

separation of prednisone and hydrocortisone was observed. As shown in Fig. 1, presence of testosterone, hydrocortisone, tetrahydrocortisone and 5-β-pregan-3α,11β,17α,21-tetrol were also detected in horse urine. Since these steroids were not added to the urine, they may have appeared from the endogenous source. In urine samples obtained from the prednisone-treated horse, only the metabolites M_1 and M_2 were detected and the parent drug was not detected (Fig. 2). However, in the prednisolone injected horse, trace amounts of the parent prednisolone were detected in urine at 24 h after injection (Fig. 3). Although the presence of prednisolone was detected only by the CI analysis, the presence of testosterone and its metabolites were confirmed in plasma (Fig. 4) and urine (Fig. 5) by both the EI and CI analyses.

Extraction efficiency and recovery

The recovery of various steroids from urine is shown in Fig. 6. A linear relationship was observed between the amount of steroids added and the amount of steroids

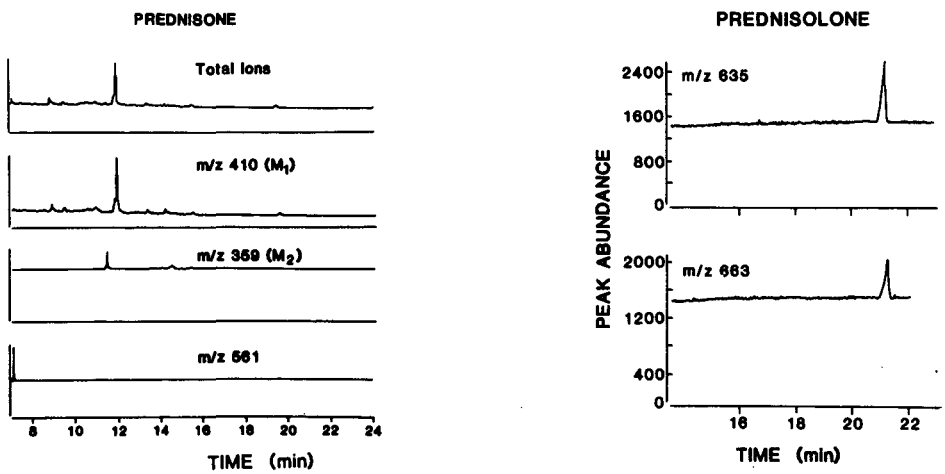

Fig. 2. Selected-ion chromatogram for prednisone and its metabolites extracted from horse urine and analyzed by CI.

Fig. 3. Selected-ion chromatogram for prednisolone extracted from horse urine and analyzed by CI-GC–MS.

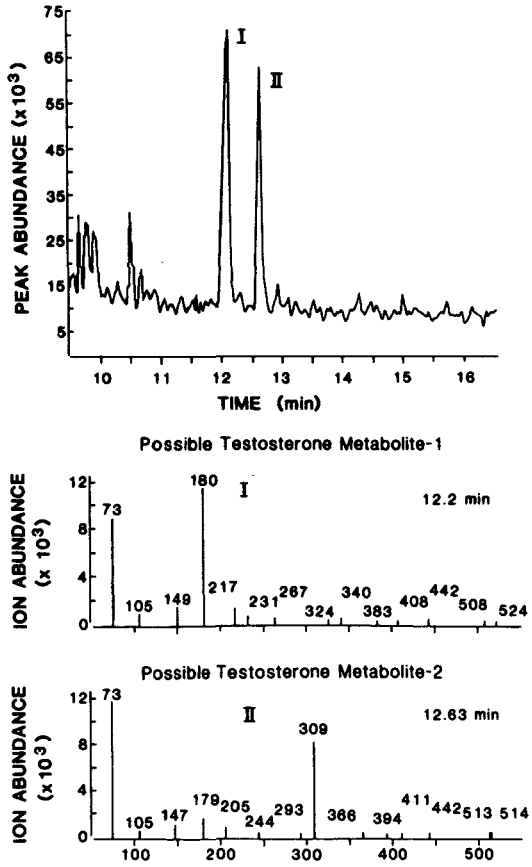

Fig. 4. Chromatographic separation and EI mass fragmentation patterns of the two possible testosterone metabolites.

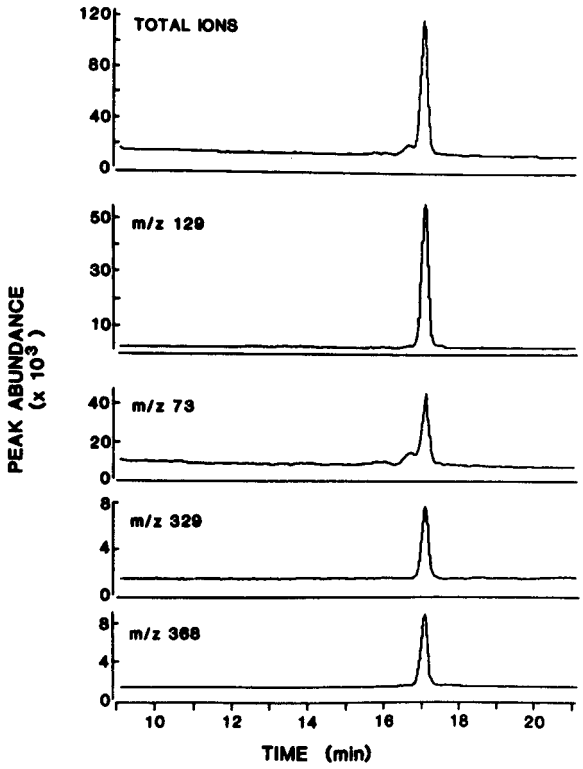

Fig. 5. Selected-ion chromatogram for testosterone extracted from plasma and analyzed by EI-GC–MS.

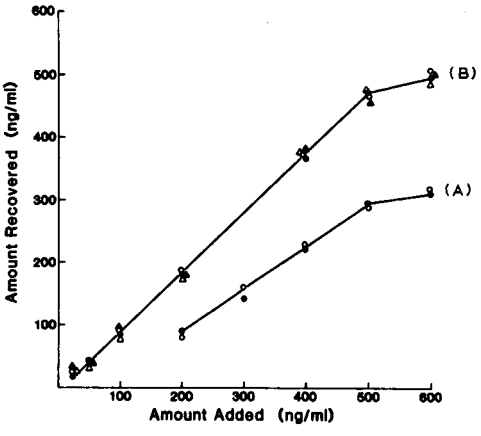

Fig. 6. Recovery of various steroids from horse urine (n = 5). (A) ○ = Recovery of prednisone determined by the EI–SIM method; ● = recovery of prednisolone determined by the EI–SIM method; (B) △ = recovery of testosterone determined by the EI–SIM method; ▲ = recovery of testosterone determined by the CI–SIM method; ● = recovery of prednisolone determined by the CI–SIM method; and ○ = recovery of prednisone determined by the CI–SIM method.

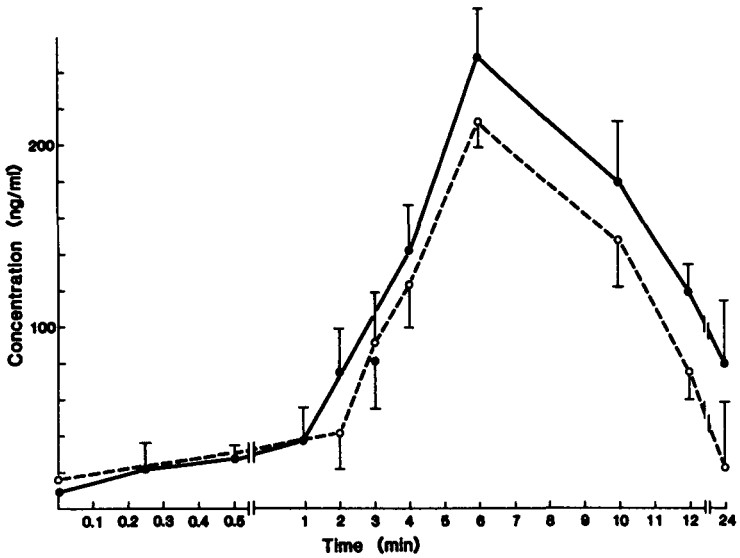

Fig. 7. Comparison of plasma testosterone levels determined by the RIA and the EI-GC–MS method described in this study. (n = 3, values are mean ±S.D.). ● = RIA; ○ = GC–MS.

TABLE III

TLC MIGRATION (R_F) IN DIFFERENT SOLVENT SYSTEMS OF VARIOUS STEROIDS

	DAV.[a]	*PA*[b]	*T-1*[c]	*9-1*[d]	*4/4/2*[e]	S_1[f]	S_2[g]
5-β-Pregan-3α,-11β,17α,21-tetrol	0.40	0.62	0.9	0.2	0.04	0.3	0.4
Prednisolone	0.44	0.70	0.9	0.26	0.04	0.4	0.5
Prednisolone-M_1	0.20	0.56	0.84	0.1	0.00	–	–
Prednisolone-M_2	0.80	0.96	0.86	0.74	0.32	–	–
Prednisone	0.50	0.82	0.9	0.4	0.1	0.4	0.5
Prednisone-M_1	0.30	0.68	0.84	0.25	0.1	–	–
Prednisone-M_2	0.80	0.94	0.9	0.25	0.28	–	–
Testosterone	0.55	0.50	0.9	0.3	0.1	–	–
Testosterone-M_1[h]	0.35	0.23	0.85	0.2	0.04	–	–
Testosterone-M_2[h]	0.76	0.13	0.9	0.4	0.1	–	–
α-Cortolone	0.18	0.45	0.85	0.04	0.04	0.1	0.2
β-Cortolone	0.18	0.45	0.85	0.04	0.04	0.1	0.2
α.Cortol	0.20	0.45	0.85	0.04	0.04	0.1	0.2
β-Cortol	0.20	0.45	0.85	0.04	0.04	–	–
11-β-Hydroxy-etiocholanolone	0.74	0.90	0.9	0.5	0.24	0.5	0.7
Tetrahydrocortisone	0.40	0.70	0.9	0.26	0.04	–	–
Hydrocortisone	0.50	0.72	0.9	0.3	0.04	–	–

[a] DAV = Ethyl acetate–methanol–concentrated ammonium hydroxide (85:10:5, v/v).
[b] PA = Chloroform–methanol–propanoic acid (72:18:10, v/v).
[c] T-1 = Methanol–concentrated ammonium hydroxide (100:1,5, v/v).
[d] 9-1 = Chloroform–ethanol (90:10, v/v).
[e] 4/4/2 = Chloroform–cyclohexane–acetic acid (40:20:20, v/v).
[f] S_1 = Ethyl acetate–acetic acid (39:1, v/v), followed by dichloromethane.
[g] S_2 = Chloroform–ethyl acetate–methanol (50:45:5, v/v) followed by DAV.
[h] Possible metabolites.

recovered from the urine. The curve lost linearity at concentrations above 500 ng/ml possibly because of the saturation of the extraction procedure. The extraction efficiency was approximately 60–70% from urine and 75–80% from plasma. The comparison of plasma testosterone levels determined from the RIA and GC–MS methods have been shown in Fig. 7. The values obtained by GC–MS were 70–80% of the values obtained by the RIA procedure. Since the RIA analysis was carried out with whole plasma (unextracted) and the GC–MS analysis with extracted plasma, the differences between the two assays may be due to the extraction efficiency of testosterone.

Cleanup of extract by TLC

The TLC procedure was necessary only if a large volume of urine was extracted to achieve high concentrations of steroids. Although the TLC cleanup provided clean mass spectra, the recovery of the procedure reduced to 45–55%. Because of the lower sensitivity, the use of TLC cleanup remains limited. For the screening of different steroids by TLC, the R_f value of steroids has been listed in Table III.

CONCLUSIONS

From the results of this study it is concluded that (1) CI–SIM provided a sensitive method for screening steroids, (2) CI–SIM was more sensitive than EI–SIM for most of the steroids except for testosterone and prednisone or prednisolone metabolites, (3) the chromatographic conditions provided clean separation of different steroids, and (4) the recovery of steroids from urine and plasma were $>70\%$.

REFERENCES

1 J. D. Bacter and G. G. Rousseau, *Glucocorticoid Hormone Action*, Springer-Verlag, New York, 1979.
2 P. A. J. Adam and R. C. Haynes, *J. Biol. Chem.*, 244 (1969) 6444.
3 R. R. MacGregor, *Ann. Intern. Med.*, 86 (1977) 35.
4 F. Hirata, E. Schiffmann, K. Venkatasubamaniaw, D. Salomon and J. Axelrod, *Proc. Natl. Acad. Sci. U.S.A.*, 77 (1980) 2533.
5 A. Granelli-Piperano, J. D. Vassali and E. Reich, *J. Exp. Med.*, 146 (1977) 1693.
6 P. L. Toutain, R. A. Brandon, H. de Pomgers, M. Alvinerie and J. D. Baggot, *Am. J. Vet. Res.*, 45 (1983) 1750.
7 T. Tobin, *Drugs and the Performance Horse*, Charles C. Thomas, Springfield, IL, 1981, p. 132.
8 A. Olivesi, D. G. Smith, G. W. White and M. Pourfarzaneh, *Clin. Chem.*, 29 (1983) 1358.
9 W. A. Colburin, *Steroids*, 24 (1974) 95.
10 W. A. Colburin and R. H. Buller, *Steroids*, 21 (1973) 833.
11 W. L. Gardiner and E. C. Horning, *Biochim. Biophys. Acta*, 115 (1966) 524.
12 S. W. Schalm, W. H. J. Summerskill and W. L. W. Mayo, *Clin. Proc.*, 51 (1976) 761.
13 J.-A. Gustafsson and J. Sjovall, *Eur. J. Biochem.*, 6 (1968) 326.
14 E. Houghton, *Biomed. Mass. Spectrum.*, 9 (1982) 459.
15 A. K. Singh, L. R. Drewes and R. J. Zeleznikan, *J. Chromatogr.*, 324 (1985) 163.
16 S. B. Matin and B. Amos, *J. Pharm. Sci.*, 67 (1978) 923.
17 C. H. Gray, M. A. S. Green, N. J. Holness and J. B. Lunnon, *J. Endocrinol.*, 14 (1956) 146.
18 A. K. Singh, U. Mishra, M. Ashraf, H. Abdennebi, K. Granley, D. Dombroviskis, D. Hewetson and C. M. Stowe, *J. Chromatogr.*, 404 (1987) 223.
19 C. G. Hammer, B. Holmstedt and R. Ryhage, *Anal. Biochem.*, 25 (1968) 532.
20 A. K. Singh, D. Hewetson, K. Jordon and M. Ashraf, *J. Chromatogr.*, 369 (1986) 83.
26. * M.C. Dumasia, P. Teale and J.K. Wellby,

Journal of Chromatography, 479 (1989) 243–250
Elsevier Science Publishers B.V., Amsterdam — Printed in The Netherlands

CHROM. 21 687

GAS CHROMATOGRAPHIC DETERMINATION OF DIQUAT AND PARAQUAT IN CROPS

J. HAJŠLOVÁ*, P. CUHRA, T. DAVÍDEK and J. DAVÍDEK
Prague Institute of Chemical Technology, Department of Food Chemistry and Analysis, Suchbátarova 5, CS-166 28 Prague 6 (Czechoslovakia)
(First received April 7th, 1989; revised manuscript received June 13th, 1989)

SUMMARY

A sensitive and reproducible gas chromatographic procedure for the determination of diquat and paraquat in potatoes and rapeseed was developed. The volatilization of analytes was carried out via their hydrogenation with sodium borohydride–nickel(II) chloride. After their isolation from the reaction mixture, the derivatives of bipiperidine were separated on a column packed with Apiezon L plus potassium hydroxide. Comparable detection limits (0.005 mg/kg) were achieved with a nitrogen–phosphorus detector and by mass fragmentography, however, the latter method was preferred for analyses of rapeseed extracts owing to its higher selectivity.

INTRODUCTION

The bipyridinium derivatives diquat (1,1′-ethylene-2,2′-bipyridinium dication) and paraquat (1,1′-dimethyl-4,4′-bipyridinium dication) are rapid-acting herbicides, killing green plants with which they come into contact. On reaching the soil they are inactivated.

When diquat and paraquat are not used for direct plant spraying (*e.g.*, for weed control before crop sowing or emergence), no significant residues are likely to be found[1,2]. On the other hand, direct treatment with these herbicidal sprays is often carried out for preharvest desiccation of various plants and consequently some residues of active ingredients may be present. As bipyridinium herbicides are toxic the monitoring of their residues in food crops is necessary.

Spectrophotometric methods based on the procedure developed by Calderbank[3] have been widely used[4,5]. Owing to the cationic nature of both diquat and paraquat, their displacement from binding sites of an organic matrix (mostly by boiling with strong sulphuric acid) has to be performed. Purification and preconcentration of analytes (usually by cation-exchange chromatography) is carried oud prior to quantitative analysis.

Various chromatographic methods for the determination of bipyridinium herbicides have also been described. A high-performance liquid chromatographic procedure with UV detection[6] was used for analyses of body fluids. After isolation from

0021-9673/89/$03.50

hydrolysed potato tubers, residues of diquat and paraquat as their heptanesulphonate ion pairs were separated on a reversed-phase column[7]. The gas chromatographic (GC) determination of bipyridinium herbicides is not possible unless they are converted into volatile products. Partly hydrogenated derivatives were reported to originate from the parent compounds (1,1′-ethyleneoctahydro-2,2′-bipyridine from diquat and 1,1′-dimethyloctahydro-4,4′-bipyridine from paraquat) when sodium borohydride was used for their reduction. GC methods with nitrogen–phosphorus detection (NPD)[8,9] utilizing this reaction for volatilization of analytes were applied to analyses of potatoes, and similarly a GC–mass spectrometric (MS) method [10] was used for the analysis of plasma samples. Another method of reducing bipyridinium compounds involves catalytic hydrogenation with platinium oxide as a catalyst. In this instance fully hydrogenated products (corresponding derivatives of bipiperidine) can be obtained. Procedures based on this principle have been used for the analysis of soil[11] vegetables[12] and body fluids[13]. Although most of the above methods involve acid hydrolysis, it has been demonstrated that this step can be omitted because efficient displacement of diquat and paraquat from an analysed matrix occurs in the course of hydrogenation[9]. Dequaternization of bipyridinium herbicides can also be achieved by pyrolysis. The main product formed, 2,2′-bipyridine from diquat and 4,4′-bipyridine from paraquat, are amenable to GC analysis. A pyrolysis GC–MS method for analyses of biological samples has been published[14].

The aim of this study was to develop a rapid and efficient method for the analysis of residues of bipyridinium herbicides in treated crops and to introduce it for routine checking purposes.

EXPERIMENTAL

Pesticide standards

Analytically pure diquat dibromide and paraquat dichloride were supplied by ICI Plant Protection Division; standard solutions (0.01 mg/ml, expressed as dication) in 0.2 *M* hydrochloric acid were prepared. Desmetryne was obtained from Supelco; a stock solution (7.2 μg/ml) in hexane was prepared.

Chemicals

All chemicals (Lachema, Brno, Czechoslovakia) were of analytical-reagent grade; solvents were distilled before use.

Hydrogenation of diquat and paraquat in model samples

An aliquot of a standard solution of bipyridinium herbicides was transferred into a separating funnel containing 2 ml of 0.2 *M* hydrochloric acid, 1 ml of 1 *M* nickel(II) chloride and 0.5 ml of toluene (antifoaming agent). Sodium borohydride (100 mg) was then carefully added, which resulted in the evolution of hydrogen and formation of a black precipitate of nickel boride. After standing for 30 min at room temperature the reaction was stopped by addition of 2 ml of 1 *M* sodium hydroxide solution. Extraction with three 5-ml portions of diethyl ether followed. To the combined extracts (dried by passing through anhydrous potassium carbonate), two drops of concentrated hydrochloric acid were added and the solvent was evaporated under reduced pressure. The residue in the flask was made alkaline with 0.2 ml of 5 *M*

sodium hydroxide solution and the analytes were extracted into 2 ml of hexane prior to GC analysis.

Analysis of potatoes

To 50 g of a representative sample of potatoes (several tubers were mixed in a blender) placed in a beaker, 50 ml of 0.2 *M* hydrochloric acid, 20 ml of 1 *M* nickel(II) chloride, 2.5 g of sodium borohydride and 5 ml of toluene were added. After 60 min, the reaction mixture was filtered through a layer of glass-wool and the filtrate was made alkaline with 30 ml of 1 *M* sodium hydroxide solution. Three portions (one 80 ml and two 50 ml) of diethyl ether were used for extraction of hydrogenated bipyridinium compounds; separation of organic and aqueous phases was achieved by centrifugation (carried out under cooling). The combined extracts were dried over anhydrous potassium carbonate and then evaporated in the presence of 0.1 ml of concentrated hydrochloric acid. To the residue in the flask, 0.3 ml of 5 *M* sodium hydroxide solution were added and the analytes were then transferred (with vigorous shaking) into a small volume (1–2 ml) of hexane containing desmetryne as an internal standard for the subsequent GC analysis.

Analysis of rapeseed

Either 5 g of ground rapeseed or 2 g of meal were placed in a beaker, to which 20 ml of distilled water, 20 ml of 0.2 *M* hydrochloric acid and 10 ml of nickel(II) chloride were added. The hydrogenation was started by addition of 1 g of sodium borohydride. After 60 min, the reaction mixture was filtered into a separating funnel (30 ml of 0.2 *M* hydrochloric acid were used for rinsing), and the pH of filtrate was adjusted to 1–2 with 50% hydrochloric acid. This solution was extracted with 25 ml of diethyl ether and the organic layer, after separation by centrifugation, was discarded. The aqueous phase was made alkaline (pH 11–12) and then extracted with three 25 ml portions of diethyl ether. The combined extracts were processed in the same way as for the analysis of potatoes.

Gas chromatography

All GC analyses were carried out on a Hewlett-Packard 5880 A chromatograph equipped with a nitrogen–phosphorus detector. The injector temperature was 230°C, the detector temperature was 300°C and the nitrogen carrier gas flow-rate was 30 ml/min. The following columns were used: (i) 2.4 m × 2 mm I.D. glass column packed with 5% Carbowax 20M plus 2% potassium hydroxide on Inerton Super (0.125–0.160 mm), with temperature programming from 160 to 220°C at 5°C/min; (ii) 2.4 m × 2 mm I.D. glass column packed with 5% Apiezon L plus 3% potassium hydroxide on Inerton Super, isothermal at 200°C.

Gas chromatography–mass spectrometry

GC–MS analyses were performed on a Shimadzu QP 1000 gas chromatograph–quadrupole mass spectrometer equipped with a 3.2 m × 1.6 mm I.D. glass column packed with 5% Apiezon L plus 3% potassium hydroxide on Inerton Super. The column temperature was 220°C, ion source temperature 280°C and ionization energy 70 eV. The flow-rate of helium carrier gas was 30 ml/min. For mass fragmentography, version 9.1 of the original Shimadzu "MF" software was used.

RESULTS AND DISCUSSION

GC methods for the analysis of residues of diquat and paraquat are mostly based on the determination of volatile dienes originating as the main products from the parent compounds by the reduction with sodium borohydride. In our experience, however, and in agreement with another study[8], the degree of hydrogenation depends on many factors (*e.g.*, reaction time, reaction temperature), which can result in a poor reproducibility. It therefore seemed more reasonable to convert bipyridinium compounds into their perhydrogenated products. This reaction was carried out with a sodium borohydride–nickel(II) chloride reduction system similar to that used by Kawase *et al.*[15] for the hydrogenation of diquat and paraquat precipitated from body fluids by reinecke reagent. However, they encountered problems with incompleteness of reduction of analytes, which they attributed to the poisoning of the catalyst by the sulphide ion released from thiocyanate contained in reineckate complexes.

In our experiments we found hydrogenation to have been completed in 30 min. Perhydrogenated paraquat and two isomers originating from diquat were the only products obtained. Although these compounds could be separated on a column packed with Carbowax 20M plus potassium hydroxide, an impurity present in the blank sample had a retention time identical with that of the peak corresponding to paraquat (see Fig. 1). This problem was overcome by the use of Apiezon L plus potassium hydroxide stationary phase (see Fig. 2). The response of the nitrogen–phosphorus detector was linear within the range tested, *i.e.*, 0.5–50 ng (injected amount). For precise quantification, both peaks corresponding to diquat must be considered, because in freshly prepared samples the peak-area ratio (first peak to the second) was 1.9 and gradually increased, reaching 3.0 within 2 days (at laboratory temperature). This phenomenon was probably due to the establishment of thermodynamic equilibrium between the *cis* and *trans* isomers of the reaction product.

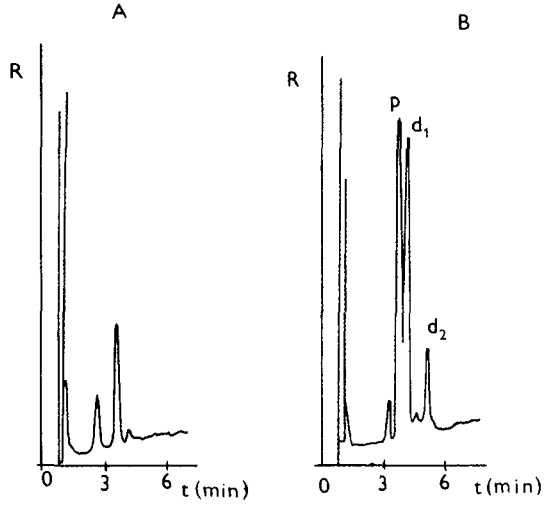

Fig. 1. Gas chromatogram of hydrogenated diquat (peaks d_1 and d_2) and paraquat (peak p) on Carbowax 20M plus KOH. (A) Blank sample; (B) model mixture (injected amount of analytes, 10 ng).

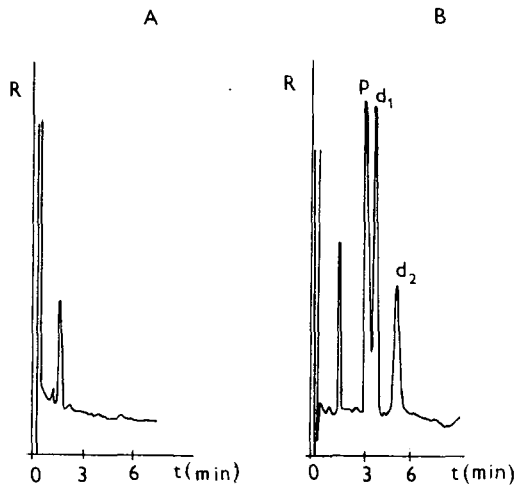

Fig. 2. Gas chromatogram of hydrogenated diquat (peaks d_1 and d_2) and paraquat (peak p) on Apiezon L plus KOH. (A) Blank sample; (B) model mixture (injected amount of analytes, 10 ng).

Almost the same procedure as that employed for the preparation of model samples was used for analyses of potato tubers. In this instance, however, a greater amount of sodium borohydride was necessary for the "direct" reduction of potato homogenate, and the reaction time also had to be extended. When products of reduction were extracted (with diethyl ether) from the reaction mixture, stable emulsions were formed. Their separation could be carried out only by centrifugation. The evaporation of an excess of solvent from the combined extracts was performed in the presence of several drops of hydrochloric acid to prevent the loss of volatile analytes.

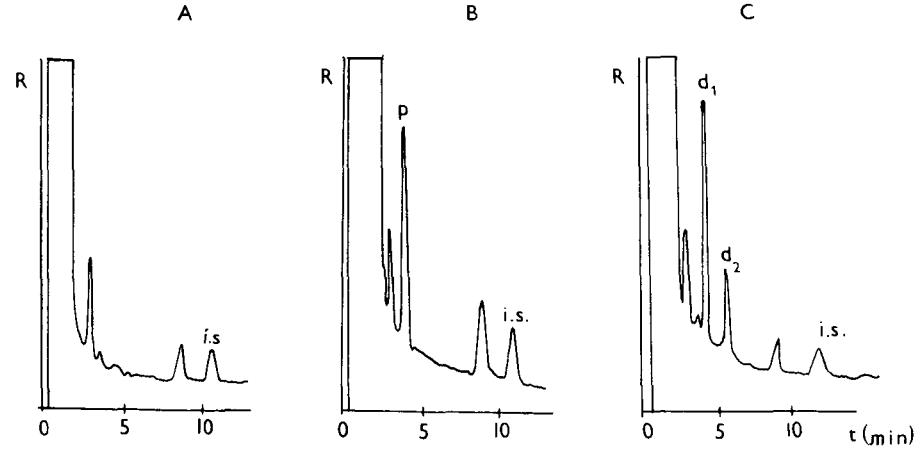

Fig. 3. Determination of bipyridinium herbicides in potatoes (column ii, see Experimental). Each injection represents 150 mg of sample. (A) Blank sample; (B) potatoes spiked with paraquat at 0.1 mg/kg; (C) potatoes spiked with diquat at 0.1 mg/kg.

TABLE I

RECOVERIES OF DIQUAT AND PARAQUAT FROM POTATOES

Compound	*Spiking level*[a] *(mg/kg)*	*Recovery*[b] *(%)*	*Relative standard deviation (%)*
Diquat	0.01	86.1	12.7
	0.04	92.3	5.6
	0.10	95.0	4.2
	1.50	96.6	3.8
Paraquat	0.04	109.8	8.2
	0.10	101.7	6.9
	1.50	100.1	4.0

[a] Expressed as dication.
[b] Mean value of five replicates.

These were released from their protonated form by alkalinization and then immediately extracted into a small volume of *n*-hexane containing desmetryne, an internal standard for GC (see Fig. 3). As can be seen form Table I, high recoveries and good reproducibility of the results were achieved by our procedure. We found that the recovery of residues did not depend on the time of post-spiking incubation, which means that the interaction of bipyridinium compounds with the plant matrix did not result in the formation of non-extractable residues. This fact favours the use of a procedure based on the "total" hydrogenation because, in contrast to our findings, Worobey and Panopio[8], who determined diquat and paraquat as partly hydrogenated products (dienes), encountered serious problems with low recoveries, the value of

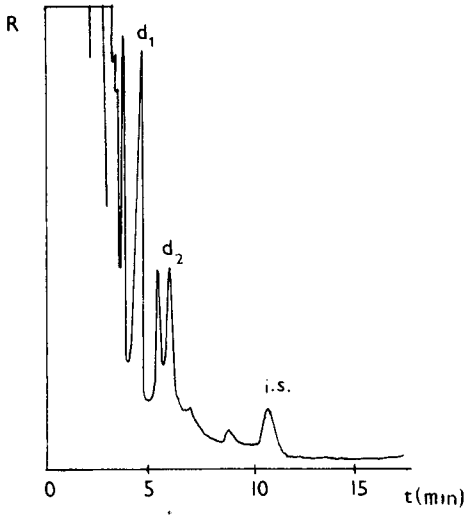

Fig. 4. GC analysis of rapeseed (column ii, see Experimental). Injection represents 15 mg of sample.

TABLE II

MASS SPECTRA OF PERHYDROGENATED PARAQUAT (p) AND ISOMERS OF DIQUAT (d_1 AND d_2)

Compound	*M.W.*	*m/z (%)*
1,1′-Dimethyl-4,4′-bipiperidine (p)	196	96(100), 44(76), 45(65), 43(61) 42(50), 58(45), 70(39), 97(33), 98(32), 196(30)
cis-1,1′-Ethylene-2,2′-bipiperidine (d_1)	194	83(100), 111(50), 98(42), 55(41), 42(38), 194(23), 43(22), 96(17), 44(15), 69(14)
trans-1,1′-Ethylene-2,2′-bipiperidine (d_2)	194	83(100), 111(47), 110(44), 42(41), 55(40), 56(40), 98(34), 44(28), 45(27), 43(25), 194(21)

which moreover depended on the way in which the spiked samples were treated (intensity of mixing, incubation time, etc.).

Rapeseed is another crop that is commonly desiccated with preparations containing bipyridinium compounds (especially diquat). Owing to the higher content of volatile nitrogen-containing compound in this plant material, an additional clean-up step had to be introduced in the sample procedure, but nevertheless some impurities were still left in the final extract (see Fig. 4). Although the gas chromatogram of an "unspiked" sample is presented here, two peaks, d_1 and d_2, with retention times identical with those of isomers of perhydrogenated diquat can be seen. As it was not known whether the rapeseed sample had been treated with diquat, mass spectrometry was therefore employed for the identification of these compounds. Table II gives electron impact mass spectrometric data for our analytes, confirming the expected structures:

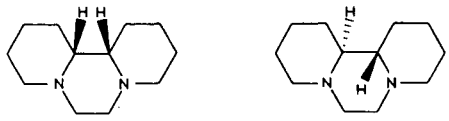

d_1 and d_2
originating from diquat

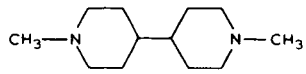

p
originating from paraquat

No significant differences existed (the sole exception was the presence of an ion of *m/z* 110 in the spectrum of d_2) in the fragmentation pathways of isomers originating from diquat; however, their absolute configuration could not be determined by this method. In all the spectra distinct molecular ions were present. Four ions were selected for mass fragmentographic analysis of rapeseed extract (see Fig. 5). The

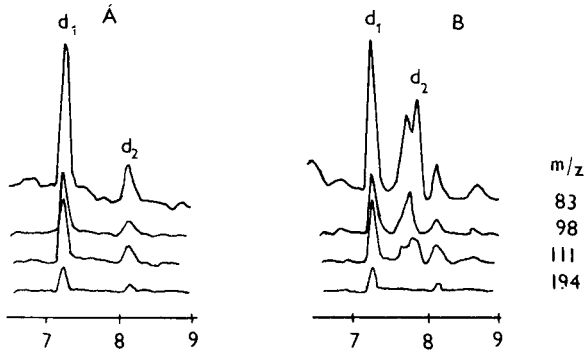

Fig. 5. Mass fragmentographic analysis of rapeseed. (A) Standard solution of hydrogenated diquat, injected amount 5 ng; (B) rapeseed, injection represents 5 mg of sample.

presence of diquat residues (at a level of 2.8 mg/kg) was found in this sample. As can be seen, the most selective ion was that of *m/z* 194 (molecular ion), but unfortunately its abundance in the spectrum was not high. Based on the monitoring of the most intense ion of *m/z* 83, the sensitivity of MS detection was comparable to that achieved by NPD. In the latter instance, however, the use of a more efficient capillary column for better resolution of the analytes (especially for levels lower than 1 mg/kg) is recommended. The recovery of diquat from both rapeseed and meal was high, *viz.*, 90.3 ± 5 and 92.8 ± 3%, respectively, at a spiking level 2 mg/kg.

We were also interested in the distribution of diquat residues between the rapeseed oil and remaining meal. A rapeseed sample containing 2.8 mg/kg of diquat was extracted with light petroleum (b.p. 40–70°C) in a Soxhlet apparatus. Nearly all the residues (99.3% of the original content) were found in the defatted rapeseed sample; the analysis of isolated oil did not reveal the presence of diquat. This finding is in agreement with the above-outlined physico-chemical properties of diquat. This bipyridinium compound is firmly bonded to the hydrophilic portion of the plant matrix and hence is not accessible for extraction with an apolar solvent.

REFERENCES

1 A. Calderbank and S. H. Yuen, *Analyst (London)*, 90 (1965) 99.
2 A. Calderbank and P. Slade, *Outlook Agric.*, 5 (1966) 55.
3 A. Calderbank, *Analyst (London)*, 86 (1961) 569.
4 J. E. Pack, *Anal. Methods Pestic. Plant Growth Regul. Food Addit.*, 5 (1967) 397.
5 J. B. Leary, *Anal. Methods Pestic. Plant Growth Regul.*, 10 (1978) 321.
6 A. Pryde and F. J. Darby, *J. Chromatogr.*, 115 (1975) 107.
7 B. L. Worobey, *Pestic. Sci.*, 18 (1987) 245.
8 B. L. Worobey and L. G. Panopio, *Anal. Lett.*, 16(A15) (1983) 1235.
9 R. R. King, *J. Agric. Food Chem.*, 26 (1978) 1460.
10 G. H. Draffan, R. A. Clare, D. L. Davies, G. Hawksworth, S. Murray and D. L. Davies, *J. Chromatogr.*, 139 (1977) 311.
11 S. U. Khan, *J. Agric. Food Chem.*, 22 (1974) 863.
12 S. U. Khan, *Bull. Environ. Contam. Toxicol.*, 14 (1975) 745.
13 C. J. Sonderquist and D. G. Crosby, *Bull. Environ. Contam. Toxicol.*, 14 (1975) 745.
14 M. A. Martens, C. H. van Peteghem and A. Heyndrickx, *Meded. Fac. Landbouwwet. Rijksuniv. Gent*, 40 (1975) 1149.
15 S. Kawase, S. Kanno and S. Ukai, *J. Chromatogr.*, 283 (1984) 231.

Journal of Chromatography, 479 (1989) 251–259
Elsevier Science Publishers B.V., Amsterdam — Printed in The Netherlands

CHROM. 21 747

HIGH-PRESSURE ADSORPTION OF CARBON DIOXIDE ON SUPERCRITICAL-FLUID CHROMATOGRAPHY ADSORBENTS

JON F. PARCHER* and JOSEPH R. STRUBINGER
Department of Chemistry, University of Mississippi, University, MS 38677 (U.S.A.)
(First received March 29th, 1989; revised manuscript received June 27th, 1989)

SUMMARY

Gibbs adsorption isotherms for sub- and supercritical carbon dioxide were measured on four common supercritical-fluid chromatography adsorbents, *viz.*, silica and octadecyl-, cyano- and diol-bonded silica, at 40°C from ambient pressure to 140 bar. All of the isotherms for supercritical carbon dioxide displayed maximum adsorption at pressures close to the critical pressure. Multilayer adsorption occurred at pressures close to the critical pressure in each system, and the type of bonded phase had little or no effect on the CO_2 adsorption isotherms. At subcritical pressures, multilayer adsorption of CO_2 occurred at relatively low pressures ($P_R \geqslant 0.4$). The adsorbed layer of "mobile" phase persisted to the highest experimental pressures (140 bar). Thus, at least a monolayer of adsorbed CO_2 will exist on the surface of adsorbent stationary phases under the conditions normally used for supercritical-fluid chromatography with CO_2 as the mobile phase. Both the density and dimensions of the adsorbed layer will vary with temperature and pressure.

INTRODUCTION

Adsorption isotherms of myriad systems have been measured at low pressures and temperatures for the investigation and interpretation of phase-transfer processes. Chromatographic adsorbents in particular have been extensively studied because of the unique duality of chromatographic systems in which the chromatographic performance is dictated by the characteristics of the phase distribution isotherm of the solutes and the mobile phase. As a consequence, the same chromatographic systems often provide an excellent means for measuring such phase distribution isotherms.

With the recently renewed interest in supercritical-fluid chromatography (SFC), the need for phase-distribution equilibria studies of the common SFC systems for the elucidation of the complex retention mechanism(s) has become apparent. However, adsorption isotherm measurements are difficult at the high pressures normally encountered with SFC. Consequently, relatively few quantitative investigations have been carried out for gas–solid *adsorption* or gas–liquid *absorption* equilibria under supercritical conditions.

In addition to the experimental difficulties, another problem is that at temper-

0021-9673/89/$03.50

atures and pressures close to the critical point, the density of the fluid phase varies dramatically with pressure and ultimately approaches that of a liquid. In which case the amount of bulk fluid occupying the region adjacent to a surface will be significant even in the absence of a strong interfacial potential between the adsorbate and adsorbent (solid or liquid). This condition necessitates the use of the Gibbs adsorption model[1,2] in which the excess adsorption is defined in terms of the amount of adsorbate present at the surface in excess of the amount that would be present if the fluid density in this interfacial region were the same as the density of the bulk fluid. It is this "excess" quantity that is obtained by direct experimental measurements. "Absolute" adsorption is defined to be the total amount of adsorbate located within a layer of arbitrarily defined thickness adjacent to the adsorbent surface. The latter quantity clearly is influenced by the choice of the layer dimensions.

In spite of the difficulties, several authors have measured the equilibrium isotherms of some systems at conditions close to the critical point. Hori and Kobayashi[3] measured the adsorption of methane on Porasil over a range of sub- and supercritical conditions. An early review by Menon[4] cited several examples of adsorption equilibria studies for inorganic gases at supercritical conditions. More recently, Findenegg[5] also discussed the sub- and supercritical adsorption of propane and ethylene on graphitized carbon black adsorbents. However, none of these investigations involved systems commonly used for SFC.

Recently, however, a few fundamental phase-distribution studies of SFC systems have been completed. Selim and Strubinger[6,7] measured the uptake of supercritical pentane in capillary columns containing SE-30 and SE-54 polymeric stationary phases. Others[8] have measured stationary phase swelling (volume changes) of up to 400–500% under SC conditions for both butane and carbon dioxide in SE-30 by measurement of the changes in the void volume of capillary columns. In addition to the studies involving liquid stationary phases, the uptake of supercritical CO_2 by octadecyl-bonded silica has recently been determined by tracer pulse chromatography over a range of sub- and supercritical temperatures and pressures[9]. Yonker and Smith[10] also used tracer pulse chromatography to measure the uptake of a common SFC modifier, 2-propanol, from CO_2 by cross-linked SE-54 in a capillary column. Lochmüller and Mink[11] performed the same type of measurements with ethyl acetate adsorbed on silica from CO_2 using another chromatographic method, *viz.*, the peak maxima method.

In each case, the sorption isotherms of systems near the critical point of the adsorbate had an unusual shape. A maximum in the excess adsorption was observed at pressures close to the critical pressure (P_c) and temperatures slightly greater than the critical temperature (T_c) in the studies which covered both sub- and supercritical conditions[3,4,9]. The supercritical systems showed decreasing adsorption with increasing pressure (at fixed temperature) and decreasing temperature (at fixed pressure). The density isotherms, on the other hand, showed normal temperature dependence in every case, *i.e.*, the amount adsorbed decreased with increasing temperature at fixed density. For this reason, density isotherms are more meaningful than pressure isotherms for the comparison of supercritical adsorption isotherms.

Multilayer adsorption is commonly observed for gas–solid systems near the critical point of the adsorbate for both sub- and supercritical conditions. The maximum amount adsorbed decreases at temperatures and pressures higher and lower

than T_c and P_c. If such multilayer adsorption occurs for supercritical CO_2, this modification of the stationary phase would have to be considered in any theoretical model for SFC retention mechanisms.

The objective of the present investigation was to determine the excess adsorption isotherms of carbon dioxide on several different types of common SFC adsorbents over a range of pressures in order to investigate the role of the stationary phase characteristics in the retention mechanism(s) observed in SFC.

EXPERIMENTAL

The experimental method used to determine the adsorption isotherms was mass spectrometric tracer pulse chromatography (MSTPC)[12,14]. Stable isotopes of CO_2 were used as the tracer probes with a mass spectrometric (MS) detection system[15,16]. The mass spectrometer was an HP-5985 gas chromatography (GC)–MS system operated in the selected ion monitor mode. The carrier gas stream was split into the GC–MS system through a short length of 5 μm I.D. fused-silica capillary tubing.

The carbon dioxide was SFC grade (Scott Specialty Gases), and $^{13}C^{18}O^{16}O$ (m/e = 47) (Merck & Co) was used as the stable tracer for the isotherm measurements. Neon, argon and krypton were used to determine the void volume of the columns. The tracer and inert gases were injected as a gaseous mixture via a gas-sampling valve that was pressurized with CO_2 to the operating pressure of the column prior to injection. More complete experimental details can be found in ref. 9.

The chromatographic columns and adsorbents are described in Table I. The surface areas for all four of the stationary phases were measured by BET adsorption of nitrogen at 77°K.

TABLE I

PHYSICAL CHARACTERISTICS OF THE CHROMATOGRAPHIC COLUMNS

Packing type	*Manufacturer*	*Column length (mm)*	*Packing weight (g)*	*Surface area (m^2/g)*
Silica	Scientific Glass Engineering	250	0.431	140
Octadecyl-silica	Scientific Glass Engineering	250	0.573	90
Cyano-silica	Keystone Scientific	100	0.214	120
Diol-silica	Keystone Scientific	100	0.192	210

RESULTS

The measured Gibbs (excess) adsorption isotherm for CO_2 on the silica adsorbent at 40°C is shown in Fig. 1, and the experimental data are given in Table II. The isotherm measurements included both sub- and supercritical conditions. At pressures of less than P_c for CO_2 (73.8 bar), the CO_2 mobile phase was a gas, and at higher pressures the mobile phase was a supercritical fluid with a density that varied from 0.32 to 0.67g/ml. In the subcritical regime, the density isotherm was nearly linear indicating relatively weak adsorbate-adsorbent and solute-solute interactions. However, the calculated monolayer capacity, assuming an area of 18 Å^2 for adsorbed

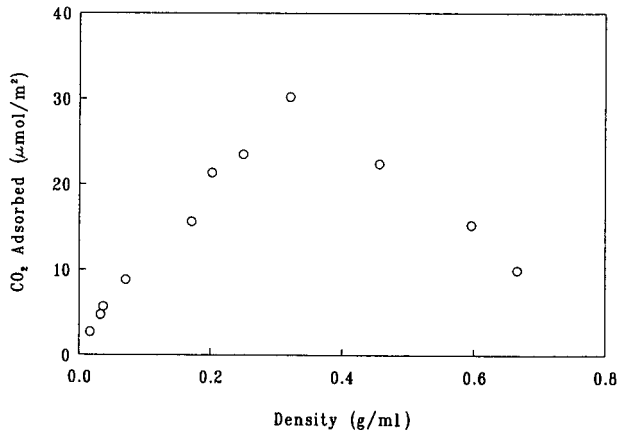

Fig. 1. Gibbs adsorption isotherm of CO_2 on Silica at 40°C.

CO_2, was only 9 μmol/m^2. Thus, at a reduced temperature of 1.03 (40°C), multilayer adsorption was observed at relatively low, subcritical pressures ($P/P_c \geqslant 0.6$). At pressures greater than P_c the *excess* amount of CO_2 adsorbed *decreased* with pressure. This apparent decrease in adsorption was actually due to the significant *increase* in the bulk density of CO_2 with pressure at pressures greater than P_c. Thus a point of maximum adsorption —about 3–4 layers— occurred at, or slightly below, the critical pressure. The unique shape of this isotherm is caused by several interrelated factors,

TABLE II

ADSORPTION ISOTHERM DATA FOR CO_2 ON SFC ADSORBENTS AT 40°C

Silica		*C_{18}-silica*		*Diol-silica*		*Cyano silica*	
Density (g/ml)	*Excess adsorbed (μmol/m^2)*	*Density (g/ml)*	*Excess adsorbed (μmol/m^2)*	*Density (g/ml)*	*Excess adsorbed (μmol/m^2)*	*Density (g/ml)*	*Excess adsorbed (μmol/m^2)*
Subcritical pressures							
0.017	2.7						
0.033	4.7					0.027	2.4
0.037	5.7	0.015	1.9	0.018	3.3	0.043	4.4
0.071	8.8	0.038	4.5	0.040	6.3	0.069	6.4
0.171	15.6	0.067	7.8	0.073	10.9	0.174	14.2
0.202	21.3	0.204	17.7	0.185	22.1	0.215	18.4
Supercritical pressures							
0.250	23.5	0.242	21.8	0.274	26.1	0.355	26.7
0.321	30.2	0.336	24.1	0.498	20.1	0.538	14.2
0.457	22.4	0.531	11.8	0.599	16.7	0.626	12.3
0.596	15.2	0.627	7.9			0.684	6.4
0.666	9.9	0.681	5.6				
		0.720	5.0				

viz., the high density and pressure of the adsorbate, temperatures close to the critical temperature, and the fact that only the excess amount of CO_2 adsorbed could be measured experimentally.

Very similar adsorption isotherms have previously been observed for supercritical propane and ethylene on graphitized carbon black[5]. With both of these adsorbates, the maximum adsorption occurred at pressures close to P_c and the adsorption observed at higher pressures decreased dramatically with pressure. The maxima in the adsorption isotherms were sharply peaked at temperatures close to T_c but more diffuse at higher temperatures. The formation of thick, adsorbed layers close to the critical point was suggested[5] to be a form of "prewetting" of the adsorbent by the supercritical adsorbate.

The exact effect of a thick layer of CO_2 adsorbed on SFC adsorbents on the retention of other solutes is uncertain. It is also unclear whether the adsorbed CO_2, which is in dynamic equilibrium with the bulk fluid phase, actually constitutes a part of the "stationary" phase. It has been shown in high-performance liquid chromatography that in some cases chromatographic solutes interact directly with an adsorbed solvent layer, particularly with bonded phases; whereas in other cases the solutes interact directly with the solid surface in a displacement process (polar solutes with silica)[17,18]. A similar mechanism may operate for SFC; however, the exact role of the stationary phase is presently unclear.

Almost all previous studies of SFC retention mechanisms have been carried out by studying the effect of physical and chemical parameters on the capacity factor (k') of different solutes. Unfortunately, this protocol gives only indirect evidence concerning the exact composition of different columns or packing types. Accurate knowledge of the packing weight, surface areas, flow-rates and void volumes, as well as k', is required for direct comparison of different columns, and very few studies of this type have been carried out with SFC systems.

The influence of the pressure drop across packed columns on the experimentally measured parameters such as k' and adsorption isotherms could possibly be significant, especially for systems near the critical point of the mobile phase[19]. A significant density (ρ) gradient may exist in a packed column even with a relatively small pressure drop across the column because of the large value of $(\partial\rho/\partial P)_T$ (where T = temperature) near the critical point. In order to evaluate the influence of the density gradient on the isotherm data in the present study, the inlet and outlet densities were calculated for each experiment. Table III contains the pressure and density data for the octadecyl-bonded silica column. The volume flow-rates used in the experiment ranged from 800 μl/min at low pressures to 50 μl/min at the highest pressures. Thus, the pressure gradients decreased with pressure and were negligible for all of the supercritical pressures. The density profiles and gradients are shown in Figs. 2 and 3. In no case was the density at the inlet significantly different from the outlet density, and there is no need for a correction applied to the experimental isotherm data.

These experiments were not typical of practical SFC conditions for two reasons: (i) the *molar flow-rate* was maintained constant, not the pressure, density or volume flow-rate, and (ii) the probe solutes were light gases, thus the flow-rates and consequently the pressure drops were much lower than those observed for SFC with high-molecular-weight solutes. However, the important point is that the experimental data obtained with the MSTPC technique do not require any correction for pressure or density gradients under the conditions used for this study.

TABLE III

PRESSURE AND DENSITY DATA FOR OCTADECYL-BONDED SILICA AT 40°C

Pressure (bar)		*Pressure Gradient*	*Density (g/ml)*		*Density Gradient*
Inlet	*Outlet*	$(\Delta P/<P>) \times 100$	*Inlet*	*Outlet*	$(\Delta\rho/<\rho>) \times 100$
10.3	7.0	38.1	0.018	0.012	39.7
21.2	19.0	10.6	0.040	0.038	11.8
33.1	32.5	1.9	0.070	0.066	6.0
60.9	60.0	1.5	0.157	0.155	2.5
69.1	68.4	1.0	0.198	0.196	2.0
84.3	83.9	0.41	0.339	0.337	1.6
96.6	96.2	0.43	0.533	0.531	0.78
110.8	110.4	0.31	0.628	0.627	0.26
124.7	124.4	0.22	0.682	0.681	0.13
138.1	137.7	0.25	0.720	0.720	0.12

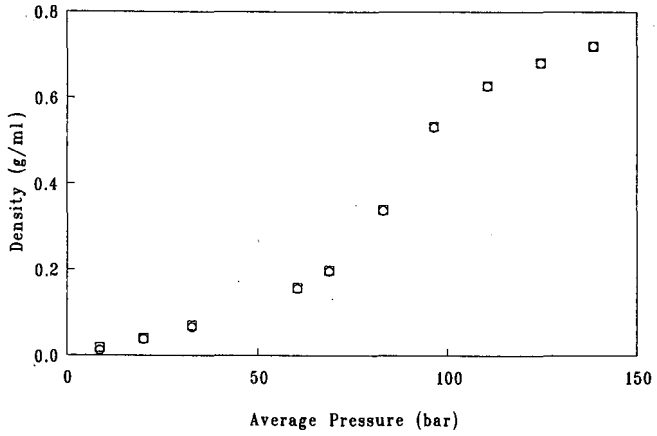

Fig. 2. Inlet and outlet densities for the C_{18}-bonded silica at 40°C. □ = Inlet; ○ = outlet.

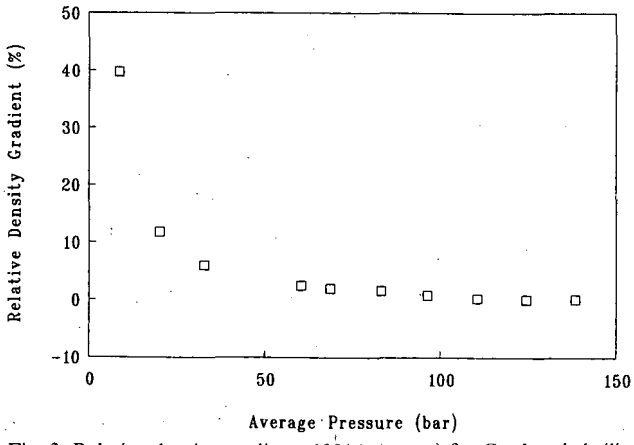

Fig. 3. Relative density gradients $100(\Delta\rho/<\rho>)$ for C_{18}-bonded silica at 40°C.

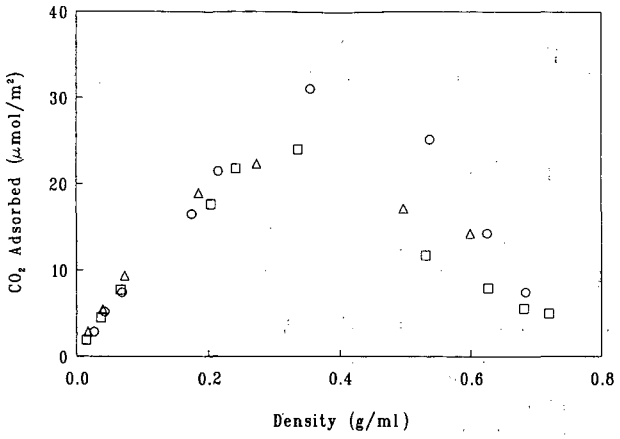

Fig. 4. Excess adsorption isotherms of CO_2 on several common SFC adsorbents at 40°C. □ = C_{18}-silica; ○ = cyano-silica; △ = diol-silica.

In order to determine the effect of different types of bonded stationary phase on the mobile phase uptake by SFC adsorbents, the adsorption isotherms of C_{18}-, diol- and cyano-bonded silica were also determined under the same experimental conditions. These isotherms are given in Table II and shown in Fig. 4. The isotherms are all very similar in shape and magnitude to the silica isotherm (Fig. 1), although there are differences especially at supercritical pressures.

The *subcritical* density isotherms for all four adsorbents were linear and nearly equivalent within experimental error. Thus, the bonded phases do not significantly affect the adsorption capacity for CO_2 (per unit surface area) of the support, and all of the SFC stationary phases studied acted as relatively inert adsorbents at subcritical pressures.

One difference in the supercritical isotherms is that the C_{18}-bonded silica appears to adsorb slightly less than the other adsorbents, including the untreated silica. This is a reflection of the non-polar character of this adsorbent compared to the others. However in every case, multilayer adsorption of CO_2 was observed at pressures greater than P_c, regardless of the surface characteristics. At high pressures (densities $\geqslant 0.7$) the *excess* adsorption isotherms converged to a value of about 5 μmol/m^2 or approximately half of the low pressure monolayer capacity. Thus, at 40°C, the density of CO_2 in the surface layer was greater than the bulk density even at 140 bar.

CONCLUSIONS

High-performance liquid chromatography studies have shown that a monolayer of the strongest solvent component of the mobile phase commonly exists on the surface of the stationary phase; that the amount adsorbed does not depend upon the composition of the mobile phase; and that chemical modification of the adsorbent surface does not affect the monolayer capacity of the solid[17,18]. The studies reported here show that somewhat similar effects are observed for SFC with CO_2 as the mobile

phase. That is, at temperatures slightly above T_c and pressures greater than P_c at least a monolayer of condensed mobile phase exists on the stationary phase adsorbent. At pressures only slightly above P_c, a thicker condensed layer of CO_2 of up to 3–4 molecular diameters is adsorbed under normal SFC conditions.

Our previous investigation[9] showed that multilayer adsorption of CO_2 was maximal at temperatures and pressures close to the critical point. The excess amount of CO_2 adsorbed decreased at higher pressures and temperatures, but never reached zero under conditions commonly employed for practical SFC. Thus, in SFC as in high-performance liquid chromatography, the stationary phase adsorbent is always "coated" by at least a monolayer of condensed mobile phase.

The effect of mobile phase "modifiers", such as alcohols, on the dimensions and composition of the adsorbed stationary phase film has not been determined. Lochmüller and Mink[11] have measured the adsorption of one such modifier, ethyl acetate, on Partisil-10 at 60°C. They observed typical Langmuir isotherms for this organic modifier —under conditions far from its critical point ($T_c = 25$°C)— on the SFC adsorbent. One unusual observation was that, at fixed concentration of the modifier in the mobile phase, the amount of modifier adsorbed on the stationary phase decreased with CO_2 pressure (density). This would indicate that the mobile phase and modifier competed for sites in the adsorbed layer. Yonker and Smith[10] measured the uptake of 2-propanol from supercritical CO_2 by a cross-linked polymer and found partition isotherms that were very similar to those shown in Figs. 1 and 4. The experimental protocol of the former study[11] mimicked the SFC technique of gradient programming at a fixed pressure, while the protocol of the latter study[10] was more relevant for the technique of density programming with a fixed mobile phase composition.

Thus, it is clear the stationary phases used for SFC *adsorb and/or absorb* both the supercritical mobile phase and polar modifiers. However, the effect of this stationary phase modification on the retention of SFC solutes is unclear. The exact effect of a polar modifier on the magnitude and composition of the adsorbed interfacial "phase" can best be determined by measurement of the binary adsorption isotherms of CO_2-modifier mixtures.

ACKNOWLEDGEMENTS

Acknowledgement is made to the National Science Foundation and to the donors of the Petroleum Research Fund, administered by the American Chemical Society, for support of this research.

REFERENCES

1 C. S. Koch, F. Koster and G. H. Findenegg, *J. Chromatogr.*, 406 (1987) 257.
2 F. Riedo and E. sz. Kováts, *J. Chromatogr.*, 239 (1982) 1.
3 Y. Hori and R. Kobayashi, *J. Chem. Phys.*, 54 (1971) 1226.
4 P. G. Menon, *Chem. Rev.*, 68 (1968) 277.
5 G. H. Findenegg, in A. L. Meyers and G. Belfort (Editors), *Fundamentals of Adsorption*, Engineering Foundation, New York, 1983, pp. 207–218.
6 M. I. Selim and J. R. Strubinger, *Fresenius' Z. Anal. Chem.*, 330 (1988) 246.
7 J. R. Strubinger and M. I. Selim, *J. Chromatogr. Sci.*, 26 (1988) 579.

8 S. R. Springston, P. David, J. Steger and M. Novotny, *Anal. Chem.*, 58 (1986) 997.
9 J. R. Strubinger and J. F. Parcher *Anal. Chem.*, 61 (1989) 951.
10 C. R. Yonker and R. D. Smith, *Anal. Chem.*, 61 (1989) 1348.
11 C. H. Lochmüller and L. P. Mink, *J. Chromatogr.*, 409 (1987) 55.
12 F. I. Stalkup and R. Kobayashi, *AIChE J.*, 9 (1963) 121.
13 F. Helfferich and D. L. Peterson, *Science (Washington, D.C.)*, 142 (1963) 661.
14 F. I. Stalkup and H. A. Deans *AIChE J.*, 9 (1963) 106.
15 J. F. Parcher and M. I. Selim *Anal. Chem.*, 51 (1979) 2154.
16 J. F. Parcher *J. Chromatogr.*, 251 (1982) 281.
17 R. P. W. Scott and P. Kucera, *J. Chromatogr.*, 112 (1975) 425.
18 R. P. W. Scott and P. Kucera, *J. Chromatogr.*, 142 (1977) 213.
19 D. E. Martire, *J. Chromatogr.*, 461 (1989) 165.

Journal of Chromatography, 479 (1989) 261–268
Elsevier Science Publishers B.V., Amsterdam — Printed in The Netherlands

CHROM. 21 679

HIGH-PERFORMANCE LIQUID CHROMATOGRAPHY AND CAPILLARY SUPERCRITICAL-FLUID CHROMATOGRAPHY SEPARATION OF VEGETABLE CAROTENOIDS AND CAROTENOID ISOMERS

H. H. SCHMITZ and W. E. ARTZ

Department of Food Science, 382 Agr. Eng. Sci. Bldg., 1304 W. Pennsylvania Ave., University of Illinois, Urbana, IL 61801 (U.S.A.)

C. L. POOR

Division of Nutritional Sciences at the University of Illinois, Champaign-Urbana, IL (U.S.A.)

and

J. M. DIETZ and J. W. ERDMAN, Jr.*

Department of Food Science, 382 Agr. Eng. Sci. Bldg., 1304 W. Pennsylvania Ave., University of Illinois, Urbana, IL 61801 (U.S.A.)

(First received March 17th, 1989; revised manuscript received June 9th, 1989)

SUMMARY

Carotenoids from carrots and tomatoes were separated with high-performance liquid chromatography (HPLC) and capillary supercritical fluid chromatography (SFC). All *trans* alpha- and beta-carotene were separated from their respective *cis*-isomers with capillary SFC. Carotenoids extracted from tomatoes included xanthophyll, lycopene and beta-carotene, while alpha- and beta-carotene were extracted from carrots. The HPLC separations were accomplished isocratically with a 25-cm column containing 5-μm ODS and methanol–acetonitrile–chloroform (47:47:6) or acetonitrile–dichloromethane (80:20). beta-Carotene *cis*-isomers were separated with SFC with a SB-cyanopropyl-25-polymethylsiloxane column, while alpha-carotene isomers were separated with two SB-cyanopropyl-50-polymethylsiloxane columns. Carotenoids from carrots and tomatoes were separated with a SB-phenyl-50-polymethylsiloxane column. Carbon dioxide with 1% ethanol was the SFC mobile phase. The eluent was monitored at 461 nm for HPLC and either 453 or 461 nm for SFC.

INTRODUCTION

Capillary column supercritical-fluid chromatography (SFC) has emerged as a very promising chromatographic technique that complements both high-performance liquid chromatography (HPLC) and gas–liquid chromatography (GLC). It is particularly effective for separations that are difficult due to limitations imposed by both HPLC and GLC[1]; *e.g.*, the thermal instability of the analyte, which would limit analysis on GLC and poor resolution due to limited theoretical plates, which can limit analysis on HPLC[2]. In addition, both selective (UV–VIS) and universal (flame

0021-9673/89/$03.50

ionization, FID) detectors can be used with capillary SFC. Supercritical carbon dioxide, with and without added modifiers, is an effective solvent for a wide variety of non-polar solutes. In addition to the normal column–solute interactions, the retention of an analyte on the column is dependent upon the density of the supercritical mobile phase[3], which can be easily altered to effect separations. The stationary phase composition and temperature, plus the solvent composition and density, provide a variety of parameters that can be programmed to separate a mixture of compounds. These conditions appear optimal for the separation of the thermally labile and difficult to separate carotenoids and their *cis-trans* isomers[4]. The high efficiency afforded by capillary columns is particularly important due to the large number of naturally occurring carotenoids (nearly 500, plus several isomers for many of them), most of which are closely related structurally[5].

Although SFC has been applied to a wide variety of compounds and mixtures in the past few years[6–11], there have been few reports on carotenoids and none on the separation of carotenoid *cis-trans* isomers[4,12,13]. Because of the relatively labile nature of the carotenoids, HPLC, rather than GLC, has been used extensively to separate and identify carotenoids[14–17] and their isomers[18,19] extracted from a variety of biological samples. The first application of SFC to carotenoids was in 1968 by Giddings *et al.*[12], who separated alpha- and beta-carotene. In 1987 Frew *et al.*[4] separated and identified several carotenoids with SFC in combination with mass spectrometry. Favati *et al.*[20] has utilized supercritical CO_2 for the extraction, but not the separation, of carotene and lutein from leaf protein concentrates. They illustrated the potential of supercritical CO_2 for selective carotenoid extraction under a variety of solvent densities.

The objectives of this work were three-fold: (1) to illustrate the carotenoid separation capabilities of SFC as compared to an isocratic HPLC system, (2) to illustrate the ability of SFC to separate closely related carotenoid geometric isomers and (3) to demonstrate the application of SFC to the analysis of carotenoids from biological systems.

EXPERIMENTAL

Standards and samples

Crystalline lycopene (L9875, from tomatoes), alpha-carotene (C0251, from carrots) and beta-carotene (C0126, from carrots) were obtained from Sigma (St. Louis, MO, U.S.A.). Carrots and tomatoes were purchased fresh locally. Carotenoid standards for SFC were dissolved in hexane (0.1%, w/v), while standards for HPLC were dissolved in chloroform at a concentration of 0.1% (w/v), and then diluted to a concentration range similar to that of the samples. Carotenoids were extracted from vegetables by blending 200 g (fresh weight) of vegetable sample in 200 ml of methanol for 5 min. The resulting puree was then filtered through a Büchner funnel with Whatman No. 1 filter-paper. The remaining vegetable tissue was extracted with 200 ml of hexane by stirring for 30 min under argon. The extraction mixture was coarsely filtered as above, and the hexane filtrate evaporated with a rotary evaporator to a volume of approximately 5 ml. The extract was stored under argon in a foil covered sample vial and stored in a freezer (−20°C) for analysis the following day.

cis-trans isomerization of the double bonds in the polyene chain for both alpha- and beta-carotene was catalyzed by iodine in hexane in daylight[21] with aliquots of the

0.1% (w/v) standard solutions. All standard and sample preparation was performed under yellow lighting (except when regular lighting was called for in the sample procedure). All solutions were filtered with a 0.2-μm filter prior to injection.

SFC apparatus

A Lee Scientific Model 501 capillary SFC (Salt Lake City, UT, U.S.A.) pump and oven were used with a Linear UV–VIS 204 detector (Reno, NV, U.S.A.). A Lee Scientific Model 501 extraction system was used, which utilizes cryofocusing to concentrate the analyte near the head of the column. The release of compressed gas through a sleeve around the cryofocusing unit results in rapid cooling to well below the supercritical point for CO_2. The analyte precipitates out of the extracting solvent (CO_2) at that point. A Model R40 refrigerated circulator (Precision Scientific Group, Chicago, IL, U.S.A.) was used to cool the pump, the Valco A90 injector (Houston, TX, U.S.A.), the extraction cell and the Linear UV/VIS detector. The Valco injection system contained a 200-nl internal loop operated in a time-split mode. The chromatographs were recorded on an Omniscribe Series B-5000 recorder (Houston Instruments, Austin, TX, U.S.A.) and a Hewlett-Packard (Avondale, PA, U.S.A.) Model 3390A integrator. The pump, oven, extraction cell and injection system was controlled by an ARC Turbo personal computer (American Research Corp., Monterey Park, CA, U.S.A.) with software written by Lee Scientific.

For the separation of the carotenoids extracted from vegetables, a SB-phenyl-50 column (10 m × 50 μm I.D., film thickness of 0.25 μm) was used with a cross-linked stationary phase containing 50% phenyl- and 50% polymethylsiloxane. For the separation of beta-carotene *cis-trans* isomers, a SB-cyanopropyl-25 column (7 m × 50 μm I.D., film thickness of 0.25 μm) was used with a cross-linked stationary phase consisting of 25% cyanopropyl and 75% polymethylsiloxane (Lee Scientific). For the separation of alpha-carotene *cis-trans* isomers, two SB-cyanopropyl-50 columns (10 m × 50 μm I.D., film thickness of 0.25 μm) were used with a cross-linked stationary phase consisting of 50% cyanopropyl- and 50% polymethylsiloxane (Lee Scientific). The mobile phase was SFC grade CO_2 containing 1% (v/v) ethanol (Scott Specialty Gases, Plumsteadville, PA, U.S.A.).

HPLC apparatus

The HPLC system consisted of a Tracor 950 chromatographic pump and 970A variable wavelength detector (Austin, TX, U.S.A.), a Rheodyne 7125 sample injector (Cotati, CA, U.S.A.), an Upchurch Uptight precolumn, packed with ODS C_{18} (Oak Harbor, WA, U.S.A.), a Supelco LC-18 (Bellefonte, PA, U.S.A.) stainless-steel column (25 cm × 4.6 mm I.D.) packed with 5-μm ODS and a Shimadzu (Kyoto, Japan) C-R3A Chromatopac integrator. The solvent system was comprised of either acetonitrile–dichloromethane (80:20)[22] or methanol–acetonitrile–chloroform (47:47:6)[23]. All solvents were filtered and degassed, and were of spectrograde quality.

SFC procedures

Alpha- and beta-carotene present in the carrot extract were separated at 50°C under isobaric conditions and a mobile phase density of 0.70 g/ml. The injection duration was 0.25 s. Carotenoids present in the tomato extract were separated at 45°C with an asymptotic density program with a 1/2 rise time constant of 30 min and

a termination time of 30 min. The initial density was 0.66 g/ml, while the convergence density was 0.72 g/ml. In effect, a mobile phase density of 0.69 g/ml was achieved after 30 min at which time the mobile phase density was held at 0.69 g/ml. Alpha- and beta-carotene *cis-trans* isomers were also separated at 50°C. The beta-carotene isomers were separated isobarically; the mobile phase density was 0.66 g/ml and the injection duration was 0.35 s. For the separation of alpha-carotene isomers the extraction cell was used as an injection system. A 1-μl volume of the isomerized alpha-carotene solution was loaded into the extraction cell. The extraction cell temperature was set at 50°C. After cryofocusing had been started and the mobile phase compressed to a density of 0.92 g/ml, a valve was adjusted to direct the supercritical carbon dioxide mobile phase through the extraction cell. During the extraction the oven was held at 45°C. After a 5-min extraction, the density was rapidly reduced to 0.52 g/ml. At that time a valve was adjusted that directed the mobile phase through the column, the cryofocusing was turned off and the temperature in the oven was increased rapidly to 50°C. A linear density ramp from 0.52 to 0.62 g/ml at 0.002 g/ml · min was run. Column eluents were monitored at 461 nm and the detector sensitivity was set at 0.02 a.u.f.s. for the vegetable and beta-carotene SFC analyses. However, for the alpha-carotene analysis the eluent was monitored at 453 nm at 0.06 a.u.f.s.

HPLC procedures

An isocratic system of methanol–acetonitrile–chloroform (47:47:6) at a flow-rate of 2.0 ml/min was used to separate alpha- and beta-carotene from carrots. An isocratic system of acetonitrile–dichloromethane (80:20) at a flow-rate of 2.0 ml/min was used to separate the carotenoids isolated from tomatoes. Column eluents were monitored at 461 nm. Lycopene, alpha-carotene and beta-carotene peaks were tentatively identified for both SFC and HPLC based on a comparison with the retention times of the standards.

RESULTS AND DISCUSSION

A comparison between the HPLC and SFC methods used to separate the vegetable carotenoids indicated improved separation with SFC. Fig. 1 shows the separation of alpha- and beta-carotene from the carrot extract achieved with SFC using the SB-phenyl column, which was clearly superior to the isocratic HPLC separation shown in Fig. 2. Fig. 3 demonstrates separation of carotenoids in the tomato extract by SFC with an asymptotic density program for the mobile phase. As with the carrot extract, the SFC separation was superior to the tomato extract separations using isocratic HPLC (Fig. 4).

In 1985, Bushway[14] investigated several isocratic HPLC methods for the separation of carotenoids from fruits and vegetables, with limited success in some cases. Ruddat and Will[15] and Wills *et al.*[17] found that gradient HPLC conditions, relative to isocratic conditions, improved the separation of complex mixtures of carotenoids and were better suited for the analysis of carotenoids from fruits and vegetables. As with gradient HPLC, SFC possesses the potential for efficiently separating complex carotenoid mixtures, and as method development continues improved separations are expected.

Figs. 5 and 6 show the separation of isomeric mixtures of alpha- and

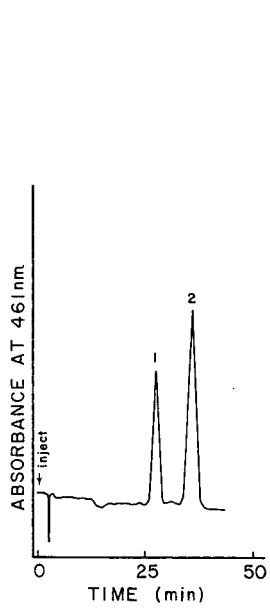

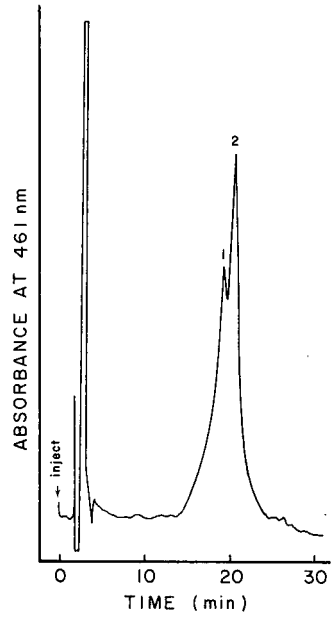

Fig. 1. SFC separation of alpha- (1) and beta-carotene (2) from carrot extract. Chromatographic conditions as described in text.

Fig. 2. HPLC separation of alpha- (1) and beta-carotene (2) from carrot extract. The mobile phase consisted of methanol–acetonitrile–chloroform (47:47:6).

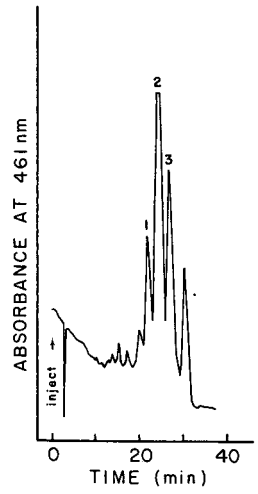

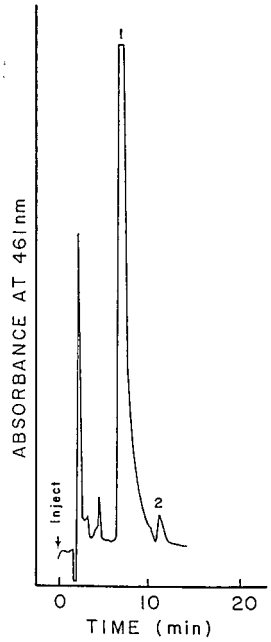

Fig. 3. SFC separation of lycopene (2), alpha- (1) and beta-carotene (3) from tomato extract.

Fig. 4. HPLC separation of lycopene (1) and beta-carotene (2) from tomato extract. The mobile phase consisted of acetonitrile–dichloroethane (80:20).

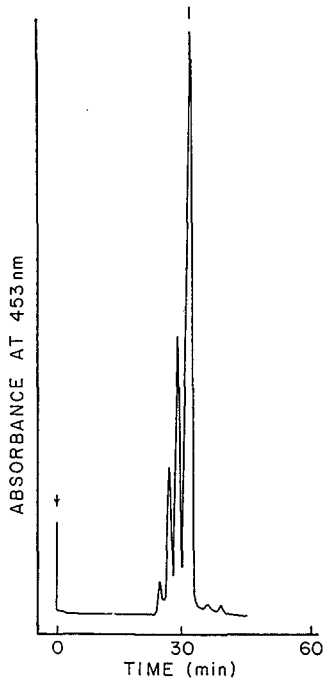

Fig. 5. SFC separation of all-*trans* alpha-carotene (1) and various *cis* isomers.

beta-carotene with SFC on cyanopropyl polymethylsiloxane column(s). The separations achieved are comparable to those obtained on HPLC for both alpha-carotene[18,19] and beta- carotene[14,18,19] isomers. Figs. 5 and 6 are the first examples of the separation of *cis-trans* carotenoid isomers with capillary SFC.

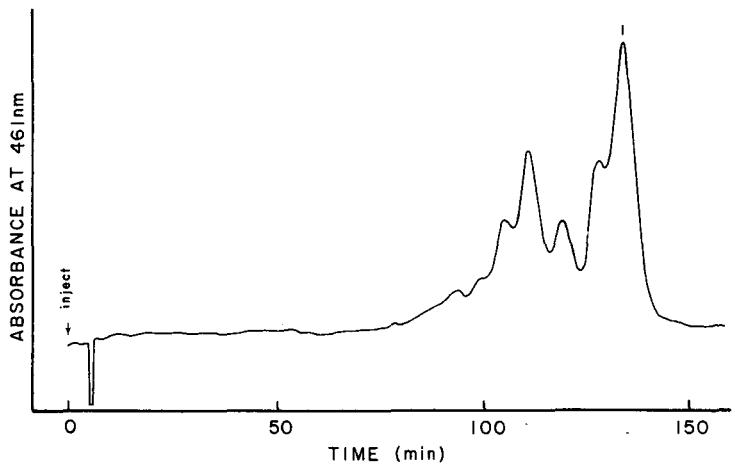

Fig. 6. SFC separation of all-*trans* beta-carotene (1) and various *cis* isomers.

Separation of *cis-trans* isomers of linoleic acid (*cis*-9,12 and *trans*-9,12) has been done with capillary SFC (12 m × 50 μm I.D., 50% cyanopropyl column)[11]. In addition, positional as well as stereoisomers, have been separated with capillary SFC[8–10]. Chang *et al.*[8] separated several series of both positional and stereoisomers with capillary SFC on a new liquid crystalline polysiloxane stationary phase. However, separation of *cis-trans* geometric isomers was not reported.

Frew *et al.*[4] suggested that the cyanopropyl stationary phase may be the most promising for carotenoid separations with SFC. The cyanopropyl column appeared to be the best of the SFC stationary phases available from Lee Scientific for the separation of carotenoids. However, due to the severe tailing of lycopene on the cyanopropyl columns, other stationary phases were examined. Consequently, a SB-phenyl-50 column was employed for the separation of samples containing lycopene, which provided separation without tailing of the lycopene in the mixtures examined.

Both pure supercritical CO_2 and supercritical CO_2 with 1% (v/v) ethanol were evaluated for their effect on the separations. Since no appreciable difference in separation efficiency was observed in the absence of the ethanol modifier with the capillary SFC columns examined, the results were not reported. During the last few years, many investigators have examined the effects of modifiers on SFC separations[24–26]. The addition of polar organic solvents as modifiers can cause significant changes in retention characteristics and peak shapes of analytes on packed column systems. Schmidt *et al.*[27] found that CO_2 with isopropanol (8%, v/v) enhanced the separation and peak shape of a series of relatively polar solutes on packed column SFC. While the addition of ethanol to the CO_2 for the separation of carotenoids in a capillary column devoid of exposed silanol or siloxane sites was not needed, a modifier may be required with packed columns or to enhance extraction from biological samples.

At the present time, the level of detection for compounds of interest in a biological matrix when using capillary SFC can often be restricted by the small amount of sample that can be injected on to the column (200–1000 nl). This problem can be largely overcome with the incorporation of an on-line extraction system, although the use of an extraction system just for injection complicates the process of injection. On-line supercritical-fluid extraction and chromatography is an interesting technique which has substantially expanded current chromatographic separation and quantitation capabilities. These techniques are currently under investigation.

CONCLUSIONS

This research illustrated some of the capabilities of SFC for carotenoid analysis. Capillary SFC has demonstrated significant potential for improvement of the separation of carotenoids and their *cis-trans* isomers relative to HPLC. A review of the literature indicates that capillary SFC is able to effect carotenoid separations that are comparable to the best current HPLC separations in other laboratories. SFC will never completely replace GLC or HPLC, but it will be an invaluable addition to the set of chromatographic tools used for separating and quantitating mixtures of compounds, particularly those compounds that are thermally sensitive, difficult to separate or exhibit problems with current extraction techniques.

ACKNOWLEDGEMENT

This research was funded in part by NIH grant CA46406-02, by NIH Biomedical Research Support grants RR07030 and RR05460, by project 50-0345 of the Agricultural Experiment Station, University of Illinois and by the IBM Corp. through the University of Illinois Research Board, Urbana, IL.

REFERENCES

1 D. W. Later, B. E. Richter and M. R. Andersen, *LC · GC*, 4 (1986) 992.
2 C. M. White and R. K. Houck, *J. High Resolut. Chromatogr. Chromatogr. Commun.*, 9(1986) 3.
3 J. C. Fjeldsted and M. L. Lee, *Anal. Chem.*, 56 (1984) 619A.
4 N. M. Frew, C. G. Johnson and R. H. Bromund, *ACS Symp. Ser.*, 366 (1987) 208.
5 J. A. Olson, in L. J. Machlin (Editor), *Handbook of Vitamins*, Marcel Dekker, New York, 1984, Ch. 1, p. 4.
6 D. W. Later, B. E. Richter, D. E. Knowles and M. R. Andersen, *J. Chromatogr. Sci.*, 24 (1986) 249.
7 D. W. Later, B. E. Richter, W. D. Felix, M. R. Andersen and D. E. Knowles, *Am. Lab. (Fairfield, Conn.)*, 18 (Aug. 1986) 108.
8 H.-C. K. Chang, K. E. Markides, J. S. Bradshaw and M. L. Lee, *J. Chromatogr. Sci.*, 26 (1988) 280.
9 H.-C. K. Chang and M. L. Lee, *J. Chromatogr. Sci.*, 26 (1988) 298.
10 L. T. Taylor, *J. Chromatogr. Sci.*, 26 (1988) 45.
11 Lee Scientific, Inc., *J. Chromatogr. Sci.*, 25 (1987) 179.
12 J. C. Giddings, L. McLaren and M. N. Meyers, *Science (Washington, D.C.)*, 159 (1968) 197.
13 D. R. Gere, *Hewlett-Packard Application Note*, 800-5, Hewlett-Packard, Avondale, PA, 1983.
14 R. J. Bushway, *J. Liq. Chromatogr.*, 8 (1985) 1527.
15 M. Ruddat and O. H. Will (III), *Methods Enzymol.*, 111 (1985) 189.
16 J. F. Fisher and R. L. Rouseff, *J. Agric. Food Chem.*, 34 (1986) 985.
17 R. B. H. Wills, H. Nurdin and M. Wootton, *J. Micronutr. Anal.*, 4 (1988) 87.
18 L. A. Chandler and S. J. Schwartz, *J. Food Sci.*, 52 (1987) 669.
19 F. W. Quackenbush, *J. Liq. Chromatogr.*, 10 (1987) 643.
20 F. Favati, J. W. King, J. P. Friedrich and K. Eskins, *J. Food Sci.*, 53 (1988) 1532.
21 L. Zechmeister, in *Cis-trans Isomeric Carotenoids, Vitamins A and Arylpolyenes*, Academic Press, New York, 1962, p. 51.
22 H. C. Furr, D. A. Copper and J. A. Olson, *J. Chromatogr.*, 378 (1986) 45.
23 C. R. Broich, L. E. Gerber and J. W. Erdman, Jr., *Lipids*, 18 (1983) 253.
24 J. R. Strubinger and M. I. Selim, *J. Chromatogr. Sci.*, 26 (1988) 579.
25 A. L. Billie and T. Griebrokk, *Anal. Chem.*, 57 (1985) 2239.
26 J. M. Levy and W. M. Ritchey, *J. Chromatogr. Sci.*, 24 (1986) 242.
27 S. Schmidt, L. G. Blomberg and E. R. Campbell, *Chromatographia*, 25 (1988) 775.

Journal of Chromatography, 479 (1989) 269–295
Elsevier Science Publishers B.V., Amsterdam — Printed in The Netherlands

CHROM. 21 690

STUDY OF THE CHANGES IN MONO-, DI- AND TRIFUNCTIONAL OCTADECYL-MODIFIED PACKINGS FOR REVERSED-PHASE HIGH-PERFORMANCE LIQUID CHROMATOGRAPHY WITH DIFFERENT ELUENT COMPOSITIONS

M. HETEM*, L. VAN DE VEN, J. DE HAAN and C. CRAMERS
Eindhoven University of Technology, Department of Chemical Technology, Laboratory Instrumental Analysis, P.O. Box 513, 5600 MB Eindhoven (The Netherlands)
and
K. ALBERT and E. BAYER
Institut für Organische Chemie, Universität Tübingen, Auf der Morgenstelle 18, D-7400 Tübingen (F.R.G.)
(First received February 7th, 1989; revised manuscript received June 12th, 1989)

SUMMARY

Two different types of silica substrates uniformly modified with reversed-phase high-performance liquid chromatographic (RP-HPLC) phases obtained with mono-, di- and trifunctional octadecylsilanes were subjected to artificial ageing under simulated routine conditions and were subsequently analysed and evaluated. Changes in the properties of the bonded phase packings were characterized and quantified with chromatographic techniques, solid-state NMR and elemental analysis. These changes were correlated with selectivity, loss of silanes, gain in silanol content and rearrangement of the silica to silane bonding. When eluents of extremely high pH were used, the multifunctional octadecylsilane stationary phases showed a higher resistance towards ligand stripping. The substrate shielding of difunctional octadecylsilanes showed superior characteristics due to direct surface attachments. The rigidity of the silica substrate used for modification influences the stability of the RP-HPLC phases, especially for the monofunctionally modified octadecylsilane stationary phase. With the use of multifunctional C_{18} silanes for modification, the influence of the characteristics of the substrate on the stability of the RP-HPLC phases was reduced compared with monofunctional C_{18}. In contrast to monofunctionally modified phases, the polar selectivity of the multifunctionally modified phases remained more or less constant after intensive use with aggressive eluents. A chromatographic characterization method for obtaining information about the stability, capacity, selectivity and silica degradation of different RP-HPLC stationary phases is also presented.

INTRODUCTION

The stability of chemically bonded phases on porous silica substrates employed in high-performance liquid chromatography (HPLC) has been the issue of several

0021-9673/89/$03.50

recent studies[1–5]. The significance of these studies becomes clear on considering the still increasing popularity of liquid–solid partition reversed-phase chromatography (RP-HPLC). The wide variations in the properties of bonded phases commercially available today for RP-HPLC applications exist as a result of considerable differences in: the structure of the silica gel generally employed as the substrate for modification and the nature of the moieties at the surface such as silanediol groups and bonded and isolated silanols[3–9], the chemical properties of the ligand moieties used for modification of the porous silica[8–15], the number and nature of reactive groups involved in ligand surface attachment, *e.g.*, chloro and ethoxy groups[10,16], and the reaction conditions for modifications[17]. These are also decisive factors with regard to the relative surface coverage of the bonded phase[13,17,18] and the type of anchoring of the ligands to the substrate[1,10,16].

It is obvious that dissimilarities in the synthesis of chemically bonded phases not only determine the selectivity, but also influence their stability towards hydrolysis. Aggressive eluents used as mobile phases in modern RP-HPLC practice cause hydrolysis of the bonded ligands at the silica surface followed by hydrolysis of the silica substrate[1–5]. Although this process normally proceeds slowly, after use for some time the properties of the stationary phase alter, indicated by changes in the capacity and eventually also in the selectivity of the reversed phase.

In this study, the interference of various eluents used in LC practice, with octadecylsilane RP-HPLC stationary phases modified on two different silica substrates and with various ligand anchorings, comprising six phases altogether, were examined by chromatography, elemental analysis and high-resolution solid-state ^{29}Si NMR.

The two silica substrates with different physical properties and chemical nature of the silica surface were uniformly modified with mono-, di- and trifunctional octadecylsilanes (C_{18}) to obtain mono-, di- and even tridentate linkages of the C_{18} ligands with the silica surface and neighbours (cross-linking). The reaction conditions employed for modification were such that for all six bonded C_{18} phases an equal relative coverage of the octadecylsilanes at the surface was obtained. Much to our surprise, identical reaction conditions could be employed. The influence of the properties of the substrate, the anchoring of the ligands on the stability of the ligand bonding to the surface and a further hydrolysis of the silica was investigated by subjecting the six modified phases to artificial ageing under simulated routine conditions.

CHARACTERIZATION

In order to describe the qualitative and quantitative changes in the RP-HPLC stationary phases, one should include both bulk and surface properties related to solid–liquid interactions determining chromatographic behaviour, as follows.

(a) Determination of bulk properties such as specific surface area, particle size, pore size distribution and total volume of the pores of the substrate[19–21]. Possible contamination with traces of metals should be regarded as important for the stability of the stationary phase. With the determination of the carbon content of the bulk phase and the specific surface area of the substrate, the average ligand surface density (α_1) can be calculated with an equation derived by Berendsen[14]:

$$\alpha_1 \text{ (mol m}^{-2}) = \frac{P_c}{S_{BET}[M_c - P_c(M_1 - 1)]} \quad (1)$$

where P_c = the amount of carbon (g/g), S_{BET} = specific BET surface area of the substrate ($m^2\ g^{-1}$), M_c = the amount of carbon per mole of bonded silane ($g\ mol^{-1}$) and M_1 = molecular weight of the silane molecule ($g\ mol^{-1}$).

(b) Characterization of surface structure elements should include the nature of various groups present on the modified surface. This surface contains a variety of siliceous groups, such as different types of silanol, siloxane bridges and octadecyl ligands. High-resolution solid-state ^{29}Si NMR proved to be a suitable technique for determining changes in the ratios of these siliceous groups[1,3,7,10,18]. Solid-state ^{29}Si NMR not only distinguishes the different types of surface modifications (mono-, di- and trifunctional) under study, but also provides details concerning surface and neighbour attachments[22,23], via siloxane bonds, of the octadecylsilanes. This provides the possibility of studying the chemical reactions underlying the changes at different eluent compositions.

Until recently, only chromatographic experiments provided overall information on the changes in solid–liquid interactions between the stationary and the mobile phase after intensive use in laboratory practice. A more detailed chromatographic characterization of the stationary phases should be aimed at in order to relate the results of other stationary phase characterization methods. In this study, the chromatographic experiments were focused on changes in the amount of bonded ligands and selectivity. Alternatively, attention can be focused on the determination of the influence of the silica substrate by applying polar test solutes such as phenols, anilines or nitrobenzene, which are indicators of substrate interaction[1,15,23]. However, a reliable determination of substrate interactions with polar components will be hindered by both a varying silanol activity and the "memory effect" of previous injections, showing irreversible adsorption of the polar components. More fundamental chromatographic characterizations of RP-HPLC stationary phases were proposed by Smith[24] and Jandera[25–27] based on mainly solvophobic interactions of the eluting compounds with organic solvent-rich mobile phases.

The retention model proposed shows a linear relationship between the logarithm of the capacity factors, k', of a homologous series and the eluent composition:

$$\log k' = a - mx \quad (2)$$

and

$$a = a_o + a_l n_c \quad (3a)$$

$$m = m_o + m_l n_c \quad (3b)$$

where x is the volume fraction of the organic part of the eluent (for binary eluents only), n_c is the incremental carbon number of a homologous series and a_o, a_l, m_o and m_l are constants to be determined by regression. The validity of the regression has been extensively discussed[1,26,27] and linearity with respect to eluent composition was shown at least in the range 60–90% (v/v) of methanol for all octadecyl-modified

stationary phases in this study. After elimination of the incremental carbon number of the eluting components from eqns. 3a and 3b, Jandera[25,26] derived

$$m = q + pa \tag{4}$$

where

$$p = m_1/a_1 \tag{5a}$$

$$q = m_o - pa_o \tag{5b}$$

As already shown by Jandera, the value of p is independent of the stationary phase. An approximate theoretical calculation of the value of p depends only on the type of eluent, especially the organic modifier[26]:

$$p \approx 2\left(1 - \frac{I_{org}}{I_{H_2O}}\right) \tag{6}$$

where I_{org} = interaction index of the organic component of the mobile phase and I_{H_2O} = interaction index of water. For binary methanol–water eluents, I_{org}/I_{H_2O} = 0.57. With eqn. 6, the theoretical value of p is 0.86 and should be independent of the fraction of organic modifier used.

The constants m_o and q in eqn. 5b describe the selectivity[26]: m_o mainly non-specific, lipophilic selectivity and q specific, polar selectivity. The value of m_o depends in practice on the character of the organic solvent in the mobile phase and the amount of bonded ligands of the stationary phase, whereas the value of q should depend more on the nature of the homologous series residue or on the stationary phase involved for characterization. The a_o value equals log k' of the molecular residue (see eqns. 2 and 3a). The a_o value of an essentially non-polar residue such as benzene should give a good indication of the phase ratio of the stationary phase used. A decrease in this a_o value expresses the loss of attached ligands. The a_o value of alkyl aryl ketones includes more specific interactions between the alkyl aryl ketone residue and the stationary phase. The nature of these interactions is more complex and includes also polar interactions with the substrate.

EXPERIMENTAL

Materials

The test components used for chromatographic characterization were all of reference grade. Alkylbenzenes (test mixtue 1) used were benzene, methylbenzene, ethylbenzene, propylbenzene and butylbenzene. Alkyl aryl ketones (test mixture 2) used as test compounds were ethanophenone, propanophenone, butanophenone, pentanophenone, hexanophenone and octanophenone (Pierce, Rockford, IL, U.S.A.). All other solvents and chemicals used for simulating routine treatments and chromatographic characterization were of analytical-reagent grade (E. Merck, Darmstadt, F.R.G.) and demineralized, deionized water (Millipore Milli-Q system, Millipore, Bedford, MA, U.S.A.) was used. All eluents were freshly prepared and filtered over 0.22-μm membrane filters (Millipore) prior to use.

Chromatography

The six octadecylsilane-modified bonded phases were prepared at the Institut für Organische Chemie of the University of Tübingen, F.R.G. The modification with methylchlorooctadecylsilane, dimethylchlorooctadecylsilane and trichlorooctadecylsilane on two different silica substrates, Hypersil (batch 5-192, Shandon Southern Products, Runcorn, U.K.) and Nucleosil 100-7 (batch 5061, Macherey, Nagel & Co., Düren, F.R.G.) was catalysed with 2,6-lutidine[18]. The bulk properties of the two silica substrates are listed in Table I.

TABLE I

BULK PROPERTIES OF THE SILICA SUBSTRATES

Property	*Hypersil*	*Nucleosil 100-7*
Batch No.	5-192	5061
Mean particle size (μm)	5 ± 1.5	7 ± 1.5
Mean pore size (nm)	12	10
Specific surface area (m^2/g)	170	350
Pore volume (ml/g)	0.7	1.0
Iron content (μg/g)	377 ± 20	76 ± 10
Total silanol content[a] (ratio × 100%)	15.6	32.8
Relative silanol ratios (× 100%)[a]		
Dihydroxysiloxane	13.5	11.6
Hydroxysiloxane	86.5	88.4
Silanol density at the surface (contents × g m^{-2})[b]	0.092	0.093

[a] Determined by deconvolution of the solid-state ^{29}Si MAS NMR spectra of the substrates.
[b] Calibrated by dividing the total silanol content by the specific surface area.

A 25-g amount of silica substrate was activated at 160°C under reduced pressure for 24 h. A sample of 0.120 mol of dimethylchloro-, methyldichloro- or trichlorooctadecyl silane was melted and dissolved in 100 ml of dry methylene chloride together with 0.15 mol of 2,6-lutidine. The mixture was added to the activated silica still under vacuum and with vigorous stirring to avoid clotting. The reaction mixture was refluxed for 5 h. The silica was then filtered and thoroughly washed with dry methylene chloride, ethanol, ethanol–water (50:50) and finally diethyl ether. The modified silicas were then dried at 50°C for 72 h. Each stationary phase was packed in columns (100 mm × 4 mm I.D.) (Knauer, Bad Homburg, F.R.G.) according to a standard packing procedure. From each series of seven columns of a typical phase, six columns were placed in an apparatus for simulating routine use after a chromatographic test to ensure reproducibility of the packing procedure, and the remaining column was used as a reference column for initial chromatographic tests. The equipment for simulating intensive routine use was described previously[1]. The artificial, strictly controlled ageing experiments consisted of continuous, separate exposure of columns packed with the C_{18} phases under well defined conditions to several eluent compositions for a period of 240 h. Basic and acidic aqueous and methanol–aqueous buffers were used (see Table II). The buffer solutions were prepared with equal amounts of buffer salt (calibrated for a total volume of 1 l of aqueous or methanol–aqueous solution), titrated in aqueous solution to the pH values 3.0 for acidic and 8.4 for basic solutions. Subsequently an equal volume of methanol was added for aqueous–methanol buffers.

TABLE II

TREATMENTS FOR SIMULATING ROUTINE-USE EXPERIMENTS

Each column purged with 7000 column volumes of a typical purging eluent; flow-rate 0.5 ml/min; time 240 h; ambient temperature.

Treatment No.	*Buffer*	*pH*	*Volume fraction of methanol in the eluent*	*Ion pairing agent and concentration (M)*
I	0.05 *M* phosphate	3.0	0	–
II	0.05 *M* phosphate	3.0	0.5	–
III	0.05 *M* phosphate	3.0	0.5	Hexylsulphonate (0.005)
IV	0.05 *M* hydrogencarbonate	8.4	0	–
V	0.05 *M* hydrogencarbonate	8.4	0.5	–
VI	0.05 *M* hydrogeancarbonate	8.4	0.5	Triethylamine (0.005)

In order to include a study of the effect of additional ionic species on bonded phases, at high pH a basic and at low pH an acidic ion-pairing agent were added to the methanol–water buffers. For economic and also practical reasons, these eluents were recirculated continuously in a closed system at a flow-rate of 0.5 ml/min. Hence during the purging process each column was purged with about 7000 column volumes of a specific eluent. As already discussed by Claessens *et al.*[1], possible saturation of the eluent with dissolved silica and/or ligands could reduce the ageing effect of the treatment. The influence of multiple sample introduction on the column is also neglected. Therefore, it seems reasonable to consider the results of the present experiments as the minimum changes during normal laboratory use for the different combinations of reversed phase and eluents.

After finishing a typical series of purging experiments, the columns were carefully rinsed with water, aqueous–methanol mixtures and methanol to prevent deposition of the buffering salts. Subsequently, the columns were subjected to chromatographic characterization with the two series of homologues, alkylbenzenes and alkyl aryl ketones, at a suitable eluent composition. These chromatographic experiments were performed with a Model 100 A pump (Beckman, Berkely, CA, U.S.A.), a Model CV-6-VHPa-N60 injection valve equipped with a 20-μl loop (Valco, Houston, TX, U.S.A.) and a Model LC-3 variable-wavelength UV detector (Pye Unicam, Cambridge, U.K.) operated at 254 nm. Injections of 5–10 μl of the test mixtures were performed. The detector signal was sampled at 10 Hz and integrated with a Nelson 3000 data system (Nelson Analytical, Cupertino, CA, U.S.A.).

Elemental analysis

The carbon content of the modified C_{18} stationary phases prior to and after simulating routine treatment was obtained with a Perkin-Elmer Model 240 Analyzer (Perkin Elmer, Norwalk, CT, U.S.A.). Tungsten oxide was added to the modified silica as a catalyst. The carbon content, P_c, and the ligand surface density, α_1, of the starting materials are given in Table III.

TABLE III

OCTADECYLSILANE-MODIFIED RP-HPLC STATIONARY PHASES UNDER STUDY, NOTATION, CARBON CONTENTS AND LIGAND SURFACE DENSITIES

Substrate	*Modification*	*Abbreviation*	*Carbon content, P_c (%, w/w)*	*Ligand surface density, α_1 (eqn. 1) (μmol m^{-2})*
Nucleosil 100-7, batch 5061	Dimethylchlorooctadecylsilane	NMO	15.9	2.38
	Methyldichlorooctadecylsilane	NDI	15.6	2.52
	Trichlorooctadecylsilane	NTR	15.6	2.62
Hypersil, batch 5-192	Dimethylchlorooctadecylsilane	HMO	8.5	2.34
	Methyldichlorooctadecylsilane	HDI	8.7	2.55
	Trichlorooctadecylsilane	HTR	8.6	2.63

Solid-state ^{29}Si NMR measurements

The solid-state ^{29}Si NMR spectra were obtained on a Bruker CXP 300 Fourier transform NMR spectrometer at 59.63 MHz. Representative samples of 150–200 mg were spun at *ca.* 3.5 kHz using aluminium oxide rotors of the standard Bruker double-bearing type. ^{29}Si Bloch decay magic angle spinning (MAS) NMR spectra of the original silica substrates were obtained with a pulse interval time of 90 s. ^{29}Si Bloch pulse MAS NMR is a time consuming technique but, when the pulse interval times exceed the relaxation times by a factor of *ca.* 5, the signal areas measured represent the absolute amounts of silicon atoms of different nature present in the sample. Typically 1000 FIDs (free induction decays) with an acquisition time of 10 ms were accumulated in 1K data points, zero-filled to 8K prior to Fourier transformation. A line broadening of 10 Hz prior to zero-filling was used. ^{29}Si cross-polarization magic angle spinning (CP-MAS) NMR spectra of all modified C_{18} stationary phases prior to and after simulated routine treatment were obtained with a cross-polarization contact time of 6 ms for the monofunctionally modified stationary phases and 2 ms for the other modified phases. These respective values were the optimum contact times for mono- and multidentate surface-linked groups. The pulse interval was 1 s. ^{29}Si CP-MAS NMR is confined to those silicon atoms not too far from protons near the surface and facilitates fast acquisition. Typically 2000 FIDs with an acquisition time of 10 ms were accumulated in 1K data points, zero-filled to 8K prior to Fourier transformation. The line broadening used was 20 Hz prior to zero-filling and Fourier transformation. The spectral width for all spectra was 20 kHz.

RESULTS AND DISCUSSION

The influence of long-term exposure to some aggressive eluents used in modern HPLC practice on the performance of a separation is illustrated best by chromatography itself. Fig. 1 depicts the chromatograms of alkylbenzenes (test mixture 1) eluted on methyldichlorooctadecylsilane-modified Nucleosil phases (NDI), before and after treatment III and IV. The characterization of the changes at the surface of the modified substrates after intensive use, the chemistry of the ageing proces, the impact on chromatography and stationary phase modification are discussed below.

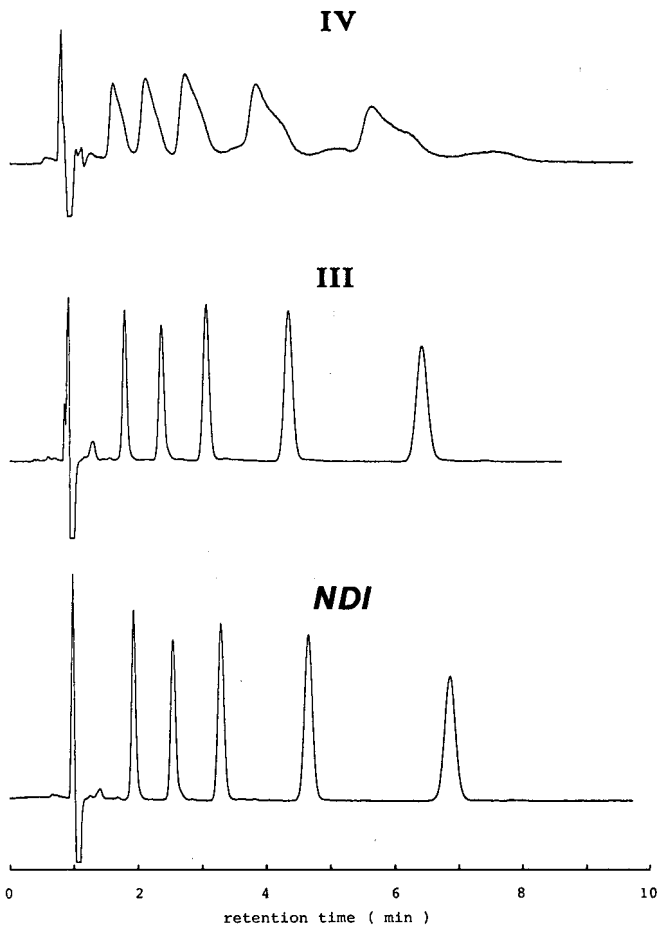

Fig. 1. Chromatograms of the untreated difunctional octadecylsilane-modified Nucleosil silica (NDI) and the identical stationary phase after treatments III and IV according to Table II. Chromatographic test conditions: test mixture 1, alkylbenzenes; water–methanol (30:70, v/v); UV detection at 254 nm.

Condensation of multifunctional silanes

The different types of surface silane modifications most relevant to this paper are collected in Table IV with their ^{29}Si NMR chemical shifts. The corresponding structural elements at the surface of the silica gel are depicted in Fig. 2.

The ^{29}Si MAS NMR spectra of both silica substrates are represented in Fig. 3. The relative amount of silanol groups, mainly hydroxysiloxane (Q_3) groups, determined from these spectra is given in Table I. Owing to the large surface area of the Nucleosil substrate and assuming that all silanol groups are located at the surface, an almost identical silanol density for both substrates was calibrated. In this study the total amount of geminal silanol, dihydroxysiloxane (Q_2) or silanediol groups of both substrates before modification did not exceed 15%. Köhler *et al.*[3] reported a geminal silanol content of 32% relative to the total amount of silanol for various substrates,

TABLE IV

MOST RELEVANT SURFACE SILANES/SILOXANES, THEIR FUNCTIONALITY, NOTATION AND TYPICAL ^{29}Si CHEMICAL SHIFTS

Modification	*Chemical (spectral) function-ality*	*Topological (network) function-ality*	*Code*	*Typical chemical shift (ppm downfield from TMS)*
Dimethyloctadecylsiloxysilane	M	1	M_1	+12
Methyloctadecylhydroxysiloxysilane	D	1	D_1	−3
Methyloctadecyldisiloxysilane	D	2	D_2	−11
Paired methyloctadecyldisiloxysilane	D	2	D'_2	−16
Octadecyldihydroxysiloxysilane	T	1	T_1	−48
Octadecylhydroxydisiloxysilane[a]	T	2	T_2	−55
Octadecyltrisiloxysilane[a]	T	3	T_3	−66
Dihydroxysiloxane	Q	2	Q_2	−91
Hydroxysiloxane	Q	3	Q_3	−101
Tetrasiloxysiloxane	Q	4	Q_4	−110

[a] Paired T_2 and T_3 groups and double-paired T_3 groups were not distinguishable.

determined by ^{29}Si CP-MAS NMR. For untreated substrates we measured a lower content of geminal silanols relative to the total silanol content, about 12% for both silica substrates. For relative comparison, representative ^{29}Si CP-MAS NMR spectra of the monofunctional octadecylsilane-modified Nucleosil substrate, the difunctional

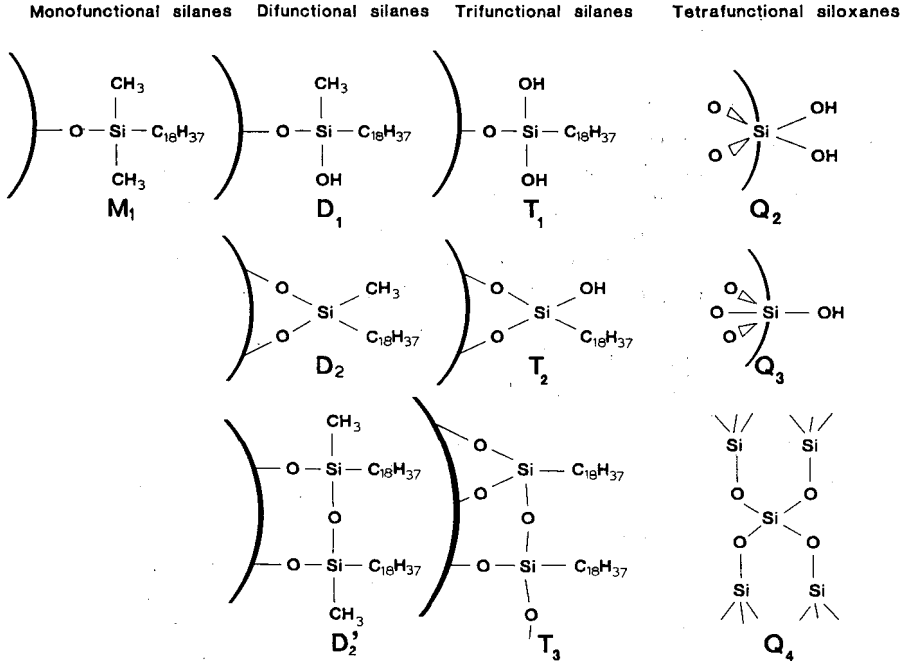

Fig. 2. Structure of the siliceous surface moieties most relevant to this paper with their notations.

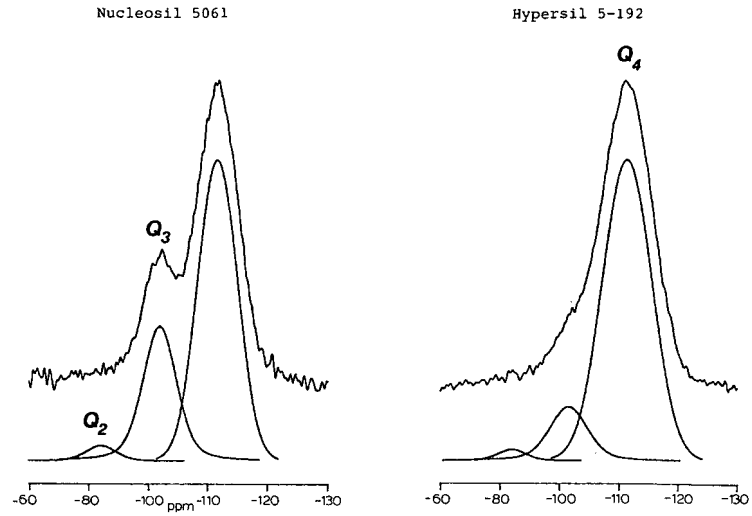

Fig. 3. ^{29}Si Bloch pulse MAS NMR spectra of the original Hypersil and Nucleosil silica substrates with the deconvoluted signals. N_s = 1000; pulse interval time, 90 s; acquisition time, 10 ms; line broadening, 10 Hz.

octadecylsilane-modified Nucleosil substrate, the trifunctional octadecylsilane-modified Nucleosil and the trifunctional octadecylsilane-modified Hypersil substrate before and after treatments I, III and IV are shown in Figs. 4, 5, 6 and 7, respectively. The spectra of mono- and difunctional octadecylsilane-modified Hypersil were identical with those of the respective mono- and difunctional octadecylsilane-modified Nucleosil stationary phases. Only the spectra of the trifunctional modified Nucleosil and Hypersil stationary phases differed. For a direct comparison between the depicted spectra, one should consider the different contact times applied for mono- and multifunctionally modified phases, 6 and 2 ms, respectively[22]. A difference in contact time will alter the ratio between the Q_3 and Q_4 signals, which generally show different optimum contact times. To prevent the spectral difference, all untreated stationary phases were also measured with a 2 ms contact time. The Q_3/Q_4 ratio of all modified Nucleosil phases was found to be 1.22 $\pm$ 0.02 and for all modified Hypersil phases this value was 0.90 $\pm$ 0.04. The small spectral deviation indicated an equal residual silanol content after modification for all Nucleosil phases and also for all Hypersil phases.

The NMR spectra of the bonded phases indicate that the di- and trifunctional modified RP-HPLC phases under study tended to form more multidentate surface and neighbour linkages of the octadecylsilane ligand, when used intensively with aqueous buffer solutions of high and low pH as eluents. Methyloctadecylhydroxysiloxysilane (D_1) and methyloctadecyldisiloxysilane (D_2) moieties reacted to form methyloctadecyldisiloxysilane, especially paired (D'_2) moieties (see also Fig. 5). A similar condensation reaction occurred with the trifunctional octadecylsilane-modified stationary phases. Octadecyldihydroxysiloxysilane (T_1) and octadecylhydroxydisiloxysilane (T_2) moieties formed on modification were dehydrated to form octadecylhydroxydisiloxysilane (T_2) and octadecyltrisiloxysilane (T_3) moieties, respectively (see

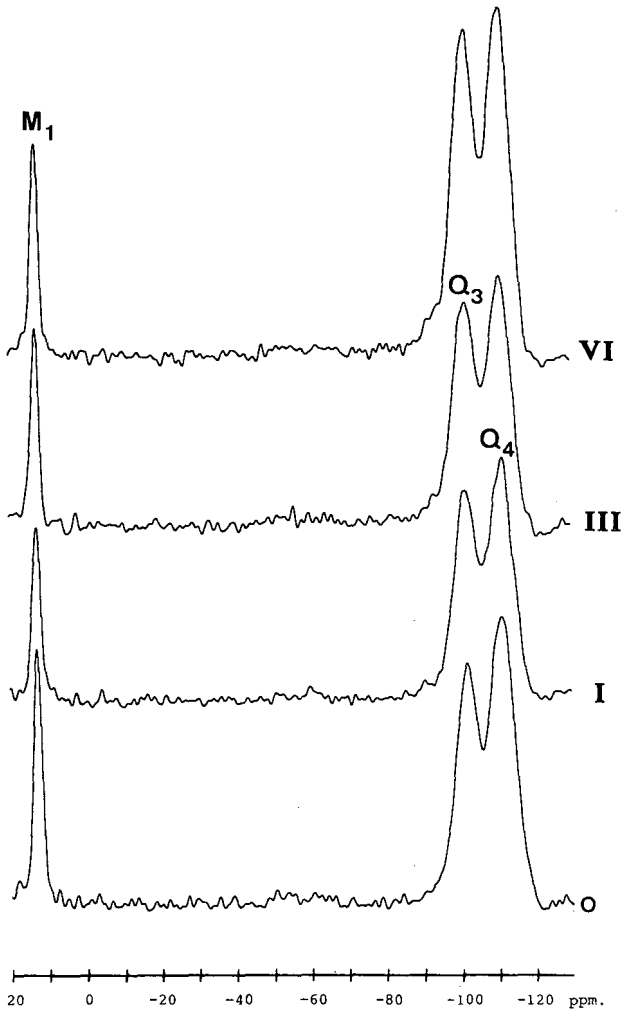

Fig. 4. ^{29}Si CP-MAS NMR spectra of monofunctional octadecylsilane-modified Nucleosil silica, before (0) and after treatments I, III and VI. $N_s = 2000$; contact time, 6 ms; interval time, 1 s; acquisition time, 10 ms; line broadening, 20 Hz.

Figs. 6 and 7). The amount of surface silanol groups did not alter accordingly. On the contrary, a slight increase in surface silanol groups was noticed. From this we can conclude that condensation of hydroxysilane moieties at the surface (D_1, T_1 and T_2) mainly occurred between anchored neighbours showing preferential polymerization across the surface. This is in agreement with the results of methyltrichlorosilane modifications of silica gels with different water contents published by Sindorf and Maciel[7]. Our results indicate that multidentate linkage with other silanes at the surface prevented hydrolysis of the anchored ligands, in contrast to the monofunctionally modified octadecyl phases. In the latter instance, a substantial increase in silanol content is found during ageing. Condensation of multifunctional silanes was more

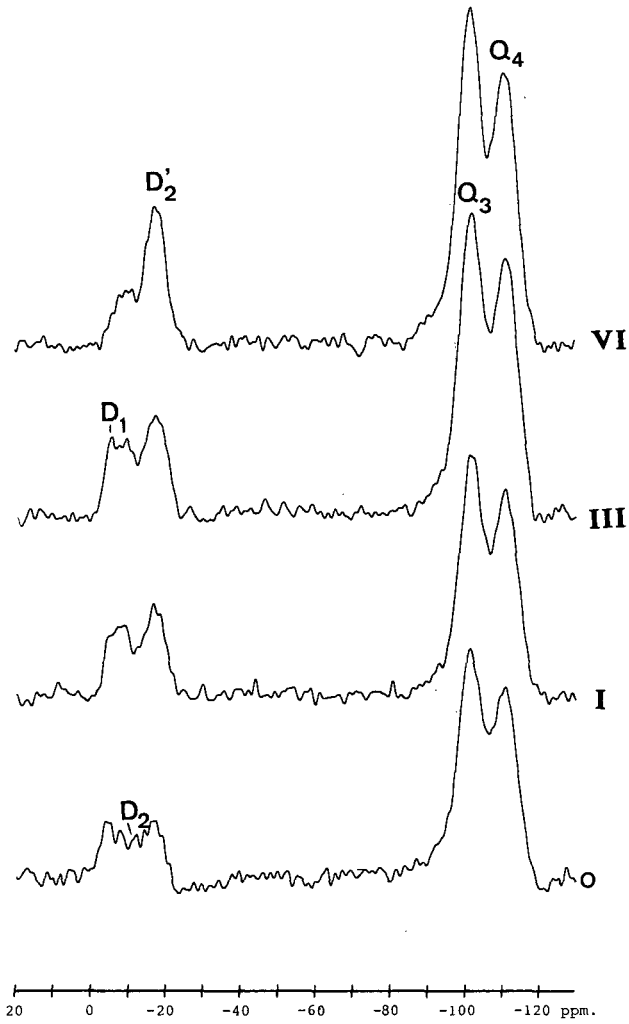

Fig. 5. ^{29}Si CP-MAS NMR spectra of difunctional octadecylsilane-modified Nucleosil silica before (0) and after treatments I, III and VI. Conditions as in Fig. 4, except contact time, 2 ms.

pronounced when buffers of high pH were used as eluents for simulation of intensive use.

The effect of ion pair agents added to aqueous–methanol buffers of low and high pH on the stationary phases studied here is not completely clear at this stage. All multifunctionally modified stationary phases except trifunctionally modified Nucleosil showed an enhanced condensation of surface silanes on addition. For trifunctional octadecylsilane Nucleosil condensation was reduced by the methanol content of the aqueous–methanol buffer.

It should be noted that the trifunctionally modified Nucleosil used for the simulation experiments already showed progress of condensation of octadecyldi-

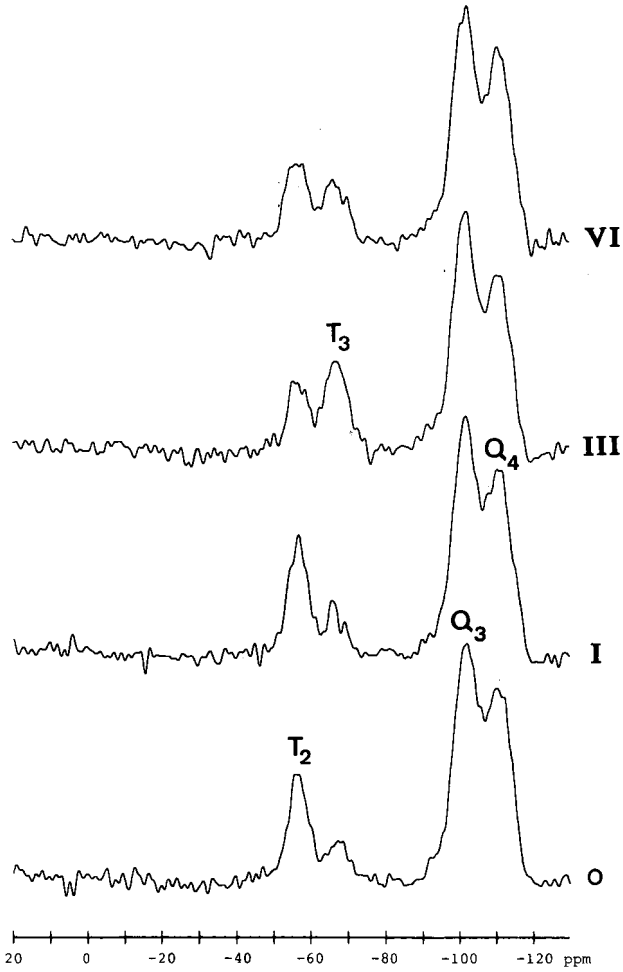

Fig. 6. ^{29}Si CP-MAS NMR spectra of trifunctional octadecylsilane-modified Nucleosil silica before (0) and after treatments I, III and VI. Conditions as in Fig. 5.

hydroxysiloxysilane (T_1) and octadecylhydroxydisiloxysilane (T_2) groups in the time elapsed between synthesis and the start of the chromatographic experiments. The concentration of T_1 groups was low and that of T_3 groups was much higher for the NTR phase than for the HTR phase used (see also Figs. 6 and 7). After a longer period no further changes at the surface of the trifunctionally modified Nucleosil were noticed.

The results of the spectroscopic and chromatographic measurements and the elemental analysis are summarized in Tables V–VII for modified Nucleosil silica and in Tables VIII–X for the modified Hypersil silica.

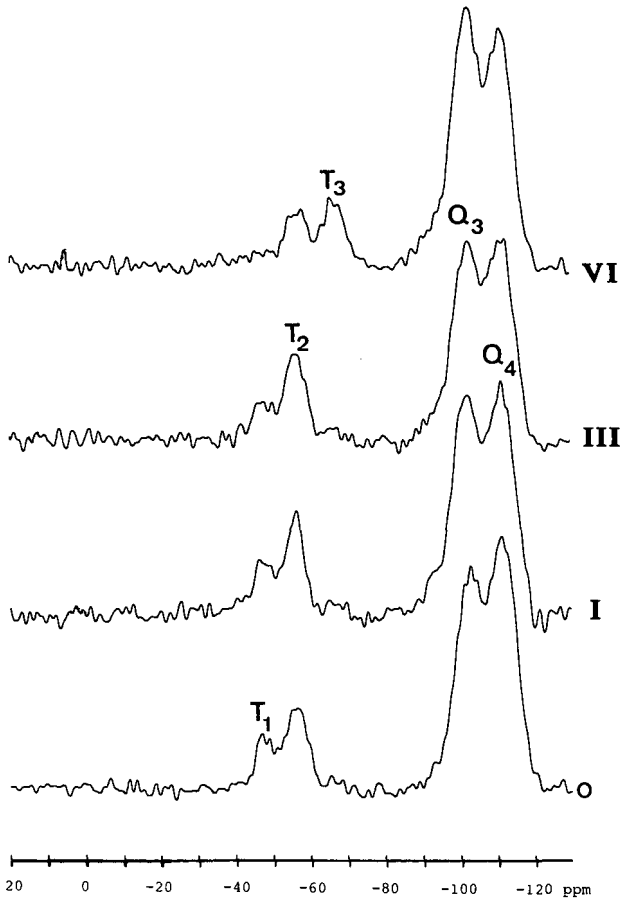

Fig. 7. ^{29}Si CP-MAS NMR spectra of trifunctional octadecylsilane-modified Hypersil silica before (0) and after treatments I, III and VI. Conditions as in Fig. 5.

TABLE V

RESULTS OF ELEMENTAL ANALYSIS, NMR EXPERIMENTS AND CHROMATOGRAPHIC MEASUREMENTS OF THE MONOFUNCTIONAL OCTADECYLSILANE-MODIFIED NUCLEOSIL SILICA BEFORE AND AFTER TREATMENTS I–VI

Mean value of p (eqn. 5a) = 0.80.

Stationary phase NMO treatment	*Ligand* α_1 *(eqn. 1)* (μmol m^{-2})	*NMR*		*Chromatography:* a_o	
		Ligand M_1	*Silanol* Q_3	*Alkyl-benzenes*	*Alkyl aryl ketones*
–	2.38	0.34	0.66	2.22	0.81
I	2.32	0.24	0.76	2.31	1.01
II	2.31	0.32	0.68	2.34	0.41
III	2.26	0.23	0.77	1.80	0.32
IV	2.06	0.23	0.77	1.73	0.25
V	2.13	0.32	0.68	1.76	0.32
VI	2.11	0.28	0.72	1.91	0.21

TABLE VI

RESULTS OF ELEMENTAL ANALYSIS, NMR EXPERIMENTS AND CHROMATOGRAPHIC MEASUREMENTS OF THE DIFUNCTIONAL OCTADECYLSILANE-MODIFIED NUCLEOSIL SILICA BEFORE AND AFTER TREATMENTS I–VI

Mean value of p (eqn. 5a) = 0.65.

Stationary phase NDI treatment	*Ligand* α_1 *(eqn. 1)* (μmol m^{-2})	*NMR*				*Chromatography:* a_0	
		Ligand			*Silanol* Q_3	*Alkyl-benzenes*	*Alkyl aryl ketones*
		D_1	D_2	D'_2			
–	2.52	0.16	0.08	0.18	0.58	1.96	0.31
I	2.45	0.19	0.03	0.16	0.62	1.76	0.15
II	2.47	0.17	0.02	0.17	0.64	1.87	0.08
III	2.50	0.15	–	0.21	0.64	1.45	−0.05
IV	2.32	0.12	–	0.22	0.66	1.36	−0.07
V	2.44	0.15	–	0.20	0.65	1.53	−0.06
VI	2.37	0.08	–	0.24	0.68	1.46	−0.12

Stationary phase hydrolysis

The influences of treatments I–VI on the capacity factors of the methyldichloro-octadecylsilane-modified Nucleosil (NDI) stationary phase for test mixture I are shown in Fig. 8 with the eluent methanol–water (80:20, v/v). The decreased capacity factors after all treatments indicate a significant loss of ligands from the surface of the reversed phase. After extrapolation to $n_c = 0$ and $x = 0$ (methanol fraction in the eluent used for characterization), the differences in capacity were expressed as the a_0 values for the alkylbenzene test mixture (see below). A typical diagram of log k', determined by regression analysis from chromatographic results, *versus* the volume

TABLE VII

RESULTS OF ELEMENTAL ANALYSIS, NMR EXPERIMENTS AND CHROMATOGRAPHIC MEASUREMENTS OF THE TRIFUNCTIONAL OCTADECYLSILANE-MODIFIED NUCLEOSIL SILICA BEFORE AND AFTER TREATMENTS I–VI

Mean value of p (eqn. 5a) = 0.85.

Stationary phase NTR treatment	*Ligand* α_1 *(eqn. 1)* (μmol m^{-2})	*NMR*				*Chromatography:* a_0	
		Ligand			*Silanol* Q_3	*Alkyl-benzenes*	*Alkyl aryl ketones*
		T_1	T_2	T_3			
–	2.62	0.02	0.24	0.10	0.64	2.06	2.44
I	2.57	–	0.22	0.11	0.67	2.38	−0.06
II	2.56	0.03	0.21	0.05	0.71	2.11	1.34
III	2.57	–	0.25	0.09	0.66	1.95	0.86
IV	2.95	–	0.09	0.20	0.71	1.35	−1.25
V	2.58	–	0.11	0.15	0.74	1.72	−0.04
VI	2.55	–	0.16	0.13	0.71	1.97	−0.83

TABLE VIII

RESULTS OF ELEMENTAL ANALYSIS, NMR EXPERIMENTS AND CHROMATOGRAPHIC MEASUREMENTS OF THE MONOFUNCTIONAL OCTADECYLSILANE-MODIFIED HYPERSIL SILICA BEFORE AND AFTER TREATMENTS I–VI

Mean value of p (eqn. 5a) = 0.84.

Stationary phase HMO treatment	*Ligand* α_1 *(eqn. 1)* (μmol m^{-2})	*NMR*		*Chromatography:* a_o	
		Ligand M_1	*Silanol* Q_3	*Alkyl-benzenes*	*Alkyl aryl ketones*
–	2.34	0.29	0.71	2.37	0.99
I	1.45	0.11	0.89	1.89	0.71
II	1.81	0.22	0.78	2.28	0.34
III	1.82	0.18	0.82	1.97	0.47
IV	1.55	0.16	0.84	2.01	−0.19
V	1.79	0.18	0.82	1.73	0.86
VI	1.63	0.17	0.83	1.98	0.06

fraction methanol (x) and the incremental carbon number of the alkylbenzene (n_c) for the methyldichlorooctadecylsilane-modified Hypersil (HDI) stationary phase after treatment V is shown in Fig. 9, where the linear dependence of the log k' values on both the eluent composition and the incremental carbon number is shown. According to eqns. 2 and 3, the a_o, m_o, a_1 and m_1 values were calculated by multiple linear regression. The validity of the regression was expressed by the correlation coefficient (r). All correlation coefficients had values between 0.995 and 0.999, indicating reliable values for all constants estimated by the regression model proposed by Jandera[25]. With eqn. 5a the matching values for p were calculated.

TABLE IX

RESULTS OF ELEMENTAL ANALYSIS, NMR EXPERIMENTS AND CHROMATOGRAPHIC MEASUREMENTS OF THE DIFUNCTIONAL OCTADECYLSILANE-MODIFIED HYPERSIL SILICA BEFORE AND AFTER TREATMENTS I–VI

Mean value of p (eqn. 5a) = 0.88.

Stationary phase HDI treatment	*Ligand* α_1 *(eqn. 1)* (μmol m^{-2})	*NMR*				*Chromatography:* a_o	
		Ligand			*Silanol* Q_3	*Alkyl-benzenes*	*Alkyl aryl ketones*
		D_1	D_2	D'_2			
–	2.55	0.07	0.20	0.05	0.68	2.09	0.49
I	2.39	0.05	0.15	0.12	0.68	1.91	−0.29
II	2.44	0.05	0.18	0.17	0.62	1.91	0.57
III	2.45	–	0.17	0.16	0.67	2.01	0.49
IV	2.29	0.04	0.14	0.11	0.71	1.90	−0.36
V	2.36	0.04	0.12	0.14	0.70	2.01	0.14
VI	2.21	0.04	0.10	0.17	0.69	1.60	0.32

TABLE X

RESULTS OF ELEMENTAL ANALYSIS, NMR EXPERIMENTS AND CHROMATOGRAPHIC MEASUREMENTS OF THE TRIFUNCTIONAL OCTADECYLSILANE-MODIFIED HYPERSIL SILICA BEFORE AND AFTER TREATMENTS I–VI

Mean value of p (eqn. 5a) = 0.84.

Stationary phase HTR treatment	*Ligand* α_1 *(eqn. 1)* (μmol m^{-2})	*NMR*				*Chromatography:* a_0	
		Ligand			*Silanol* Q_3	*Alkyl-benzenes*	*Alkyl aryl ketones*
		T_1	T_2	T_3			
–	2.63	0.18	0.18	–	0.64	1.97	0.51
I	2.51	0.07	0.22	–	0.71	1.76	0.31
II	2.54	0.10	0.22	–	0.68	1.82	0.48
III	2.57	0.10	0.23	–	0.67	1.80	0.41
IV	2.69	–	0.12	0.15	0.73	1.23	−0.86
V	2.40	0.02	0.15	0.11	0.72	1.54	−0.06
VI	2.38	–	0.12	0.14	0.76	1.37	−0.70

Both elemental analysis and solid-state ^{29}Si NMR measurements showed a significantly larger loss of ligands for monofunctionally modified stationary phases, especially for the Hypersil substrate, after simulation of intensive use. The effect of ligand loss was also registered by the a_0 values determined for the alkylbenzene and alkyl aryl ketone homologous series. From theory it should be concluded that there is

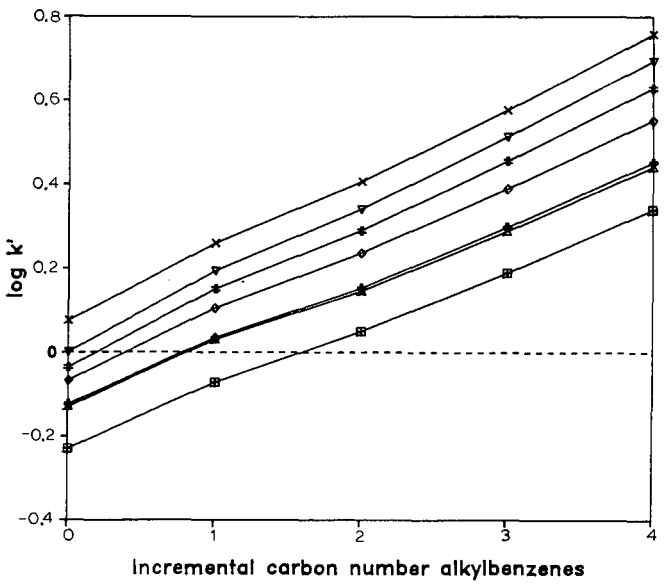

Fig. 8. Influence of treatments I–VI on the capacity factor k' determined by chromatography for alkylbenzenes (text mixture 1). Eluent: methanol–water (80:20, v/v). ×, NDI, no treatment; ▽, NDI, II; ≠, NDI, I; ◇, NDI, V; +, NDI, III; △, NDI, VI; □, NDI, IV.

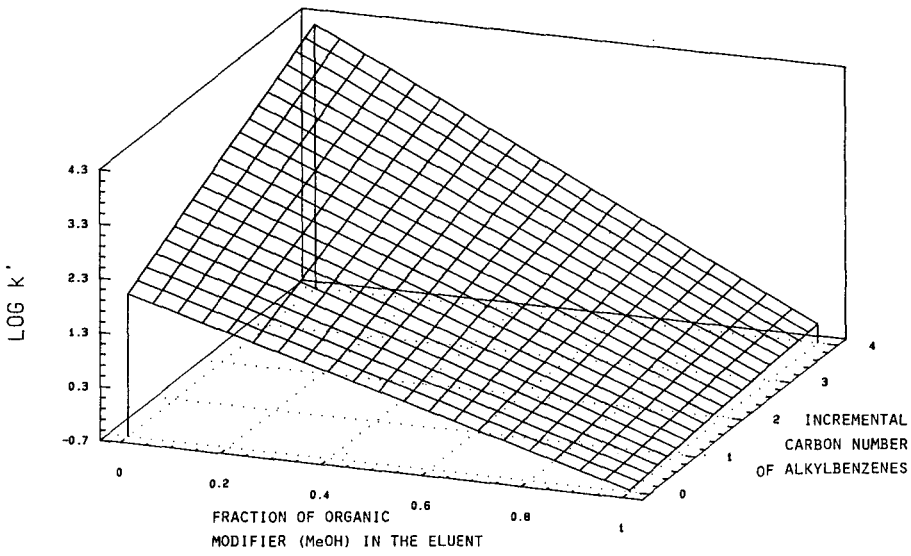

Fig. 9. Graphical representation of the regression function for k' with the volume fraction organic modifier (here methanol) in the eluent measured between $x = 0.6$ and 0.9 and extrapolated for x between 0 and 1, and the incremental carbon number of the alkylbenzene homologous series for the difunctional octadecylsilane-modified Hypersil silica (HDI) after treatment V.

a correlation between especially the a_0 values determined for alkylbenzenes and the ligand density α_1 calculated with eqn. 1 after elemental analysis, both indicating eventual stripping of ligands from the surface of the silica. However, the observed correlation between α_1 and a_0 (alkylbenzene residue) for both stationary phases was poor, with correlation coefficients of r (Nucleosil) = 0.70–0.86 and r (Hypersil) = 0.56–0.85. Plots of the α_1 values as a function of the a_0 (alkylbenzene residue) values for both the Nucleosil and the Hypersil stationary phases are depicted in Figs. 10 and 11, respectively.

The a_0 values fluctuated to a larger extent than the α_1 values, especially for multifunctionally modified phases. The observed deviation between α_1 and a_0 values is due to the fact that α_1 is an averaged bulk value determined from the probably changed specific surface area and the relative carbon content, which is also influenced by hydrolysis of the substrate. On the other hand, the a_0 value seemed to be more sensitive to irregularities in the packing, such as local distortion of the ligand film and the packed bed, and chromatographic parameters.

New stationary phases with increasing ligand density showed a good correlation between the a_0 (alkylbenzene residue) and α_1 values. The bonded phases modified with multifunctional silanes were more stable, in contradiction with results reported earlier[1]. This earlier study already contained a restrictive remark regarding the possible influence of a lower surface coverage of ligands for the trifunctional modified stationary phase studied. We can now conclude that the influence of different surface coverage is of major importance for the comparison of the stability of ligand anchoring on silica-based substrates, at least for multifunctionally derivatized materials. For

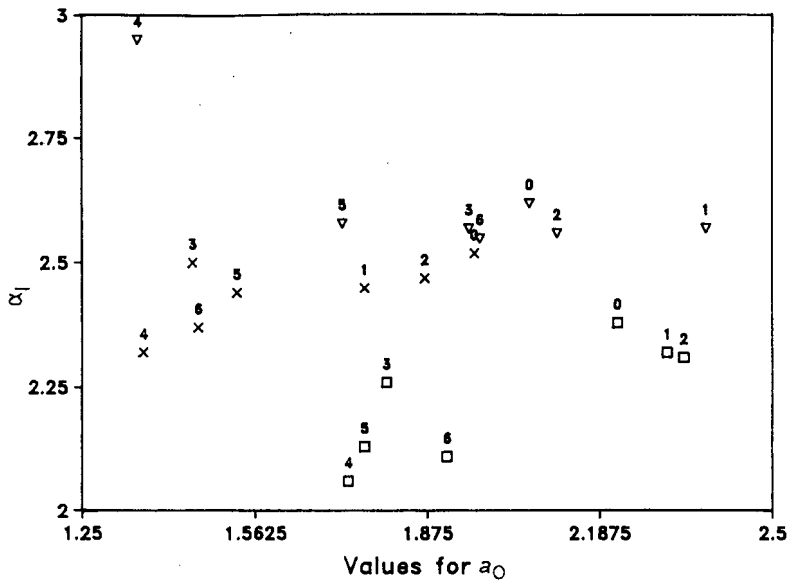

Fig. 10. Octadecyl ligand surface density α_1 (μmol m^{-2}) *versus* a_o (alkylbenzenes) for modified Nucleosil stationary phases before (0) and after each treatment (numbers 1–6 represent treatments I–VI). □, NMO; ×, NDI; ▽, NTR.

more stable stationary phases, full coverage of the surface with ligands is desirable. Hydrolysis of octadecyl ligands was reduced by eluents containing 50% (v/v) methanol. Most severe hydrolyses of octadecylsilanes were determined after use of

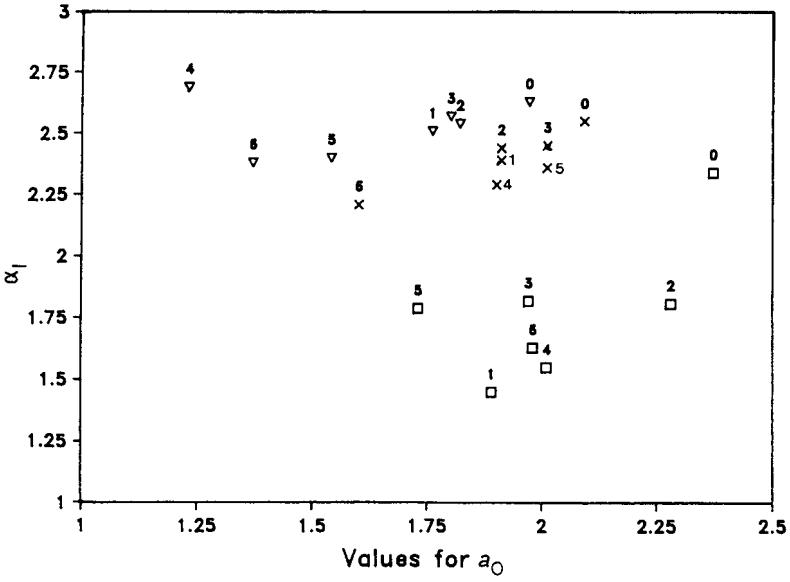

Fig. 11. Octadecyl ligand surface density α_1 (μmol m^{-2}) *versus* a_o (alkylbenzenes) for modified Hypersil stationary phases before (0) and after each treatment (numbers 1–6 represent treatments I–VI). □, HMO; ×, HDI; ▽, HTR.

high pH buffer eluents, especially with treatment IV. Elemental analysis sometimes showed an "increase" in the ligand density at the surface after treatment. This, however, is caused by rapid dissolution of the silica substrate rather than by extra hydrolysis of the silane ligands during ageing. The relatively higher hydrolysis of substrate material was only observed in this study for trifunctionally derivatized stationary phases. The same results, mainly for trifunctional modifications, were reported earlier[1]. Ligands attached to silica with trifunctional silanes were the most resistant towards hydrolysis when exposed to aggressive HPLC eluents compared with identically modified mono- and difunctional analogues. However, at high pH the shielding of the surface by polymerization did not prevent hydrolysis of the silica substrate, leading to a less preferable situation.

In a recent study, Kirkland *et al.*[28] used bridged "bidentates", containing two monofunctional silicon atoms with short alkyl ligands (C_1–C_4) instead of the difunctional alkylsilanes used for modification of the silica substrate in most other studies. They also noticed that these "bidentates" showed a higher resistance towards hydrolysis of the anchored silanes. We have noticed before that the anchoring of longer alkylsilane modifications was more stable owing to the shielding effect of these longer alkyl chains[1]. In this study, with difunctionally modified C_{18} phases the loss of ligands at the surface after the exposure treatments was limited to less than 10% relative to the initial carbon content, showing the highest stability towards hydrolysis by aggressive eluents. Compared with the short alkyl ligand modification described earlier[1], the multifunctional octadecylsilane-modified stationary phases studied here show extremely high stabilities. Therefore, in order to improve the stability of alkyl-modified reversed phases with alkyl ligands longer than C_4, the use of multifunctional alkylsilanes must be considered. This seems particularly true for bifunctional derivatized stationary phases.

Cracked particles and small channels formed through the packed column caused double and split peaks in chromatograms, as shown for the NDI phase after treatment IV in Fig. 1. These columns showed such a severe drop in column efficiency that any further use for chromatographic separations was inadvisable. For the trifunctionally modified phases, more severe peak splitting occurred than for the difunctionally modified phases, indicating superior substrate shielding in the latter case.

The relative deviations of the results determined by the characterization methods used in this study are listed in Table XI. The relative deviations (RD) of the reported values were calibrated by comparing the determined values before and after treatment with the value before treatment (see eqn. 7):

$$\mathrm{RD} = \frac{\sum_{i=1}^{n} \left| X_{\mathrm{after}} - X_{\mathrm{before}} \right|}{n} \cdot \frac{1}{X_{\mathrm{before}}} \tag{7}$$

where X is the value determined by a specific characterization method and n is the number of experiments or treatments performed.

These relative deviations give a summary of the results listed in Tables V–X for comparison of the stabilities of the stationary phases examined. From the relative deviations for elemental analysis and solid-state ^{29}Si NMR experiments it can be

TABLE XI

RELATIVE DEVIATION OF THE RESULTS DETERMINED BY ELEMENTAL ANALYSIS, NMR EXPERIMENTS AND CHROMATOGRAPHIC MEASUREMENTS FOR THE STATIONARY PHASES UNDER STUDY

Stationary phase	*Elemental analysis:* α_1	*NMR*		*Chromatography:* a_0	
		Total ligand	*Silanol*	*Alkyl-benzenes*	*Alkyl aryl ketones*
NMO	0.076	0.206	0.106	0.142	0.564
NDI	0.037	0.152	0.118	0.198	1.004
NTR	0.038	0.167	0.094	0.131	1.005
HMO	0.284	0.414	0.169	0.166	0.625
HDI	0.076	0.068	0.032	0.096	0.759
HTR	0.051	0.199	0.112	0.186	0.114

concluded that on the Nucleosil substrate the di- and trifunctional octadecysilane stationary phases were more stable than the monofunctional octadecylsilane phase for the same surface coverage. The relative deviations of a_0 (alkylbenzene) did not give a clear indication of the stability of the Nucleosil stationary phases. However, the trifunctional octadecyl phase was already altered by condensation before characterization and chromatographic treatments. This alteration could possibly have had a positive influence on the stability compared with the trifunctionally modified Hypersil stationary phase. On the Hypersil silica, however, the difunctional octadecylsilane modification manifested the highest stability after exposure to the HPLC eluents with the characterization methods used in this study. Compared with commercially available reversed-phase monofunctional octadecyl Hypersil phases, the ligand density in this study was relatively low [$\alpha_1 = 2.34$ compared with α_1 (commercial Hypersil C_{18}) = 3.41]. This probably explains the poor stability of the HMO stationary phase compared with a previous study[1].

Selectivity

Selectivity in RP-HPLC depends on both the mobile and the stationary phase used. To judge the selectivity of the mobile phase, the mean values of p are listed in Tables V–X. These p values were in agreement with the theoretical value for methanol–water eluents ($p = 0.86$) calculated by Jandera[26]. The only exception was found for the NDI stationary phase with a mean value of $p = 0.65$. This deviation was found after regression for both homologous test mixtures and was double checked. No reasonable explanation could be found for this deviation from the theoretical value.

More specific stationary phase–solute interactions were obtained from the values of m_0 for lipophilic and q for polar selectivity. The plots of m_0 *versus* a_0 for both homologue residues on the Nucleosil and Hypersil stationary phases are depicted in Figs. 12 and 13, respectively. As already pointed out by Jandera[26,27], there is a good correlation between the non-polar contribution to the selectivity m_0 and the capacity factor of the stationary phase represented by a_0 values. The correlation coefficients were r (alkylbenzenes) = 0.92–0.98 and r (alkyl aryl ketones) = 0.97–0.996. As

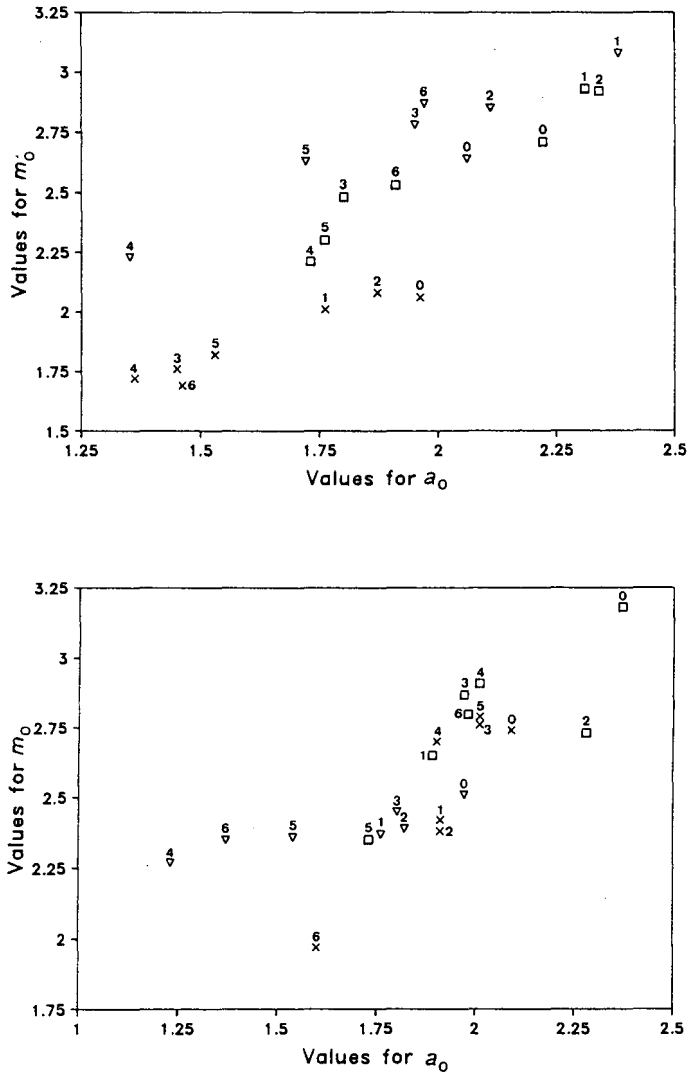

Fig. 12. Chromatographically determined m_o values (lipophilic selectivity) *versus* a_o for the alkylbenzene homologous series on modified Nucleosil (top) and Hypersil (bottom) stationary phases before (0) and after each treatment (numbers 1–6 represent treatments I–VI). Top: □, NMO; ×, NDI; ▽, NTR. Bottom: □, HMO; ×, HDI; ▽, HTR.

expected, a decrease in the amount of bonded ligands caused by intensive use caused a decrease in non-specific lipophilic selectivity.

Plots of the polar selectivity q *versus* a_o values for the alkyl aryl ketone residue both on Nucleosil and Hypersil stationary phases are shown in Fig. 14. The influence of the exposure treatments on the polar selectivity varied depending on the type of modification and the silica substrate. For the monofunctionally modified phases a decrease in the capacity factor and lipophilic selectivity implies also a decrease in

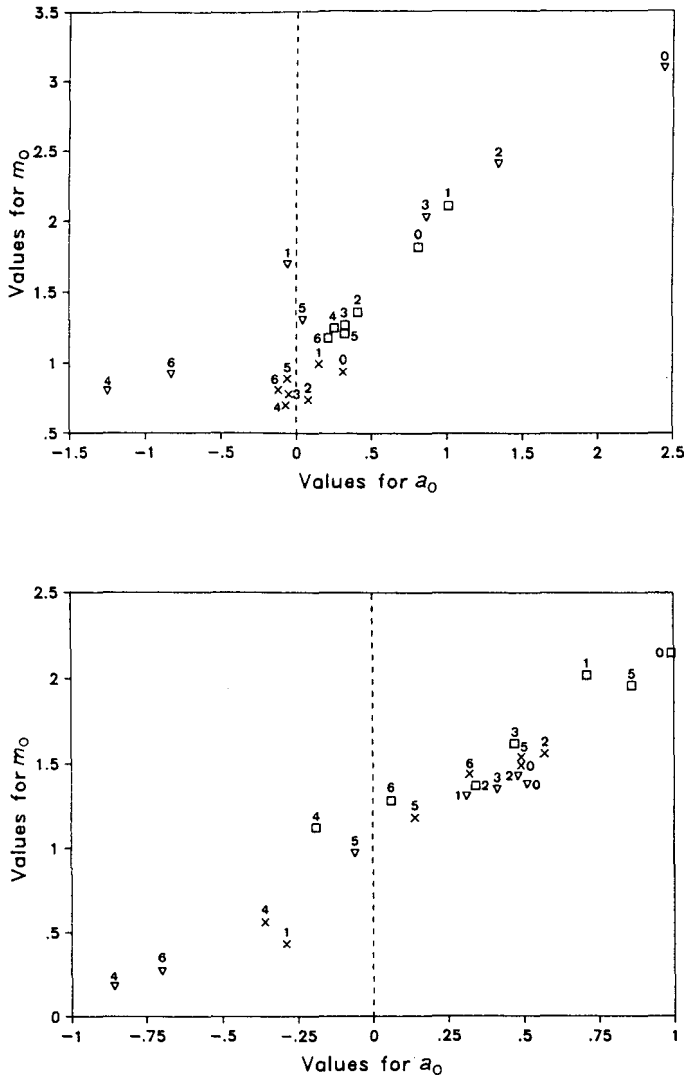

Fig. 13. Chromatographically determined m_0 values (lipophilic selectivity) *versus* a_0 for the alkyl aryl ketone homologous series on modified Nucleosil (top) and Hypersil (bottom) stationary phases before (0) and after each treatment (numbers 1–6 represent treatments I–VI). Top: □, NMO; ×, NDI; ▽, NTR. Bottom: □, HMO; ×, HDI; ▽, HTR

polar selectivity for alkyl aryl ketones, and especially for the HMO stationary phase an extreme decrease in the q value occurred. This polar selectivity seemed to decrease with the loss of ligands and the gain in silanol groups at the surface, against expectation.

Multifunctionally modified stationary phases, especially difunctionally modified phases, show an almost constant value of q after hydrolysis and condensation of the remaining ligands at the surface. It seems that the residual silanols are better shielded by the surface cross-linked ligands, except for the trifunctional octadecyl-

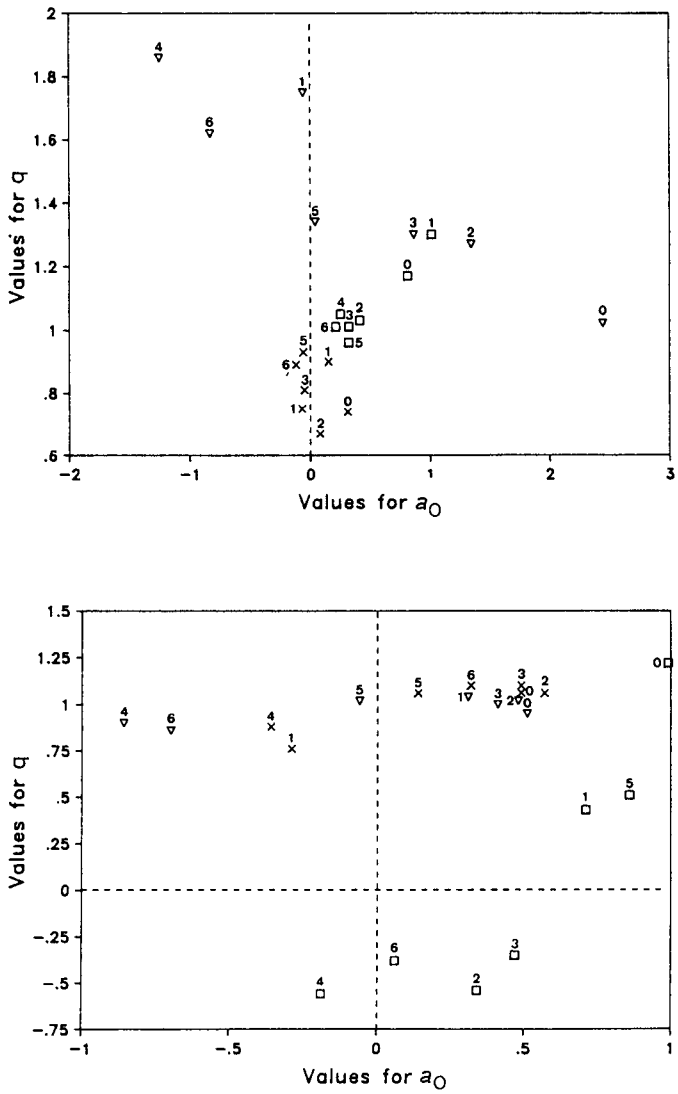

Fig. 14. Chromatographically determined q values (polar selectivity) and a_o values for the alkyl aryl ketone homologous series on modified Nucleosil (top) and Hypersil (bottom) stationary phases before (0) and after each treatment (numbers 1–6 repesent treatments I–VI). Top: □, NMO; ×, NDI; ▽, NTR. Bottom: □, HMO; ×, HDI; ▽, HTR.

modified Nucleosil phase. The substrate shielding of this stationary phase seems poor, indicated also by higher q values after several treatments. Substrate shielding by siloxane bridges directly at the surface, which occurs especially with bidentate, difunctional octadecyl-modified phases, D_2 and D'_2 groups, prevented ligand and substrate hydrolysis and showed a remaining selectivity after the exposure treatments. Difunctionally modified stationary phases with a bidentate linkage are to be preferred in RP-HPLC with aggressive eluents.

In contrast with results published by Jandera[27] on polar selectivity and the value of q for solutes, we found that the value of q (alkyl aryl ketones) did not indicate more specific polar interactions between the solute and the increasing amount of silanol groups measured by solid-state ^{29}Si NMR. Probably the "polarity" of the alkyl aryl ketone residue (steric hindrance of the benzene ring) and the shielding of the silanol groups formed, also due to a higher degree of mobility and irregularities in the octadecyl film[29] after the exposure treatments, influenced these specific polar interactions negatively. More polar residues of homologous series are currently being investigated for future characterization of a more pronounced and discriminating value for the polar selectivity of different stationary phases before and after long-term exposure to aggressive eluents. As expected for the alkylbenzene residue, the value of q did not change much. More or less equal q values were determined even for the different silica substrates used for modification, owing to the rather apolar residue of the alkylbenzene homologous series.

Exposure treatments, a practical guide

A comparison between the effects of different exposure treatments can be used to evaluate the choice of the eluents listed in Table II. From the results of the different characterization techniques, it is obvious that eluents of both low and high pH should be included in the series of exposure treatments. For the aqueous buffer with pH 8.4, used in treatment IV, severe degradation of the silica substrate was always observed. However, for more discriminating information about the stability of modified phases, the pH of the aqueous buffer should be selected at *ca.* 7.5, especially for less-stable RP-HPLC phases. Mixed eluents containing organic modifiers with aqueous buffers can be used with higher aqueous pH values, because the presence of the modifier decreases silica degradation. Although the effect of addition of ion pairing agents on the stability of the modified phases was moderate, the exclusion of these ionic species from the exposure treatments will deprive the experiments of additional, useful information. The present study involved a wide variety of eluents for exposure treatments.

For routine laboratory interest, a comparison of different stationary phases should be carried out with a more aggressive eluent than those used in practice to decrease the exposure time. Especially when aqueous eluents with abnormal pH values (below 4 and above 7) are to be used, one should consider "ageing" of the stationary phases. Information about the stability, selectivity, capacity and silica degradation can be obtainad by the chromatographic characterization method described above combined with information on the column efficiency.

CONCLUSIONS

Condensation of the multifunctional octadecylsilanes at the surface of the silica substrate prevented hydrolysis of the anchored ligands even after long-term exposure to aggressive eluents. For stationary phases synthesized in order to achieve identical degrees of silylation, we conclude that the bifunctional octadecylsilane stationary phases exhibited the best overall stability towards hydrolysis of the anchored ligands and hydrolysis of the silica substrate, especially when buffers of high pH were used as eluents.

Difunctionally modified stationary phases with bidentate linkage are to be preferred in RP-HPLC with aggressive eluents. The decrease in capacity and lipophilic selectivity observed after long-term exposure was less pronounced for the multifunctionally derivatized stationary phases. Most multifunctionally modified octadecyl stationary phases showed an almost unchanged polar selectivity after intensive use. For the monofunctional phases a severe decrease in polar selectivity was determined.

For Nucleosil and Hypersil silica, differences in the type of silica substrate used appeared to have much less influence on hydrolysis for multifunctionally modified stationary phases than for monofunctionally modified phases. Of the two monofunctional octadecylsilane reversed phases, the Nucleosil-based phase seemed to be more resistant to aggressive eluents. The connection between the major substrate properties and stabilities of the stationary phases after modification will be the subject of further research in these laboratories.

ACKNOWLEDGEMENTS

We thank Mr. M. Kunst and Miss B. Pfleiderer for preparing the stationary phases, Mr. E. van Steen for assistance and Mr. H. Eding for the elemental analyses of the stationary phases. We thank Mr. H. Claessens for stimulating discussions and support. Further, the authors gratefully thank Mrs. Denise Tjallema for her expeditious handling of the manuscript. These investigations were supported by the Netherlands Foundation for Chemical Research (SON) with financial aid from the Netherlands Organization for Scientific Research (NWO).

REFERENCES

1 H. A. Claessens, J. W. de Haan, L. J. M. van de Ven, P. C. de Bruijn and C. A. Cramers, *J. Chromatogr.*, 436 (1988) 345–365.
2 T. G. Waddell, D. E. Leyden and M. T. DeBello, *J. Am. Chem. Soc.*, 103 (1981) 5303–5307.
3 J. Köhler, D. B. Chase, R. D. Farlee, A. J. Vega and J. J. Kirkland, *J. Chromatogr.*, 352 (1986) 275–305.
4 J. Köhler and J. J. Kirkland, *J. Chromatogr.*, 385 (1987) 125–150.
5 N. Sagliano, R. A. Hartwick, J. Bass, B. Woods and N. T. Miller, *paper presented at the 12th International Symposium on Column Liquid Chromatography, Washington, DC, June 19–24, 1988.*
6 Cs. Horvath (Editor), *High Performance Liquid Chromatography*, Vols. 1 and 2, Academic Press, New York, 1980.
7 D. W. Sindorf and G. E. Maciel, *J. Am. Chem. Soc.*, 105 (1983) 3767–3776.
8 E. Bayer, K. Albert, J. Reiners, M. Nieder and D. Müller, *J. Chromatogr.*, 264 (1983) 197–213.
9 H. Engelhardt and H. Müller, *J. Chromatogr.*, 218 (1981) 395–407.
10 H. A. Claessens, C. A. Cramers, J. W. de Haan, F. A. H. den Otter, L. J. M. van de Ven, P. J. Andree, G. J. de Jong, N. Lammers, J. Wyma and J. Zeeman, *Chromatographia*, 20 (1985) 582–586.
11 A. M. Krstulovic, P. R. Brown, *Reversed-Phase High Performance Liquid Chromatography*, Wiley, New York, 1982.
12 J. L. Glajch, J. G. Gluckman, J. G. Charinkofsky, J. M. Minor and J. J. Kirkland, *J. Chromatogr.*, 318 (1985) 23–29.
13 R. D. Golding, A. J. Barry and M. F. Barke, *J. Chromatogr.*, 384 (1987) 105–116.
14 G. E. Berendsen, *Ph.D. Thesis*, Delft, 1980.
15 M. C. Hennion, C. Picard and M. Caude, *J. Chromatogr.*, 166 (1978) 21–35.
16 C. Lüllmann, H. G. Genieser and B. Jastorff, *J. Chromatogr.*, 323 (1985) 273–280.
17 J. N. Kinkel and K. K. Unger, *J. Chromatogr.*, 316 (1984) 193–200.
18 E. Bayer, A. Paulus, B. Peters, G. Laup, J. Reiners and K. Albert, *J. Chromatogr.*, 364 (1986) 25–37.
19 W. Noll, *Chemie und Technologie der Siliconen*, Verlag Chemie, Weinheim, 1968.

20 R. K. Iler, *The Chemistry of Silica*, Wiley, New York, 1979.
21 K. K. Unger, *Porous Silica*, Elsevier, Amsterdam, 1979.
22 J. M. J. Vankan, J. J. Ponjeé, J. W. de Haan and L. J. M. van de Ven, *J. Colloid Interface Sci.*, 126 (1988) 604–609.
23 H. Engelhardt, B. Dreyer and H. Schmidt, *Chromatographia*, 16 (1982) 242–246.
24 R. M. Smith, *Anal. Chem.*, 56 (1984) 256–262.
25 P. Jandera, *Chromatographia*, 19 (1984) 101–112.
26 P. Jandera, *J. Chromatogr.*, 314 (1984) 13–36.
27 P. Jandera, *J. Chromatogr.*, 352 (1986) 91–110.
28 J. J. Kirkland, J. L. Glajch and R. D. Farlee, *Anal. Chem.*, 61 (1989) 2–11.
29 K. Albert, B. Evers and E. Bayer, *J. Magn. Reson.*, 62 (1985) 428–436.

Journal of Chromatography, 479 (1989) 297–306
Elsevier Science Publishers B.V., Amsterdam — Printed in The Netherlands

CHROM. 21 718

MEASUREMENT OF DEOXYGUANOSINE/THYMIDINE RATIOS IN COMPLEX MIXTURES BY HIGH-PERFORMANCE LIQUID CHROMATOGRAPHY FOR DETERMINATION OF THE MOLE PERCENTAGE GUANINE + CYTOSINE OF DNA

MOSTAFA MESBAH[a] and WILLIAM B. WHITMAN*
Department of Microbiology, University of Georgia, Athens, GA 30602 (U.S.A.)
(First received December 28th, 1988; revised manuscript received May 5th, 1989)

SUMMARY

The ratio of deoxyguanosine and thymidine can be determined in a complex mixture containing the major ribonucleosides and deoxynucleosides, the minor deoxynucleosides, and the nucleotide monophosphates by high-performance liquid chromatography. The isocratic procedure utilizes a C_{18} column and a solvent of methanol–triethylamine phosphate (pH 5.1). A single analysis requires 15 min. Within the range of 0.5–1.5 μg of total deoxynucleosides per sample, the determination is very precise and the relative standard deviation is about 0.1%. From the deoxyguanosine/thymidine ratio, a precise determination of the mole percentage guanine + cytosine of double-stranded DNA is calculated.

INTRODUCTION

High-performance liquid chromatography (HPLC) has proven to be a useful method for analysis of nucleotides, nucleosides and bases in biological tissues, blood and other materials[1–7]. An important application of these techniques is the determination of the mole percentage guanine + cytosine (mole-% G+C) of DNA[8–13]. The free nucleosides or bases are produced by enzymatic or acid hydrolysis, and the quantity of each component is measured by HPLC. Because dCyd and dAdo are frequently modified in DNA, both the minor and major nucleosides or bases must be separated to determine the total composition. Moreover, fairly large errors of about 1% are usually associated with the quantification of the individual components of DNA[10,12]. Considering that the mole-% G+C of DNA varies over a fairly narrow range of 25–75 mole-%[14], this error seriously compromises the usefulness of the technique.

A modification of the HPLC technique is to determine the ratio of dGuo and

[a] Present address: Department of Pharmacognosy, Faculty of Pharmacy, University of Assiut, Assiut, Egypt.

0021-9673/89/$03.50

dThd in enzymatic digests of double-stranded DNA[15]. The mole-% G+C is then calculated from the formula:

$$\text{mole-\%} = [1 + Y(\text{dT/dG})]^{-1}$$

where dT and dG are the peak areas for dThd and dGuo, respectively, and Y is a ratio of the molar response factor of dG/dT, which is determined from a standard DNA of known sequence. Thus, Y = [measured peak area ratio of (dG/dT) obtained from the standard DNA hydrolysate] × [value of the mole ratio of (dT/dG) that is calculated from the sequence of the standard DNA]. Because dGuo and dThd are not modified in DNA, the minor nucleosides do not have to be measured. The chromatography is also potentially simpler because only two nucleosides need to be determined. Most importantly, the precision and accuracy may be much higher because it does not depend upon the preparation of individual standards for each of the nucleosides. In this paper, we describe an HPLC procedure for the determination of dGuo/dThd ratios in the complex mixtures of nucleosides which result from the enzymatic degradation of DNA. Over the range of 0.5–1.5 μg of total deoxynucleosides the relative standard deviation of this procedure is on the order of 0.1%.

EXPERIMENTAL

Apparatus

Equipment for HPLC was obtained from Beckman (Berkeley, CA, U.S.A.). It included two Model 110A high-pressure pumps, a Model 420 controller, an Altex Model 210 injector with 20 μl sample loop, and a Model 160 fixed-wavelength absorbance detector with a 254-nm filter and quartz-mercury ultraviolet lamp. The data was collected with a Model 3390A Hewlett-Packard (Avondale, PA, U.S.A.) integrator. The integrator used the default conditions except for attenuation and chart speed, which were set at 4 and 0.5 cm/min, respectively. For the standard chromatographic conditions, an Econosphere C_{18} reversed-phase column (Alltech Assoc. Deerfield, IL, U.S.A.) was used. The particle size was 5 μm, and the column dimensions were 250 × 4.6 mm I.D. In some cases, an Econosphere C_{18} reversed-phase column with a 3-μm particle size and dimensions of 150 × 4.6 mm I.D. was used. The column temperature was controlled with a water jacket and a refrigerated circulating water bath.

Chromatographic conditions

Unless it is specified differently, conditions included a flow-rate of 1.0 ml/min at a temperature of 37°C. The solvent contained 12% methanol and 20 m*M* triethylamine phosphate (TEAP), pH 5.1. The solvent was prepared by combining 40 ml of 0.5 *M* TEAP, pH 5.1, with about 750 ml of glass distilled water. HPLC-grade methanol (120 ml; J. T. Baker Ch.) was added, and the volume was adjusted to 1 l. The solvent was then filtered through a 0.45-μm cellulose triacetate membrane (GA-6 Metricel; Gelman Sciences, Ann Arbor, MI, U.S.A.). Triethylamine, 99% minimum concentration, was obtained from Kodak (Rochester, NY, U.S.A.). If the reagent had a noticeable yellow color, it was purified by vacuum distillation. To prepare the 0.5 *M* TEAP solution, triethylamine was diluted with water, the pH was adjusted to

5.1 with 85% phosphoric acid, and the solution was brought to its final volume. When the column was not in use, the flow-rate was reduced to 0.1 ml/min. When the machine was not to be operated for more than two weeks, the column was washed with water followed by 70% (v/v) methanol. When the column pressure exceeded 2000 p.s.i., the filters and precolumn were changed. Piston seals were also changed frequently.

Enzymatic hydrolysis of DNA

The DNA was suspended in 10 m*M* Tris–HCl, 0.1 m*M* Na_2EDTA, pH 7.2 at a concentration of 0.5–1.5 mg/ml. A portion of this solution, 25 μl, was transferred to a 1.5-ml disposable centrifuge tube, heated for 2 min in a boiling water bath, and cooled rapidly in ice water. The following reagents were then added: 50 μl of 30 m*M* sodium acetate buffer, pH 5.3; 5 μl of 20 m*M* $ZnSO_4$; and 3 μl of nuclease P1 (1 unit). The sample was then incubated for 1 h at 37°C. Then 5 μl of alkaline phosphatase (5 units) and 5 μl of 0.1 *M* glycine buffer, pH 10.4, were added. The sample was then incubated an additional 6 h at 37°C. The P1 nuclease solution was stored in aliquots at −20°C. It contained 1 mg/ml of nuclease P1 from *Penicillium citrinum* (Sigma, 340 units per mg protein) in 30 m*M* sodium acetate buffer, pH 5.3, and 0.5 m*M* $ZnSO_4$. The alkaline phosphatase solution contained 1 mg/ml of bovine intestinal mucosa alkaline phosphatase (Sigma, Type V11-NT, 1060 units per mg of protein) in 0.1 *M* glycine buffer, pH 10.4, and it was prepared by dilution of the stock enzyme immediately before use.

Materials

Biochemicals were obtained from Sigma. *Methanococcus voltae* DNA was purified by phenol extraction as described previously[16].

RESULTS

Chromatographic conditions

The major ribonucleosides and deoxyribonucleosides produced by enzymatic hydrolysis of nucleic acids were separated by isocratic HPLC. Because the dGuo/dThd ratio is especially important for the determination of the mole-% G+C, the chromatographic conditions were varied systematically to determine the optimal conditions for measuring dGuo and dThd. The parameters chosen for careful study, methanol concentration and temperature, are important factors in the chromatography of ribonucleosides[17]. In addition, several potential sources of error were identified.

The retention times of the nucleosides were very sensitive to the methanol concentration and the column temperature (Fig. 1 and 2). Four major effects were observed. One, as the temperature increased, the resolution of the nucleosides and the ratio of the peak height to peak width increased (data not shown). This effect was expected due to the increased efficiency of most reversed-phase columns at higher temperatures. Two, as the temperature increased, the retention times of the nucleosides decreased (Fig. 1). Because of the increased column efficiency, the resolution of most of the nucleosides was adequate even at 55°C. Three, as the temperature increased, the order of elution of 5-methyldeoxycytidine (dmCyd) changed (Fig. 1).

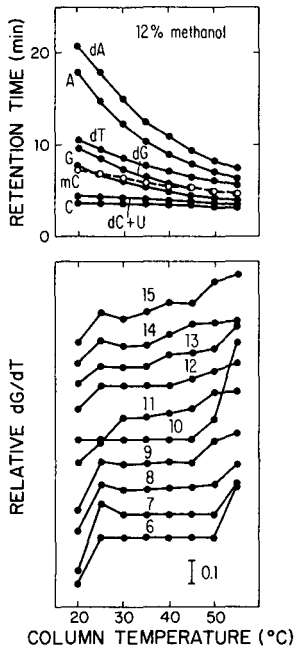

Fig. 1. Effect of column temperature on the elution of nucleosides and the apparent dGuo/dThd ratio. (Top) Retention time of the major nucleosides at 12% methanol. (Bottom) Effect of temperature and methanol concentration on the apparent dGuo/dThd ratio. The apparent dGuo/dThd ratio is the ratio of the observed peak areas for each nucleoside. Numbers above each line refer to the percentage methanol. The bar is equal to a change in the ratio of 0.1.

Thus, at 12% methanol, dmCyd coeluted with Guo at 25°C and with dGuo at 45–55°C. This effect caused an increase in the apparent dGuo/dThd ratio at high temperatures. Likewise, very similar results were obtained with hydrolysates of DNA which

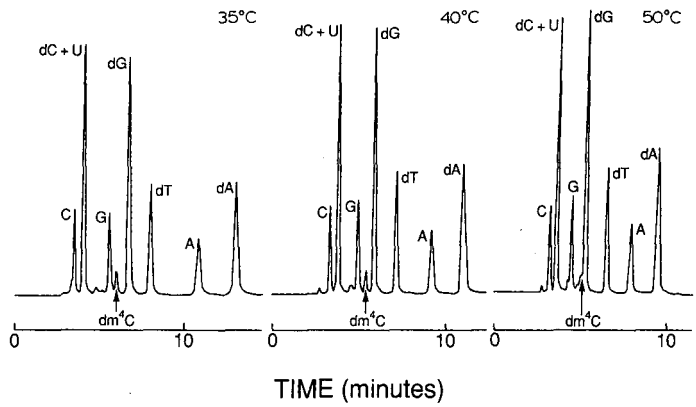

Fig. 2. Chromatography of enzymatic hydrolysates of *Methanococcus thermolithotrophicus* nucleic acids at 35, 40 and 50°C. This DNA contains 0.26 mole-% 4-methyldeoxycytidine, m^4dC[18]. This sample also contained 25% RNA. The apparent dGuo/dThd ratios were: 0.9801 at 35°C, 0.9834 at 40°C and 1.0209 at 50°C.

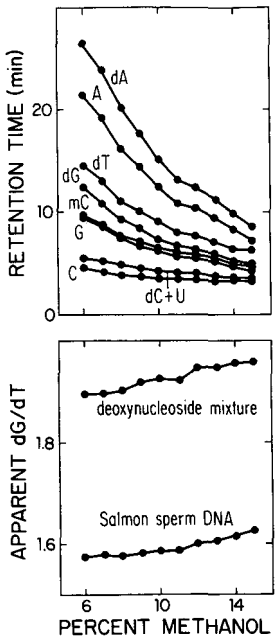

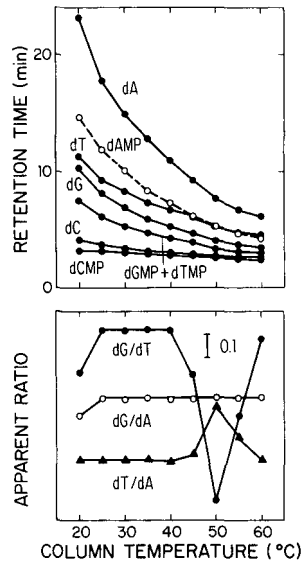

Fig. 3. Effect of methanol concentration on the elution of nucleosides and the apparent dGuo/dThd ratio. The temperature was 35°C.

Fig. 4. Elution of deoxynucleotide monophosphates and effect on the apparent nucleoside ratios. The mixture of nucleoside standards contained 20% of the monophosphates. Chromatography was at 12% methanol.

contained 4-methyldeoxycytidine, which coeluted with dmCyd in this system (Fig. 2). In contrast to dmCyd, no interference was observed by N^6-methyldeoxyadenosine (dmAdo), which eluted several minutes after dAdo under most conditions (data not shown). Four, as the methanol concentration increased the retention times of the nucleosides decreased (Fig. 3). At high methanol concentrations, dGuo was poorly resolved from dmCyd and Guo. Also associated with an increase in methanol concentration was an increase in the apparent dGuo/dThd ratio. This effect was probably not due to the coelution of the nucleosides because it was also observed at methanol concentrations where the nucleosides were well resolved (Fig. 3). Instead, the peak shape of the nucleoside may have changed, which would effect the integration of the peak and the apparent ratio. Therefore, to obtain reproducible dGuo/dThd ratios, the concentration of methanol must be constant.

For determination of the mole-% G+C, nucleic acid was enzymatically degraded to nucleosides. Small amounts of the monophosphates frequently remained after the degradation. Therefore, it was important to determine where the monophosphates eluted to recognize samples with incomplete degradation. In addition, the monophosphates may interfere with the measurement of the nucleosides and introduce an error in addition to the incomplete degradation. For instance, dAMP coeluted with dThd between 45 and 60°C, and it was a potential source of error in that temperature range (Fig. 4). Similarly, AMP eluted close to dGuo and GMP coeluted with dCyd in this same temperature range (Fig. 5). Thus, in mixtures containing the

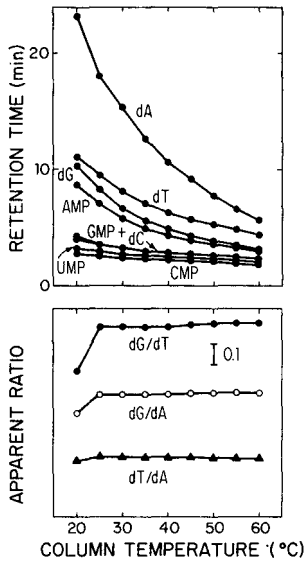

Fig. 5. Elution of ribonucleotide monophosphates and effect on the apparent nucleoside ratios. The mixture of nucleoside standards contained 40% of the monophosphates. Chromatography was at 12% methanol.

monophosphates there was a small increase in the apparent dGuo/dThd and dGuo/dAdo ratios, while the apparent dThd/dAdo ratio was unchanged.

To determine the dGuo/dThd ratio, the optimal conditions were near 12% methanol and 37°C for the Econosphere C_{18} column with a 5-μm particle size. Under these conditions, the nucleosides were well resolved from each other as well as from dmCyd, dAMP and AMP. Importantly, the apparent ratio was unaffected by changes in column temperature of ± 5°C (Fig. 1). Although the apparent ratio changed with the methanol concentration, dmCyd was also well separated from dGuo and dThd at 11 and 13%. Therefore, the system was not sensitive to small changes in these parameters.

Column

Substitution of the column with another column of the same manufacture had little effect on the chromatography. However, when a column with a 3-μm particle size and smaller dimensions (150 × 4.6 mm I.D.) was substituted, the chromatographic conditions had to be changed to resolve dGuo and dThd adequately. The conditions for the best separation with this new column were quickly found using a mixture of nucleosides and nucleotides which were difficult to resolve. Thus, the best separation of Guo, Ado, dGuo, dThd, mdCyd, AMP and dAMP was accomplished with 8% methanol at 38°C. Under these chromatographic conditions, mdCyd and AMP eluted before dGuo, dAMP eluted after dThd, and dGuo and dThd were well resolved. Moreover, the analysis was completed in 11 min, which was slightly faster than obtained with the larger, 5-μm particle column. Importantly, the separations necessary for determination of the mole-% G+C could be obtained with more than one type of C_{18} reversed-phase column.

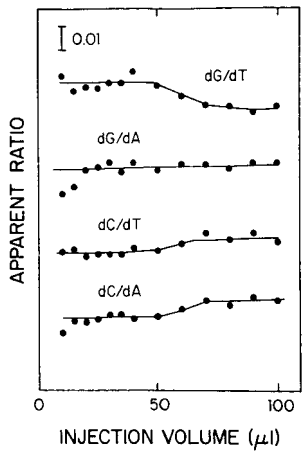

Fig. 6. Effect of injection volume on the apparent nucleoside ratios. The sample was a mixture of dCyd, dmCyd, dGuo, dThd and dAdo in distilled water. The chromatographic conditions were 12% methanol and 37°C. Correlation coefficients for the injection volumes *versus* the apparent dGuo/dThd, dGuo/dAdo, dCyd/dThd and dCyd/dAdo ratios were −0.667, 0.358, 0.611 and 0.659, respectively. For $n = 33$, all these correlation coefficients except for the dGuo/dAdo ratio were significant at $P = 0.01$.

Buffer

The concentration of the buffer TEAP had little effect on the chromatography at concentrations between 10 and 30 m*M*. At concentrations below 10 m*M*, the chromatography was seriously impaired. For instance, for 5, 10, 20 and 30 m*M* TEAP, the apparent dGuo/dThd ratios of a nucleoside mixture were 2.209 ± 0.004, 2.238 ± 0.008, 2.233 ± 0.006 and 2.234 ± 0.005, respectively. Consequently, 20 m*M* TEAP was used in subsequent chromatography.

Sample volume

When the quantity of sample was kept constant, the injection volume had little effect on the chromatography. Between 10 and 40 μl, the sample volume had no significant effect on the apparent nucleoside ratios of a mixture of dCyd, dmCyd, dGuo, dThd and dAdo (Fig. 6). Above 50 μl, a small but significant correlation was observed between the injection volume and the nucleoside ratios. In a separate experiment, the apparent dGuo/dThd ratios for 5, 10, 15 and 20 μl dilutions of a nucleoside mixture were 2.290 ± 0.002, 2.286 ± 0.003, 2.289 ± 0.002 and 2.286 ± 0.002, respectively. Therefore, no significant effects of sample volume were found down to 5 μl; and for routine experiments, the volume was maintained between 5 and 20 μl.

Sample size

The sample size had a small but significant effect on the chromatography of the nucleosides. When the injection volume was kept constant, the apparent dGuo/dThd ratio of a synthetic mixture decreased slightly between 0.5 and 4.2 μg (Fig. 7). Although not significant, a decrease of similar magnitude was also observed for the apparent dGuo/dAdo ratio. Below 0.3 μg of the mixture or 75 ng of each nucleoside, the reproducibility of the analyses decreased dramatically (Fig. 7). Similar results

were also obtained with enzymatically degraded nucleic acid which contained 40% RNA (Fig. 8). In this case, dCyd was not measured because it coeluted with Urd. Although the decrease in the apparent dGuo/dThd ratio was not significant in this experiment, the magnitude of the decrease was similar to that observed with the nucleoside mixture, and significant decreases in the dGuo/dThd ratios were observed in other experiments (data not shown).

The effect of the sample size on the nucleoside ratios was very small. For the apparent dGuo/dThd, dGuo/dAdo, dCyd/dThd and dCyd/dAdo ratios, the relative slopes of the replots *versus* sample size of the synthetic mixtures were −0.125, −0.113, −0.042 and −0.049% per μg, respectively, over the range of 0.5–4.2 μg. Thus, ratios involving dGuo were most affected. In this case, most of the decrease was due to samples larger than 1.5 μg. When these were excluded from the analysis, the correlation coefficient decreased to 0.0295 ($n = 10$), and the relative slope increased to

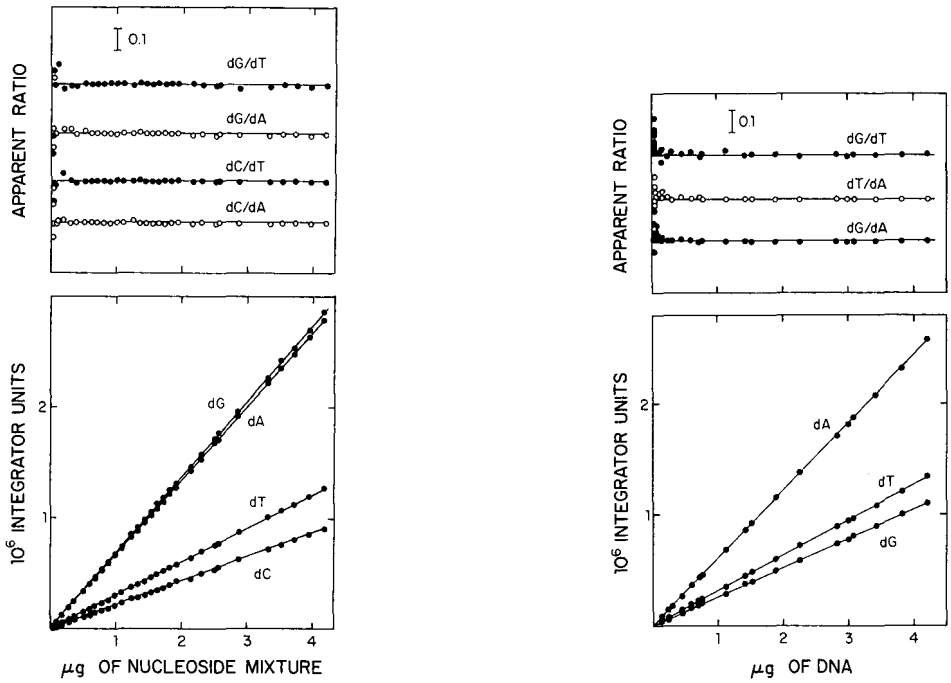

Fig. 7. Linearity of the integrator response with sample size for a nucleoside mixture. The mixture contained equimolar amounts of dCyd, dThd, dGuo and dAdo. The injection volume was 20 μl. The correlation coefficients for the sample size (0.5–4.2 μg) *versus* the apparent dGuo/dThd, dGuo/dAdo, dCyd/dThd and dCyd/dAdo ratios were −0.624, −0.381, −0.141 and −0.081, respectively. For $n = 25$, only the correlation coefficient for dGuo/dThd was significant at $P = 0.01$. All others were not significant at $P = 0.05$.

Fig. 8. Linearity of the integrator response with sample size for enzymatically degraded nucleic acid. The nucleic acid was from *M. voltae* and contained 40% RNA. Therefore, dCyd was not determined. The correlation coefficients for the sample size (0.45–4.2 μg) *versus* the apparent dGuo/dThd, dGuo/dAdo and dThd/dAdo ratios were −0.201, −0.178 and −0.032, respectively. For $n = 15$, these values are not significant at $P = 0.05$.

TABLE I

DETERMINATION OF THE APPARENT DEOXYNUCLEOSIDE RATIOS

Ratios (± the standard error of the mean) were calculated as the mean quotient of the integrated peak areas from each injection or as the slope of the replot of the integrated peak area of each nucleoside *versus* the peak areas of the other nucleosides (see text). For the nucleoside mixture, data from 25 measurements were analyzed. For the *M. voltae* DNA, data from eighteen measurements were analyzed. The measurements are shown in Figs. 7 and 8.

Ratio	*Quotient method*	*Slope method*
Nucleoside mixture		
dGuo/dThd	2.251 ± 0.001	2.245 ± 0.002
dGuo/dAdo	1.030 ± 0.001	1.027 ± 0.002
dCyd/dThd	0.716 ± 0.001	0.716 ± 0.001
dCyd/dAdo	0.328 ± 0.000	0.327 ± 0.001
M. voltae DNA		
dGuo/dThd	0.828 ± 0.002	0.824 ± 0.001
dGuo/dAdo	0.434 ± 0.001	0.433 ± 0.001
dThd/dAdo	0.524 ± 0.002	0.525 ± 0.001

+0.01% per μg. Neither of these were significant at $P = 0.05$. Thus, for sample sizes of 0.5–1.5 μg, there was no effect of sample size.

The equations to calculate the G+C content from the ratios of nucleosides assumed that the peak areas of the nucleosides were proportional to the quantity chromatographed and that replots of the peak area for each nucleoside *versus* the sample size extrapolated to a common origin. Because the sample size could not be measured directly with the necessary level of precision (0.1% R.S.D.), other tests of the data in Figs. 7 and 8 were devised to test these relationships. First, for each chromatographic run, the peak area for each nucleoside was replotted against the peak area for the other nucleosides. The correlation coefficients for all pairwise comparisons of the peak areas for the nucleosides were found to be greater than 0.99997 for the nucleoside mixture and 0.99994 for the digested DNA (data not shown). Because these values were very close to one, the integrated peak area of the nucleosides must have been nearly linear over this range of sample sizes. Second, all the replots extrapolated very close to the origin, to within ± 0.9 ng of nucleoside for the mixture and ± 1.9 ng of nucleoside for the digested DNA. In both cases, these values were less than twice the standard error and were not significant. Third, the nucleoside ratios were calculated from the slopes of these replots and compared to the ratios determined from each run (Table I). The ratios were very close. Therefore, by these relatively sensitive criteria, the integrator response was close to linear between 0.3 and 4.2 μg of DNA or nucleosides, and the integrator response for the nucleosides extrapolated to a common origin.

DISCUSSION

The dGuo/dThd ratios in complex mixtures of nucleosides can be determined

very precisely by HPLC. However, care must be taken to insure that dmCyd is resolved from dGuo and that, if nucleotide monophosphates remain after the degradation, they are resolved from both dGuo and dThd. The most common contaminant of DNA is RNA, and ribonucleosides do not interfere with the determination. Moreover, the determination is rapid and can be performed on standard equipment. Although the determination is somewhat sensitive to sample size, if the samples and standards are between 0.5 and 1.5 μg of total deoxynucleosides per injection this effect is negligible. The precision of this method is then on the order of 0.1%. Therefore, for DNA with a composition of 50 mole-% G+C, the precision is on the order of 0.05 mole-%, which represents a 5–10-fold increase in the precision for the determination of mole-% G+C of DNA.

ACKNOWLEDGEMENTS

This work was supported by grant DMB83-51355 from the National Science Foundation, the Georgia Power Company and the University of Georgia Research Foundation.

REFERENCES

1 R. J. Simmonds and R. A. Harkness, *J. Chromatogr.*, 226 (1981) 369.
2 M. Ryba, *J. Chromatogr.*, 219 (1981) 245.
3 A. H. Csárnyi, M. Vajda and J. Sági, *J. Chromatogr.*, 204 (1981) 213.
4 A. A. Miller, *J. Chromatogr.*, 228 (1982) 165.
5 H. Martinez-Valdez, R. M. Kothari, H. V. Hershey and M. W. Taylor, *J. Chromatogr.*, 247 (1982) 307.
6 S. P. Assenza, P. R. Brown and A. P. Goldberg, *J. Chromatogr.*, 277 (1983) 305.
7 S. M. Payne and B. N. Ames, *Anal. Biochem.*, 123 (1982) 151.
8 C. Y. Ko, J. L. Johnson, L. B. Barnett, H. M. McNair and J. R. Vercellotti, *Anal Biochem.*, 80 (1977) 183.
9 K. C. Kuo, R. A. McCune, C. W. Gehrke, R. Midgett and M. Ehrlich, *Nucleic Acids Res.*, 8 (1980) 4763.
10 C. W. Gehrke, R. A. McCune, M. A. Gama-Sosa, M. Ehrlich and K. C. Kuo, *J. Chromatogr.*, 301 (1984) 199.
11 C. F. Mischke and E. Wickstrom, *Anal. Biochem.*, 105 (1980) 181.
12 A. Wakizaka, K. Kurosaka and E. Okuhara, *J. Chromatogr.*, 162 (1979) 319.
13 J. Tamaoka and K. Komagata, *FEMS Microbiol. Lett.*, 25 (1984) 125.
14 J. DeLey, *J. Bacteriol.*, 101 (1970) 738.
15 M. Mesbah, U. Premachandran and W. B. Whitman, *Inter. J. Syst. Bacteriol.*, 39 (1989) 159.
16 W. B. Whitman, J. Shieh, S. Sohn, D. S. Caras and U. Premachandran, *Syst. Appl. Microbiol.*, 7 (1986) 235.
17 C. W. Gehrke, K. C. Kuo and R. W. Zumwalt, *J. Chromatogr.*, 188 (1980) 129.
18 M. Ehrlich, M. A. Gama-Sosa, L. H. Carreira, L. G. Ljungdahl, K. C. Kuo and C. W. Gehrke, *Nucleic Acids Res.*, 13 (1985) 1399.

Journal of Chromatography, 479 (1989) 307–317
Elsevier Science Publishers B.V., Amsterdam — Printed in The Netherlands

CHROM. 21 662

ANALYSIS OF DENSITY-FRACTIONATED RAT RED BLOOD CELLS OF DIFFERENT AGES BY PARTITIONING IN TWO-POLYMER AQUEOUS PHASE SYSTEMS

HARRY WALTER*

**Laboratory of Chemical Biology-151, Veterans Administration Medical Center, Long Beach, CA 90822 (U.S.A.), and the Department of Physiology and Biophysics, University of California, Irvine, CA 92717 (U.S.A.)*

and

EUGENE J. KROB

Laboratory of Chemical Biology, Veterans Administration Medical Center, Long Beach, CA 90822 (U.S.A.)

(Received April 14th, 1989)

SUMMARY

Rats were injected with radioactive iron and bled at different times thereafter. This gave rise to cell populations in which the bulk of labeled cells corresponded in age to the time elapsed between injection and bleeding. Such cell populations were centrifuged and the 7–10% least dense and the 7–10% most dense cells subjected to counter-current distribution in a charge-sensitive two-polymer aqueous phase system which fractionates cells on the basis of surface properties. While it is known that there is a tendency for cell density to increase with cell age and that rat red cells of different ages have characteristic partititon ratios, we were able, by applying partitioning analysis to density-separated cells, to gather data not obtainable by use of either method alone. These include: (1) the demonstration of two very young cell populations having different surface properties in the most dense fraction; (2) the finding that in the least dense layer labeled mature erythrocytes (at least those labeled 18 days and beyond) and unlabeled red cells have overlapping distribution curves which indicate that the label in the top fraction can represent young or early middle-aged but never old cells; and (3) the presence, as judged by surface properties, of some middle-aged red cells, in addition to old cells, in the most dense cell layer.

INTRODUCTION

To study the senescence of red blood cells many investigators have attempted cell fractionations based on age-associated alterations in physical properties [for a recent review, see ref. 1]. Cohort labeling (*e.g.*, with ^{59}Fe) of the youngest cells in the population and tracing, at different subsequent times, the location of the bulk of labeled cells (which approximate in age the time elapsed between injection and bleeding) in the separatory method indicates whether an age-dependent fractionation has occurred. Thus centrifugation has revealed that at least a general correlation exists

0021-9673/89/$03.50

between increasing cell age and density in some species (*e.g.*, human, rat) while counter-current distribution of rat red cells in charge-sensitive two-polymer aqueous phase systems[2] indicates that the surface charge-associated properties of reticulocytes increase rapidly as these cells become young mature erythrocytes while the latter undergo a systematic diminution in partition ratios during their entire life-span.

As the labeled cells age they predominate, as indicated above, in fractions corresponding to cells of higher density. However, cells (except when very young) never band in a narrow density range but rather tend to spread with cell age[3]. Even in the case of young cells small quantities (order of 0.5%) of the labeled cells can also be found in the 7–10% highest density cell layer. Whether labeled cells in a layer other than the one in which they are concentrated are similar to the bulk of labeled cells or represent a distinct cell subpopulation is subject to conjecture. We therefore studied an additional physical parameter of labeled cells, obtained at different times following isotope injection, in high and low density fractions: their surface properties by counter-current distribution in a charge-sensitive two-polymer aqueous phase system.

EXPERIMENTAL

Animal injection and bleeding

Male Sprague-Dawley rats (Charles River Labs., Wilmington, MA, U.S.A.), weighing 275–400 g, were used. Injection of rats with 15–80 μCi of [^{59}Fe]ferrous citrate (ICN, Irvine, CA, U.S.A.) via the saphenous vein as well as the ^{59}Fe-counting procedures used have previously been detailed[4]. Rats were exsanguinated by heart puncture at different times (16 h to 49 days) after injection. About 4 ml of blood were collected in each of two blue-top (sodium citrate) vacutainer tubes.

Murphy centrifugation procedure

A somewhat modified Murphy centrifugation procedure[5] for the fractionation of red blood cells of different ages was used. The Sorvall centrifuge (RC-5) rotor (SS-34) was incubated overnight at 30°C and then spun for 1 h with the centrifuge set to the same temperature. The blood, collected as described above, was first centrifuged (using a 15 ml disposable plastic centrifuge tube) on a table model at 1200 *g* for 30 min in the cold room. The plasma was removed and saved. The buffy coat was aspirated and the plasma added back to the cells. The latter were resuspended and centrifuged once again in a similar manner. The plasma was aspirated and the cells were well mixed. A 0.2-ml volume of cells was taken as the "unfractionated" sample. The remaining red cells were transferred into round-bottom polycarbonate tube (77 × 10.9 mm) (Damon/IEC Division, Needham Heights, MA, U.S.A.) and centrifuged in the Sorvall unit at 26 900 *g* for 60 min at 30°C. The small amount of remaining plasma was aspirated and the top 7–10% of the cells was removed with a 1-ml plastic pipette and represents the "top" fraction. Cells were then slowly aspirated. Prior to aspirating the last 0.5 ml of cells to be discarded, the sides of the tube were rinsed down with isotonic aqueous salt solution (saline) using a Pasteur pipette. The wash solution was aspirated as was the last 0.5 ml of cells to be discarded. With a 1-ml plastic pipette the 7–10% of cells on the bottom were collected and represent the "bottom" fraction. The cells constituting the top, bottom and unfractionated samples were washed three times with saline and finally suspended in 10 ml saline. Aliquots of

these cell suspensions were counted electronically while others were used in counter-current distribution experiments and/or to determine the specific activity ratios of cells in top/cells in unfractionated (or top/bottom) fractions (see below).

Electronic cell counting

Aliquots of washed cells, suspended in saline were electronically counted using a Celloscope (Particle Data, Chicago, IL, U.S.A.) operating on the Coulter principle and fitted with a 76-μm orifice tube.

Determination of specific radioactivity of Murphy-method fractionated cells

Aliquots of top, unfractionated and bottom cell suspensions, each containing $2 \cdot 10^8$ cells, from a Murphy experiment, were centrifuged, the supernatant solution discarded and the cells lysed in 10 ml of a 20 mos*M* sodium phosphate buffer, pH 7.2. After high-speed centrifugation (to remove the stroma) the absorbance of the supernatant solution was read at 540 nm on a Gilford spectrophotometer. ^{59}Fe radioactivity was determined by counting a known aliquot (2.5–3 ml) on a Beckman scintillation well-counter set for ^{59}Fe.

Preparation of phase system

A phase system, selected and prepared as previously described, was used[2]. It contained 5% (w/w) dextran T500, lot No. LL 01035 (Pharmacia LKB, Piscataway, NJ, U.S.A.), 5% (w/w) poly(ethylene glycol) 8000 (PEG, "Carbowax 8000", Union Carbide, Long Beach, CA, U.S.A.), 210 (or 220) mos*M* sodium phosphate buffer, pH 7.4, 60 (or 46) mos*M* sodium chloride and 5% (w/w) heat-inactivated fetal bovine serum (FBS). Such a phase system has an electrostatic potential difference between the phases (top phase positive) and is charge-sensitive (see refs. 2 and 6 for detailed discussion).

The phase system was permitted to equilibrate in a separatory funnel at 4–5°C. Top and bottom phases were then separated.

Counter-current distribution of red blood cells

Our counter-current distribution apparatus (Workshop, Chemical Center, University of Lund, Sweden) consists of two circular Plexiglas plates, one stator and one rotor, having 120 cavities with a bottom phase capacity of 0.7 ml[7]. Counter-current distribution of cells was carried out as previously described[4]. All cavities received 0.5 ml of bottom phase. Aliquots of "unfractionated" cells and "top" and "bottom" cells (from a Murphy centrifugation, see above) corresponding to $2 \cdot 10^9$ cells were centrifuged and the supernatant solutions discarded. The cells were resuspended, using a Pasteur pipette, in 2.3 ml of top phase ("load mix"). Cavities 0–2 received 0.7 ml of one load mix, cavities 40–42 received 0.7 ml of the second load mix and cavities 80–82 the third load mix. All other cavities received 0.7 ml of top phase. Counter-current distribution was then carried out at 4–5°C using a 6-min settling and a 27.5-s shaking time. Thirty or 39 transfers (see Figures) were completed.

Analysis of cells after counter-current distribution

After counter-current distribution the cells in each cavity were collected, by use of a fraction collector, directly into plastic centrifuge tubes. Saline (0.7 ml) was added

to each tube thereby reducing the polymer concentrations and giving rise to a single homogeneous suspending medium. Cells in each three adjacent tubes were pooled. They were centrifuged at 1200 *g* for 10 min, the supernatant solution was discarded, and the cells were lysed by addition of 3 ml of 20 mos*M* sodium phosphate buffer, pH 7.2. The tubes were then centrifuged at high speed to remove the stroma and the hemoglobin absorbance and ^{59}Fe radioactivity was determined as described above.

Presentation of data

The fractionation of rat labeled red blood cells by the Murphy centrifugation procedure is given as the ratio of specific activity (cpm/hemoglobin absorbance) of cells in the top layer to cells in the original, unfractionated cells, T/U[8]. For longer times after injection the ratio of specific activity of cells in the bottom layer to cells in the original, unfractionated cells, B/U, is also presented.

Counter-current distribution curves of total cells are shown in terms of hemoglobin absorbance (at 540 nm). Distributions of labeled (^{59}Fe) cell populations are in counts/min (cpm). A relative specific activity is also presented through the distribution curves and reflects, most sensitively, the extent of displacement and, hence, of difference between the labeled and unlabeled red cell populations. It is defined as:

$$\frac{\text{cpm/unit hemoglobin absorbance in a given cavity}}{\text{cpm/unit hemoglobin absorbance in the original cell population prior to counter-current distribution}}$$

The data depicted in the graphs are representative of at least three separate experiments with individual rats.

RESULTS AND DISCUSSION

Cell age-related fractionation of rat red blood cells by centrifugation

Rats were injected with [^{59}Fe]ferrous citrate and bled at different times (from 16 h to 49 days) thereafter. Erythrocyte populations were thus obtained in which the predominantly labeled cells corresponded in age to the time elapsed between injection and bleeding (*i.e.*, reticulocytes, mature young to old erythrocytes)[1].

Such cell populations were subjected to a Murphy-method centrifugation. The specific radioactivity (in cpm/hemoglobin absorbance) of the original, unfractionated cells as well as of cells constituting the top 7–10% of the centrifuged cell column was determined as a ratio of specific activities of top cells/unfractionated cells (T/U). As previously reported[8], this ratio was approximately constant at 3–4 (range 3.1–3.9) during the first 7 days of the experiment suggesting that reticulocytes (constituting the primary labeled cell population for at least 24 h after isotope injection) and mature young erythrocytes (at the later bleeding times) are both enriched in the top 7–10% layer of centrifuged red cells[a]. Cells in the bottom fraction contained about 0.5% of the labeled young cells.

[a] It should be noted that if one were to express data as specific activity ratios of 7–10% of cells in top/7–10% of cells in bottom at *short* times after isotope injection they would be of the order of 50–250. This variability in the ratio is caused by the low specific activities associated with the bottom fraction at such short times after injection and has prompted us to present specific activity ratios of cells in top/cells in unfractionated cells at these earlier times.

The T/U ratio diminished with time after isotope injection being about 2.2 at 13–14 days, 1.6 at 18–21 days, 0.6 at 28–33 days and 0.4 at 40–49 days[8]; while the analogous B/U ratio increased, from about 0.2 at 18–21 days to 0.8 at 35–36 days and 1.6 at 40–49 days.

Surface properties of rat labeled red blood cells, at different times after ^{59}Fe injection, in top and bottom fractions obtained by Murphy-method centrifugation: analysis by counter-current distribution

Murphy-method fractionated cells as described above were subjected to counter-current distributions. Results of a typical series of such experiments (with cells obtained at different times after injection of rats with isotope) are depicted in Figs. 1–5. The upper panel of each figure presents the counter-current distribution pattern of unfractionated cells, U, the middle panel the counter-current distribution of cells from the top layer, T, of a Murphy-method centrifugation and the lower panel the counter-current distribution of cells from the bottom layer, B, of the centrifugal column.

The top panels of Figs. 1–5 show the previously reported charge-associated surface alterations that accompany rat red blood cell maturation and aging in the peripheral blood[2]. At 16 h after isotope injection (Fig. 1, U) it is the reticulocytes that are labeled. They have a lower partition ratio (presumably lower surface charge-associated properties) than the bulk of the peripheral red cells as evidenced by the position of the distribution of labeled cells (open circles) to the left of the distribution of unlabeled cells (solid circles). The extent of displacement is clearly indicated by the relative specific activity curve (solid triangles).

The partition ratio of reticulocytes increases rapidly[9] during maturation to the youngest erythrocytes (42 h, Fig. 2, U) and, subsequently, slowly diminishes (Figs. 3–5, U) over the entire 55-days life-span of the mature erythrocyte. The oldest erythrocytes in the peripheral blood have a partition ratio that is close to that of the reticulocytes (compare Figs. 1, U, and 5, U, and see ref. 2).

As is evident from all five figures, the least dense cells (T) have a higher partition ratio (*i.e.*, are to the right), most dense cells, B, a lower partition ratio and the original, unfractionated cells, U, an intermediate partition ratio[10–12]. This result (indicated, for easier viewing, by the arrows in Fig. 1) is in line with the fact (see above) that young mature erythrocytes have a high, old mature erythrocytes a low partition ratio[a].

To study the surface properties of labeled red blood cells associated, at different times during their life-span, with cell populations of low and high mean densities we compared the relative partition ratios (*i.e.*, positions in the graphs) of labeled cells from the top and bottom of a cell column after a Murphy-method centrifugation and of unfractionated samples.

In Fig. 1, the reticulocytes associated with centrifuged cells from the top, T, have the same partition ratio as reticulocytes in the unfractionated cell population, U, implying that their charge-associated surface properties, as reflected by partitioning, are the same. The labeled cells in the centrifugate from the bottom, B (representing the small percentage of total labeled cells as indicated by the relative cpm scales on the

[a] The youngest reticulocytes, which have a low partition ratio, constitute a very small percentage of the total peripheral red cell population. They thus do not affect the higher partition ratio of cells of lower density (primarily mature younger erythrocytes) obtained on Murphy centrifugation.

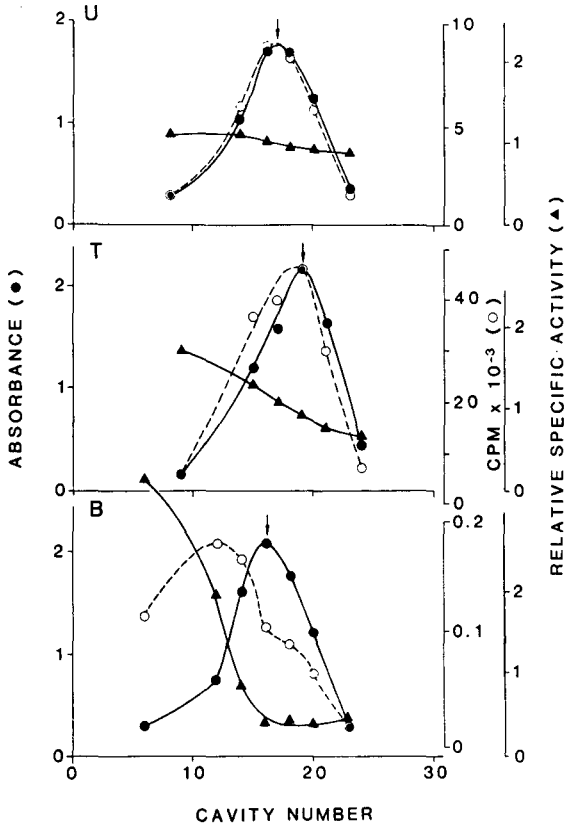

Fig. 1. Rats were injected with [^{59}Fe]ferrous citrate and bled at different times thereafter. This gave rise to rat cell populations in which the bulk of labeled cells corresponds in age to the time elapsed between injection and bleeding. Such cell populations were fractionated, in succession, on the basis of density and surface properties. Cells were centrifuged and the top layer, T, containing predominantly young cells, the bottom layer, B, containing older cells, and an aliquot of unfractionated cells, U, were subjected to counter-current distribution in a charge-sensitive two-polymer aqueous phase system (see text for composition). Thirty transfers were carried out at 4–5°C using 6-min settling and 27.5-s shaking times. The run was analyzed for total cell distribution (●, in terms of hemoglobin absorbance at 540 nm) and labeled cell distribution (○, in terms of cpm). A relative specific activity is also presented (▲) with 1.0 being the specific activity of each sample prior to counter-current distribution. Note that the unlabeled bulk of cells in T have a higher partition ratio (*i.e.*, are to the right) than those in B, while U cells have an intermediate ratio (see arrows above the distribution curves of total cells). In this figure results are depicted with blood collected 16 h after injection when it is the reticulocytes that are labeled and most of the label is in T and least in B (note cpm scales). See text for discussion.

three panels) are composed of two subpopulations. Those with the higher partition ratio consist of cells similar in partitioning behavior to reticulocytes found in the top fraction[a]. An analogous experiment done with blood obtained at 42 h after ^{59}Fe injection (Fig. 2, B) shows that the two cell subpopulations remain in evidence with the left peak diminishing in relative size. This process continues for about 3–4 (some-

[a] For easier viewing this is indicated in Fig. 2, depicting an analogous experiment with red cells collected 42 h after injection, by the broken-line arrows.

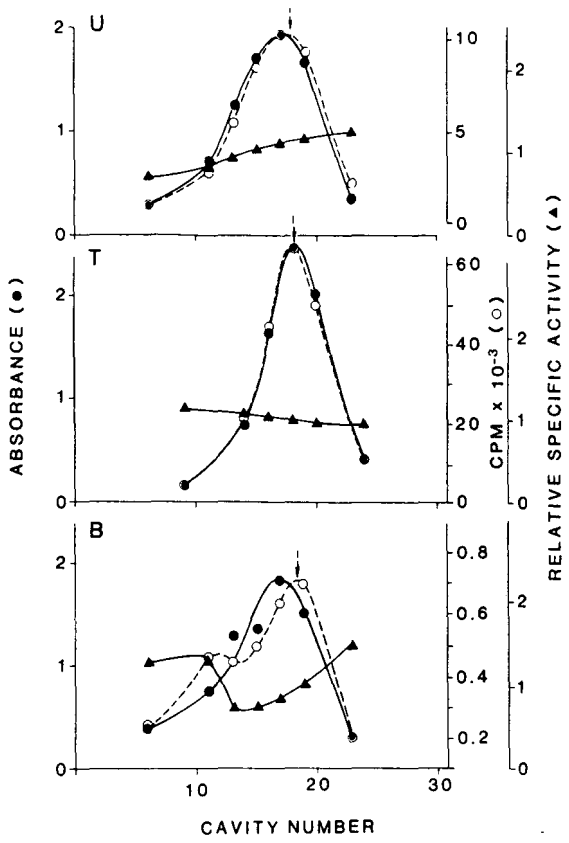

Fig. 2. Experiment as in Fig. 1 except that blood was collected 42 h after injection when the label is predominantly in mature young erythrocytes. For easier visualization of the similar positions of labeled cells in T and U and those having the higher partition ratio in B a broken arrow has been placed over each of the isotope peaks. See text for details.

times even 6) days following isotope injection after which the left peak disappears.

We have previously traced, by partitioning, the surface alterations that accompany erythroid cell differentiation in the rat bone marrow[13] and reticulocyte maturation in the peripheral blood (see ref. 9, Figs. 1 and 2 and discussion above) and have found that these processes are accompanied by increases in the cells' partition ratios. It is therefore tempting to speculate that the labeled red cells with the lower partition ratio associated with the centrifugal bottom cell fraction are representative of the youngest cells in the peripheral blood.

In the case of mice the youngest red cells are more dense than older cells during the first day or so after release from the bone marrow and then (possibly after restructuring in the spleen[14]) become less dense[15]. Whether a small percentage of rat reticulocytes behaves in a similar manner is not known. Alternatively, it is possible that the labeled rat cell populations in the bottom are qualitatively representative of those in the top fraction but that, due to differences in physical properties (*e.g.*, a differential tendency to adhere to other cells), cells with lower partition ratios appear to a rela-

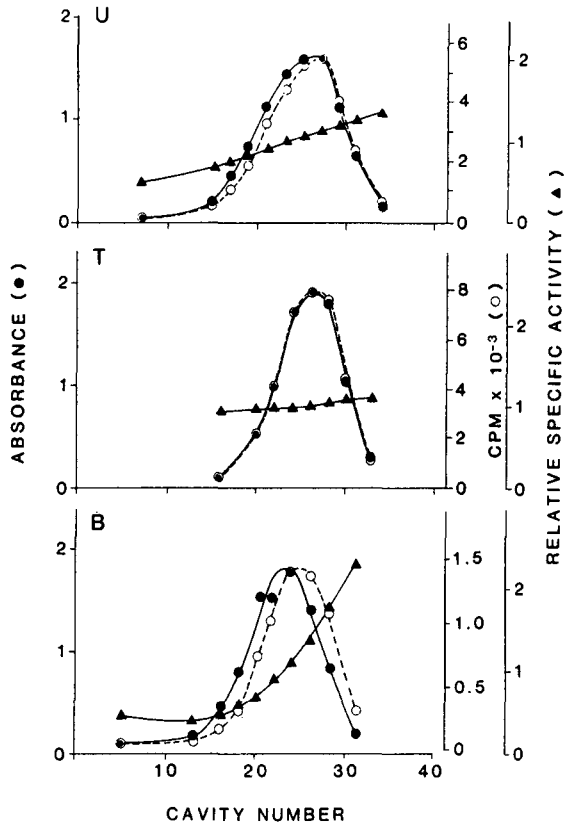

Fig. 3. Experiment as in Fig. 1 except that the blood was collected 18 days after isotope injection when the label is predominantly in early middle-aged cells. Thirty-nine transfers were carried out. See text for discussion.

tively greater extent in the bottom fraction than do those with the higher partition ratios.

At 6–7 days after isotope injection (data not shown) labeled cells in unfractionated, top and bottom fractions have the same partition ratio which is slightly greater (*i.e.*, is displaced to the right) than that of unlabeled cells in the least dense (T) fraction. Hence the labeled cells at this time are younger than the mean age of the 7–10% least dense cells.

Fig. 3 depicts results with rat erythrocytes containing labeled cells 18 days after isotope injection. These have mean surface properties similar to those of the young, lower-density cells in the top fraction in a Murphy-method centrifugation, as indicated by the virtual overlap of labeled and total cell distributions (Fig. 3, T). The labeled cells also have the same partition ratios (*i.e.*, positions) in the bottom fraction and in the unfractionated cell sample (Fig. 3, B and U). Thus, 18-days labeled cells in low- and high-density fractions have the same mean surface properties, those associated with early middle-aged rat erythrocytes[2,16].

At 35 days after isotope injection (Fig. 4) labeled cells overlap not only with the

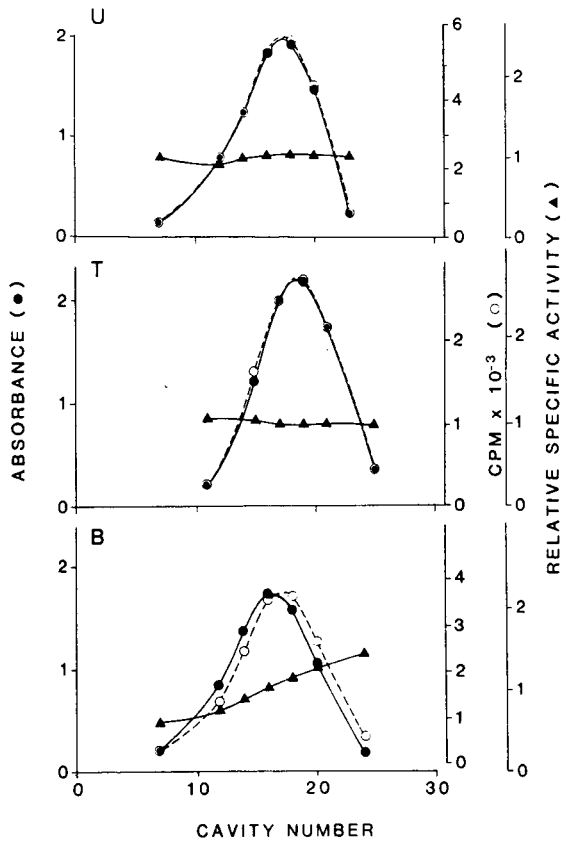

Fig. 4. Experiment as in Fig. 1 except that the blood was collected 35 days after isotope injection when the label is predominantly in middle-aged cells. See text for discussion.

distribution of unfractionated cells (Fig. 4, U) but also with that of low-density (younger) cells (Fig. 4, T) as indicated by specific activity ratios of 1.0 through the distribution curves in both cases. Since red blood cells in unfractionated and low-density fractions have different partition ratios (see discussion above and arrows in Fig. 1), the labeled cells in the two parts of the figure must represent different cell subpopulations. The labeled cells in the low-density fraction are younger than the mean age of those in the unfractionated cells. Reutilization of ^{59}Fe (refs. 1 and 16) in the formation of young cells, as older cells break down and release their ^{59}Fe, is the most likely basis for this result. The labeled unfractionated cells (Fig. 4, U) have the same partition ratio (associated with middle-aged erythrocytes[2,16]) as the labeled cells in the high-density fraction (Fig. 4, B).

Fig. 5 shows results obtained with erythrocytes 48 days after isotope injection. At this time labeled and unlabeled cells are found to overlap in both the least dense (Fig. 5, T) and most dense (Fig. 5, B) fractions. Since the partition ratios of these cells differ (again see discussion above and arrows in Fig. 1) it is apparent that the labeled cells in these two fractions also differ. They reflect subpopulations of different cell age:

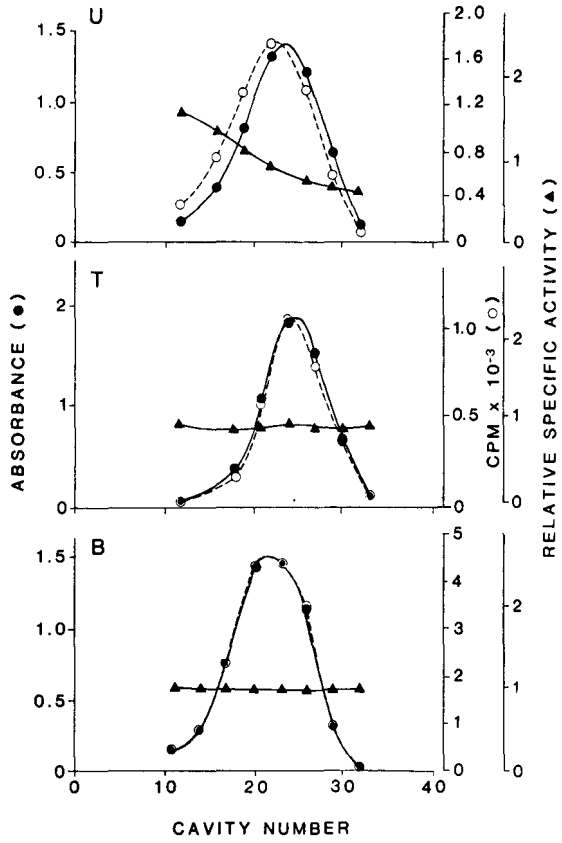

Fig. 5. Experiment as in Fig. 3 except that the blood was collected 48 days after isotope injection when the label is predominantly in old cells. See text for discussion.

younger cells with higher partition ratio (Fig. 5, T) and older cells with lower partition ratio (Fig. 5, B). Labeled cells in the unfractionated sample (Fig. 5, U) have the same partition ratio as those in the most dense fraction as might be expected since more of the label is now in the older cells and the unfractionated sample represents a mean.

ACKNOWLEDGEMENT

This work was supported by the Medical Research Service of the Veterans Administration.

REFERENCES

1 M. R. Clark, *Physiol. Rev.*, 68 (1988) 503.
2 H. Walter, in H. Walter, D. E. Brooks and D. Fisher (Editors), *Partitioning in Aqueous Two-Phase Systems: Theory, Methods, Uses, and Applications to Biotechnology*, Academic Press, Orlando, FL, 1985, pp. 327–375.

3 R. C. Leif and J. Vinograd, *Proc. Natl. Acad. Sci. U.S.A.*, 51 (1964) 520.
4 H. Walter, E. J. Krob, A. Pedram, C. H. Tamblyn and G. V. F. Seaman, *Biochim. Biophys. Acta,* 860 (1986) 650.
5 J. R. Murphy, *J. Lab. Clin. Med.*, 82 (1973) 334.
6 D. E. Brooks, K. A. Sharp and D. Fisher, in H. Walter, D. E. Brooks and D. Fisher (Editors), *Partitioning in Aqueous Two-Phase Systems. Theory, Methods, Uses, and Applications to Biotechnology*, Academic Press, Orlando, FL, pp. 11–84.
7 P.-Å. Albertsson, *Anal. Biochem.*, 11 (1965) 121.
8 H. Walter, E. J. Krob, R. B. Wenby and H. J. Meiselman, *Cell Biophys.*, in press.
9 H. Walter, A. Miller, E. J. Krob and G. S. Ascher, *Exptl. Cell Res.*, 69 (1971) 416.
10 H. Walter, E. J. Krob, C. H. Tamblyn and G. V. F. Seaman, *Biochem. Biophys. Res. Commun.*, 97 (1980) 107.
11 H. Walter and E. J. Krob, *Cell Biophys.*, 5 (1983) 205.
12 H. Walter and E. J. Krob, *Cell Biophys.*, 5 (1983) 301.
13 H. Walter, E. J. Krob and G. S. Ascher, *Exptl. Cell Res.*, 79 (1973) 63.
14 S. H. Song and A. C. Groom, *Can. J. Physiol. Pharmacol.*, 50 (1972) 400.
15 M. Morrison, C. W. Jackson, T. J. Mueller, T. Huang, M. E. Dockter, W. S. Walker, J. A. Singer and H. H. Edwards, *Biomed. Biochim. Acta,* 42 (1983) 107.
16 H. Walter and F. W. Selby, *Biochim. Biophys. Acta*, 112 (1966) 146.

Journal of Chromatography, 479 (1989) 319–325
Elsevier Science Publishers B.V., Amsterdam — Printed in The Netherlands

CHROM. 21 684

HIGH-PERFORMANCE LIQUID CHROMATOGRAPHIC DETERMINATION OF SECONDARY CARDIAC GLYCOSIDES IN *DIGITALIS PURPUREA* LEAVES

YOUICHI FUJII*, YUKARI IKEDA and MITSURU YAMAZAKI
School of Pharmacy, Hokuriku University, 3 Ho, Kanagawa-machi, Kanazawa 920-11 (Japan)
(First received April 6th, 1989; revised manuscript received June 12th, 1989)

SUMMARY

An analytical method for the determination of secondary cardiac glycosides in *Digitalis purpurea* leaves by high-performance liquid chromatography (HPLC) is described. The procedure consisted of extraction of dry leaf powder with ethanol–chloroform (2:1) and clean-up by Sep-Pak cartridges prior to HPLC analysis. HPLC was performed on an octylsilyl bonded silica column, using acetonitrile–methanol–water (4:4:5) for trisdigitoxosides and acetonitrile–methanol–water (8:30:43) for strospeside; the effluent was monitored by ultraviolet detection (at 220 nm). Quantitation of these cardiac glycosides was carried out by the internal standard method. The amounts of digitoxin, gitoxin, gitaloxin and strospeside per 100 mg of dry leaf powder were estimated to be 22.6, 14.0, 54.7 and 1.9 μg, respectively. The method is sufficiently sensitive and reproducible to assay secondary glycosides in *Digitalis purpurea* leaves.

INTRODUCTION

The digitalis glycosides are well known as a group of important medical therapeutic agents for the treatment of heart disease. *Digitalis purpurea* leaves contain secondary glycosides such as digitoxin, gitoxin, gitaloxin and strospeside which are produced by the enzymatic conversion of primary glycosides of purpurea glycoside A, purpurea glycoside B, glucogitaloxin and digitalinum verum, respectively.

Previously published methods of determining secondary glycosides in *Digitalis purpurea* leaves have utilized paper chromatographic[1] and thin-layer chromatographic (TLC)[2–5] techniques, but they did not always yield accurate quantitation of cardiac glycosides in the leaves. High-performance liquid chromatography (HPLC) appears to be more suitable for the determination of secondary glycosides. The separation of various mixtures of these compounds was accomplished by use of a normal-phase silica column[6–8] and a reversed-phase C_{18} column[8]. In addition, Nachtmann *et al.*[9] have proposed the separation of digitalis glycosides by HPLC following precolumn derivatization with 4-nitrobenzoyl chloride. However, there have been few attempts to introduce HPLC for the quantitation of cardiac glycosides in the extract of *Dig-*

0021-9673/89/$03.50

italis purpurea leaves. Wichtl *et al.*[10] have carried out the quantitation of digitoxin and several primary glycosides in the leaves using gradient elution, but not data on gitoxin, gitaloxin and strospeside were given.

In the previous paper of this series we reported the micro-HPLC analysis of purpurea glycoside A, purpurea glycoside B and glucogitaloxin in *Digitalis purpurea* leaves[11]. The present study focuses on the quantitative method for secondary cardiac glycosides from the extract of such leaves, which involves clean-up with Sep-Pak cartridges followed by HPLC on a reversed-phase C_8 column with ultraviolet (UV) detection (at 220 nm).

EXPERIMENTAL

Instruments

The HPLC system consisted of a JASCO 880-PU pump (Japan Spectroscopic, Tokyo, Japan), a Model KHP-UI-130 injector (Kyowa Seimitsu, Tokyo, Japan), a Model UV-8010 detector (Tosoh, Tokyo, Japan) monitoring the absorbance at 220 nm and a Chromatopac C-R3A data processor (Shimadzu, Kyoto, Japan). The stainless-steel column (150 mm × 4.6 mm I.D.) was packed with Chemcosorb 5 C_8-U (Chemco Scientific, Osaka, Japan). This was a reversed-phase column containing 5-μm porous silica particles linked covalently with octylsilyl groups.

Materials

Gitoxin and digoxin were obtained from E. Merck (Darmstadt, F.R.G.), gitaloxin and strospeside from Boehringer Mannheim (Mannheim, F.R.G.), digitoxin from Wako (Osaka, Japan) and Sep-Pak cartridges from Waters (Milford, MA, U.S.A.). The chemical structures of digitoxin, gitoxin, gitaloxin and strospeside are given in Fig. 1. 14α,15α-Epoxy-"β"-anhydrodigitoxin (internal standard I) was synthesized in four steps from digitoxin according to the procedure of Sawlewicz *et al.*[12] and recrystallized repeatedly from methanol. Digoxigenin bisdigitoxoside (internal standard II) was also prepared from digoxin by the method of Haack *et al.*[13]. All of these compounds were checked for homogeneity by TLC, and solvents were purified by redistillation prior to use.

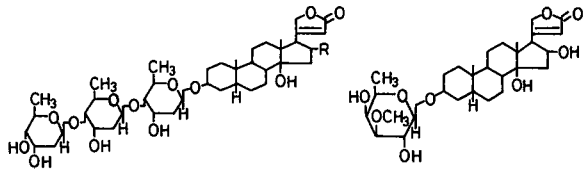

Fig. 1. Structures of the secondary glycosides investigated.

Preparation of the leaf powder

Leaves of *Digitalis purpurea* L. plant in the second year were collected in the medicinal botanical garden (Kanazawa, Japan) of Hokuriku University on June 21. The harvested leaves were quickly washed with water and immediately stored at

−4°C for 17 months. The frozen leaves were freeze-dried in a Neocool Model DC-55A apparatus (Yamato Scientific, Tokyo, Japan), and then dried using phosphorus pentoxide under reduced pressure at room temperature. The dried leaves were pulverized and sifted through a sieve of mesh width 500 μm. The leaf powder obtained was further dried under reduced pressure for 5 days.

Extraction and clean-up procedures

About 50 mg of leaf powder were accurately weighed and added to ethanol–chloroform (2:1) (25 ml) containing 14α,15α-epoxy-"β"-anhydrodigitoxin (44.69 μg) and digoxigenin bisdigitoxoside (1.18 μg) as internal standards. After ultrasonication for 1 h in an ultrasonic cleaning bath, the extract was filtered and evaporated to dryness using a rotary evaporator. The residue was dissolved in chloroform–acetic acid (100:0.1) (2 ml) and applied to the Sep-Pak silica cartridge. Chloroform–acetic acid (100:0.1) (28 ml) and chloroform–methanol–acetic acid (100:5:0.01) (25 ml) were successively passed through the cartridge. After evaporation of the latter fraction, the residue obtained was dissolved in methanol–water–acetic acid (10:30:0.04) (1 ml) and loaded on the Sep-Pak C_{18} cartridge. After washing with methanol–water–acetic acid (10:30:0.04) (9 ml), secondary glycosides and internal standards were eluted with methanol–water–acetic acid (20:10:0.03) (20 ml). The eluate was evaporated to dryness *in vacuo*.

Determination of secondary glycosides

For the simultaneous determination of trisdigitoxosides, the extract pretreated above was dissolved in acetonitrile–methanol–water (4:4:5) (0.5 ml) and analyzed by HPLC. The remaining solution was dried under a gentle stream of nitrogen, and the resulting material was redissolved in acetonitrile–methanol-water (8:30:43) (0.1 ml) and used for the determination of strospeside by HPLC.

A 10-μl volume of each sample was injected into the liquid chromatograph and the flow-rate was adjusted to 0.5 ml/min. The separations were performed under ambient conditions. The mobile phase for each separation is listed with each chromatogram. Digitoxin, gitoxin, gitaloxin and strospeside in *Digitalis purpurea* were determined by the internal standard method. Calibration graphs were constructed using the average peak areas from three chromatograms.

TLC procedure

Normal-phase and reversed-phase TLC were performed on 5 cm × 10 cm high-performance silica gel 60 F_{254} plates (E. Merck) with a preadsorbent spotting area and 5 cm × 10 cm $KC_{18}F$ plates (Whatman, Clifton, NJ, U.S.A.), respectively. Aliquots (2 μl) of the solutions were spotted with Drummond Microcap micropipettes on TLC plates. The plates were developed in glass chambers that were lined with paper and preequilibrated with mobile phase for 10 min. After air drying, the plates were checked by fluorescence quenching of the layers under UV light around 254 nm, and then sprayed with concentrated sulphuric acid and heated in an oven at 120°C for 5 min.

RESULTS AND DISCUSSION

Our initial effort was directed to the chromatographic separation of secondary glycoside mixtures and the selection of the internal standard. The separation was achieved by using two kinds of isocratic solvent systems, because the polarity of strospeside is much different from that of a group of trisdigitoxosides. 14α,15α-Epoxy-"β"-anhydrodigitoxin (internal standard I) and digoxigenin bisdigitoxoside (internal standard II) were found to be the most suitable for the separations of trisdigitoxosides and strospeside, respectively. HPLC was performed on an octylsilyl bonded silica column using a ternary solvent mixture of acetonitrile, methanol and water. A detection wavelength of 220 nm was employed on the basis of the α,β-unsaturated lactone ring attached at the C-17 position of the steroid nucleus. Fig. 2 shows the chromatogram of a mixture of trisdigitoxosides (digitoxin, gitoxin and gitaloxin) and internal standard I. These compounds were separated into four peaks using acetonitrile–methanol–water (4:4:5) as the eluent. The retention times for gitoxin, gitaloxin, digitoxin and internal standard I were 10.6, 13.2, 20.4 and 23.3 min, respectively. On the other hand, the separation of strospeside and internal standard II was accomplished when acetonitrile–methanol–water (8:30:43) was employed as the mobile phase, as illustrated in Fig. 3.

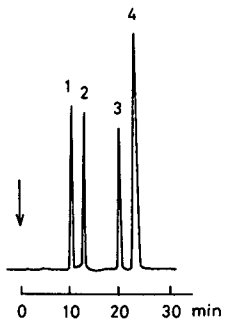

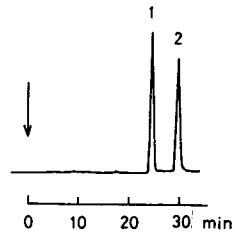

Fig. 2. Separation of a mixture of digitoxin, gitoxin, gitaloxin and internal standard I. Peaks: 1 = gitoxin; 2 = gitaloxin; 3 = digitoxin; 4 = 14α,15α-epoxy-"β"-anhydrodigitoxin. Conditions: Chemcosorb 5 C_8-U column (150 mm × 4.6 mm I.D.); mobile phase, acetonitrile–methanol–water (4:4:5); flow-rate, 0.5 ml/min; UV monitor at 220 nm; sample volume, 10 μl.

Fig. 3. Separation of a mixture of strospeside and internal standard II. Peaks: 1 = strospeside; 2 = digoxigenin bisdigitoxoside. Mobile phase: acetonitrile–methanol–water (8:30:43). Other conditions as in Fig. 2.

On the basis of these data, the determination of secondary glycosides in *Digitalis purpurea* leaves was carried out. The dried leaf powder was extracted with ethanol–chloroform (2:1) by ultrasonication. Many coexisting materials in the extract exert a significant influence on the HPLC separation of these glycosides. Therefore, Sep-Pak cartridges packed with silica gel and ODS-bonded silica gel were used in a clean-up step prior to HPLC. The purified material was subjected to HPLC using the two types of mobile phases as described above. Figs. 4 and 5 depict representative chromatograms of trisdigitoxosides and strospeside, respectively, in the extract after

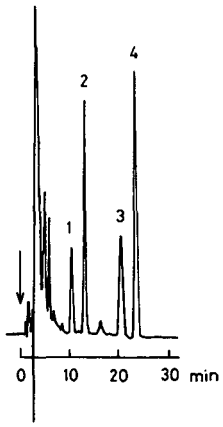

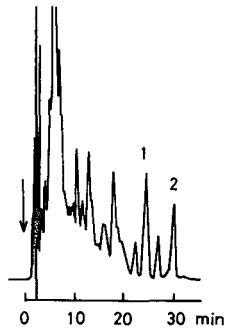

Fig. 4. Chromatogram of the extract of *Digitalis purpurea* leaves for the determination of digitoxin, gitoxin and gitaloxin. Peaks: 1 = gitoxin; 2 = gitaloxin; 3 = digitoxin; 4 = 14α,15α-epoxy-"β"-anhydrodigitoxin. Conditions as in Fig. 2.

Fig. 5. Chromatogram of the extract of *Digitalis purpurea* leaves for the determination of strospeside. Peaks: 1 = strospeside; 2 = digoxigenin bisdigitoxoside. Conditions as in Fig. 3.

incorporation of the internal standards. From chromatograms of the extract in the absence of the internal standards, the coexisting substances present were ascertained not to interfere with the peaks due to internal standards I and II. The eluate corresponding to each peak on the chromatograms was collected and evaporated *in vacuo*. The materials obtained were analyzed by both normal-phase TLC (digitoxin, R_F 0.61; gitaloxin, R_F 0.59; gitoxin, R_F 0.49 and strospeside, R_F 0.38) using cyclohexane–ethyl acetate–ethanol–acetic acid (9:5:4:0.02) as a developing solvent and reversed-phase TLC (strospeside, R_F 0.56; gitoxin, R_F 0.47; gitaloxin, R_F 0.40 and digitoxin, R_F 0.32) using acetonitrile–0.5 *M* NaCl (10:13). No impurities were detected on both TLC plates on exposure to UV light around 254 nm and visualization using concentrated sulphuric acid spray. These results indicated single components in each zone with retention times corresponding to digitoxin, gitoxin, gitaloxin and strospeside. Linear calibration graphs were obtained by plotting the peak area ratios, y, of each trisdigitoxoside to internal standard I and of strospeside to internal standard II against the amount of each compound, x (μg). The regression equations, ranges of linearities, R, and correlation coefficients, r, were $y = 0.0340\,x - 0.0020$ (R 2–20 μg, $r = 0.997$) for digitoxin, $y = 0.0315\,x - 0.0007$ (R 2–16 μg, $r = 0.997$) for gitoxin, $y = 0.0246\,x + 0.0060$ (R 5–40 μg, $r = 0.999$) for gitaloxin and $y = 1.017\,x - 0.002$ (R 0.1–2.0 μg, $r = 0.999$) for strospeside.

The quantitation of trisdigitoxosides and strospeside in *Digitalis purpurea* by the proposed method was then undertaken. The assay results obtained from ten determinations of dry leaf powder samples are compiled in Table I. The data indicate that the average contents of digitoxin, gitoxin, gitaloxin and strospeside per 100 mg of the dry leaf powder were 22.6, 14.0, 54.7 and 1.9 μg, respectively. The amount of strospeside in the leaves was considerably lower, as compared with the other compounds. The coefficients of variation were found to be within 2.8–6.6%. The recovery

TABLE I

CONTENTS OF THE SECONDARY GLYCOSIDES IN *DIGITALIS PURPUREA* LEAVES OBTAINED BY THE PRESENT METHOD

Values are the amounts per 100 mg of a dry leaf powder sample.

Glycoside	*Found (μg)*		*Mean ± S.D. (μg)*	*C.V. (%)*
Digitoxin	21.31	23.73		
	21.38	23.45		
	22.55	23.15		
	23.17	20.80		
	23.47	22.95	22.6 ± 1.0	4.6
Gitoxin	15.43	13.15		
	14.30	14.04		
	13.70	14.06		
	14.78	13.42		
	13.53	13.45	14.0 ± 0.7	5.0
Gitaloxin	53.42	54.35		
	55.17	56.42		
	53.13	53.82		
	53.61	57.57		
	55.97	53.35	54.7 ± 1.5	2.8
Strospeside	1.77	1.91		
	1.83	1.97		
	2.11	1.96		
	2.03	1.71		
	2.05	1.88	1.9 ± 0.1	6.6

was examined by adding pure secondary glycosides to dry leaf powder samples and following the procedure described. Added glycosides equivalent to half of the amount of each glycoside contained in the leaves were recovered sufficiently, more than 96%. The values of the coefficient of variation and recovery indicated the quantitative usefulness of this HPLC method.

In the present study, the HPLC determination of secondary glycosides was achieved by using two different isocratic solvent systems and two internal standards because of the large differences in polarities of trisdigitoxoside and strospeside. The pretreatment with Sep-Pak cartridges was much more efficient and convenient than the previous method[14] consisting of a solvent-partition sequence and preparative TLC. Gitaloxin is known readily to lose the formyl group at position C-16 giving rise to gitoxin, especially under alkaline conditions. Therefore, a very small amount of acetic acid was added to the eluent used with the Sep-Pak cartridges, in order to prevent deformylation of gitaloxin. Our value for gitaloxin in comparison with gitoxin was higher than previous results obtained by paper chromatography[1] or TLC[3,4]. On the other hand, the content of strospeside in the leaves was almost the same as that reported by Lugt and Noordhoek-Ananias[4]. In conclusion, digitoxin, gitoxin, gitaloxin and strospeside in *Digitalis purpurea* leaves can be analyzed with good resolution and reproducibility by the HPLC method described. This technique may be useful for estimation of the quality of *Digitalis* leaves.

ACKNOWLEDGEMENT

The authors thank the staff of the medicinal botanical garden of Hokuriku University for providing the leaves of *Digitalis purpurea.*

REFERENCES

1 P. A. Linley, *Planta Med.*, 23 (1973) 272.
2 M. A. Elkiey, Z. F. Ahmed, E. M. Abdelkader and S. M. Abdelwahab, *J. Pharm. Sci. U.A.R.*, 5 (1964) 139.
3 Ch. B. Lugt, *Planta Med.*, 23 (1973) 176.
4 Ch. B. Lugt and L. Noordhoek-Ananias, *Planta Med.*, 25 (1974) 267.
5 S. M. Khafagy and A. N. Girgis, *Planta Med.*, 25 (1974) 350.
6 P. H. Cobb, *Analyst (London)*, 101 (1976) 768.
7 P. A. Linley and A. G. M. Mohamed, *J. High Resolut. Chromatogr. Chromatogr. Commun.*, 4 (1981) 239.
8 F. Erni and R. W. Frei, *J. Chromatogr.*, 130 (1977) 169.
9 F. Nachtmann, H. Spitzy and R. W. Frei, *J. Chromatogr.*, 122 (1976) 293.
10 M. Wichtl, W. Wichtl-Bleier and M. Mangkudidjojo, *J. Chromatogr.*, 247 (1982) 359.
11 Y. Fujii, Y. Ikeda and M. Yamazaki, *J. High Resolut. Chromatogr. Chromatogr. Commun.*, 10 (1987) 137.
12 L. Sawlewicz, H. H. A. Linde and K. Meyer, *Helv. Chim. Acta*, 51 (1968) 1353.
13 E. Haack, F. Kaiser and H. Spingler, *Naturwissenschaften*, 44 (1957) 633.
14 Y. Fujii, H. Fujii and M. Yamazaki, *J. Chromatogr.*, 258 (1983) 147.

Journal of Chromatography, 479 (1989) 327–334
Elsevier Science Publishers B.V., Amsterdam — Printed in The Netherlands

CHROM. 21 682

HYDROPHOBIC INTERACTION CHROMATOGRAPHY OF PROTEINS ON SEPARON HEMA

I. THE EFFECT OF AN INITIAL SALT CONCENTRATION ON THE SEPARATION OF PROTEINS

IMRICH KLEINMANN, JAN PLICKA, PETR ŠMÍDL and VRATISLAV SVOBODA*
Institute for Research, Production and Application of Radioisotopes, Radiová 1, 102 27 Prague 10 (Czechoslovakia)

(First received November 1st, 1988; revised manuscript received June 14th, 1989)

SUMMARY

The influence of an initial salt concentration, φ_0, on the gradient separation of proteins using hydrophobic interaction chromatography on Separon HEMA 1000 was investigated. The results obtained were compared with the retention times and peak widths calculated according to a mathematical model.

INTRODUCTION

High-performance hydrophobic interaction chromatography is a widely used technique for the separation of proteins. A number of reports[1–18] dealing both with the theoretical and the practical aspects of the method has been published. For the separation of proteins, generally a linear gradient of decreasing salt concentration, usually of ammonium sulphate in a low concentration of buffer at constant pH, is used. The resolution is inversely proportional to the square root of the gradient slope, g[17] (dimension M/ml). The gradient slope is usually changed by choosing various gradient times, t_g. The influence of the initial salt concentration on the resolution of protein peaks has been of little interest up to now[1,2,4,7]. The increased retention of proteins with increasing initial salt concentration and the effect on the recovery during separation were usually stressed.

Some other studies related to the gradient elution of proteins, mainly by reversed-phase chromatography, have been published recently[19–22].

The effect of the initial salt concentration at the gradient on the retention time, t_R, or on the peak width, σ_R^2, may be theoretically explained by applying, *e.g.*, the basic equation[23] describing the mass balance of the given component on the column at the point x and time t

$$\frac{\partial C(x,t)}{\partial t} + \frac{1-\varepsilon}{\varepsilon} \cdot \frac{\partial \bar{C}(x,t)}{\partial t} = D \cdot \frac{\partial^2 C(x,t)}{\partial x^2} - u \cdot \frac{C(x,t)}{\partial x} \quad (1)$$

0021-9673/89/$03.50

where u = the velocity of the mobile phase in cm/s, D = the axial dispersion coefficient in cm^2/s, ε = the fraction of the column void volume, $\bar{C}$ = the concentration of solute in the stationary phase in M of the stationary phase and C = the concentration of solute in the mobile phase in M. l is a distance reached by a pertinent component from the top of the column in a given time interval. l is an independent variable in the differential forms of eqns. 2 and 3.

In the case of equilibrium linear chromatography, the analytical solution of eqn. 1 exists, for the condition of the Dirac input signal. It has been published, *e.g.*, by Kučera[24] in the form of the relationships for the nth normalized statistical and central moments of the elution curve, for example for the first moment, μ_1', and the second central moment, μ_2 where L = the column length and k' = the capacity factor.

$$\mu_1' = t_R = \frac{L}{u}(1 + k') + \frac{2D}{u^2}(1 + k') \tag{2}$$

$$\mu_2 = \sigma_R^2 = 2D \cdot \frac{L}{u^3}(1 + k')^2 + \frac{8D^2}{u^4}(1 + k')^2 \tag{3}$$

Eqn. 2 in a differential form is used to compute the retention time, t_R, at gradient elution. Both k' and D are changed along the column during the movement of a pertinent component:

$$dt_R = \frac{1 + k'}{u} \cdot dl + \frac{1}{u} \cdot \frac{dk'}{dl} \cdot dl + 2\frac{1 + k'}{u^2} \cdot \frac{dD}{dl} \cdot dl + \frac{2D}{u^2} \cdot \frac{dk'}{dl} \cdot dl \tag{4}$$

$l \in \langle 0, L \rangle$

Similarly for the computation of σ_R^2, eqn. 3 in a differential form is used:

$$d\sigma_R^2 = 2D \cdot \frac{(1 + k')^2}{u^3} \cdot dl + \frac{2l}{u^3}(1 + k')^2 \frac{dD}{dl} + \frac{4Dl}{u^3}(1 + k') \frac{dk'}{dl} \cdot dl +$$

$$+ \frac{16D}{u^4}(1 + k')^2 \frac{dD}{dl} \cdot dl + \frac{16D^2}{u^4}(1 + k') \frac{dk'}{dl} \cdot dl \tag{5}$$

If these equations are used for the description of gradient elution chromatography, the peak sharping has to be taken in account[25,26]. This occurs due to the difference in the rate of movement of the two peak wings. This correction of eqn. 5 may be expressed in differential form as:

$$d\sigma_{RC} = d\sigma_R - d\sigma_C \tag{6}$$

It is possible to evaluate the correction term $d\sigma_C$ by numerical solution of eqns. 4–6 (see below).

EXPERIMENTAL

The stainless-steel column (100 mm × 4 mm I.D.) was packed with Separon HEMA 1000, 10 μm (Tessek, Prague, Czechoslovakia). A Spectra Physics 8700 XL gradient pump (San José, CA, U.S.A.) was employed. Proteins were injected on the column always after the dwell time of the gradient system had elapsed (time necessary for the change in mobile phase composition to reach the top of the column, in our case 7.5 min at a flow-rate of 0.5 ml/min). All proteins used in this study (lysozyme, ovalbumin, transferrin, ribonuclease A, carbonic anhydrase, myoglobin and cytochrome *c*) were obtained from Sigma (St. Louis, MO, U.S.A.). Proteins were dissolved in 0.1 *M* phosphate buffer, pH 7.0, containing the initial concentration of ammonium sulphate chosen for a given gradient. Volumes of 20–60 μl of each protein solution were injected on the column. The UV detector Uvicord S 2138 (Pharmacia-LKB, Bromma, Sweden) was operated at 275 nm and connected to a 4290 Spectra Physics integrator.

The void volume was determined as the retention volume of pure phosphate buffer injected on the column washed with the solution of ammonium sulphate in phosphate buffer. The values obtained in this way were in good agreement with the retention volumes of non-retained hydrophilic proteins (cytochrome *c*, myoglobin) in sufficiently low concentration of salt, and also with results described earlier[27].

RESULTS AND DISCUSSION

In the case of isocratic elution of proteins, as in refs. 16 and 18, the logarithm of the capacity factor, log k', is usually proportional to the molar concentration of ammonium sulphate φ, see Fig. 1. The differences between the individual proteins

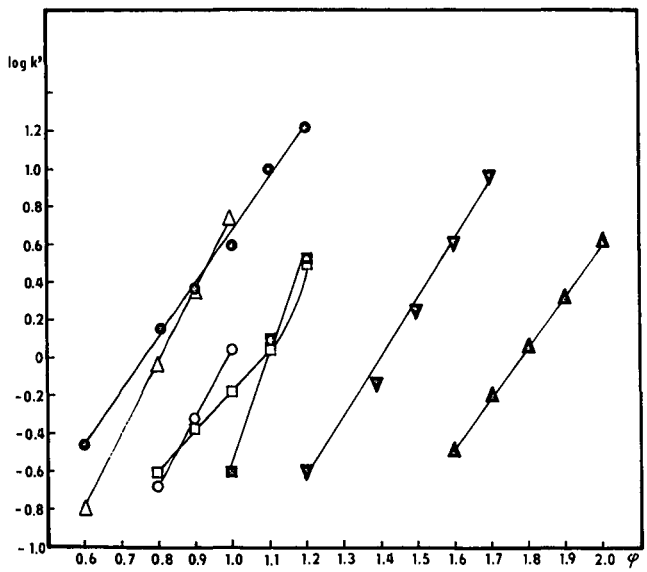

Fig. 1. The dependences of the logarithm of the capacity factor (log k') on the concentration of ammonium sulphate [$\varphi(M)$] in 0.1 *M* phosphate buffer pH 7.0 for the isocratic elution of proteins: ■, transferrin; □, ribonuclease A; △, carbonic anhydrase; ○, ovalbumin; ●, lysozyme; ▼, myoglobin; ▲, cytochrome *c*.

consist above all in the slope of the dependence of log k' *vs.* φ and in the concentration range in which this dependence can be investigated. Up to a certain salt concentration, the protein is not retained and is eluted with the void volume of column. When this salt concentration is exceeded, the elution volume of the protein increases but a pronounced increase in peak width occurs at the same time so that the number of theoretical plates decreases monotonously. At higher salt concentrations further measurement is impossible. The dependence for ribonuclease A suggests a pronounced non-linear increase in log k' in the concentration range 1.1–1.2 M $(NH_4)_2SO_4$. Further experiments were carried with lysozyme, ovalbumin and transferrin. These proteins differ in the relative molecular mass and in the slope of the dependence of log k' *vs.* φ.

The significant influence of the initial salt concentration on the course of the gradient elution is documented in Table I. First, a constant gradient time was chosen. In the range of $\varphi_0 = 0.9$–1.4 M, the gradient slopes (see values of g in Table I) increased by 50% due to the initial concentration. The resolution of the pair transferrin–ovalbumin was increased by a factor of three, whereas that of ovalbumin–lysozyme decreased by approximately 40%. The experiments given in lines 7 and 8 of Table I demonstrate that these changes in resolution are caused by the influence of the initial salt concentration. The gradient time was adjusted so as to obtain the same gradient slope as in lines 2 and 6. It is seen that, regardless of the same g value, the resolutions are different. It is usually thought that the steeper the gradient, the lower is the resolution. Comparison of lines 6 and 9 in Table I shows that the ratio of the slopes of the dependence of log k' *vs.* salt concentration can play an important rôle. Whereas the gradient slope, g, increased by a factor of three caused a decrease in the resolution of the pair transferrin–ovalbumin, on contrary the resolution of the pair ovabumin–lysozyme increased. Analogous results were obtained in Jandera's study on reversed-phase separation of pesticides[19]. The influence of the initial eluent composition is discussed in connection with the different slopes of the dependences of log k' *vs.* eluent composition. Chromatograms corresponding to the experiments in lines 1 and 6 of Table I are given in Figs. 2 and 3. It is interesting to follow the elution of an impurity contained in transferrin. While the t_R of this impurity does not change, its peak is eluted after the peak of transferrin when $\varphi_0 = 0.9$ M and before it when $\varphi_0 = 1.4$ M.

TABLE I

DEPENDENCE OF THE RESOLUTION OF TRANSFERRIN (1), OVALBUMIN (2) AND LYSOZYME (3) ON THE INITIAL CONCENTRATION OF AMMONIUM SULPHATE, φ_0

No.	φ_0 *(M)*	t_{grad} *(min)*	g *(M/ml)*	$R_S^{1,2}$	$R_S^{2,3}$
1	0.9	60	0.0300	0.45	1.78
2	1.0	60	0.0333	0.85	1.54
3	1.1	60	0.0366	1.04	1.71
4	1.2	60	0.0400	1.38	1.20
5	1.3	60	0.0433	1.44	1.00
6	1.4	60	0.0466	1.51	1.02
7	1.4	84	0.0333	1.45	1.09
8	1.0	43	0.0466	0.73	1.26
9	1.4	20	0.1400	0.92	1.62

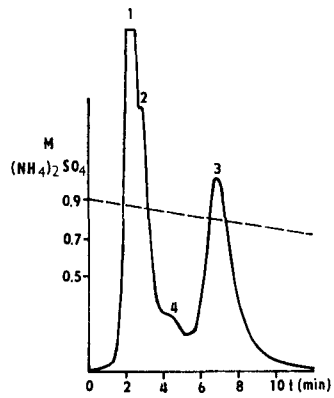

Fig. 2. The separation of transferrin (1), ovalbumin (2), and lysozyme (3) and the impurity in transferrin (4). Column: 100 mm × 4 mm I.D. packed with Separon HEMA 1000, d_p = 10 μm. Decreasing gradient of ammonium sulphate in 0.1 *M* phosphate buffer pH 7.0. Gradient time: 60 min. Flow-rate: 0.5 ml/min. Initial concentration of ammonium sulphate: 0.9 *M*.

For the practical utilization of isocratic dependences $\log k' = f(\varphi)$, the application of the model described in the Introduction may be advantageous. The relationships $\log k'$ *vs.* φ and D *vs.* φ (D was determined from the peak width using eqn. 3) measured in the isocratic mode for transferrin, ovalbumin and lysozyme were utilized for the numerical calculations of t_R and W ($W = 4\sigma$). The dependences $\log k'$ *vs.* φ and D *vs.* φ are described by eqns. 7 and 8 within the limits of the salt concentrations used during the experiments.

$$\log k' = A + B\varphi \tag{7}$$

$$D = a + b\varphi \tag{8}$$

Parameters A, B, a and b for the three proteins discussed were determined by linear regression. The results including the correlation coefficients are summarized in Table II.

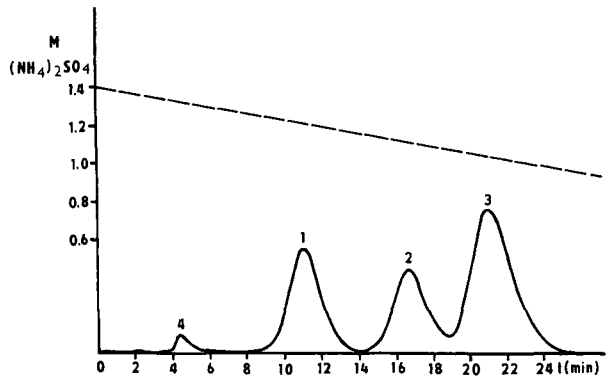

Fig. 3. Separation as in Fig. 2 but with initial concentration of 1.4 *M* ammonium sulphate.

TABLE II

PARAMETERS OF EQNS. 7 AND 8 FOR TRANSFERRIN, OVALBUMIN AND LYSOZYME DETERMINED FROM THE EXPERIMENTAL DEPENDENCES log k' *vs.* φ AND D *vs.* φ

Dependence	*Transferrin*	*Ovalbumin*	*Lysozyme*
$\log k' = A + B\varphi$			
A	−6.255	−3.598	−1.981
B	5.689	3.646	2.659
Correlation coeff.	0.9900	0.9988	0.9894
$D = a + b\varphi$			
a	−0.062	−0.038	−0.005
b	0.071	0.059	0.017
Correlation coeff.	0.9784	0.9999	0.9813

In the numerical solution the value of Δl was first chosen (in this case $\Delta l = L/100$). Then the values of t_R were computed step-by-step at Δl, $2\Delta l$, $3\Delta l$, ... $100\Delta l$ as the sums of corresponding values of Δt_{R_i} (i = 1,2,3, ... 100) (see eqn. 4). A given gradient is considered, of course. Similarly the values of $\sigma_{R_i}^2$ corresponding to Δl, $2\Delta l$, $3\Delta l$, ... $100\Delta l$ (see eqn. 5) are computed. These $\sigma_{R_i}^2$ correspond to the σ_R^2 of a peak eluted from a column of length Δl, $2\Delta l$, $3\Delta l$, ... $100\Delta l$. However the correction is performed for each point with respect to peak focusing. For this purpose, σ_R (expressed in units of time) is converted into the peak width on the column, $\tilde{W}_l$ (expressed in units of length) utilizing eqn. 9

$$\frac{l - (\tilde{W}_l)_i}{t_{R_i} - 2\sigma_{R_i}} = \frac{1}{t_{R_i} + 2\sigma_{R_i}} \quad \begin{matrix} l = i\Delta l \\ i = 1,2, \ldots, 100 \end{matrix} \tag{9}$$

which can be transformed into:

$$(\tilde{W}_l)_i = \frac{4l\sigma_{R_i}}{t_{R_i} + 2\sigma_{R_i}} \tag{10}$$

Then the speed of the rear edge (index r) and front edge (index f) of the peak is determined

$$v_{r(f)} = \frac{u}{1 + k'_{r(f)}} \tag{11}$$

and the correction of the peak width is calculated:

$$(W_c)_i = \Delta t_{R_i}(v_{r,i} - v_{f,i}) \tag{12}$$

The peak width on the column is defined more precisely acoording to

$$(W_l)_i = (\tilde{W}_l)_i - (W_c)_i \tag{13}$$

and used in eqn. 9 to calculate a more precise value of σ_{R_i}. The whole computation is repeated until $l = L$ (i = 100).

TABLE III

EXPERIMENTAL AND CALCULATED RETENTION TIMES, t_R (min), AND PEAK WIDTHS, W (ml), OF PROTEINS FOR VARIOUS INITIAL CONCENTRATIONS OF AMMONIUM SULPHATE, φ_0

t_{grad} = 60 min. First the experimental and then the calculated values are given.

φ_0 (M)	*Transferrin*		*Ovalbumin*		*Lysozyme*	
	t_R	W	t_R	W	t_R	W
0.9	2.12	0.70	2.80	0.80	6.89	1.50
	1.96	0.61	2.74	0.95	5.85	1.14
1.0	2.53	0.0	4.23	1.30	9.09	1.85
	2.33	0.75	3.82	1.23	8.38	1.56
1.1	3.47	1.16	5.93	1.20	11.53	2.08
	3.46	0.92	5.77	1.64	11.59	2.02
1.2	5.25	1.20	9.67	2.00	14.79	2.25
	6.00	1.19	8.65	2.11	15.14	2.45
1.3	7.81	1.60	13.51	2.35	18.15	2.30
	9.59	1.20	13.09	2.11	18.25	2.36
1.4	11.14	1.70	16.79	2.05	21.14	2.20
	13.34	1.15	16.89	2.02	22.76	2.22

The calculated values of t_R and W for a gradient time of 60 min and $\varphi_0 \in \langle 0.9, 1.4 \rangle$ are presented together with the experimental values in Table III. The simplified definitions $k' = 0$ for the lower φ values ($\varphi < 0.8$ for transferrin and ovalbumin and $\varphi < 0.6$ for lysozyme, see Fig. 1) and $k' \to \infty$ for $\varphi > 1.2$ certainly contribute to the differences between the experimental and calculated data, especially in the case of transferrin.

The differences between the computed values of t_R and W (see Table III) and the same values obtained by numerical solution of eqn. 1[28] for gradient elution were not greater than 10%. However, the computing time needed was 100 times shorter in the case of the data in Table III.

If the relationship for t_R, known from the literature[19], was applied values two times smaller than the experimental data were obtained. The reason for the unsuccessful application of the analytical relationship for t_R is probably the limited range of the salt concentration in which log k' is a linear function of this parameter.

On the other hand, if the correction to peak focusing was not considered, the values of W calculated as described above were two times greater than experimental results.

The agreement between the experimental data and the values calculated according to the model used here is quite good. From the standpoint of resolution, the difference between the computed and the experimental data is, of course, more pronounced. However, the qualitative trend is maintained; thus the computation corresponds to the conclusions concerning the influence of φ_0 revealed by Table I.

CONCLUSION

Both the experimental results and the model used confirm that the resolution of protein peaks in hydrophobic interaction chromatography on Separon HEMA 1000 depends mainly on the choice of the initial concentration of salt, φ_0, in the gradient elution. This is caused by the different functions of log k' *vs.* φ and D *vs.* φ of the proteins. The effect of different gradient conditions (starting composition, gradient steepness and gradient shape) may be predicted from the isocratic measurements.

REFERENCES

1 Y. Kato, T. Kitamura and T. Hashimoto, *J. Chromatogr.*, 298 (1984) 407.
2 D. L. Gooding, M. N. Schmuck and K. N. Gooding, *J. Chromatogr.*, 296 (1984) 107.
3 P. Štrop, *J. Chromatogr.*, 294 (1984) 213.
4 J. L. Fausnaugh, L. A. Kennedy and F. R. Regnier, *J. Chromatogr.*, 317 (1984) 141.
5 J. L. Ochoa, *Biochemie*, 60 (1978) 1.
6 S. C. Coheen and S. C. Engelhorn, *J. Chromatogr.*, 317 (1984) 55.
7 W. R. Melander, Ds. Corradini and Cs. Horváth, *J. Chromatogr.*, 317 (1984) 67.
8 W. R. Melander and Cs. Horváth, *Arch. Biochem. Biophys.*, 183 (1977) 200.
9 P. Štrop, F. Mikeš and Z. Chytilová, *J. Chromatogr.*, 156 (1979) 239.
10 P. Štrop and D. Čechová, *J. Chromatogr.*, 207 (1981) 55.
11 P. Štrop, D. Čechová and V. Tomášek, *J. Chromatogr.*, 259 (1983) 255.
12 Y. Kato, T. Kitamura and T. Hashimoto, *J. Chromatogr.*, 266 (1983) 49.
13 S. C. Coheen and R. S. Matson, *J. Chromatogr.*, 326 (1985) 235.
14 N. T. Miller and B. L. Karger, *J. Chromatogr.*, 326 (1985) 45.
15 N. T. Miller, B. Feibush and B. L. Karger, *J. Chromatogr.*, 316 (1985) 519.
16 R. Jansen, K. K. Unger, H. Giesche, J. N. Kinkel and M. T. W. Hearn, *J. Chromatogr.*, 397 (1987) 91.
17 S. Yamamoto, M. Nomura and Y. Sano, *J. Chromatogr.*, 409 (1987) 101.
18 A. Katti, Y. F. Maa and Cs. Horváth, *Chromatographia*, 24 (1987) 646.
19 P. Jandera and M. Špaček, *J. Chromatogr.*, 366 (1986) 107.
20 J. L. Glajch, M. A. Quarry, J. F. Vasta and L. R. Snyder, *Anal. Chem.*, 58 (1986) 280.
21 L. R. Snyder and M. A. Stadalius, in Cs. Horváth (Editor), *High Performance Liquid Chromatography. Advances and Perspectives*, Vol. 4, Academic Press, Orlando, FL, 1986.
22 B. F. D. Ghrist and L. R. Snyder, *J. Chromatogr.*, 459 (1988) 25.
23 J. C. Smit, H. C. Smit and E. M. De Jage, *Anal. Chim. Acta*, 122 (1980) 1.
24 E. Kučera, *J. Chromatogr.*, 19 (1965) 237.
25 P. Jandera and J. Churáček, *J. Chromatogr.*, 91 (1974) 223.
26 V. Svoboda, *Radioisotopy*, 18 (1977) 775.
27 V. Svoboda and I. Kleinmann, *J. Chromatogr.*, 366 (1986) 107.
28 J. Plicka, V. Svoboda, I. Kleinmann and A. Uhlířová, *J. Chromatogr.*, 469 (1989) 29.

Journal of Chromatography, 479 (1989) 335–344
Elsevier Science Publishers B.V., Amsterdam — Printed in The Netherlands

CHROM. 21 688

DETERMINATION OF GLUTATHIONE IN SCOTS PINE NEEDLES BY HIGH-PERFORMANCE LIQUID CHROMATOGRAPHY AS ITS MONOBROMOBIMANE DERIVATIVE

G. WINGSLE*, G. SANDBERG and J.-E. HÄLLGREN
Department of Forest Genetics and Plant Physiology, The Swedish University of Agricultural Sciences, S-90183 Umeå (Sweden)
(First received September 27th, 1988; revised manuscript received June 15th, 1989)

SUMMARY

A method for determination of glutathione in its reduced (GSH) and oxidized (GSSG) forms in Scots pine extracts by reversed-phase high-performance liquid chromatography utilizing monobromobimane as the derivatization reagent was developed. The recovery and the precision for GSH in pine needles was high, *ca.* 99 and 3.6%, respectively. The determination of GSSG showed lower recovery (*ca.* 80%) and poorer precision (13.3%). The identity of the putative GSH-bimane derivative was confirmed indirectly by gas chromatography–mass spectrometry. GSH comprised 77% of water-extractable thiols in pine needles, and the ratio GSSG/GSH was low (0.024).

INTRODUCTION

Glutathione (γ-L-glutamyl-L-cysteinylglycine) is thought to be the major low-molecular-weight thiol in most living eucaryotic cells. Although convincing evidence for its wide distribution has not been established in the plant kingdom[1], it is suggested to be involved in numerous processes in the cell[2] such as a component of the hydrogen-scavenging system in chloroplasts[3].

Traditionally, quantitative analyses of reduced glutathione (GSH) in plants have been performed by titration of the total amount of free thiols with the sulphhydryl reagent 5,5′-dithiobis(2-nitrobenzoic acid) (DTNB)[4]. A more reliable procedure for the determination of GSH and also the oxidized form of glutathione (GSSG) is based on the highly specific enzyme glutathione reductase (E.C. 1.6.4.2)[5]. In the presence of reduced nicotinamide–adenine dinucleotide phosphate (NADPH) this enzyme catalyses the reduction of GSSG to GSH and with the addition of DTNB to the reaction mixture, the stoichiometric formation of the 5-thio-2-nitrobenzoic acid (TNB) occurs.

Recently, the rapid development of high-performance liquid chromatography (HPLC) has rendered alternative procedures for analysis of thiols, and techniques for the separation, derivatization and detection of GSH have been described. Saetre and

0021-9673/89/$03.50

Rabenstein[6] presented a method based on a mercury electrochemical detection, and Reeve *et al.*[7] utilized Ellmans reagents to convert GSH and GSSG into the mixed disulphides of TNB which were separated by reversed-phase HPLC. An alternative HPLC technique for determining thiols is based on carboxymethylation of the thiol group to block thiol–disulphide exchange reactions[8]. Free amino groups are then converted into 2,4-dinitrophenyl derivatives by reaction with 1-fluoro-2,4-dinitrobenzene, providing a chromatophoric group that can be detected at the nanomole level. Another procedure has been described by Newton *et al.*[9] for determination of thiols at the picomole level. This method is based on the conversion of thiols into fluorescent derivatives with monobromobimane (mBBr) and separation of the bimane derivatives by reversed-phase HPLC.

Glutathione, as well as other thiols, is considered to be an important metabolite in relation to the phytotoxicity of air pollutants to plants. In experiments with Scots pine[10] and *Picea abies*[11] it has been shown that GSH can serve as an indicator of the phytotoxic effects of compounds such as SO_2 and O_3. However, the analysis of glutathione in conifer extracts requires special precautions, both during the initial extraction and the subsequent analysis. GSH oxidizes readily[12] and conifers are known to contain a number of compounds including high levels of phenolic compounds and terpenes[13], that might interfere in the analysis. Adaption of an analytical method for quantitative analysis of glutathione in conifer tissues therefore necessitates careful examination to optimize the procedure.

The aim of the present study was to investigate possibilities of adapting the method by Newton *et al.*[9] for the analysis of GSH and GSSG in extracts from conifer needles. Quantitative analysis by reversed-phase HPLC with fluorescence detection of GSH-bimane derivatives in pine extracts was examined in terms of accuracy and precision. The identity of the putative GSH-bimane HPLC peak was subsequently confirmed by gas chromatography–mass spectrometry (GC–MS).

EXPERIMENTAL

Millipore water was used in all steps of analysis.

Extraction of plant material

Extraction was performed in a cold room (4°C) by grinding 200 mg needles of Scots pine (*Pinus sylvestris* L.) in liquid nitrogen in a mortar. The plant material was then transferred to a glass column and eluted twice with a total of 5 ml of an ice cold medium consisting of water or 0.1 m*M* dithiothreitol (DTT) and 1 m*M* EDTA. The whole procedure was completed within 10 min. An aliquot of the extract was used for determination of GSH or GSSG.

Derivatization

Typically, 500 μl of sample or standard were added to a premixed solution of 200 μl 0.1 *M* Tris–HCl (pH 8), 100 μl 4 m*M* mBBr in a 3-ml test-tube. The samples were mixed vigorously and the reaction continued for 30 min in darkness at 25°C. A 150-μl volume of glacial acetic acid was then added to stop the reaction, and the samples were diluted to a final volume of 1 ml in water. Prior to HPLC analysis the samples were centrifuged at 7000 *g* (Labofuge 6000, Heraeus) for 10 min. Samples

eluted with 5-sulphosalicylic acid (5%, v/v) were derivatized with mBBr according to Anderson and Meister[12].

GSSG was determined in extracts or standard samples after alkylation of GSH by derivatization with the sulphhydryl reagent 2-vinylpyridine[14]. This was achieved by vigorously mixing 2-ml samples with 100 μl 0.1 *M* Tris–HCl (pH 6.5) and 40 μl 9.3 *M* 2-vinylpyridine in test-tubes. After 60 min at 25°C, excess of 2-vinylpyridine was removed by partitioning the sample three times against 150-μl volumes of diethyl ether. Then the GSH content of one part of the sample was determined and used as a blank and the other part was used for the determination of GSH after GSSG had been reduced to GSH. This was carried out by adding 50 μl 4 m*M* NADPH and 2 μl glutathione reductase from spinach (*ca.* 59 units ml^{-1}, Sigma) to the derivatization mixture with mBBr as described above.

Derivatization of GSH and GSSG utilizing 9-fluorenylmethyl chloroformate (FMOC) was performed according to Näsholm *et al.*[15].

High-performance liquid chromatography

Solvents were delivered at a flow-rate of 1 ml min^{-1} by a Waters liquid chromatographic system consisting of two M 45 pumps, a dynamic solvent mixer and a M 680 gradient master. Samples were introduced off-column via a Valco loop injector fitted with a 25-μl loop. Reversed-phase separations were carried out on a 250 mm × 4.6 mm I.D. ODS-Hypersil (5 μm) column eluted from 0 to 20 min with an isocratic system using 85% of solution A [10% methanol (v/v) and 0.25% glacial acetic acid (v/v), adjusted to pH 3.9 with NaOH] and 15% of solution B [90% methanol (v/v) and 0.25% glacial acetic acid (v/v), adjusted to pH 3.9 with NaOH], followed by 100% of solution B to regenerate the column. The column effluent was directed to a Shimadzu Model RF fluorimeter (excitation at 379 nm, emission at 475 nm).

The separation and detection of GSH and GSSG-FMOC derivatives by reversed-phase HPLC was performed according to procedures described for amino acids by Näsholm *et al.*[15], with a slight modification of the solvent programme. The separation was carried out with the following percentages of methanol in buffer (7 ml glacial acetic acid and 1 ml triethylamine to 1 l water, adjusted to pH 4.2 with NaOH): 0–15 min, 55%; 15–20 min, 55–65%; 20–40 min, 65%; 40–50 min, 100% and 50–60 min, 55%.

GC–MS analysis

Qualitative analysis of GSH in an extract from pine needles was carried out using the procedure outlined in Fig. 1. Approximately 90 nmol of the putative GSH-

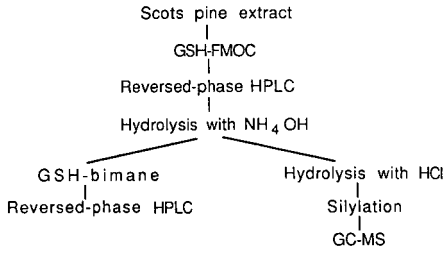

Fig. 1. Qualitative analysis of reduced glutathione in Scots pine.

FMOC peak from reversed-phase HPLC of a Scots pine extract were collected and 200 μl concentrated ammonium hydroxide were added for 12 h at 100°C to perform base hydrolysis of the FMOC derivative. An aliquot of the sample was thereafter reduced to dryness with a stream of nitrogen and dissolved in 200 μl medium (0.1 m*M* DTT and 1 m*M* EDTA). This sample was taken for determination of GSH by derivatization with mBBr and analysis by reversed-phase HPLC to confirm the peak identity. The other part of the base hydrolysed putative GSH-FMOC fraction was reduced to a dryness with a stream of nitrogen and hydrolysed with 6 *M* HCl under vacuum for 24 h at 100°C. Thereafter the sample was again reduced to dryness, dissolved in 100 μl acetonitrile and silylated with bis(trimethylsilyl)trifluoroacetamide (100 μl, 80°C for 12 h). Mass spectrometric analysis of concentrated aliquots was performed with a HP 5890 gas chromatograph linked via a direct capillary inlet to an HP 5970B mass selective detector equipped with an HP 9000 computer system. Samples were introduced in the splitless mode (splitless time 2 min) at 225°C onto a 25 m × 0.31 mm I.D. cross-linked methyl silicone capillary column with a 0.52-μm film. The column temperature was initially held at 60°C for 3 min, then raised at 30°C min^{-1} to 130°C than at 7°C min^{-1} to 235°C. The interface temperature was maintained at 250°C. The retention time for air was 63 s.

GSH standards and the total water extractable thiol concentration in Scots pine needles were estimated by the method described by Grill *et al.*[16].

RESULTS

Extraction

The maximum yield of GSH was achieved by grinding approximately 200 mg needles in liquid nitrogen in a mortar and extracting the material with 5 ml ice-cold medium, consisting of 0.1 m*M* DTT and 1 m*M* EDTA or water, 1.103 and 1.146 μmol GSH (g fresh weight)$^{-1}$, respectively (Table I). Extraction of the plant material with additional medium, or by using extended extraction times, did not improve the yield. In addition, hot ethanol also gave low yields of GSH[17]. The stability of GSH during the extraction was tested after 0, 15 and 60 min after initial extraction in the presence of 0.1 m*M* DTT and 1 m*M* EDTA or 5-sulphosalicylic acid (results not shown). It was found that GSH is stable within the time used for the assay. A slight

TABLE I

COMPARISON OF DIFFERENT EXTRACTION MEDIA AS REGARDS THE YIELD OF GLUTATHIONE EXTRACTED FROM PINE NEEDLES

The samples were derivatized with monobromobimane and the values are the averages of three separate extractions, except for 5-sulphosalicylic acid (n = 2). Data are mean ± S.D.

Extraction	*GSH* (*μmol/g f.wt.*)	*Yield* (*%*)
Water	1.146 ± 0.033	100 ± 2.9
0.1 m*M* DTT/1 m*M* EDTA	1.103 ± 0.024	96.3 ± 2.2
Ascorbate (0.15%)	0.884 ± 0.008	77.1 ± 0.9
5-Sulphosalicylic acid (5%)	0.924 ± 0.007	80.6 ± 0.7

reduction of GSSG standards by 0.1 m*M* DTT and 1 m*M* EDTA was however detected (3.1%) when compared to samples dissolved in water.

Derivatization

Samples and standards showed maximum derivatization efficiency at a buffer pH of 8–9 (Fig. 2). The derivatization efficiency with time indicated that a derivatization time of 15 min was sufficient.

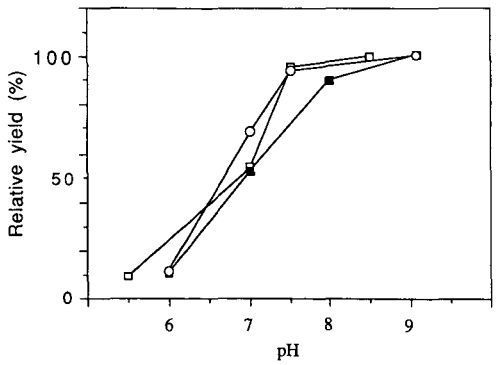

Fig. 2. pH dependence of the yield of reduced glutathione from a standard and an extract of Scots pine. 0.1 *M* sodium phosphate buffer was used in the derivatization mixture in the range pH 5–7, and 0.1 *M* Tris–HCl in the range pH 8–9. Standards were dissolved in 0.1 m*M* DTT/1 m*M* EDTA and needles were eluted in 0.1 m*M* DDT/1 m*M* EDTA or 0.15% ascorbate. ○ = standard; □ = extract in 0.1 m*M* DTT/1 m*M* EDTA; ◘ = extract in 0.15% ascorbate.

HPLC separation

The chromatographic conditions used give a separation of the GSH-bimane derivative peak from other components in the pine needle extract (Fig. 3). There was no significant background interference with the analysis and when GSH was masked with 2-vinylpyridine prior to derivatization no GSH-bimane peak was detectable (data not shown). Using FMOC as a chromatographic group it was possible to get a separation of both GSSG and GSH from pine needle extract (Fig. 4). The GSSG-FMOC peak was identified by spiking the sample with standard GSSG-FMOC (Fig. 4b).

Identification of GSH from a pine extract by GC–MS analysis

The putative GSH-bimane derivative peak from HPLC was identified by using the procedure outlined in Fig. 1.

Silylated amino acids produce characteristic ions at $M^+ - 15$, $M^+ - 43$ and $M^+ - 117$ corresponding to loss of $-CH_3$, $-COCH_3$ and $-COO-TMS$ respectively[18], but also ions with *m/z* 73 $[Si(CH_3)_3]$ and 147 $[(CH_3)_3SiOSi(CH_3)_2]$ are diagnostic for silylated amino acids.

Retention times in the GC system for the putative N-trimethylsilyl esters of Gly, CySH and Glu of a hydrolysed GSH fraction from HPLC were 9.11, 12.70 and 13.64 min. In all GC peaks the base fragments for the corresponding amino acid were present [$M^+ - 117$, *m/z* 174, 220 and 246 for Gly, CySH and Glu, respectively (Table

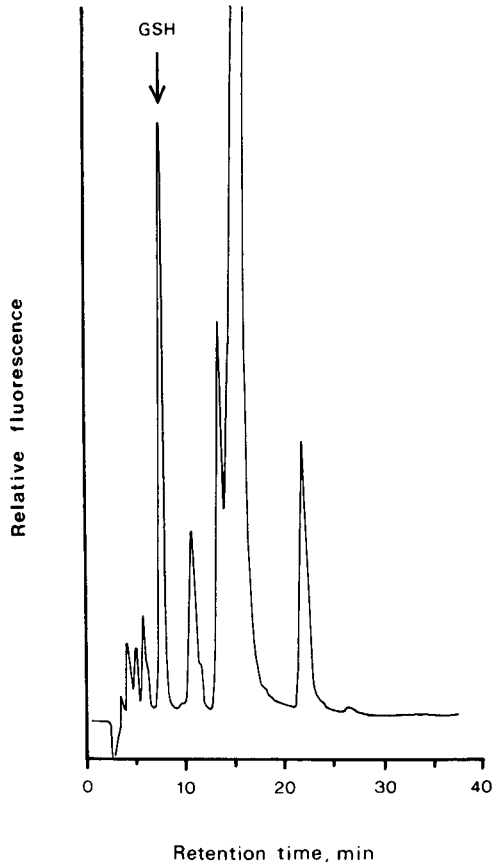

Fig. 3. Representative chromatogram of reduced glutathione (GSH) from an extract of Scots pine needles derivatized with monobromobimane.

III)], together with *m/z* 73 and 143. Only the putative Glu peak produced a detectable M^+ [Glu(TMS)$_3$], together with *m/z* 84 and 156, which were specific for the Glu and Gln derivatives. The largest fragment of the putative CySH was *m/z* 322 corresponding to $M^+ - 15$ (bis-TMS). In addition, a fragment at *m/z* 218 (TMS–NHCHCOO–TMS) was present, which represents loss of the side chain from the molecular ion of CySH[18]. Ions at *m/z* 174 and 86 are diagnostic for the structure RCH_2NH_2, and both were present in the putative Gly peak [*m/z* 174, $(TMS)_2N^+=CH_2$; 86, $(CH_3)_2Si^+=CH_2$][18]. In addition, a characteristic ion for CySH at *m/z* 248 was also observed in this spectrum.

Recovery and precision

The accuracy of the method was determined by comparing standards with standards of different concentrations mixed with subsamples from pine needle extract. The amount of GSH-bimane derivatives detected was linear (tested by least squares linear regression) in the concentration range tested. The recovery of 50 and

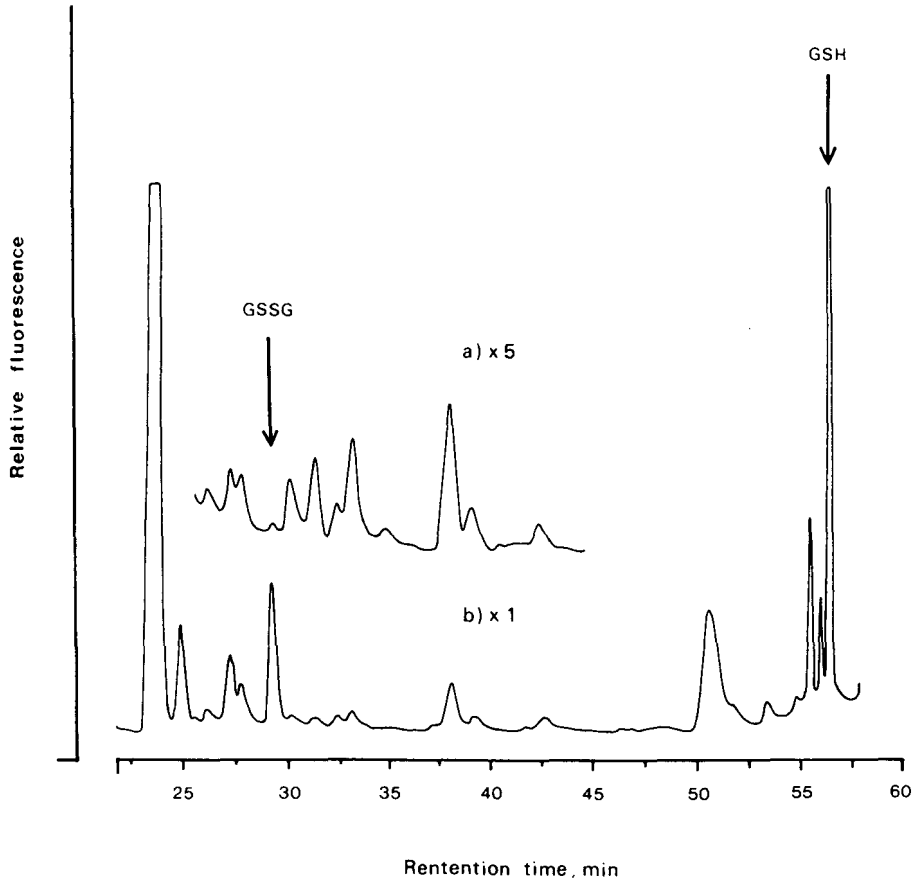

Fig. 4. (a) Chromatogram of Scots pine needles extract derivatized with 9-fluorenylmethyl chloroformate (FMOC). (b) As in (a) but spiked with 200 pmol GSSG derivatized with FMOC.

250 nmol GSH added to extracts was 99 and 100.3%, respectively (Table II). Recoveries from extracts spiked with 1 and 2 nmol GSSG were 80 and 86.7%, respectively (Table II).

The precision of the method was calculated as the standard deviation of the amount of GSH and GSSG determined in subsamples of three individual pine extracts. The precision was 3.6% for the determination of GSH and 13.3% for GSSG (Table II).

Analysis of GSH, GSSG and water-extractable thiols from a pine extract

Pine needles collected outdoors in April (1987) in Umeå were analysed for GSH, GSSG and water-extractable thiols and the averages from two samples were 0.201, 0.0045 and 0.26 μmol (g fresh weight)$^{-1}$, respectively.

TABLE II

RECORDER RESPONSES FROM STANDARDS AND STANDARDS OF DIFFERENT CONCENTRATIONS MIXED WITH SUBSAMPLES FROM A PINE NEEDLE EXTRACT

Samples were derivatized with monobromobimane and prepared for analysis as described in the text. Data are mean ± S.D. of three samples.

Amount added (μM)	*Recorder response (mV, relative unit)*		*Recovery (%)*
	Standard	*Standard + extract*	
GSH			
0.00	–	13.0 ± 0.5	–
0.05	69.0 ± 0.9	81.2 ± 1.4	99
0.25	354.0 ± 1.2	368.0 ± 4.2	100.3
GSSG			
0.000	–	9.8 ± 1.3	–
0.001	20.2 ± 2.3	24.0 ± 4.2	80
0.002	37.6 ± 2.7	41.1 ± 2.0	86.7

TABLE III

CHARACTERISTIC AND ABUNDANT IONS IN THE 70 eV ELECTRON IMPACT MASS SPECTRA OF AMINO ACIDS FROM A HYDROLYZATE OF GLUTATHIONE FROM PINE NEEDLES

Amino acid	M^+ *[m/z (%)]*	$M^+ - 15$ *[m/z (%)]*	*Base peak (m/z)*	*Other characteristic ions [m/z (%)]*	
CySH	–	322(3)	220	218(88)	100(22)
Glu	363(2)	348(5)	246	156(16)	84(8)
Gly	–	276(6)	174	248(17)	86(15)

DISCUSSION

In the present study the method of Newton *et al.*[9], using mBBr as a chromatophore, originally devised for determining thiols in red blood cells, was applied to extracts from Scots pine needles. The method developed for extraction of GSH from pine needles and detection of the GSH-bimane derivative by reversed-phase HPLC was shown to be acceptable both with regard to recovery (*ca.* 99%) and precision (3.6%) (see Table II). The recovery of GSH was similar to the value reported by Fahey *et al.*[19] for red blood cells (97%). After grinding the needles in liquid nitrogen, the extraction with 0.1 m*M* DTT and 1 m*M* EDTA or water both showed high yields of GSH. Usually extraction of GSH from biological samples has shown a need for rapid acidification, because of rapid autooxidation at pH > 7 and the effect of γ-glutamyl transpeptidase[20]. However, acidification was not necessary when GSH was analysed in pine needles. This may be due to the acidic nature of the unbuffered pine extract which was typically pH 4.5–5.5. Oxidation of GSH did not occur in the pine extract. This was indicated by the amount of GSH remaining unchanged when derivatized up to 45 min after extraction. Further evidence of the stability of GSH is the

fact that yields were not enhanced when tissue was extracted with 5-sulphosalicylic acid. This indicates that both extraction with a low concentration of DTT (0.1 m*M*) or water can be used successfully when GSH is extracted from pine needles. However, since a small amount of the GSSG (3.1%) in standard solution is reduced to GSH, water is preferable when GSSG is analysed. The DTT would not interfere with the GSH analysis when the GSSG concentration or any other reducible GSH conjugate is low compared to the concentration of GSH. This is obviously the case when pine needles were extracted by 0.1 m*M* DTT since no increase in the yield of GSH was detected when 0.1 m*M* DTT was used compared to water alone (Table I). Reproducible results were obtained when samples were derivatized with 0.5 m*M* mBBr in 25 m*M* Tris–HCl at pH 8 for 15 min. The reaction of bromobimanes with GSH are second order and dependent on pH, the active nucleophile being the thiolate anion, GS-(ref. 21). Although mBBr reacts preferentially with thiols, it also reacts with amines, phosphate, carboxylates and other nucleophiles and thus may interfere with the analysis[22]. Kosower and Kosower[23] also showed that amine buffers give an higher background if used above pH 8 due to the amine acting as a nucleophile. It is thus preferable to derivatize at a pH that does not enhance nucleophilic reactions that could interfere with the analysis. Tests of the stability of GSH in pine needles during storage at −80°C for up to 3 weeks indicated no change in endogenous GSH levels.

The analyses of GSSG from pine extracts showed lower recoveries (*ca.* 80%) and poorer precision (13.3%) than obtained with GSH (see Table II). The procedure for measuring GSSG, after the conversion of GSSG into GSH by glutatione reductase, is more complicated than the determination of GSH and this may account for the lower recoveries and less precise estimates. One possible reason for the low recovery is that phenolic and tannin compounds interacted with the enzyme and decreased the yield of GSH.

The reversed-phase HPLC separation of the GSH-bimane derivative was performed with a slight modification of the isocratic system described by Anderson and Meister[12]. This eluted the GSH-bimane derivative as a single peak. It was not possible to characterize this peak by GC–MS, although its identity was confirmed by GC–MS of rederivatized amino acid components of the GSH-FMOC peak. Lower amounts of N-trimethylsilyl esters of CySH were detected compared to esters of Glu and Gln. However, CySH is not stable to strong acid[24]. Using FMOC as a chromatophoric group it was possible to make qualitative determinations of both GSH and GSSG in an extract of Scots pine needles by HPLC.

A comparison of the amount of GSH to the total water-extractable thiols shows that GSH made up 77% of the low-molecular-weight thiols in Scots pine needles collected outdoors in April. This value is lower than the 96% reported for *Picae abies* by Grill *et al.*[16]. However, it is in agreement with values reported for non-glutathione thiols from hardened citrus leaves[17]. The ratio GSSG/GSH was low (0.024), in agreement with published data on other species[17,25].

ACKNOWLEDGEMENTS

The technical assistance of Jan Forsgren and valuable comments on the manuscript by Einar Jensen are gratefully acknowledged. Financial support was provided by the Swedish Council for Forestry and Agricultural Research.

REFERENCES

1 T. Kassai and P. O. Larson, in W. Herz, H. Grisebach and G. W. Kirby (Editors), *Progress in the Chemistry of Organic Products,* Vol. 39, Springer, Vienna 1980, p. 243.
2 H. Rennenberg, *Phytochemistry*, 21 (1982) 2771.
3 K. Asada and M. Takahashi, in D. J. Kyle, C. B. Osmond and C. J. Arntzen (Editors), *Photoinhibition*, Elsevier, Amsterdam, 1987, Ch. 10, p. 227.
4 G. L. Ellman, *Arch. Biochem. Biophys.*, 82 (1959) 70.
5 F. Tietze, *Anal. Biochem.*, 27 (1969) 502.
6 R. Saetre and D. L. Rabenstein, *J. Agric. Food Chem.*, 26 (1978) 982.
7 J. Reeve, J. Kuhlenkamp and N. Kaplowitz, *J. Chromatogr.*, 194 (1980) 424.
8 D. J. Reed, J. R. Babson, P. W. Betty, A. E. Brodie, W. W. Ellis and D. W. Potter, *Anal. Biochem.*, 106 (1980) 55.
9 G. L. Newton, R. Dorian and R. C. Fahey, *Anal. Biochem.*, 114 (1981) 383.
10 G. Wingsle, T. Näsholm, T. Lundmark, A. Ericsson and J. E. Hällgren, in S. Schulte-hostede (Editor), *2nd International Symposium on Air Pollution and Plant Metabolism, April 6–9, 1987, Workshops and Poster Presentations*, GSF-Bericht 9/87, München, 1988, p. 62.
11 H. Mehlhorn, G. Seufert, A. Schmidt and K. J. Kunert, *Plant Physiol.*, 82 (1986) 36.
12 M. E. Anderson and A. Meister, *Proc. Natl. Acad. Sci. U.S.A.*, 80 (1983) 707.
13 B. Nyman, *Phytochemistry*, 24 (1985) 2939.
14 O. W. Griffith, *Anal. Biochem.*, 106 (1980) 207.
15 T. Näsholm, G. S. Sandberg and A. Ericsson, *J. Chromatogr.*, 396 (1987) 225.
16 D. Grill, H. Esterbauer and U. Klösch, *Environ Pollut,* 17 (1979) 187.
17 C. L. Guy, J. V. Carter, G. Yelenosky and C. T. Guy, *Cryobiology*, 21 (1984) 443.
18 H. Iwase, Y. Takeuchi and A. Murai, *Chem. Pharm. Bull.*, 27 (1979) 1307.
19 R. C. Fahey, G. L. Newton, R. Dorian and E. M. Kosower, *Anal. Biochem.*, 111 (1981) 357.
20 M. E. Anderson, *Methods Enzymol.*, 113 (1985) 548.
21 A. E. Radkowsky and E. M. Kosower, *J. Am. Chem. Soc.*, 108 (1986) 4527.
22 R. C. Fahey and G. L. Newton, *Methods Enzymol.*, 147 (1987) 85.
23 N. S. Kosower and E. M. Kosower, *Methods Enzymol.*, 147 (1987) 76.
24 D. C. Carpenter, *J. Am. Chem. Soc.*, 53 (1931) 1812.
25 W. Bielawski and K. Joy, *Phytochemistry*, 25 (1986) 2261.

Journal of Chromatography, 479 (1989) 345–352
Elsevier Science Publishers B.V., Amsterdam — Printed in The Netherlands

CHROM. 21 716

HIGH-PERFORMANCE LIQUID CHROMATOGRAPHIC SEPARATION OF *E*- AND *Z*-MONOLIGNOLS AND THEIR GLUCOSIDES

NORMAN G. LEWIS*, Ma. ESTELA J. INCIONG, KALI P. DHARA and ETSUO YAMAMOTO
Departments of Wood Science and Forest Products and Biochemistry, Virginia Polytechnic Institute and State University, Blacksburg, VA 24061 (U.S.A.)
(Received April 28th, 1989)

SUMMARY

Photoirradiation of the *E*-monolignols, *E*-*p*-coumaryl, coniferyl and sinapyl alcohols gave mixtures of the corresponding *E*/*Z* monolignols. Similar treatments of the glucosides, *E*- and *Z*-coniferin, *Z*-isoconiferin and *Z*-syringin afforded comparable *E*/*Z* mixtures. Without derivatization, separation of the individual *E*- and *Z*-monolignols, and the *E*- and *Z*-monolignol glucosides could only be obtained by high-performance liquid chromatography. This development now permits the long-awaited facile analysis of plant extracts for *E*/*Z* monolignol and corresponding glucoside composition.

INTRODUCTION

Lignins are complex polyphenolic polymers present in terrestrial vascular plants, and which have essential structural and defense functions. For some time, it has generally been accepted that they are formed exclusively via random dehydrogenative polymerization of the three *E*-monolignols, *p*-coumaryl (**1**), coniferyl (**2**) and sinapyl (**3**) alcohols[1].

In woody angiosperms and gymnosperms, the exact mechanism of transport of the *E*-monolignols **1**–**3** from the cytoplasm into the lignifying cell wall has not yet been unequivocally demonstrated. It is, however, thought that they are transported into the wall as glycosidic conjugates, such as *E*-coniferin (**5**) and *E*-syringin (**6**). (Interestingly, the glucoside **4** has never been isolated.) Action of a β-glucosidase in the cell wall regenerates the *E*-monolignols **1**–**3**, and lignification then proceeds in a reaction requiring H_2O_2 and peroxidase for initiation of the free-radical polymerization[1]. The importance of the metabolic pathway to lignins cannot be underestimated as lignins are, next to cellulose, the most abundant organic substances in nature.

In spite of lignin's abundance in plant tissue, the precursor monolignols and glucosides are often found only in trace quantities. In most studies, their identification relies solely upon thin-layer chromatographic comparison with authentic (*E*) standards.

0021-9673/89/$03.50

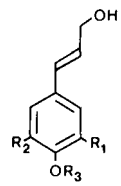

1, R_1, R_2, R_3 = H

2, R_1 = OCH_3, R_2, R_3 = H

3, R_1, R_2 = OCH_3, R_3 = H

4, R_1, R_2 = H, R_3 = Glc

5, R_1 = OCH_3, R_2 = H, R_3 = Glc

6, R_1, R_2 = OCH_3, R_3 = Glc

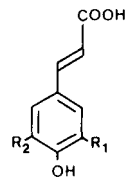

7, R_1, R_2 = H

8, R_1 = OCH_3, R_2 = H

9, R_1 = OCH_3, R_2 = OH

10, R_1, R_2 = OCH_3

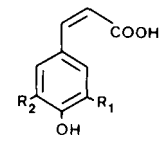

11, R_1, R_2 = H

12, R_1 = OCH_3, R_2 = H

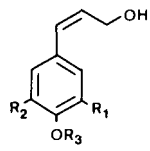

13, R_1, R_2, R_3 = H

14, R_1 = OCH_3, R_2, R_3 = H

15, R_1, R_2 = OCH_3, R_3 = H

16, R_1 = OCH_3, R_2 = H, R_3 = Glc

17, R_1, R_2 = OCH_3, R_3 = Glc

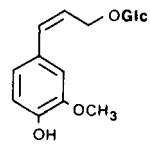

18

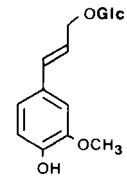

19

In contrast to woody plants, grasses and herbaceous plants contain significant amount of cell-wall-bound hydroxycinnamic acids, *e.g.*, **7**–**10**[2–12]. These acids can be covalently linked to both polyoses (hemicelluloses)[8,10,11,13–16] and lignin[17–20]. Interestingly, these bound acids, *e.g.*, *p*-coumaric and ferulic acids, exist as mixtures of *E*- (**7**,**8**) and *Z*- (**11**,**12**) isomers, respectively[10,21–23]. All current evidence leans towards a photochemical mechanism for isomerization[23]. This is because (1) such acids are rapidly photochemically interconverted *in vitro*[10,21–23] and *in vivo*[21,23] and (2) plants grown in the presence of light contain mixtures of *E* and *Z* isomers, whereas etiolated plants contain only *E* isomers[21,23].

Unlike the hydroxycinnamic acids, it has been generally assumed that monolignols exist only in the *E* configuration. It was, therefore, rather surprising to discover that American beech (*Fagus grandifolia*) bark contained significant quantities of *Z*-monolignols, *Z*-coniferyl (**14**) and *Z*-syringyl (**15**) alcohols[24], and the glucosides, *Z*-coniferin (**16**) and *Z*-syringin (**17**)[25]. Importantly, the corresponding *E* isomers

could not be detected in this tissue. A third glucoside, *Z*-isoconiferin (**18**) was also isolated[25,26], where glucosylation had occurred at the allylic hydroxyl group; this compound had previously been described as faguside in European beech (*Fagus sylvatica*)[26].

In this paper, we describe a high-performance liquid chromatography (HPLC) method suitable for the separation of *E*- and *Z*-monolignols and their corresponding glucosides. This method allows us to rapidly quantify the amounts of both *E* and *Z* isomers in plant tissue. In this regard, it should be noted that most silica gel thin-layer chromatographic methods give only partial or no separation of these *E*/*Z* isomers.

MATERIALS AND METHODS

Instrumentation

The instrumentation in these experiments employed two Waters Model 510 solvent delivery systems fitted with a Model 721 system controller, a WISP Model 710B automatic injection module and a Model 990 photodiode array detector equipped with a NEC Power Mate 2, a Waters 990 Plotter and a NEC pinprinter CP6. Chromatographic separations used Waters Novapak C_{18} (150 mm × 3.9 mm, stainless steel) columns. For the separation of the *E* (**1**–**3**) and *Z* (**13**–**15**) monolignols, the column was eluted with degassed, filtered (0.45 μm) methanol–water (15:85, v/v). The flow-rate was 1.3 ml min $^{-1}$, and detection at 262 nm. Separation of the *E*- and *Z*-glucosides (**5**,**6**,**16**–**19**) employed two Novapak columns in series, with a mobile phase consisting of degassed, filtered (0.45 μm) acetonitrile–water (15:85, v/v) at 0.7 ml min $^{-1}$, and detection at 257 nm. ^{1}H NMR spectra were separately obtained in both $C^2H_3O^2H$ and $(C^2H_3)_2CO$ solutions, using tetramethylsilane (TMS) as an internal standard. Instrumentation employed a 270-MHz Bruker WP-270SY spectrometer.

*Preparation of E- and Z-coniferyl alcohols (**2**,**14**)*

Z-Coniferyl alcohol (**14**) was prepared as described previously[24]. E-Coniferyl alcohol (**2**) was obtained in 52% yield, via direct reduction of *E*-methyl ferulate using "ATE" complex[27] [diisobutylaluminumhydride (DIBAL-H) and *n*-butyllithium, *n*-BuLi] in anhydrous tetrahydrofuran (THF)[24], and then recrystallized from peroxide-free diethyl ether–light petroleum (b.p. 37–54°C) (1:1).

*Photoisomerization of E- and Z-coniferyl alcohols (**2**,**14**)*

E-Coniferyl alcohol (**2**) (5.99 mg, 33.3 μmol) was predissolved in methanol (0.665 ml) in a quartz tube (4 mm O.D., 2.5 mm I.D.), which was then purged with nitrogen. The resulting 0.05 *M* solution of coniferyl alcohol (**2**) was irradiated for 15 min, at a distance of 30.5 cm, with a Lifeguard mercury arc lamp (Philips, 400 W) whose outer glass shell had been removed. The energy fluence rate of the light below 320 nm, as determined by an UVX digital radiometer equipped with a short wave sensor (UVP, San Gabriel, U.S.A), varied from 48.6 to 113.0 mW cm^{-2}, depending upon the experiment. HPLC analysis of the resulting reaction mixture, with detection at 262 nm, showed the presence of two components having elution volumes of 17.15 and 20.64 ml, and identical to those of authentic *E*- and *Z*-coniferyl alcohols (**2**,**14**), respectively. The UV spectrum of each component was also obtained during HPLC

separation, using a Waters 990 photodiode array detector: *E*-coniferyl alcohol (**2**) (λ_{max} 211, 262 nm); *Z*-coniferyl alcohol (**14**) (λ_{max} 211, 256 nm). Final product verification was obtained by ^{1}H NMR analysis of the reaction mixture, where integration of the olefinic resonances showed an *E*/*Z* ratio of 1.2:1. Following irradiation, the total recovery of *E*- and *Z*-coniferyl alcohols was 35.2%.

*Preparation of E- and Z-p-coumaryl (**1,13**) and sinapyl (**3,15**) alcohols*

Both *E*-*p*-coumaryl (**1**) and *E*-sinapyl (**3**) alcohols were prepared in a manner analogous to that described for *E*-coniferyl alcohol (**2**), *i.e.*, via reduction of the methyl esters of the corresponding hydroxycinnamic acids[24,27].

Photochemical isomerization of 0.05 *M* solutions of monolignols **1** and **3** could readily be achieved by 15 min irradiation as before. For *E*-*p*-coumaryl alcohol (**1**), irradiation afforded a mixture of two components having elution volumes of 11.73 and 14.00 ml, corresponding to *E*-*p*-coumaryl (**1**) and *Z*-*p*-coumaryl (**13**) alcohols, respectively. Analysis of the UV spectrum of each product was obtained during HPLC separation: *E*-*p*-coumaryl alcohol (**1**) (λ_{max} 205, 259 nm); *Z*-*p*-coumaryl alcohol (**13**) (λ_{max} 202, 253 nm). Again final verification of product identity was carried out by analysis of the ^{1}H NMR spectrum of the mixture; integration of the olefinic resonances gave an *E*/*Z* ratio of 1:1.1. Following irradiation, recovery of *E*/*Z* alcohols was 79.5%.

In a similar manner, irradiation of *E*-sinapyl alcohol (**3**) gave two components having elution volumes of 23.11 and 29.42 ml, corresponding to *E*- and *Z*-sinapyl alcohols (**3** and **15**), respectively. UV (λ_{max}): *E*-sinapyl alcohol (**3**) (220, 271 nm); *Z*-sinapyl alcohol (**15**) (217, 265 nm). Product confirmation was again obtained by analysis of the ^{1}H NMR spectrum; integration of olefinic resonances gave a 1.4:1 *E*/*Z* ratio. Recovery of *E*/*Z* sinapyl alcohols after photoirradiation was 33%.

*Preparation of Z-coniferin (**16**), Z-isoconiferin (**18**), Z-syringin (**17**) and E-coniferin (**5**)*

Glucosides **16**–**18** were isolated and purified to homogeneity exactly as described[25]. *E*-Coniferin (**5**) was synthesized in 50% yield, via "ATE-complex" reduction[27] of the condensation product of *E*-methyl ferulate and acetobromoglucose.

*Photoisomerization of E- and Z-coniferins (**5,16**)*

E-Coniferin (**5**) (17.38 mg, 50.8 μmol) was dissolved in methanol (1.015 ml) in a quartz tube under nitrogen as before. The solution was then irradiated for 15 min with an open-face mercury arc lamp (energy fluence rate of 94.2–138.0 mW cm^{-2}) at a distance of 30.5 cm. HPLC analysis of the resulting reaction mixture, monitored at 257 nm, showed the presence of two components having elution volumes of 3.44 and 3.98 ml, and corresponding to *E*- and *Z*-coniferins (**5**,**16**), respectively. The UV spectrum of each component was obtained during HPLC separation. UV (λ_{max}): *E*-coniferin (**5**) (212, 257 nm) and *Z*-coniferin (**16**) (212, 254 nm). Final product identification employed ^{1}H NMR analysis of the reaction mixture; integration of olefinic resonances gave a 2:1 *E*/*Z* ratio. Recovery of *E*/*Z* coniferins (**5**,**16**) after photoirradiation was 98.6%. In a similar manner, *Z*-coniferin (**16**) was irradiated to afford a 1:2 mixture of *E*/*Z* coniferins (**5**,**16**). Recovery of *E*/*Z* coniferins (**5**,**16**) after photoirradiation was 77.5%.

*Photoisomerization of Z-syringin (**17**) and Z-isoconiferin (**18**)*

Z-Syringin (**17**) (18.1 mg, 48.6 μmol) in methanol (0.972 ml) was irradiated with an open-face mercury arc lamp (energy fluence rate of 94.2–138.0 mW cm^{-2}) for 30 min at a distance of 30.5 cm, to give a mixture of *E*/*Z* isomers (**6**,**17**) in a 1:4.5 ratio as evidenced by ^{1}H NMR. (This represented the best conversion that we were able to effect; longer irradiation times resulted in severe losses of sample.) The HPLC elution volumes of *E*- and *Z*-syringins (**6**,**17**) were 3.65 and 4.34 ml, respectively, as evidenced by absorption at 257 nm. UV (λ_{max}): *E* isomer **6** (221, 263 nm); *Z* isomer **17** (215, 257 nm). Recovery of *E*/*Z* glucosides (**6**,**17**) was 99.5%. In an analogous manner, *Z*-isoconiferin (**18**) (16.08 mg, 47.0 μmol) in methanol (0.939 ml) was irradiated for 20 min, to afford a mixture of *E*/*Z* isoconiferins (**19**,**18**) in a 1:3.5 ratio, as evidenced by ^{1}H NMR. Elution volumes were 5.06 and 5.75 ml, respectively. UV (λ_{max}): *E* isomer **19** (206, 266 nm) and *Z* isomer **18** (212, 257 nm). Recovery of *E*/*Z* isoconiferins (**19**,**18**) was 19.4%.

RESULTS AND DISCUSSION

Until now, there have been no reports of the photochemical interconversions of *E*- and *Z*-monolignols and their glycosidic conjugates. This is in direct contrast to the situation for hydroxycinnamic acids **7**,**8**,**10**, whose facile photoisomerization with UV-A light (320–400 nm) has been well documented[10,21,–23].

Examination of the occurrence of hydroxycinnamic acids **7**–**10**, *Z*-monolignols **14**,**15** and their glucosides **16**–**18** in plant material reveals some rather interesting differences. In etiolated plants, only the *E* isomers of hydroxycinnamic acids, *e.g.* **7**,**8** are known to occur, whereas in light-grown plants mixtures of both *E* and *Z* isomers are present because of light-triggered reactions. The situation in beech bark is rather different, since only the *Z*-monolignols **14**,**15** and their glucosides **16**–**18**, and not the corresponding *E* isomers are found. To account for their formation, appropriate radiolabelling experiments with both *E* and *Z* precursors suggested that *Z*-coniferyl alcohol (**14**) formation occurred via direct isomerization of the corresponding *E* isomer **2**[28]. However, since these experiments were conducted in the absence of light, this suggested that the isomerization of the monolignols was not photochemically induced. This is in direct contrast to the *E*/*Z* isomerization of the hydroxycinnamic acids.

Since an enzyme capable of isomerizing *E*- and *Z*-monolignols has not been isolated to date, we sought to identify the conditions required for the photochemical interconversion of *E*- and *Z*-monolignols and their glucosides. Initial experiments were conducted with pure samples of *E*- and *Z*-coniferyl alcohols (**2**,**14**), respectively. Chromatographic conditions for their separation were established using a Waters Novapak C_{18} column eluted with methanol–water (15:85, v/v).

We next investigated the effects of photoirradiation of *E*- and *Z*-coniferyl alcohols (**2**,**14**) using, as the light source, a mercury arc lamp whose outer glass shell had been removed. For *E*-coniferyl alcohol (**2**), rapid photochemical isomerization was observed within 15 min to afford a 1.2:1 ratio of *E*- and *Z*-isomers as evidenced by ^{1}H NMR integration of the olefinic resonances (see Materials and methods section). A similar treatment with the *Z*-monolignol **14** afforded *E*/*Z* monolignols in a 1:2 ratio.

The elution volume, detected at 262 nm, and the UV spectrum of each mono-

lignol was recorded during chromatographic separation, using a Waters 990 photodiode array detector, and compared to that of authentic standards. Thus, the component eluted at 17.15 ml had a UV spectrum (λ_{max} 262, 211 nm) and an elution volume identical to that of *E*-coniferyl alcohol (**2**). In a similar manner, the component eluted at 20.64 ml (λ_{max} 256, 211 nm) was identical to *Z*-coniferyl alcohol (**14**).

Having demonstrated that individual photochemical treatment of *E*- and *Z*-coniferyl alcohols (**2,14**) resulted in *E*/*Z* isomerization, we next synthesized *E*-*p*-coumaryl (**1**) and *E*-sinapyl (**3**) alcohols via direct reduction of the methyl esters of the corresponding hydroxycinnamic acids **7** and **10**. Reduction was carried out using "ATE" complex, produced from DIBAL-H and *n*-BuLi[24,27]; recrystallization of each monolignol gave *E*-*p*-coumaryl (**1**) and *E*-sinapyl (**3**) alcohols in 60 and 45% yields, respectively.

In a similar manner to that employed for *E*/*Z* coniferyl alcohols **2,14**, samples of pure *E*-*p*-coumaryl (**1**) and *E*-sinapyl (**3**) alcohols were irradiated in solution for 15 min. For *E*-*p*-coumaryl alcohol (**1**), two components were present in the reaction mixture in an approx. 1:1.1 ratio, as evidenced by ^{1}H NMR integration of the olefinic resonances and HPLC analysis. The first component eluted had an elution volume (11:73 ml), UV (λ_{max} 259, 205 nm) and ^{1}H NMR spectra identical to that of *E*-*p*-coumaryl alcohol (**1**). On the other hand, the component eluted at 14.00 ml had a ^{1}H NMR spectrum consistent with that of *Z*-*p*-coumaryl alcohol (**13**), *i.e.*, the olefinic resonances at 5.67 and 6.42 ppm had a coupling constant of J = 11.7 Hz indicating a *cis* configuration. Additionally, its UV spectrum (λ_{max} 253, 202 nm) corresponded to that expected for the *Z*-isomer **13**. Photoirradiation of *E*-sinapyl alcohol (**3**) also produced a mixture of two components in approximately 1.4:1 ratio from ^{1}H NMR integration of olefinic resonances and HPLC analyses. The first component had an elution volume (23.11 ml) and UV spectrum (λ_{max} 271, 220 nm) identical to that of *E*-sinapyl alcohol (**3**), whereas the second had an elution volume (29.42 ml), UV spectrum (λ_{max} 265, 217 nm) and olefin ^{1}H NMR coupling constant, J = 11.7 Hz consistent for *Z*-sinapyl alcohol (**15**).

Fig. 1 shows the HPLC profile of a mixture of all six *E*- and *Z*-monolignols (**1–3,13–15**). It is noteworthy that the separation of the isomers follow the sequential order of *p*-coumaryl (**1**): coniferyl (**2**): sinapyl (**3**) alcohols due to the effect of the bulky methoxyl groups. Additionally, the *Z* isomers were also less polar than the

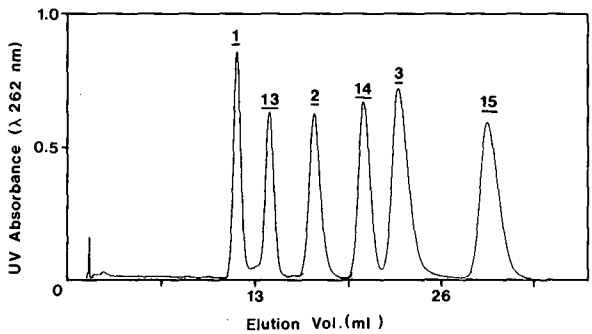

Fig. 1. HPLC elution profile of *E*/*Z* monolignols **1–3,13–15**. Elution details: Waters Novapak C_{18} column eluted with methanol–water (15:85, v/v) at a flow-rate of 1.3 ml min^{-1}. Numbers refer to structures previously shown.

corresponding *E* isomers, presumably due to an increased electronic interaction of the allylic hydroxyl group with the aromatic ring, and also due to a lower degree of delocalization of π-electrons in the molecular framework.

We next turned our attention to the photochemical isomerism of the *E* and *Z* isomers of coniferin (**5**,**16**). *E*-Coniferin (**5**) was prepared in 50% yield via direct reduction of the condensation product of *E*-methyl ferulate and acetobromoglucose with "ATE" complex[27], whereas *Z*-coniferin (**16**) was isolated from beech bark[25]. Chromatographic conditions for the separation of the individual glucosides required two Novapak C_{18} columns in series, which were eluted with acetonitrile–water (15:85, v/v) with detection at 257 nm. Photochemical irradiation of the *E* isomer **5** resulted in formation of both *E* and *Z* isomers in approximately 2:1 ratios, as evidenced by ^{1}H NMR analysis of the reaction mixture. Product identification of the two components again relied upon elution volumes, UV and ^{1}H NMR spectra. Thus *E*-coniferin (**5**) (λ_{max} 257, 212 nm) had an elution volume of 3.44 ml, whereas the corresponding *Z* isomer **16** (λ_{max} 254, 212 nm) was eluted at 3.98 ml. In a comparable fashion, *E*- and *Z*-mixtures of both syringin (**6**,**17**) and isoconiferin (**19**,**18**) were prepared by photoirradiation of the corresponding *Z* isomers, obtained from beech bark as before.

Fig. 2 shows the HPLC chromatogram of the six glucosides *i.e.*, *E*/*Z*-coniferin (**5**,**16**), syringin (**6**,**17**) and isoconiferin (**19**,**18**). Again, separation of the *E*/*Z* glucosides, coniferin and syringin, followed the general trend already noted for the *E*/*Z* monolignols.

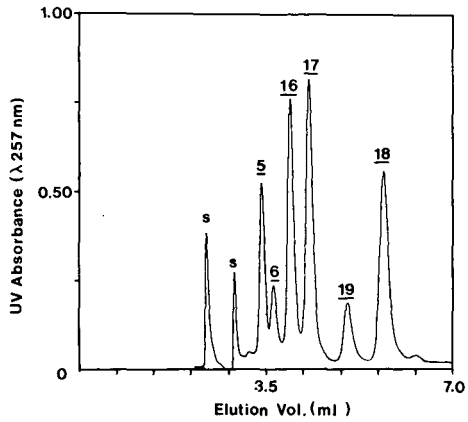

Fig. 2. HPLC elution profile of *E*/*Z* monolignol glucosides **5**,**6**,**16**–**19**. Elution details: two Waters Novapak C_{18} columns in series, eluted with acetonitrile–water (15:85, v/v) at a flow-rate of 0.7 ml min^{-1}. Numbers refer to structures previously shown; s = absorbance from solvents used in sample preparation.

CONCLUSIONS

This HPLC technique now permits the facile and rapid analysis of plant extracts, not only for the determination of *E*-monolignol and glucoside contents, but also for the corresponding *Z* isomers. Using this method, more meaningful chemotaxonomical studies of plants for these components can now be obtained, *i.e.*, the general significance of both *E*- and *Z*-monolignols and their glucosides, in various plants can now be determined.

This study also demonstrates that under suitable photochemical conditions, facile *E*/*Z* isomerization can be induced. However, unlike the hydroxycinnamic acids **7**,**8** which exist as mixtures of both *E* and *Z* isomers in graminaceous plants, only the *Z* isomers are detectable in beech bark tissue. If a simple photochemical process was in effect for the isomerization of *E*/*Z*-monolignols, then it would be expected that both isomers would accumulate in the bark. The underlying reasons for the exclusive accumulation of *Z* isomers in beech bark tissue needs to be determined.

ACKNOWLEDGEMENTS

The authors wish to thank the U.S. Department of Energy (grant DE-FG 05-88ER13883) for financial assistance.

REFERENCES

1 K. Freudenberg and A. C. Neish, *Constitution and Biosynthesis of Lignin*, Springer, Berlin, 1968.
2 D. C. C. Smith, *J. Chem. Soc.*, (1985) 2347–2351.
3 H. A. Stafford, *Plant Physiol.*, 37 (1962) 643–649.
4 S. El-Basyouni and G. H. N. Towers, *Can. J. Biochem.*, 42 (1964) 203–210.
5 P. J. Harris and R. D. Hartley, *Nature (London)*, 259 (1976) 508–510.
6 H. U. Markwalder and K. Neucom, *Phytochemistry*, 15 (1976) 836–837.
7 R. D. Hartley and P. J. Harris, *Biochem. Syst. Ecol.*, 9 (1981) 189–203.
8 Y. Kato and D. J. Nevins, *Carbohydr. Res.*, 137 (1985) 139–150.
9 S. C. Fry, *Planta*, 157 (1983) 111–123.
10 M. M. Smith and R. D. Hartley, *Carbohydr. Res.*, 118 (1983) 65–80.
11 A. Kato, J. Azuma and T. Koshijima, *Chem. Lett.*, (1983) 137–140.
12 H. Ohashi, E. Yamamoto, N. G. Lewis and G. H. N. Towers, *Phytochemistry*, 26 (1987) 1915–1916.
13 A. Kato, J. Azuma and T. Koshijima, *Holzforschung*, 38 (1984) 141–149.
14 I. Mueller-Harvey, R. D. Hartley, P. J. Harris and E. H. Curzon, *Carbohydr. Res.*, 148 (1986) 71–85.
15 A. Kato, J. Azuma and T. Koshijima, *Agric. Biol. Chem.*, 51 (1987) 1691–1693.
16 R. N. Antenucci, *Ph.D. Thesis*, Virginia Polytechnic Institute and State University, Blacksburg, VA, 1988.
17 T. L. Eberhardt, *M.S. Thesis*, Virginia Polytechnic Institute and State University, Blacksburg, VA, 1988.
18 N. G. Lewis, E. Yamamoto, J. B. Wooten, G. Just, H. Ohashi and G. H. N. Towers, *Science (Washington, D.C.)*, 237 (1987) 1344–1346.
19 A. Scalbert, B. Monties, J. Y. Lallemand, E. Guittet and C. Rolando, *Phytochemistry*, 24 (1985) 1359–1362.
20 N. G. Lewis, R. A. Razal, K. P. Dhara, E. Yamamoto, G. H. Bokelman and J. B. Wooten, *J. Chem. Soc., Chem. Commun.*, (1988) 1626–1628.
21 G. Engelsma, *Plant Physiol.*, 54 (1974) 702–705.
22 R. D. Hartley and E. C. Jones, *Phytochemistry*, 16 (1977) 1531–1534.
23 E. Yamamoto and G. H. N. Towers, *J. Plant Physiol.*, 117 (1985) 441–449.
24 E. Morelli, R. N. Rej, N. G. Lewis, G. Just and G. H.N. Towers, *Phytochemistry*, 25 (1986) 1701–1705.
25 N.G. Lewis, Ma. E. J. Inciong, H. Ohashi, G. H. N. Towers and E. Yamamoto, *Phytochemistry*, 17 (1988) 2119–2121.
26 J. Harmatha, H. Lubke, I. Rybarik and M. Mahdalik, *Collect. Czech. Chem. Commun.*, 43 (1978) 774–780.
27 S. Kim and K. H. Ahn, *J. Org. Chem.*, 49 (1984) 1717–1724.
28 N. G. Lewis, P. Dubelsten, T. L. Eberhardt, E. Yamamoto and G. H. N. Towers, *Phytochemistry*, 26 (1987) 2729–2734.

Journal of Chromatography, 479 (1989) 353–360
Elsevier Science Publishers B.V., Amsterdam — Printed in The Netherlands

CHROM. 21 717

SEPARATION OF ALGAL ORGANIC OSMOLYTES BY HIGH-PERFORMANCE LIQUID CHROMATOGRAPHY

N. W. KERBY*, R. H. REED and P. ROWELL
A.F.R.C. Research Group on Cyanobacteria and Department of Biological Sciences, University of Dundee, Dundee DD1 4HN (U.K.)
(Received April 20th, 1989)

SUMMARY

A method is described for the separation and quantification of a range of low-molecular-weight organic solutes, which are major osmolytes, in crude ethanolic extracts of marine algae. The method relies on the use of a silica amine modified column and refractive index detection. The acetonitrile to water ratio was varied to maximise separations. The method is suitable for the detection of simple carbohydrates, amino acids and their derivatives and is particularly suitable for the separation of the isomeric hexitols, altritol and mannitol, found in the brown alga *Himanthalia elongata*.

INTRODUCTION

Many phototrophic organisms, including algae, accumulate organic solutes as intracellular osmotica when grown under saline conditions. The accumulated organic compounds are often the major low-molecular-weight photoassimilate(s)[1] and include saccharides[2], heterosides[3], amino acids[4] or their methylated derivatives (betaines)[5] and sulphonium compounds[6]. Interest in the significance of low-molecular-weight organic solutes as osmotica in algal cells has led to the development of a range of procedures to identify and quantify these compounds. Natural abundance ^{13}C nuclear magnetic resonance (NMR) spectroscopy is the most appropriate technique to use for preliminary screening, since it identifies all organic solutes present in solution in osmotically significant amounts[7]. However, the insensitivity of ^{13}C NMR techniques necessitates either prolonged analysis times, prior concentration of algal material or access to a powerful, high-field strength spectrometer, making the technique less suitable for routine sample analysis. Consequently, such analysis and quantification of solutes is more frequently performed using one or more chromatographic procedures.

The chromatography of mono- and disaccharides has recently been reviewed[8]. Techniques have included thin-layer chromatography[9], column chromatography[10], gas–liquid chromatography[3], pyrolysis gas chromatography[11] and thin-layer electrophoresis/scanning reflectance densitometry[12]. More recently, high-performance

0021-9673/89/$03.50

liquid chromatography (HPLC) has been used to separate and quantify plant betaines and sulphonium compounds, *e.g.* β-dimethylsulphoniopropionate on a strong cation-exchange material with low-wavelength ultraviolet absorbance detection[13]. Analysis of low-molecular-weight carbohydrates by HPLC has been reviewed by Honda[14] and, unlike HPLC of amino acids and nucleosides, no general conditions have been established that allow the simultaneous analysis of all the different monosaccharides, due to the diversity of structures. Most conventional chromatographic procedures are time-consuming, requiring several purification steps prior to analysis and the organic solutes cannot always be recovered after separation and quantification. HPLC offers the potential for the non-destructive analysis of free (underivatised) solutes. However, separation of carbohydrates by normal-phase, reversed-phase and adsorption chromatography generally involves pre-column derivatisation. The need for derivatisation is usually related to the requirements of detection and not to altering the chromatographic separation of carbohydrates[8]. Reversed-phase chromatography is commonly used in the separation of simple sugars; both alkylated cyano-bonded and amino-bonded phases have been employed. Adding a small amount of a polyfunctional amine modifier to the mobile phase, to impregnate the silica column, overcomes the problems of the low solubility of carbohydrates and other solutes in the mobile phase and that of insufficient resolution[15]. Additionally, inclusion of aliphatic amines in the mobile phase ensures stability of the column by constantly renewing the surface of the stationary phase. However, silica columns modified in this way can undergo slow dissolution. Therefore, rigid walled steel columns are unsuitable for long term use, in contrast to plastic, radial compression silica columns.

The method described below combines the use of an aliphatic silica amine modifier (Waters SAM 1) with a radial compression silica cartridge and an isocratic separation system (acetonitrile–water–SAM), giving good separation of a range of algal organic osmolytes from crude ethanolic extracts, with quantification by refractometric detection. In contrast to earlier methods, the procedure is sufficiently simple and accurate to be used with large sample numbers, with automation.

MATERIALS AND METHODS

Sample collection and preparation

Prasiola stipitata Suhr in Jessen, *Enteromorpha intestinalis* (L.) Link, *Pelvetia canaliculata* (L.) Dcne et Thur. and *Himanthalia elongata* (L.) S. F. Gray were collected from Fife Ness (Nat. Grid Ref. NO639098), Fife, U.K. and were washed in filtered seawater prior to blotting dry. Samples (1 g) of algal vegetative tissue were extracted for 24 h in 5 ml 80% (v/v) ethanol at room temperature. Following freeze-drying of the ethanol extracts, the residue from each sample was dissolved in 100 μl of Milli Q water and centrifuged at 10 000 *g* for 5 min. Aliquots (10 μl) were loaded onto a Waters 10 cm × 8 mm Silica Pak cartridge (8SM HP4μ) fitted in a Waters Radial Compression Unit and were eluted at a flow-rate of 3 ml min^{-1} at room temperature. Solutes eluting from the column were detected using a refractometer, with the mobile phase as a reference. Fractions were collected, where necessary, using a Pharmacia Frac 100 fraction collector.

HPLC equipment

A Waters Maxima 820 chromatography workstation was used to collect data and control a Waters 510 pump. Low-molecular-weight organic compounds were detected with a Waters differential refractometer (R401) and the eluent was also monitored at 254 nm using a Waters LC spectrophotometer. Aliquots (10 μl) were injected onto the column via a Rheodyne injector.

Column conditioning and the mobile phase

Prior to analysis, columns were conditioned with 500 ml of a column conditioning solution, acetonitrile–water–SAM 1 reagent (Waters) (77:3:20, v/v/v) at a flow-rate of 1 ml min^{-1}. Following the first 50 ml, the solution was recycled.

The acetonitrile–water–SAM 1 ratio in the mobile phase was varied from 77:21:2 to 85:13:2 (v/v/v). Milli Q (Millipore) water was used throughout, the mobile phase was filtered through 0.22-μm Durapore filters and degassed by sonication in a water-bath (Cole Parmer) prior to use.

Chemicals

All chemicals were of the highest grade available and were purchased either from BDH (Poole, Dorset, U.K.), Millipore (U.K.) (Watford, U.K.) (for Waters products) or Rathburn Chemicals (Walkerburn, U.K.).

RESULTS

Various low-molecular-weight organic solutes, including carbohydrates, amino acids and betaine, are found in algae and, therefore, an HPLC method for the separation of such compounds is required. To investigate the effect of increasing the acetonitrile concentration in the mobile phase on the separation of a number of low-molecular-weight organic solutes (Table I) the acetonitrile concentration was varied from 77 to 85% (v/v) (Fig. 1). Increasing the acetonitrile concentration delayed the elution of individual solutes. Retention times for the individual components of the standard mixture are given in Table I. Mannitol and proline were incompletely resolved at 77% (v/v) acetonitrile. However, baseline separation was achieved when the acetonitrile concentration was increased to 82% (v/v). A further rise in acetonitrile concentration to 85% (v/v) resulted in inferior separation of these two solutes due to peak spreading. It should be noted that trehalose was not detected with a mobile phase containing 82 or 85% (v/v) acetonitrile and sucrose was also absent when 85% acetonitrile was employed (Fig. 1c, d; Table I). Therefore, optimal separation of diverse low-molecular-weight solutes, similar to those found as intracellular osmotica in algae, can be achieved by altering the water content of the mobile phase. A linear response for mannitol over the range 75–7500 nmol was found (data not shown), confirming that the method is suitable for quantitative analysis.

Fig. 2 shows the elution profile of an 80% (v/v) ethanolic extract of the green alga *Enteromorpha intestinalis* using 77% (v/v) acetonitrile in the mobile phase. The profile was characterised by a peak (retention time 3.8 min) which also had a correspondingly high UV absorption at 254 nm (data not shown) with identical chromatographic features to NaCl. This peak was detected in all marine algal samples tested and is due presumably to carry over of (sea)salt in marine samples. Ethanolic extracts

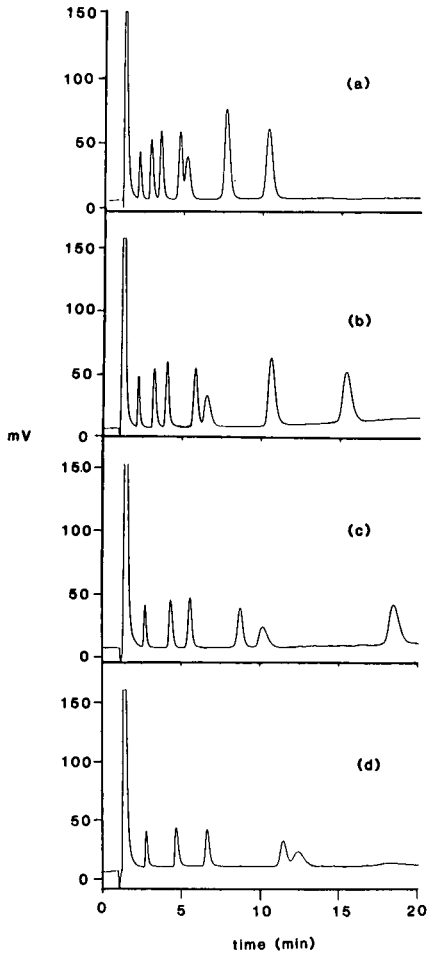

Fig. 1. Standards chromatographed using a mobile phase with increasing acetonitrile concentration. Organic solutes were detected by refractive index. (a) 77% (v/v), (b) 80% (v/v), (c) 82% (v/v), (d) 85% (v/v) acetonitrile. 500 nmol of each standard (see Table I) were applied in 10 μl of Milli Q water.

of fresh wateralgae did not contain this peak (data not shown). The peak eluting at 4.9 min was shown to be β-dimethylsulphoniopropionate (DMSP) by alkaline hydrolysis using 17% (w/v) NaOH and also using purified DMSP as a standard[16]. A small, broad peak which eluted at 7.6 min corresponded to sucrose. DMSP had previously been shown to be the major intracellular organic solute in *E. intestinalis*, with sucrose present as a trace constituent[17].

The separation of four intracellular organic solutes from ethanolic extracts of *Prasiola stipitata* using 80% (v/v) acetonitrile is shown in Fig. 2b. The peak at 4.9 min corresponded to salt and those at 4.2, 5.9, 7.0 and 11.6 min to ribitol, sorbitol, proline and sucrose, respectively. These solutes have previously been identified in marine algae by NMR (ref. 17, and our unpublished data). The two polyols and the amino acid proline appeared to be the major low-molecular-weight organic solutes and

TABLE I

RETENTION TIMES FOR LOW-MOLECULAR-WEIGHT ORGANIC SOLUTES AS A FUNCTION OF THE PERCENT ACETONITRILE IN THE MOBILE PHASE.

The elution profiles for these low-molecular-weight organic solutes are shown in Fig. 1. NR = not resolved within 20 min.

Solute	*Retention time (min)*			
	% acetonitrile in the mobile phase			
	77	*80*	*82*	*85*
Glycerol	2.16	2.20	2.70	2.79
Betaine	2.89	3.19	4.31	4.70
Ribitol	3.52	4.00	5.55	6.68
Mannitol	4.73	5.80	8.75	11.50
Proline	5.19	6.52	10.15	12.44
Sucrose	7.67	10.58	18.43	NR
Trehalose	10.35	15.33	NR	NR

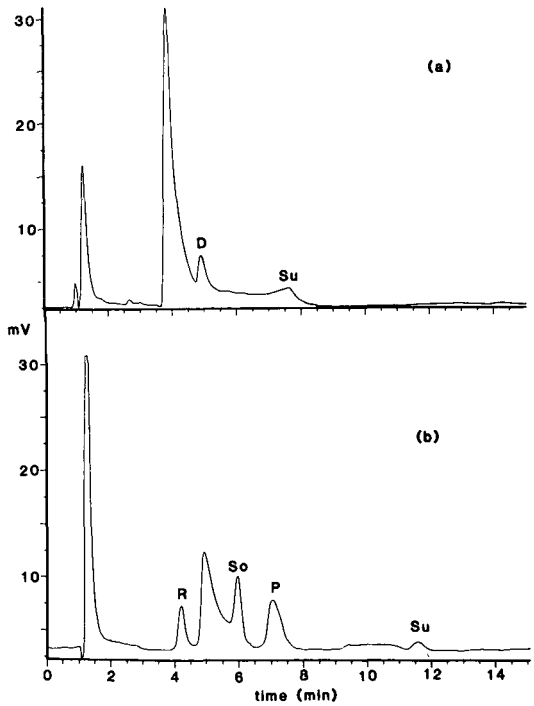

Fig. 2. Elution profile of an ethanolic extract of (a) *Enteromorpha intestinalis* using 77% (v/v) acetonitrile, and (b) *Prasiola stipitata* using 80% (v/v) acetonitrile. D = DMSP; P = proline; R = ribitol; So = sorbitol; Su = sucrose.

sucrose was identified as a minor component in *P. stipitata*, as in *E. intestinalis* (Fig. 2a). A mobile phase of 80% (v/v) acetonitrile was required to maximise the separation of these components.

The hexitol mannitol is the major photoassimilate in members of the Phaeophyta[18] and accumulates in response to osmotic shock[19]. A single peak of mannitol is detected in the majority of brown algae, *e.g.*, *Fucus* spp., *Ascophyllum nodosum* and *Laminaria* spp. However, the isomeric hexitol, altritol, has been shown to accumulate to osmotically significant amounts in *Himanthalia elongata* and in several related Australian species using natural abundance ^{13}C NMR spectroscopy[20,21]. Fig. 3a

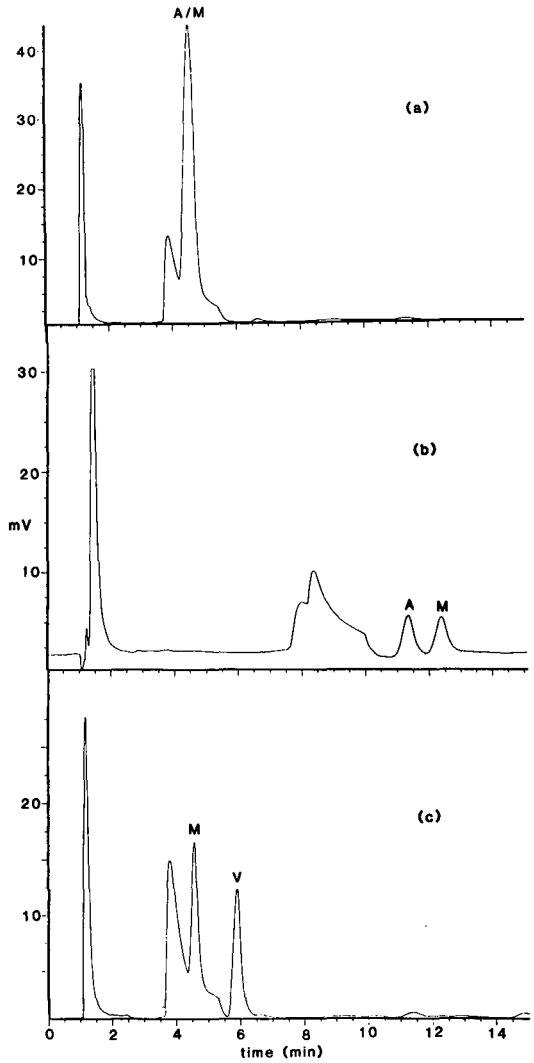

Fig. 3. Elution profile of an ethanolic extract of (a) *Himanthalia elongata* using 77% (v/v) acetonitrile, (b) *H. elongata* using 85% (v/v) acetonitrile and (c) *Pelvetia canaliculata* using 77% (v/v) acetonitrile. A/M = altritol/mannitol; A = altritol; M = mannitol; V = volemitol.

shows an elution profile for *H. elongata* using 77% (v/v) acetonitrile in the mobile phase. In addition to the salt peak at 3.9 min, a single large peak eluted with a retention time of 4.5 min which had similar chromatographic properties to mannitol and is due to both hexitols. Similarly, these isomers are not resolved by conventional gas–liquid chromatography[22] and paper chromatography[23]. Increasing the acetonitrile concentration to 85% (v/v) in the mobile phase resulted in the complete resolution of both hexitols (altritol 11.3 min and mannitol 12.4 min; Fig. 3b). The mannitol peak was confirmed using authentic mannitol whereas the identity of altritol was confirmed, following collection of the fractions, by gas–liquid chromatography[24]. Gas–liquid chromatographic separation of these hexitols requires long run times of over 1 h and gives broad peaks which are incompletely resolved. However, it is an adequate method for identification. Fig. 3c shows the separation of a hexitol (mannitol, retention time 4.6 min) and a heptitol (volemitol, retention time 5.9 min) in ethanolic extracts from the brown alga *Pelvetia canaliculata*. Volemitol is restricted to this species and shows a smaller response than mannitol to changes in salinity[19].

DISCUSSION

The method described here provides a reliable and rapid means of separating and quantifying a range of low-molecular-weight organic solutes and is especially suitable for algal samples containing compounds of diverse structure, *e.g.*, polyols, sugars, amino acids, quaternary ammonium and tertiary sulphonium compounds, which are present in osmotically significant amounts. Sample preparation is minimal, with no requirement for derivatisation. Good separation is achieved by varying the acetonitrile concentration, with short run times. The method is non-destructive and fractions can be collected with good recovery.

In all marine algal samples tested a peak due to the carry over of seasalt, during sample preparation, was present. This was unavoidable since rinsing in distilled water to remove adhering seawater would result in the loss of low-molecular-weight intracellular constituents[25]. However, by changing the amount of acetonitrile in the mobile phase the salt may be resolved from the intracellular components.

This method is particularly suitable for the separation of the two isomeric hexitols, altritol and mannitol, found in the brown alga *Himanthalia elongata*. Baseline separation can be achieved with an acetonitrile concentration of 85% (v/v) in the mobile phase within 15 min, providing significant advantages over techniques previously employed.

The separations reported here rely on the use of an amino-bonded silica column, modified with an aliphatic silica amine. Increasing the water content of the mobile phase speeds up elution on amino-bonded columns. Such separations have been assumed to be due to normal-phase partition chromatography. However, controversy over the mechanism of separation exists; some prefer to regard this as reversed-phase adsorption while others consider that three mechanisms are involved, *i.e.*, adsorption, partition and surface tension (see ref. 14).

ACKNOWLEDGEMENTS

We thank the Agricultural and Food Research Council for financial support and Gail Alexander for her helpful comments.

REFERENCES

1 B. P. Kremer, *Oceanogr. Mar. Biol. Annu. Rev.*, 19 (1981) 41–94.
2 E. Blumwald and E. Tel-Or, *Arch. Microbiol.*, 132 (1982) 168-172.
3 R. H. Reed, J. C. Collins and G. Russell, *J. Exp. Bot.*, 31 (1980) 1539–1554.
4 T. L. Setter and H. Greenway, *Aust. J. Plant Physiol.*, 6 (1979) 47–60.
5 R. H. Reed, *Br. Phycol. J.*, 24 (1989) 21–37.
6 R. H. White, *J. Mar. Res.*, 40 (1982) 529–535.
7 L. J. Borowitzka, in L. G. Paleg and D. Aspinall (Editors), *The Physiology of Drought Resistance in Plants*, Academic Press, Sydney, 1981, pp. 97–130.
8 K. Robards and M. Whitelaw, *J. Chromatogr.*, 373 (1986) 81–110.
9 G. A. Codd and W. D. P. Stewart, *Arch. Mikrobiol.*, 94 (1973) 11–28.
10 N. W. Kerby, P. Rowell and W. D. P. Stewart, *Arch. Mikrobiol.*, 141 (1985) 244–248.
11 P. I. A. Szilagyi, D. E. Schmidt and J. P. Green, *Anal. Chem.*, 40 (1968) 2009–2013.
12 J. Gorham, S. J. Coughlan, R. Storey and R. G. Wyn Jones, *J. Chromatogr.*, 210 (1981) 550–554.
13 J. Gorham, *J. Chromatogr.*, 287 (1984) 345–351.
14 S. Honda, *Anal. Biochem.*, 140 (1984) 1–47.
15 K. Aitzetmuller, *J. Chromatogr.*, 156 (1978) 354–358.
16 R. H. Reed, *Mar. Biol. Lett.*, 4 (1983) 173–181.
17 D. M. Edwards, R. H. Reed and W. D. P. Stewart, *Mar. Biol.*, 95 (1987) 583–592.
18 R. G. S. Bidwell, *Can. J. Bot.*, 45 (1967) 1557–1565.
19 R. H. Reed, I. R. Davison, J. A. Chudek and R. Foster, *Phycologia*, 24 (1985) 35–47.
20 J. A. Chudek, R. Foster, I. R. Davison and R. H. Reed, *Phytochemistry*, 23 (1984) 1081–1082.
21 P. J. Wright, M. N. Clayton, J. A. Chudek, R. Foster and R. H. Reed, *Phycologia*, 26 (1987) 429–434.
22 P. M. Holligan and E. A. Drew, *New Phytol.*, 70 (1971) 271–295.
23 R. F. Jones, *Biol. Bull. (Woods Hole, Mass.)*, 110 (1958) 169–178.
24 P. J. Wright and R. H. Reed, *J. Exp. Mar. Biol. Ecol.*, 93 (1985) 183–190.
25 R. H. Reed and P. J. Wright, *Mar. Ecol. Prog. Ser.*, 29 (1986) 205–208.

Journal of Chromatography, 479 (1989) 361–367
Elsevier Science Publishers B.V., Amsterdam — Printed in The Netherlands

CHROM. 21 678

DETERMINATION OF VITAMIN U AND ITS DEGRADATION PRODUCTS BY HIGH-PERFORMANCE LIQUID CHROMATOGRAPHY WITH FLUORESCENCE DETECTION

C. P. LEUNG* and W. K. H. LEUNG
Government Laboratory, 12 Oil Street, North Point (Hong Kong)
(First received March 28th, 1989; revised manuscript received June 3rd, 1989)

SUMMARY

A high-performance liquid chromatographic method has been developed for the determination of vitamin U in tablets and capsules. Threonine was employed as the internal standard throughout the assay. The *o*-phthalaldehyde derivatives were prepared and then chromatographed isocratically on a reversed-phase C_{18} column. The optimum reaction time for both vitamin U and threonine at pH 10.5 is 5 min. Vitamin U and its major degradation product in the dosage forms, *viz.*, methionine sulphoxide, were separated and quantified with a relative standard deviation of about 1%, using a fluorescence detector with excitation and emission wavelengths at 340 and 450 nm respectively. A linear relationship has been established between the peak area ratio of vitamin U/threonine and the concentration of vitamin U over the range of 2.5–50 μg/ml.

INTRODUCTION

Vitamin U (DL-methionine-S-methylsulphonium chloride) is an anti-ulcer vitamin extracted from cabbage leaves and other green vegetables[1]. The extracts and the synthetic compound have been widely used in Asia for the treatment of gastric disorder in conjunction with antacids and anticholinergic agents. There are more than ten over-the-counter formulations containing vitamin U available locally in Hong Kong. Most are in the form of plain tablets, capsules and sugar-coated tablets, in which the vitamin U is mixed with other active ingredients, the amounts present in each tablet or capsule being in the range of 4 to 50 mg. In one preparation, vitamin U is embedded centrally in a shell of antacids in a composite tablet. There are only a few reports in the literature on the determination of vitamin U. One involves the assay of dosage forms by amperometric titration[2] and the other the study of vitamin U metabolism in human and animals by gas and column liquid chromatography[3]. The former method is not selective as it cannot differentiate vitamin U from its degradation products in dosage forms. The latter method is quite complicated to perform, requires special apparatus for the generation of dimethyl sulphide from vitamin U and again lacks selectivity for the assay of dosage forms.

Vitamin U is very hygroscopic and is hydrolysed rapidly in alkaline media. When

0021-9673/89/$03.50

compounded in tablets or capsules with other basic ingredients such as aluminium hydroxide and magnesium hydroxide, decomposition may occur upon absorption of moisture from the atmosphere. Specific methods for the separation of vitamin U from its degradation products are therefore required for the analysis of vitamin U preparations.

When applying the high-performance liquid chromatographic (HPLC) method for the determination of vitamin U, one major problem encountered is that vitamin U has no UV or visible absorption characteristics. Reversed-phase chromatographic systems with short wavelength UV detection (210 nm) have been tested without success. *o*-Phthalaldehyde (OPA) has been demonstrated to be very useful for the precolumn and postcolumn fluorigenic detection of amines and amino acids[4–9]. Making use of the primary amine functional group of vitamin U, derivatization with OPA yields the corresponding fluorescent isoindole which can be detected by a fluorescence detector.

The OPA derivatives of methionine and its sulphone have been chromatographed by reversed-phase HPLC[9]. However, there is no report on the HPLC separation of vitamin U and its degradation products. This paper reports the development of a reversed-phase HPLC method for the quantitation of vitamin U and its major degradation product by derivatization with OPA and fluorescence detection.

EXPERIMENTAL

Instruments

An ISCO Model 2350 HPLC pump (Isco, Lincoln, NE, U.S.A.) was used at a flow-rate of 1.7 ml/min. Analysis was performed using a 250 mm × 4.6 mm I.D. stainless-steel column packed with 7-μm ODS particles (Cat. No. CP-10-5; Chemco Scientific, Osaka, Japan) using a Chemco slurry packing apparatus Model 124AA. The sample was injected into the column using a Rheodyne 7125 injector (Rheodyne, Cotati, CA, U.S.A.) with a 20-μl loop. The column effluents were monitored with a Beckman 157 fluorescence detector (Beckman Instruments, Berkeley, CA, U.S.A.) equipped with a coloured glass excitation filter (305–395 nm) and a wide band interference emission filter (430–470 nm). The integrator used was a Shimadzu Chromatopac C-R3A (Shimadzu, Kyoto, Japan) operated by the 100-mV output from the detector.

Reagents

Methanol and acetonitrile were HPLC grade, obtained from Ajax (Auburn, Australia). OPA was obtained from Sigma (St. Louis, MO, U.S.A.). Analytical reagent grade anhydrous disodium hydrogenphosphate and sodium dihydrogenphosphate dihydrate (Riedel-de Haen, Hannover, F.R.G.) were used to prepare a buffer solution. 2-Mercaptoethanol was from E. Merck (Darmstadt, F.R.G.). The internal standard, DL-threonine, and DL-methionine sulphoxide were obtained from BDH Chemicals (Poole, U.K.) and TCI (Tokyo Kasei Kogyo, Tokyo, Japan) respectively.

Mobile phase

A stock phosphate buffer solution was prepared by dissolving 5.8 g of sodium

dihydrogenphosphate dihydrate and 15.4 g of anhydrous disodium hydrogenphosphate in 500 ml of water.

In the preparation of the mobile phase, 80 ml of acetonitrile were first placed in a 500-ml stoppered measuring cylinder, followed by 25 ml of the stock phosphate buffer solution and water was then added to make up the volume. The mobile phase was degassed with an ultrasonic bath prior to use. The volume of acetonitrile may have to be slightly modified in order to obtain the optimum chromatographic performance.

Derivatization reagents

Borate buffer. 0.5 *M* Sodium borate (31 g in 1 l of water) was adjusted to pH 10.5 with potassium hydroxide pellets.

OPA solution. About 50 mg of OPA were dissolved in 5 ml of methanol. This solution was freshly prepared daily.

2-Mercaptoethanol solution. A 5-μl volume of 2-mercaptoethanol was added to 5 ml of methanol. This solution was also freshly prepared daily.

Vitamin U stock standard solution

About 10 mg of vitamin U were accurately weighed and dissolved in 200 ml of water.

Vitamin U working standard solutions

To four 100-ml volumetric flasks were added respectively 5, 10, 25 and 50 ml of the stock standard solution and made up to the mark with water. These working standard solutions contained respectively 2.5, 5, 12.5 and 25 μg/ml of vitamin U.

Internal standard solution

About 3 mg of DL-threonine were weighed and dissolved in 100 ml of water.

DL-Methionine sulphoxide standard solution

About 3 mg of DL-methionine sulphoxide were accurately weighed and dissolved in 100 ml of water.

Sample preparation

Twenty capsules or tablets were weighed and powdered. An accurately weighed quantity of the powder equivalent to about 2 mg of vitamin U was transferred to a 100-ml volumetric flask and about 90 ml of water were added. The contents of the flask were sonicated for 30 min and then made up to the mark with water. The mixture was filtered through Whatman No. 542 filter-paper. The first 10-ml portion of the filtrate was discarded and the remainder collected in a glass-stoppered flask.

Derivatization procedure

Volumes of 100 μl of each of the vitamin U working standard solutions and sample solutions were quantitatively transferred to 5-ml reaction vials. A 50-μl volume of internal standard solution was added, followed by 50 μl of borate buffer, and the solution was mixed thoroughly. Volumes 100 μl each of OPA and 2-mercaptoethanol solution were then added and mixed. A 4-ml volume of methanol was added to stop the reaction after 5 min. The resulting solutions were injected into the liquid chromatograph.

RESULTS AND DISCUSSION

A study was carried out at room temperature to select the time for completion of the derivatization reaction of vitamin U and the internal standard (threonine) with OPA. The reaction conditions described above were used with various reaction times. As shown in Figs. 1 and 2, the optimum reaction time for completion of derivatization of both vitamin U and the internal standard is 5–10 min. The results for D-methionine sulphoxide which is the major degradation product of vitamin U (*vide infra*) were similar. Thus room temperature for 5 min was chosen as the derivatization condition throughout the determination. The OPA derivatives were found to be stable for more than 1 h.

Under the experimental conditions established, a linear relationship between the peak area ratio (vitamin U/threonine) and concentration of vitamin U was demonstrated over the range of 2.5–50 μg/ml and the correlation coefficient, r, was found to be 0.9990. The peak area ratio (DL-methionine sulphoxide/threonine) was also linearly related to the concentration of DL-methionine sulphoxide over the range of 5–50 μg/ml and r was 0.9999. Typical chromatograms of DL-methionine sulphoxide and vitamin U are shown in Fig. 3, the amounts injected being 14 and 12 ng respectively.

Since more than ten over-the-counter formulations containing vitamin U are available in Hong Kong, four typical ones were selected on the basis of their differences

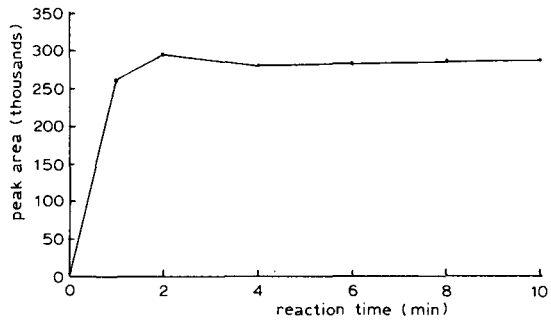

Fig. 1. Variation of the peak area of vitamin U with reaction time.

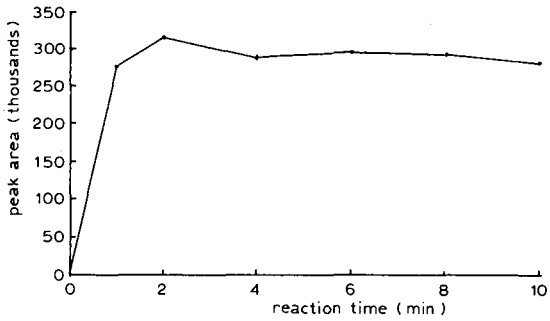

Fig. 2. Variation of the peak area of DL-threonine (the internal standard) with reaction time.

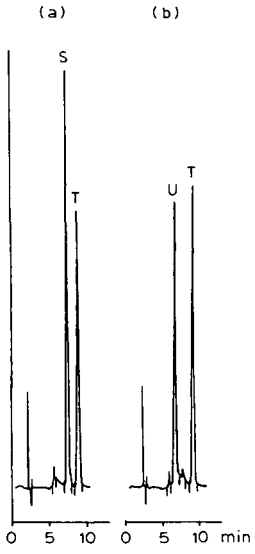

Fig. 3. Chromatograms of (a) DL-methionine sulphoxide (14 ng) and (b) vitamin U (12 ng). Peaks: U = vitamin U; S = DL-methionine sulphoxide; T = DL-threonine.

in dosage forms, origin and the presence of other active ingredients. The results of analysis of these four commercial samples using the HPLC method proposed are shown in Table I. The intra-assay coefficients of variation were between 0.3 and 1.4%, while the inter-assay coefficients of variation were between 0.4 and 2.9% in the range of 2.5–50 μg/ml of vitamin U.

Antacids and anticholinergic agents such as aluminium hydroxide, magnesium trisilicate, atropine, scopolamine and hyoscyamine were found not to interfere with the derivatization and HPLC separation when present at the analysis concentrations. A recovery experiment was carried out on a freshly prepared synthetic mixture containing a known amount of vitamin U and with appropriate quantities of aluminium hydroxide and magnesium trisilicate. The recovery was found to be 99.1 ± 0.6%.

Vitamin U is stable when dry, but not after absorbing moisture and in the presence of antacids which are usually basic in nature. Based on its structure, there are several possible degradation products, *viz.*, methionine sulphoxide, methionine sulphone, methionine and homoserine. However, it is noteworthy that the reference standard solutions did not show any significant loss in vitamin U content after standing at room temperature for 75 days, showing that the degradation might be the result of the presence of the alkaline medium.

Chromatograms of the four samples examined are shown in Fig. 4. Compared with the chromatogram of standard vitamin U, it was observed that for the first three samples the vitamin U peak was smaller than expected and there was a relatively large second peak which was present in very small quantity in the standard. Subsequent analysis showed that this peak corresponded to methionine sulphoxide which should be the major degradation product of vitamin U in the first three samples in which vitamin U was in direct contact with the antacids. Absorption of moisture might be the

TABLE I

DETERMINATION OF VITAMIN U AND METHIONINE SULPHOXIDE IN PHARMACEUTICAL PREPARATIONS

Preparation	*Origin*	*Labelled contents*	*Percentage of labelled content found*[a]	
			Vitamin U	*Methionine sulphoxide*[b]
Plain tablet	Japan	Vitamin U 4.17 mg Aluminium magnesiumsilicate 67 mg Scopolia extract 1.7 mg Carboxymethylcellulose calcium 10.5 mg	24.5 ± 0.3	46.6 ± 0.3
Capsule	Hong Kong	Vitamin U 30 mg Belladonna dry extract 15 mg Dried aluminium hydroxide gel 150 mg Magnesium hydroxide 150 mg	8.7 ± 0.1	49.2 ± 0.8
Sugar-coated tablet	China	Vitamin U 50 mg Dried aluminium hydroxide gel 123 mg Magnesium trisilicate 50 mg	35.3 ± 0.5	34.4 ± 0.6
Composite tablet	Japan	Inner tablet: vitamin U 25 mg diastase 60 mg Outer tablet: sodium glycyrrhizinate 33 mg glucuronic acid 17 mg dried aluminium hydroxide gel 160 mg magnesium trisilicate 145 mg	98.1 ± 0.3	0.7[c]

[a] Mean of five determinations, with standard deviation.
[b] Calculated as the equivalent of vitamin U.
[c] This is an approximation as the peak area lies outside the calibration range.

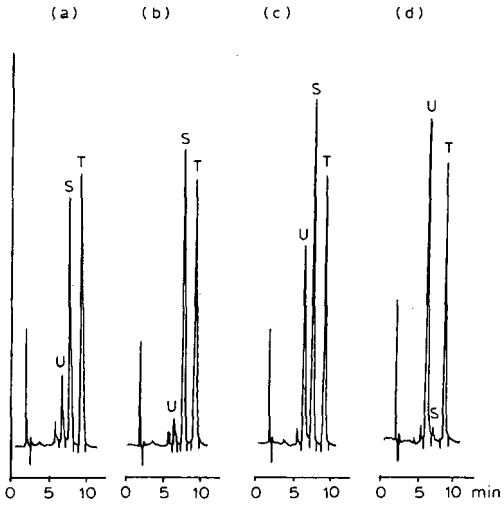

Fig. 4. Chromatograms of (a) plain tablet, (b) capsule, (c) sugar-coated tablet, (d) composite tablet; peaks as in Fig. 3.

cause of degradation. Quite surprisingly, methionine, methionine sulphone and homoserine were not detected.

For the last sample of a composite tablet, little decomposition of vitamin U was observed. It should therefore be the most stable dosage form as the vitamin U is separated from the antacids and is protected from moisture by the outer shell. As expected, the sugar-coated tablet was relatively more stable than the plain tablet and capsule because of better protection from atmospheric moisture.

ACKNOWLEDGEMENT

We thank the Government Chemist of Hong Kong for permission to publish this paper.

REFERENCES

1 *The Merck Index*, Merck & Co., Rahway, NJ, 10th ed. 1983, p. 1439.
2 M. I. Lebeveva, B. I. Isaeva, A. N. Dubovitskaya and M. V. Terekhina, *Farmatsiya (Moscow)*, 33 (1984) 79, *Anal. Abstr.*, 46 (1984) 8E22.
3 A. A. Bezzubov and N. N. Gessler, *J. Chromatogr.*, 273 (1983) 192.
4 M. Roth, *Anal. Chem.*, 43 (1971) 880.
5 M. Roth and A. Hampaï, *J. Chromatogr.*, 83 (1973) 353.
6 T. P. Davis, C. W. Gehrke, C. W. Gehrke, Jr., T. D. Cunningham, D. Thomas, K. C. Kuo, K. O. Gerhardt, H. D. Johnson and C. H. Williams, *Clin. Chem.*, 24 (1978) 1317.
7 L. D. Mell, *J. Liq. Chromatogr.*, 1 (1978) 261.
8 R. E. Subden, *J. Chromatogr.*, 166 (1978) 310.
9 P. Lindroth and K. Mopper, *Anal. Chem.*, 51 (1979) 1667.

Journal of Chromatography, 479 (1989) 369–376
Elsevier Science Publishers B.V., Amsterdam — Printed in The Netherlands

CHROM. 21 724

HIGH-PERFORMANCE LIQUID CHROMATOGRAPHIC DETERMINATION OF BENZIL IN AIR AS AN INDICATOR OF EMISSIONS DERIVED FROM POLYESTER POWDER COATINGS

JARI PUKKILA and HELMI KOKOTTI
University of Kuopio, P.O. Box 6, SF-70211 Kuopio 21 (Finland)
and
KIMMO PELTONEN*
Institute of Occupational Health. Topeliuksenkatu 41 a A, SF-00250 Helsinki (Finland)
(First received March 16th, 1989; revised manuscript received June 20th, 1989)

SUMMARY

A method to estimate occupational exposure to emissions from the curing of polyester powder paints was developed. The method is based on the monitoring only of a certain marker compound in workroom air in order to make the determinations easier. Benzil, reproducibly emitted from all the powders tested, was chosen as the indicator for curing (220°C)-derived emissions. A method for the air sampling and high-performance liquid chromatographic benzil is described. Aspects of the use of marker compounds are discussed.

INTRODUCTION

The industrial hygiene aspects of powder coating treatments have been studied in our laboratory for some years. The principle of measuring certain marker compounds only was adapted to enable estimations of powder-related occupational health risks. Previous studies were concerned with epoxy resin based powder coatings[1,2]. These studies have since been extended to include polyester-based powder coatings, the second most popular powder material in use in Finland.

The purpose of this study was to choose a suitable indicator from among the compounds released during the thermal curing of several commercial polyester powder coatings. The existence of a marker in workroom air is a sign of emissions into that air and thus a measure of air quality.

Laboratory curing experiments were performed in the search for a marker which is reproducibly emitted at the curing temperatures. Benzil proved to be a suitable marker, and has been analysed by gas–liquid chromatography (GLC)[3,4] and high-performance liquid chromatography (HPLC)[5]. There are, however, no literature data on the air sampling of benzil. In this paper we propose a method for the air sampling of benzil and for its liquid chromatographic determination. Air samples were collected on combinations of 13-mm glass fibre filters and silica sorbent tubes and were analyzed by HPLC with UV detection.

0021-9673/89/$03.50

EXPERIMENTAL

Laboratory curing of powders

Three commercial polyester coating powders were cured in laboratory experiments. The compounds released were collected and chromatographed with GC to obtain the corresponding emission profiles. Curing experiments were carried out with a device based on a movable oven system, described elsewhere[6]. A 10-g amount of powder was spread over a length of 100 cm in a glass tube (1500 mm x 17 mm I.D.). An oven was moved along the tube at 1 cm/min. The oven temperature was set at 220°C which is a typical curing temperature for polyester powders. Synthetic air (20% oxygen, 80% nitrogen) was drawn through the tube at 500 ml/min.

A 37-mm glass fibre filter (Sartorius, Cat. No. SM13400) in a 37-mm filter holder was connected to the outlet of the sample tube by PTFE tubing. A spiral glass cold trap was connected after the filter to collect the volatiles, and was cooled with solid CO_2. After sampling, the filter was extracted in a test-tube with 2.0 ml of dichloromethane. The contents of the spiral trap were eluted with 1.0 ml of dichloromethane.

Selection of the marker

The air samples in dichloromethane from the curing experiments were concentrated to 200 μl and 1.5 μl were injected into an Hewlett-Packard 5790A gas chromatograph equipped with a flame ionization detector and operated in a splitless mode. The compounds emitted were separated with a BP-5 fused-silica column (25 m × 0.22 mm I.D.: SGE, Australia) with a 0.25-μm film. The peaks of interest were identified with a Hewlett-Packard 5890 gas chromatograph equipped with an HP 5970 mass-selective detector. The temperature programme started from 30°C held for 1 min and reached 275°C in 55 min.

Air sampling of benzil

Air atmospheres containing benzil were produced to test the sampling performance of 13-mm glass fibre filters and silica air sampling tubes connected together or separately. Benzil or powder materials were placed in the bend of a J-shaped glass tube (300 mm × 5 mm I.D.) which was inserted in a laboratory oven. The J-tube was heated at 220°C. No attempt was made to make the vaporization linear. The outlet arm of the J-tube was connected to a 1-l empty impinger bottle which was connected

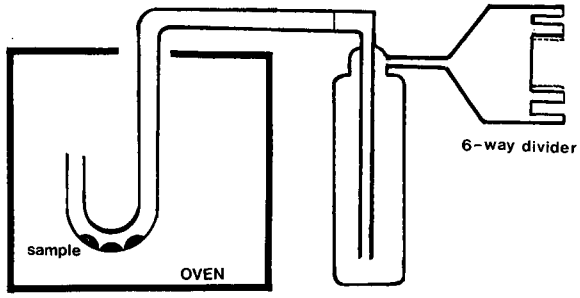

Fig. 1. A schematic diagram of the J-tube assembly.

to a six-way glass divider for simultaneous comparisons between different collection media. A schematic diagram of the J-tube assembly is shown in Fig. 1. Rather spacious glass tubing was utilized for reasons of conditional similarity for the laboratory and workroom sampling. The purpose was to allow cooling of the air stream before sampling better to simulate the sampling conditions in a workroom. However, this experimental set-up subjected benzil to severe adsorption on the walls of the apparatus.

Two filter cassettes containing the filters were connected in series. The filters (13 mm, Type AE, Cat. No. 225-16; SKC, Eighty Four, U.S.A.) were analyzed separately, as were the analytical and back-up sections of the silica tubes (70 mm x 6 mm, 150/75 mg packing, Cat. No. 226-10, SKC). Air was drawn through each arm of the six-way system by personal air-sampling pumps (Model 222-3, SKC) at the rate of 200 ml/min.

Desorption tests

The desorption of benzil from the 13-mm filters was studied by injecting 30 μl of standard solutions of benzil in methanol onto the filters. The filter loadings were 0.1, 0.2 and 0.5 μg. The filters were allowed to dry and were then immersed in 1.0 ml of methanol. Desorption from the silica tubes was studied by adding the content of a tube to 1.0 ml of a standard methanol solution. The concentrations of these solutions were 0.2, 0.5 and 1.0 μg/ml. Overnight phase equilibration for both types of samples was carried out before analysis.

Liquid chromatography

Air samples of benzil were analyzed with a Pye Unicam Model 100A liquid chromatograph equipped with a Pye Unicam LC-XP gradient programmer and a Shimadzu SPD-6A UV detector operated at 260 nm. The column was a Spherisorb ODS^{-2} (5 μm, 150 mm $\times$ 4.6 mm I.D.; Phase Separations, U.K.). The mobile phase was water–methanol (40:60), flow-rate 1.0 ml/min. External standards in methanol were made from 98% pure benzil (Cat. No. B515-1, Aldrich).

RESULTS AND DISCUSSION

Air samples collected on the 37-mm filter and cold trap from the laboratory curing experiments were subjected to GC to obtain the emission profiles. The curing experiment was repeated twice for each powder material. The two emission profiles of a particular polyester coating material were very similar. Fig. 2 shows a chromatogram of a curing air sample. Gas chromatograms of the three coating materials were investigated to find common peaks in all of them. The filter sample contained high-boiling compounds while the more volatile fraction of the emissions was found in the cold trap.

A marker compound should preferably not be a common contaminant found in industrial environments like formaldehyde or phthalates. A marker should also be present in the emissions at concentrations exceeding trace level to enable convenient field sampling times. The marker emissions should also be repeatable from experiment to experiment, indicating a constant emission mechanism.

In these experiments the peak corresponding to benzil fulfilled the aforemen-

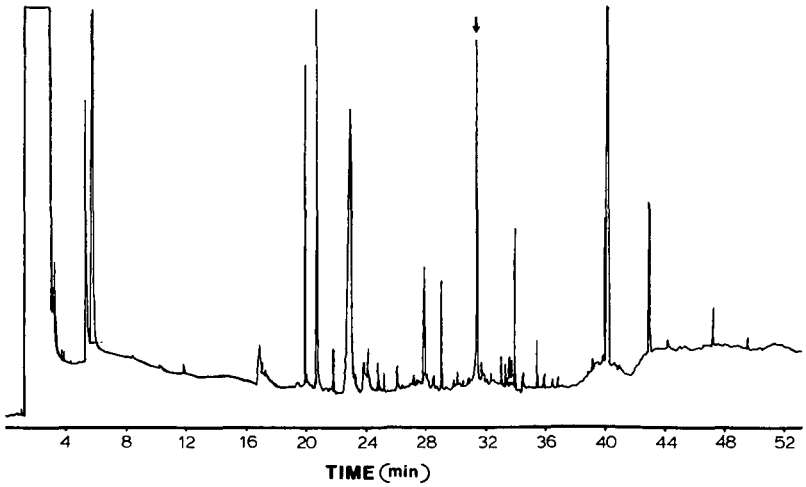

Fig. 2. A GC chromatogram of a curing air sample collected on a filter. The arrow points to the benzil peak.

tioned requirements. Benzil is probably used in polyester coating powders as an air release agent. It can thus be found also in uncured powders. The amounts of benzil in powders from different suppliers are comparable, making its use as a marker independent of the origin of the paint.

Benzil is a solid at ambient temperature and air sampling on filters is thus an obvious choice. The sampling characteristics of silica air-sampling tubes were, however, also tested. For simultaneous performance testing a six-way sampling train was employed. The benzil loading in the J-tubes was varied to give different benzil atmospheres. Adsorption on the walls of the long glass tubing preceding the collection area was considerable. This was considered irrelevant since the experimental conditions at the collection zone thus better represent the actual conditions in a workroom where the sampled air is at about room temperature, and the sample molecules to be collected typically have airborne residence times much longer than if sampled directly from the hot air stream coming from the outlet arm of the J-tube without the impinger bottle. The air concentration at the inlet zone of the collection media was estimated from the liquid chromatographic peaks of the 5-l samples by assuming 100% collection efficiency for the highest peak. These estimations are inaccurate but are indicative of the magnitude of the concentrations, and are referred to as apparent concentrations. The concentrations can not be estimated from the amount of the starting material in the J-tube because of the adsorption on the walls. Benzil was applied to the tube as methanol solutions of known concentrations which were allowed to dry before heating and sampling. The sampling efficiency was estimated by monitoring the amount of benzil found in the back-up sections or the second filter. The assumption was made that effective sampling occurred if the back-up sections remained clean.

The desorption efficiency of benzil into methanol from the collection media was determined before sampling experiments. The results for the silica and the 13-mm filters are shown in Table I. Methanol proved to be an efficient solvent for this purpose.

TABLE I

DESORPTION INTO METHANOL

R.S.D. = Relative standard deviation.

Standard solution (μg/ml)	*Recovery (%), mean ± R.S.D. (n = 4)*		*Amount on filter (μg)*
	Silica	*Filter*	
0.2	100.6 ± 1.5	97.7 ± 1.9	0.1
0.5	99.5 ± 0.4	96.8 ± 0.8	0.2
1.0	100.9 ± 1.0	96.0 ± 0.5	1.6

From the air-sampling experiments it is evident that benzil exists at low concentrations in a form collectable more efficiently on sorbent tubes than on filters. A combination of filters and sorbent tubes is thus needed to cover a broad concentration range. The silica tubes we used have a 150-mg packing in the front section and a 75-mg packing in the rear. The fraction of benzil collected on filters is likely to represent that which is in the aerosol phase. The recoveries from the filters became increasingly larger than from the tubes with increasing air contamination. The aerosol formation in the sampling train is supposed to be roughly complete after such a long and voluminous sample path.

The sampling on filters and silica tubes or their combinations was examined with widely different J-tube loadings. The amounts recovered from each of the sections of the different sampling trains are shown in Table II. The results are the averages of two determinations. The total recoveries from the tubes, at the two lowest air concentrations, were larger than those from the filter. The order of collection efficiency was reversed at higher concentrations where the recovery from filters and filter-tube combinations becomes approximately equal, reflecting the low proportion of the gas phase component. A combination of a filter and tube is needed since the expected contamination levels in workroom air are at the lower end of the concentration range of this experiment. It is also noteworthy that the rear sections of the silica tubes in the combinations contained no benzil in all the tests performed. It is the cleanliness of the back-up sections that is considered a measure of the effectiveness of sampling. Low recoveries from the collecting media as a percentage of the starting material in the J-tube is not due to breakthrough but mostly due to adsorption on the walls of the tubing. Benzil was indeed recovered from the tubing walls by rinsing with methanol. However, quantitative analyses from the walls were not performed.

The effect of extended sampling time on recovery was also examined. Additional clean laboratory air was drawn through the sampling train after sampling the standard 5-l samples from the J-tube. It was shown that the additional sampling did not result in the appearance of benzil in the rear section of the tube. It seems that the gaseous fraction of benzil collected in the tube is effectively retained in the front section of the tube. The back-up section contained no benzil even after an additional clean air sampling of 48 l. However, benzil gradually disappeared completely from the filter during the extended sampling of clean laboratory air while the loading of the front section of the tube increased. Benzil seems to be evaporated or sublimed from

TABLE II

RECOVERIES FROM SILICA TUBES AND THEIR COMBINATIONS WITH THE FILTERS

Amount on J-tube (μg)	*Sample volume (l)*	*Recovery from the tubes and filters (μg)*					
156	5	Silica	front	1.55	Filter		0.48
			rear	–	Silica	front	0.60
						rear	–
	12				Filter		0.08
					Silica	front	0.96
						rear	–
	20				Filter	–	
					Silica	front	1.01
						rear	–
209	5				Filter		2.20
					Silica	front	2.41
						rear	–
	48				Filter		–
					Silica	front	4.32
						rear	–
256	5	Silica	front	2.08	Filter		5.29
			rear	0.17	Silica	front	1.13
						rear	–
522	5	Silica	front	11.37	Filter		23.43
			rear	1.21	Silica	front	1.21
						rear	–
1044	5	Silica	front	31.01	Filter		90.96
			rear	7.58	Silica	front	1.38
						rear	–

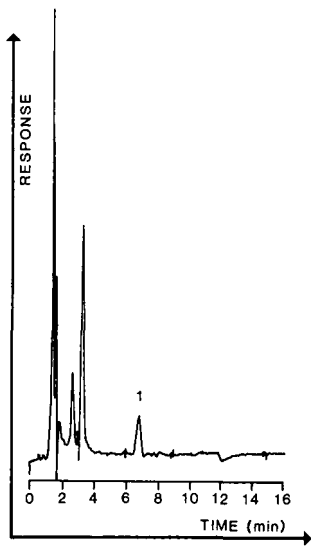

Fig. 3. An HPLC chromatogram of a curing air sample with about 80 mg of powder in the J-tube. The benzil peak (1) represents about 0.35 μg collected on the filter-tube combination or 7 ng injected for HPLC.

the filter when clean air is drawn through the filters and collected on the front section in the gas phase. The total amount of benzil recovered from the filter-tube combination did not alter significantly as a function of the additional sampling volume. A recovery of 93% was obtained (from the 5-l reference sample) after 4 h of additional clean air sampling from the tube combination. It appears that at least 48 l can be sampled at 200 ml/min. The sampling of clean air between contaminated atmospheres has a real-world basis because the emissions from the curing ovens are usually periodical, varying according to the amount of paint powder and/or the number of objects together with the processing conditions. The evaporation or sublimation of filter-bound solid material during extended sampling has been reported earlier[7,8].

The efficiency of the silica tube for collecting benzil in an essentially gaseous phase was tested by connecting the tubes directly to the outlet arm of the J-tube. As mentioned earlier, the experimental conditions hardly represent those of an actual workroom. The results would, however, be indicative of the ability of the tube to retain benzil in the gaseous phase. Samples were collected at 200 ml/min for 25 and 120 min corresponding to 5- and 24-l samples. Recoveries were 85–88% of the original J-tube loadings of 1 and 5 μg. Again the back-up sections of every tube contained no benzil. This indicates that at least 24 l of essentially gaseous atmospheres can be sampled, although the situation may be different when continuous atmospheres with linear evaporation rates are collected.

In the method we are proposing, benzil is determined with resersed-phase liquid chromatography using methanol–water (60:40) as the eluent. The UV detector is operated at 260 nm. The detection minimum giving a 1-cm peak is about 40 ng/ml corresponding to 0.85 $\mu g/m^3$ for a 48-l air sample. An HPLC chromatogram of an air sample obtained from an laboratory curing experiment is shown in Fig. 3. A major

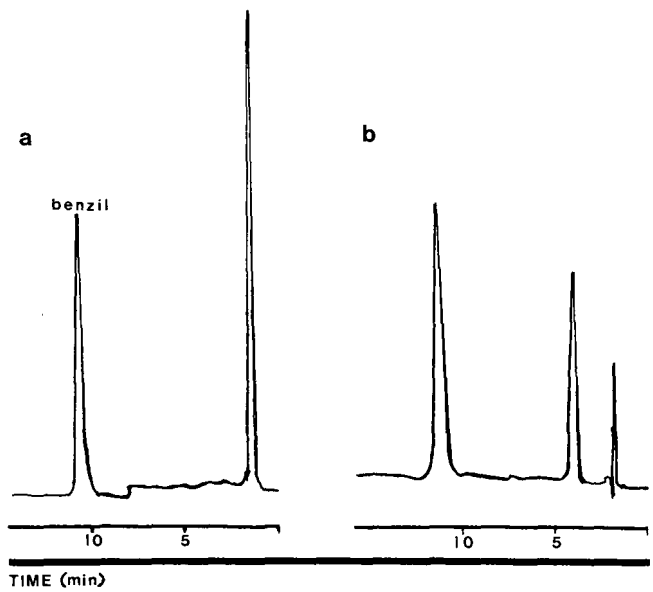

Fig. 4. An HPLC separation of benzil and benzilic acid. Eluents: (a) methanol–water (60:40): (b) methanol– 0.025 *M* KH_2PO_4 (60:40). pH 2.8 adjusted by orthophosphoric acid.

proportion of the compounds released during the curing process are more polar than benzil. Benzil can thus be well separated from the other emission components by reversed-phase chromatography.

Benzil is prone to form benzilic acid in a reaction known as the benzilic acid rearrangement. The stability of the standards in methanol was therefore monitored. Refrigerated but daily used standards were, however, stable over a period of at least 2 weeks. Standards stored on open shelves at room temperature gradually transformed mainly to benzilic acid over the same period of time. An HPLC separation of benzil and benzilic acid is shown in Fig. 4. Benzilic acid was not found in the air samples. We therefore believe that the action of sampling does not trigger the rearrangement reaction.

CONCLUSION

A method is described for the estimation of occupational emissions due to thermal curing of polyester powder coatings. The health effects of the emissions are caused by the combined action of the compounds present. It is therefore the emission levels rather than the concentrations of particular toxic compounds that are of interest. Emission levels are proportional to the concentration of a marker compound in workroom air. Benzil was selected as a marker for curing-derived emissions and is determined in the air by collecting it on combinations of 13-mm glass fibre filters and silica sorbent tubes. Air samples are analyzed by HPLC with UV detection.

ACKNOWLEDGEMENTS

Financial support from the Finnish Work Environmental Fund is gratefully acknowledged.

REFERENCES

1 J. Pukkila, K. Peltonen and T. Savolainen, *J. Chromatogr.*, 438 (1988) 443–446.
2 K. Peltonen and J. Pukkila, *J. Chromatrogr.*, 439 (1988) 375–380.
3 R. Schwartz and R. Mathews, *J. Chromatogr.*, 126 (1976) 113–116.
4 W. Brubaker and M. Ogliaruso, *J. Chromatogr.*, 324 (1985) 450–454.
5 M. Ross, D. Lines, K. Brain and R. Stevens, *Anal. Biochem.*, 87 (1978) 267–271.
6 K. Peltonen, *J. Anal. Appl. Pyrolysis*, 10 (1986) 51–57.
7 U. Knecht, C. Lämmler and S. Tobias, *Fresenius' Z. Anal. Chem.*, 326 (1987) 25.
8 J.-O. Levin, *Chemosphere*, 17 (1988) 671.

Journal of Chromatography, 479 (1989) 377–386
Elsevier Science Publishers B.V., Amsterdam — Printed in The Netherlands

CHROM. 21 683

USE OF ACHIRAL ION-PAIRING REAGENTS WITH CHIRAL STATIONARY PHASES

WILLIAM H. PIRKLE*, JEN-PING CHANG[a] and JOHN A. BURKE, III
School of Chemical Sciences, University of Illinois, Urbana, IL 61801 (U.S.A.)
(First received April 6th, 1989; revised manuscript received June 13th, 1989)

SUMMARY

The influence of the structure and concentration of achiral ion-pairing additives upon the retention and enantioselectivity of N-3,5-dinitrobenzoyl derivatives of α-amino acids and 2-aminophosphonic acids on a commercial (*R*)-N-(2-naphthyl)-alanine-derived chiral stationary phase has been examined. A mobile phase of methanol–aqueous phosphate buffer was used and the effect of methanol concentration was studied.

Increasing the concentration of the alkyltrimethylammonium ion-paring reagent enhances retention and enantioselectivity of N-3,5-dinitrobenzoyl derivatives of both α-aminocarboxylic acids and 2-aminophosphonic acids. An increase in the chain length of the alkyl portion of the ion-pairing reagent gives increased retention but no significant change in selectivity for the enantiomers. The concentration of the organic modifier in the mobile phase dramatically affects the retention of the enantiomers. A minimum in enantioselectivity occurs at about 60% methanol.

INTRODUCTION

In most of the papers from this laboratory describing the development of bonded chiral stationary phases (CSPs) for the direct chromatographic separation of enantiomers[1–5], standard mobile phases of hexane and 2-propanol are used to facilitate the comparison of the various CSPs. These mobile phases usually afford near-maximum enantioselectivity but are not necessarily optimal for any given application, for other mobile phases can significantly affect band shapes, resolution factors, and peak dispersions. Reversed phase solvents can also be used although they almost always afford less enantioselectivity than does hexane-2-propanol and may, in the case of ionic analytes, lead to undesirably rapid elution. Addition of lipophilic ion pairing reagents to reverse mobile phases can increase the retention of ionic analytes and alter selectivity as is well known[6]. Pettersson and Schill[7] have used chiral ion-pairing agents in conjunction with achiral columns to separate enantiomers. Schill *et*

[a] On sabbatical leave from the Shanghai Institute of Materia Medica, Chinese Academy of Sciences, Shanghai 20031, China.

0021-9673/89/$03.50

al.[8] as well as Hermansson and Eriksson[9] have also studied the use of α-glycoprotein chiral stationary phases with aqueous mobile phases and indicate that charged and uncharged additives affect retention and, in many cases, afford significant improvement of chiral recognition of analyte enantiomers. The reason for the enhancement of chiral recognition is stated to be one enantiomer of the ion-pair "fits better in the chiral active site of the protein due to steric reasons"[9]. Owing to the complexity of the protein, this may or may not be an adequate explanation.

This paper reports the reversed-phase chromatographic behavior of enantiomers of the N-3,5-dinitrobenzoyl (DNB) derivatives of both α-amino acids and 2-aminophosphonic acids on a commercial (*R*)-N-(2-naphthyl)alanine-derived chiral stationary phase, **1**, using a mobile phase of methanol–aqueous phosphate buffer in conjunction with achiral ion-pairing agents of general type **2**. The CSP is well characterized structurally and mechanistically[10,11]

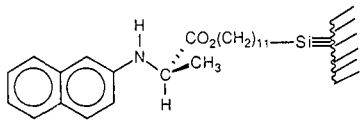

(R)-1

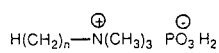

2 n = 5, 6, 7, 8, 12

EXPERIMENTAL

Apparatus

Chromatography at ambient temperature was performed using an Altex-100 A pump, an Altex 210 injector valve with a 20-μl loop, a Beckman Model 155 fixed-wavelength UV detector operating at 254 nm, and a Kipp & Zonen BD 41 chart recorder. A Regis (*R*)-N-(2-naphthyl)-alanine 250 × 4.6 mm I.D. column was used.

Chemicals

The ion-pair reagents: pentyl, hexyl, heptyl, octyl and dodecyl trimethylammonium phosphate were supplied by Regis. Analytes used in this study were available from prior studies. Methanol was purchased from Fischer. All other chemicals were reagent grade and used without further purification.

RESULTS AND DISCUSSION

From an initial investigation of the separation of the enantiomers of the DNB derivatives of 2-aminohexanoic acid and 2-aminobutylphosphonic acid using a mobile phase of methanol–0.01 *M* aqueous phosphate buffer (pH 6.86), is was found that the undesirably small capacity factors (k') of the analytes can be increased by addition of lipophilic quaternary ammonium ions to the mobile phase, Fig. 1. This was not

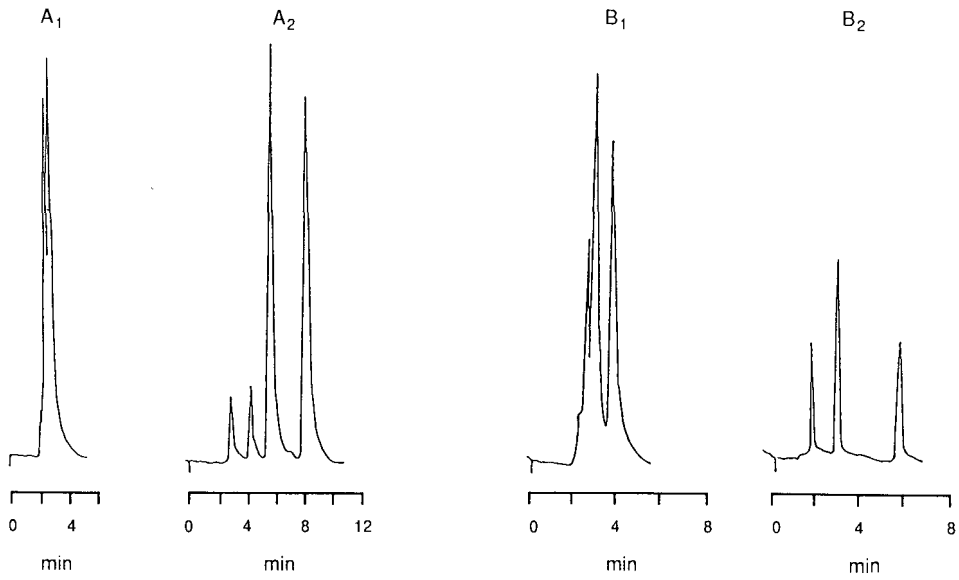

Fig. 1. Separations of the enantiomers of (A) N-(3,5-dinitrobenzoyl)-2-aminobutylphosphonic acid using methanol–0.01 *M* aqueous phosphate buffer (60:40, v/v) pH 6.86 and (B) N-(3,5)-dinitrobenzoyl)-2-aminohexanoic acid using methanol–0.01 *M* aqueous phosphate buffer pH 6.86 (70:30, v/v). In chromatograms A_1 and B_1, no ion-pairing agent was present. In A_2 and B_2, 5 m*M* ion-pairing agent had been added to the mobile phase. These agents were hexyltrimethylammonium phosphate and heptyltrimethylammonium phosphate respectively. The flow-rate was 1 ml/min in each case.

unexpected, for the eleven carbon connecting arm used to link the chiral selector to the silica affords an appreciable lipophilic character to this CSP. Thus, retention occurs by both adsorption and partitioning processes. To better understand the lipophilic effects which contribute to retention, the relationships between retention, selectivity, structure and concentration of the pairing ions were investigated. From Fig. 2, it may be seen that an increase in the concentration of the dodecyltrimethylammonium reagent from 0.25 to 5 m*M* causes a significant increase in the capacity factors of both enantiomers of the DNB derivatives of leucine and 2-aminopentanoic acid until a limiting value is reached. More significantly, the separation factor, α, for both sets of enantiomers increases as the concentration of the ion-paring reagent is increased (Fig. 3). For the enantiomers of DNB-leucine, α is increased from 2.0 to 2.9 by the addition of 8 m*M* ion-pairing reagent. For all cases, the elution order of the analytes is that expected from prior studies of the chiral recognition mechanism used by this CSP[10]. For DNB α-amino acids of the type employed, **3**, the elution order from (*R*)-**1** is (*S*) before (*R*). For DNB-2-aminoalkyl phosphonic acids of type **4**, the order is (*R*) before (*S*) owing to the Cahn–Ingold–Prelog priority sequence. The presumption is that both types of analytes are resolved by the general mechanism previously described[10].

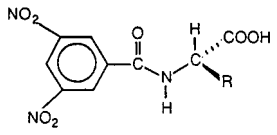

3

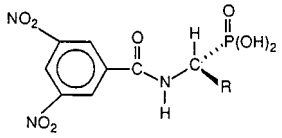

4

The process by which the ion-pairing reagent increases retention is readily understood from prior work. The ion-pairing reagent interacts reversibly with the stationary phase to provide surface charge and with the analyte enantiomers to afford enantiomeric ion pairs. Both the so-called "ion pair" and "dynamic ion exchange" retention processes are presumably in operation[6]. Consequently, the curves which relate retention and enantioselectivity to the concentration of a given ion-pairing reagent are complex, for they are ordained by the values of the various equilibrium constants. Interestingly, plots of α *vs.* ion-pairing reagent concentration do not "flatten out" as do the plots of k' *vs.* reagent concentration. Both plots might have been expected to show similar curvature if the plots reflect only the extent of the pair formation in solution. Increasing the concentration of a given ion-pairing reagent will increase the surface charge of the stationary phase until the latter becomes saturated. Surface charge facilitates the retention of both enantiomers equally and does not itself contribute to chiral recognition. The retention component contributed by surface charge augments that afforded by the chiral recognition process, thus influencing the

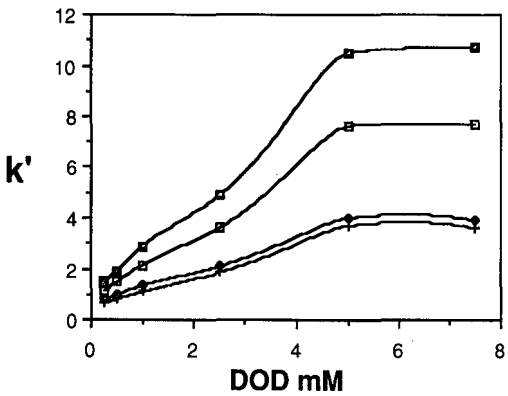

Fig. 2. Influence of the concentration of dodecyltrimethylammonium phosphate, DOD, in the methanol–aqueous phosphate buffer pH 6.86 (80:20, v/v) upon the retention of the enantiomers of the N-3,5-dinitrobenzoyl derivatives of leucine and 2-aminopentanoic acid. (+) (*S*)-DNB-2-aminopentanoic acid; (□) (*R*)-DNB-2-aminopentanoic acid; (◆) (*S*)-DNB-leucine; (■) (*R*)-DNB-leucine. The flow-rate was 1 ml/min. The curves for the two (*S*)-enantiomers are essentially coincident. The lower curve (+) has been displaced slightly for clarity.

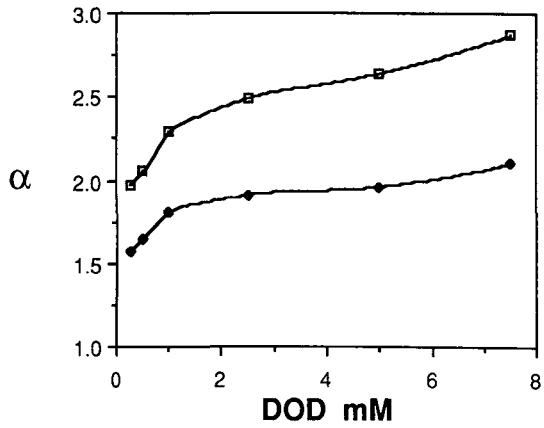

Fig. 3. Influence of the concentration of dodecyltrimethylammonium phosphate, DOD, in the mobile phase upon the separation factors for the enantiomers of DNB-leucine (□) and DNB-2-aminopentanoic acid (◆). Mobile phase and flow-rate were as in Fig. 2.

shapes of the plots of either k' or α *versus* ion-pairing reagent concentration. Additionally, one must consider the possibility that the ion-pairing reagent, by interacting with residual silanol groups on the silica[12], reduces the extent of non-enantioselective adsorption. That is, retention now more nearly occurs by only those processes which distinguish between the enantiomers. The reduction in retention through loss of the non-enantioselective processes might somewhat offset the increase in retention afforded by the higher concentration of ion-pairing reagent. Loss of non-enantioselective retention would also tend to increase enantioselectivity.

The increase in enantioselectivity can be explained in another way. The CSP used for these studies has but one significant chiral recognition mechanism available to it for the analytes under study. One of the interactions involved is hydrogen bonding of the CSPs N–*H* to the oxygens of the C-terminal carboxyl group. This process is enantioselective, occuring more extensively for the more retained enantiomer, not just because it is more retained but because of the interactions involved. In methanol–water, the heavily solvated carboxylate ion must undergo some desolvation upon interaction with CSPs N–*H*. This enantioselective desolvation reduces the exothermicity of $\Delta\Delta H$ and, consequently, reduces the magnitude of the negative $\Delta\Delta G$ value. A structural change which reduces the initial extent of solvation of the C-terminal carboxyl (*e.g.* conversion from carboxylate to an ion pair or to an ester) will reduce the extent of enantioselective desolvation with a consequent increase in the separation factor, α, of the enantiomers. The other major interactions involved in the chiral recognition process, π–π bonding and hydrogen bonding of the DNBN*H* to the CSP's carbonyl oxygen, may also entail enantioselective desolvation. However, the extent of solvation (or desolvation) of these groups is not expected to be much influenced by the presence of absence of the ion pairing reagent. For example, the ion pairing reagent has little effect upon the enantioselectivity shown on CSP **1** by esters of DNB-amino acids.

Rather interestingly, the length of the alkyl group of the ion-pairing reagent affects retention strongly but has only a modest effect on enantioselectivity (Table I).

TABLE I

EFFECT OF ALKYL CHAIN LENGTH, *n*, OF THE **2** ALKYLTRIMETHYLAMMONIUM ION-PAIRING REAGENTS ON ENANTIOSELECTIVITY OF TYPE **3** AND TYPE **4** ANALYTES USING (*R*)-CSP **1**.

Mobile phase: 5 m*M* pairing ion in methanol–0.01 *M* phosphate (70:30, v/v) (pH = 6.86); flow-rate: 1 ml/min.

R	α		
	n = 6	*n* = 8	*n* = 12
Type **3**: *α-amino acids*			
n-Butyl	3.09	2.96	2.92
n-Propyl	2.65	2.53	2.46
Ethyl	2.28	2.25	2.12
Methyl	2.08	1.98	1.93
Type **4**: *2-aminoalkylphosphonic acids*			
n-Octyl	2.79	2.69	2.67
n-Heptyl	2.48	2.54	2.57
n-Hexyl	2.30	2.51	2.46
n-Pentyl	2.25	2.38	2.37
n-Butyl	2.13	2.24	2.25
n-Propyl	1.97	2.12	2.10

The greater the length of the alkyl group, the more extensively these reagents partition into the stationary phase and the greater the surface charge of the latter. As mentioned previously, surface charge increases the retention of these anionic enantiomers equally. Indeed, plots of log *k'* *vs.* the number of methylene groups in the ion-pairing reagents alkyl substituent are linear, the lines for a pair of enantiomers being parallel. In Fig. 4A, the logarithms of the capacity factors noted for the more strongly retained enantiomers of three DNB-2 aminoalkylphosphonic acids are plotted against the number of carbons in the alkyl group of the pairing ion for three different 0.5 m*M* alkyltrimethylammonium ion-pairing reagents. The linear relationship between log *k'* and the number of carbons in the alkyl group of the paring ion is consistent with either the ion pairing or the dynamic retention mechanisms advocated for achiral ion pairing[6]. With each added methylene group in the alkyl portion of the 5 mM ion pairing reagent, the log of the capacity factor of each enantiomer increases by *ca.* 0.1 unit.

As mentioned, increasing the length of the alkyl substituent of the ion-pairing reagent does have a modest effect upon enantioselectivity. Increasing the length of the alkyl group from hexyl to dodecyl produces a slight drop in enantioselectivity for the DNB α-amino acids and a slight gain for the DNB 2-aminophosphonic acids. The origin of these small effects is unclear. The size of these effects can be judged from Fig. 4B and from the data in Table I. This situation is not unlike that which one obtains for the reversed-phase separation of the enantiomers of several DNB-α-amino acid esters. There is little change in α as the length of the alkoxy group of the ester is changed (Table II). It is evident that whatever lipophilic interactions may be undergone by the alkyl portion of the ion-pairing reagent (or the alkoxyl of the ester) with the CSP, these have but a slight influence on chiral recognition. Curvature noted in a

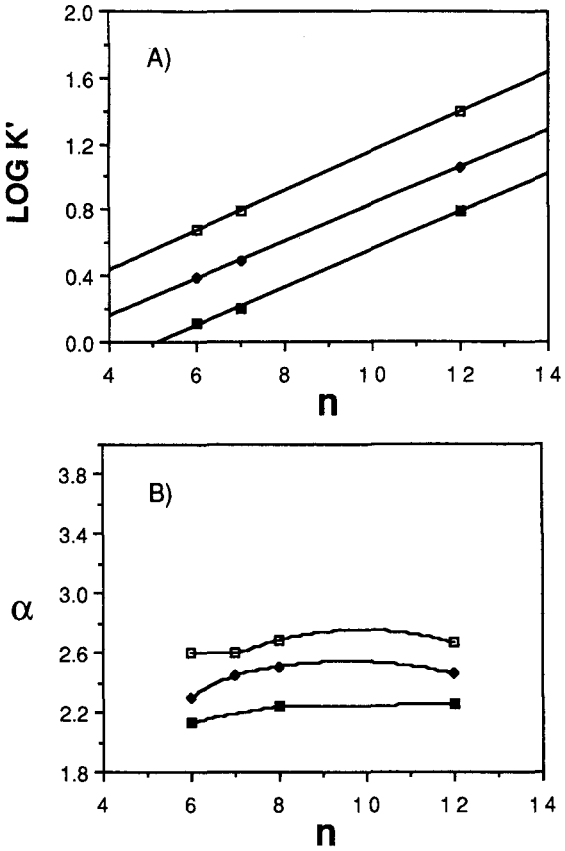

Fig. 4. (A) The dependence of log k' for the (*S*)-enantiomers of several DNB-2-aminoalkylphosphonic acids on the number, n, of methylene groups in the alkyl portion of the type **2** ion pairing reagents. (□) DNB-2-aminooctylphosphonic acid; (◆) DNB-2-aminohexylphosphonic acid; (■) DNB-2-aminobutylphosphonic acid. The mobile phase was 5 m*M* pairing ion in methanol–0.01 *M* phosphate buffer pH 6.86 (70:30, v/v). (B) The dependence of the separation factors for the enantiomers of several DNB-2-aminoalkylphosphonic acids on the number, n, of methylene groups in the alkyl portion of the type **2** ion pairing reagents. (□) DNB-2-aminooctylphosphonic acid; (◆) DNB-2-aminohexylphosphonic acid; (■) DNB-2-aminobutylphosphonic acid. The mobile phase was 5 m*M* pairing ion in methanol–0.01 *M* phosphate buffer pH 6.86 (70:30, v/v).

TABLE II

EFFECT OF THE LENGTH OF THE ALKOXYL GROUP OF ESTERS OF TYPE 3 α-AMINO-ACIDS ON ENANTIOSELECTIVITY, α, USING THE (*R*)-N-(2-NAPHTHYL)ALANINE CHIRAL STATIONARY PHASE

Mobile phase: methanol–water (90:10, v/v); flow-rate: 1 ml/min.

R	α		
	Ethoxyl	*Butoxyl*	*Octoxyl*
n-Propyl	2.27	2.13	2.09
n-Hexyl	2.35	2.31	2.32
n-Decyl	2.50	2.48	2.48
n-Tetradecyl	2.48	2.47	2.50

α *vs.* n plots stems largely (Fig. 4B) from the behavior of the least retained enantiomers which elute slightly "too late" when the shorter chain ion-pairing reagents are used. "Too late" means that these log k'_1 values fall slightly above an otherwise linear log k'_1 *vs.* n plot. The origin of this effect is unknown.

The major inference drawn from the data in Table I and Fig. 4A and B is that the length of the alkyl portion of these ion-pairing reagents has little effect upon the association constants for either ion-pair formation or dynamic ion exchange. Hence, the length of the alkyl group has little effect upon α but does affect retention in the usual manner.

Effect of methanol concentration

If retention and enantioselectivity are influenced by ion-pair formation and by enantioselective desolvation, one certainly expects that the concentration of methanol

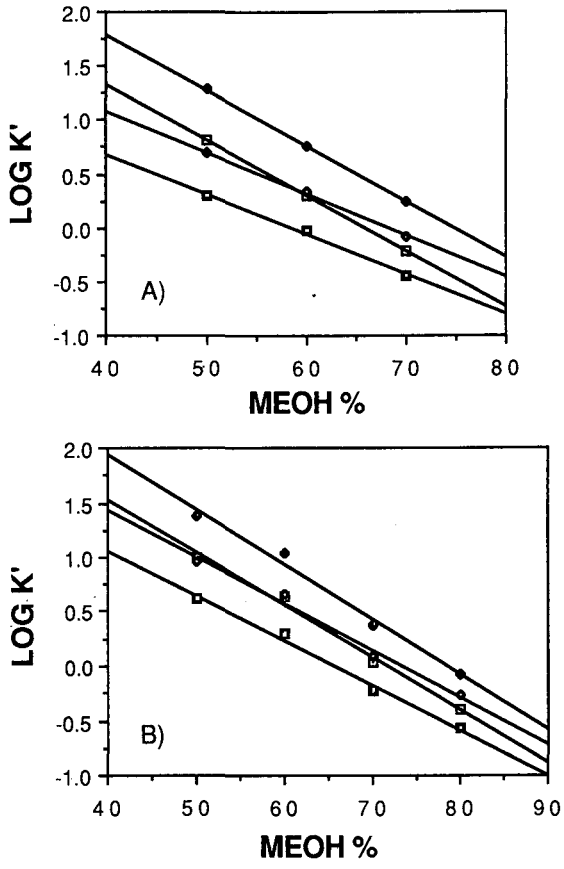

Fig. 5. The effect of the methanol content of the mobile phase on the retention of DNB-α-amino acids and DNB-2-aminoalkylphosphonic acids. A: (◘) (*S*)-DNB-2-aminobutanoic acid; (◇) (*R*)-DNB-2-aminobutanoic acid; (□) (*S*)-DNB-2-aminohexanoic acid; (◆) (*R*)-DNB-2-aminohexanoic acid. B: (◘) (*R*)-DNB-2-aminobutanoic acid; (◇) (*S*)-DNB-2-aminobutanoic acid; (□) (*R*)-DNB-2-aminohexylphosphonic acid; (◆) (*S*)-DNB-2-aminohexylphosphonic acid. In all instances, mobile phase was as indicated in Fig. 1 but containing 5 m*M* hexyltrimethylammonium phosphate.

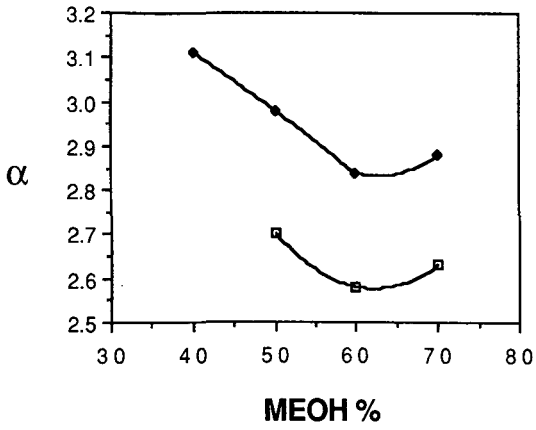

Fig. 6. Effect of the composition of the methanol–aqueous buffer mobile phase on the enantioselectivity of DNB-α-amino acids. (◆) 2-aminohexanoic acid; (□) 2-aminopentanoic acid. The mobile phases were 5 m*M* in hexyltrimethylammonium phosphate.

in the mobile phase should affect these parameters. Higher methanol concentration reduces retention by increasing the solubility of the lipophilic analyte in the mobile phase. Plots of the logs of the capacity factors of the enantiomers of several DNB-α-amino acids and DNB-2-aminoalkyl-phosphonic acids as a function of methanol concentration are shown in Fig. 5A and B. These plots are depicted as linear and of comparable slope. In actuality, the data points are slightly sinusoidal of the depicted lines. Consequently, methanol concentration also influences enantioselectivity (Fig. 6), a minimum being noted at *ca.* 60% methanol. The occurence of a minimum might have been anticipated, for some mobile phase composition will afford maximum solvation where a maximum degree of enantioselective desolvation will occur upon interaction with the CSP and a minimum value of α will be observed. Superimposed upon this is the effect of mobile phase composition on the extent of ion-pair formation. The recent report by Katz et al.[13] that methanol–water (60:40, v/v) solutions contain the maximum concentration of methanol–water associate is worth mentioning, for the minimum of α noted at this composition may not be coincidental. However, no minimum in retention occurs in 60% methanol. In this regard, these systems differ from several of those reported in ref. 11.

CONCLUSION

Achiral ion-pairing reagents have no unusual influence upon the chromatographic behavior of the enantiomers of DNB-amino acids on the N-(2-naphthyl)-alanine CSP. Their use does increase retention and enantioselectivity in an explainable manner but leads to no lipophilic interactions which contribute significantly to chiral recognition. This is not to say that there are no lipophilic interactions whatsoever, but the effect of these interactions upon chiral recognition (*e.g.*, the curvature of the α *versus n* plots in Fig. 4B) are small and their origin is obscure. The bulk of the increased enantioselectivity which is observed is attributed to a reduction in the extent of solvation of the analytes carboxylate anion group upon ion-pair formation and a

consequent reduction in the enthalpic component of the enantioselective desolvation which occurs upon adsorption onto the CSP. Similar reductions in the extent of enantioselective desolvation may partially account for the effects of ion-pairing reagents on the enantioselectivity noted using protein CSPs[8,9].

ACKNOWLEDGEMENT

This work was supported by a grant from the National Science Foundation.

REFERENCES

1 W. H. Pirkle and D. W. House, *J. Org. Chem.*, 44 (1979) 2169.
2 W. H. Pirkle, J. M. Finn and J. L. Schreiner, *J. Org. Chem.*, 103 (1981) 3964.
3 W. H. Pirkle, T. C. Pochapsky, G. S. Mahler, D. E. Corey, D. S. Reno and D. M. Alessi, *J. Org. Chem.*, 51 (1980) 4991.
4 W. H. Pirkle and T. J. Sowin, *J. Chromatogr.*, 396 (1987) 83–92.
5 W. H. Pirkle and J. E. McCune, *J. Chromatogr.*, 441 (1988) 311–322.
6 W. R. Melander and C. Horvath, in M. T. W. Hearn (Editor), *Ion-Pair Chromatography (Chromatographic Science Series,* Vol. 31), Marcel Dekker, New York, 1985.
7 C. Pettersson and G. Schill, *J. Liq. Chromatogr.*, 9 (1986) 291.
8 G. Schill, I. W. Wainer and S. A. Barkham, *J. Liq. Chromatogr.*, 9 (1986) 641.
9 J. Hermansson and M. Eriksson, *J. Liq. Chromatogr.*, 9 (1986) 621.
10 W. H. Pirkle and T. C. Pochapsky, *J. Am. Chem. Soc.*, 109 (1987) 5975.
11 W. H. Pirkle, J. A. Burke, III and S. Wilson, *J. Am. Chem. Soc.*, in press.
12 G. B. Cox and R. W. Stout, *J. Chromatogr.*, 384 (1987) 315–336.
13 E. D. Katz, C. H. Lochmüller and R. P. W. Scott, *Anal. Chem.*, 61 (1989) 349–355.

Journal of Chromatography, 479 (1989) 387–400
Elsevier Science Publishers B.V., Amsterdam — Printed in The Netherlands

CHROM. 21 738

EFFECT OF SOME OPERATIONAL VARIABLES ON THE EFFICIENCY OF ION CHROMATOGRAPHIC SEPARATIONS

DENNIS R. JENKE*
Baxter Healthcare, Corp., William B. Graham Science Center, Round Lake, IL 60073 (U.S.A.)
(First received February 27th, 1989; revised manuscript received June 27th, 1989)

SUMMARY

The influence of injection mass, eluent composition and operating temperature on the efficiency of six commercially available ion chromatography columns was examined. Efficiency was linearly related to injection mass even at masses well below the column overload limit. The linear relationship was maintained at injection masses approaching the method's quantitation limit. Injection mass had little influence on the nature of the efficiency *versus* linear velocity relationship. Changing the concentration of the eluent ion (ionic strength) in the mobile phase influenced efficiency; however, the nature of the effect was analyte and column specific. Modifying the speciation of the mobile phase at constant ionic strength produced a marked effect on efficiency with the multivalent form of the eluent ion producing a better efficiency. For silica based stationary phases, addition of up to 10% by volume methanol had no impact on chromatographic performance. Increasing the column temperature increased efficiency at high linear velocities but decreased efficiency at low linear velocity in accord with theoretical expectations.

INTRODUCTION

Optimization of separation efficiency in the application of a chromatographic methodology is critical in situations involving multi-solute separations in complex matrices wherein the assurance of specificity and/or accurate and reproducible quantitation is paramount. The utility of ion chromatography (IC), as it matures as an analytical technology, will, in many applications, depend on the optimization of operational variables with respect to separation efficiency. In a previous study, it was observed that mobile phase linear velocity had some influence on the efficiency of IC separations for representative commercially available stationary phases[1]. In this study, the effect of eluent ion charge and concentration, injection mass, organic modifier content and operating temperature on efficiency for six commercially available stationary phases was examined.

0021-9673/89/$03.50

EXPERIMENTAL

Apparatus

The chromatographic system consisted of the following components: ABI (Ramsey, NJ, U.S.A.) Model 400 pump and 757 UV detector, Alcott (Norcross, GA, U.S.A.) Model 728 autosampler, Rheodyne (Cotati, CA, U.S.A.) Model 7010 electronically actuated injector and an appropriate stripchart recorder. Columns examined are described in Table I. All components between the injector and detector were connected with the minimum possible length of 0.007 in. I.D. stainless-steel tubing to minimize extra-column void volume and heat transfer. The chromatographic system was unchanged in any respect over the entire course of this experimentation. In the experiments designed to evaluate temperature effects, the mobile phase reservoir was placed in a water bath from which heated water was circulated into a column jacket. Approximately 3 m of tubing, also in the water bath, was placed between the pump and the injector. Such an approach should minimize the generation of radial thermal gradients, which may influence the efficiency–temperature relationship[2,3], in the column.

Operating conditions

The mobile phases used in all experiments were potassium hydrogenphthalate (KHP) buffers and, prepared from reagent or HPLC-grade chemicals and were filtered through 0.2-μm filters prior to use. Analytes were detected indirectly using a "vacancy" chromatographic approach at wavelengths of either 250 or 270 nm. The samples used throughout contained from 5 to 600 ppm each of chloride, nitrate, and sulfate and were prepared from their sodium salts. The sample injection size was 10 μl and all flow-rates were measured throughout the course of the experimentation.

Design

Each column evaluated was used as received by the vendor and exhibited performance consistent with the supplied test chromatograms. Columns were equilibrated with a particular mobile phase at a particular operating temperature for a

TABLE I

COLUMNS EXAMINED

Designation	*Supplier*	*Backbone type*	*Length (mm)*	*I.D. (mm)*	*Particle size (μm)*	*Functional group*[a]
269-013	Wescan	Silica	100	4.6	5	QA
269-031	Wescan	Polymer	100	4.1	10	QA
301TP	Vydac	Silica	250	4.6	10	QA
PRP-X100	Hamilton	Polymer[b]	150	4.1	10	QA
AS-5A	Dionex	latex[c]	150	4.0	5	P
IonPak A	Waters	polymethacrylate[d]	50	4.6	10	QA

[a] QA = Quaternary amine; P = propriatary.
[b] Copolystyrene divinylbenzene.
[c] Agglomerated.
[d] gel.

period of not less than 3 h prior to the initiation of any efficiency evaluation. After equilibration, each column was "conditioned" by making five injections of a sample containing 100 ppm of each analyte while the system was operating at a flow-rate of 1 ml/min. After conditioning, the individual column were equilibrated to a particular flow-rate (ranging from 0.1 to 4.0 ml/min) and the appropriate samples were injected in replicate. Where appropriate, the experimental conditions were then changed, the column re-equilibrated as necessary and more injections were made. Flow-rate changes were made in a random order for each column tested. Appropriate properties of the resultant chromatograms were then measured from the stripchart recordings. Under the chromatographic conditions used in this study, the measured peak asymmetry was less than 1.1 in all cases and the signal to noise was (usually) greater than 100; thus these two quantities will not greatly influence the accuracy of the efficiency calculations[4,5].

Calculations

The following equations were used to calculate chromatographic performance and operating parameters:

$$N = 5.545(t_1/w_{1/2})^2 \tag{1}$$

$$R = 2(t_2 - t_1)/(w_{b,2} + w_{b,1}) \tag{2}$$

$$h = L/(Nd_p) \tag{3}$$

$$v = (Ld_p)/(D_m t_0) \tag{4}$$

$$A_s = a/b \tag{5}$$

where N = number of theoretical plates; R = resolution; A_s = peak asymmetry factor; h = reduced plate height; v = reduced velocity; t = retention time or distance; a/b = ratio of the distances from a perpendicular (dropped from the apex of the peak to the baseline) to the rear side and front side of the peak, measured at 10% peak height; $w_{1/2}$ = peak width at half peak height; w_b = peak width at the baseline; L = column length; d_p = particle size of the stationary phase; t_0 = retention time of an unretained solute; D_m = solute diffusion coefficient in the mobile phase (taken as $5 \cdot 10^{-6}$ cm^{-2} s^{-1} as being typical of low-molecular-weight solutes in water[6]); and 1 and 2 refer to two analytes for which the retention time of 2 is greater than that of 1.

RESULTS AND DISCUSSION

Effect of injection mass

The ion-exchange capacity of the stationary phases evaluated is generally quite small (0.03 to 0.2 mequiv./g) and since the columns employed are relatively short, the total exchange capacity of these columns is not large. Thus one expects that the efficiency of IC separations would be greatly influenced by the amount of analyte injected, especially as this amount approaches a significant fraction of the total exchange capacity and column overloading occurs. Undeed, Haddad *et al.*[7] observe

that at a sample loading of 70 μg, most IC columns are greatly overloaded and that even at a loading of 7 pgl some peak distortion may occur. Similar peak shape distortions as a function of sample loading are reported by Jenke and Pagenkopf[8]. In this research, column overloading was minimized by using injection masses of 10 μg or less per analyte and the absence of apparent overloading was demonstrated (by a peak shape evaluation) in peak asymmetry values of 1.1 or less for all peaks evaluated. However, it is clear from the efficiency evaluation that some overloading, as a manifestation in a reduction in efficiency, was produced at injection masses greater than approximately 2–4 μg. The typical effect of sample injection mass on the measured efficiency at constant linear velocity for the different columns evaluated is shown in Fig. 1; in all cases a linear relationship exists between these two quantities. Correlation coefficients for the best fit lines in all cases are 0.99 or greater. In general, the effect of injection mass on efficiency is decreased as analyte retention (capacity factor, k') increases, although no simple correlation between these quantities can be made from the data generated in this study. This finding is in partial agreement with theoretical relationships established for chromatographic separations in general. In these models, based on the assumption of a Langmuir interaction isotherm and the absence of mixed isotherm effects, the relationship derived between efficiency, injection mass and solute retention (capacity factor) can be written[9]:

$$1/N = 1/N_0 + \tfrac{3}{8}[k'/(1 + k')]^2(W_x/W_s) \quad (6)$$

where: N_0 = efficiency at low injection mass; W_x = injection mass; and W_s = column capacity. Clearly the data in Fig. 1 reflects the linear relationship (with an intercept

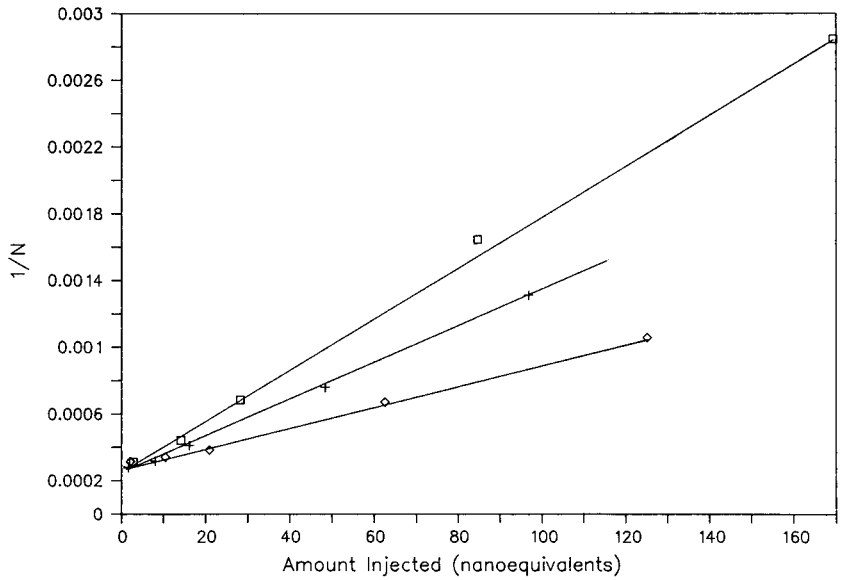

Fig. 1. Effect of injection mass on column efficiency. Column, Wescan 269-013; mobile phase, 1 m*M* KHP, pH 6; flow-rate, 1 ml/min. Approximate capacity factors are: chloride (□), 2.0; nitrate (+), 3.2; and sulfate (◇), 9.0.

independent of analyte identity) between $1/N$ and W_x predicted by this equation; however, equally clear is that the observed effect of k' on efficiency is not only different but in fact the opposite of that predicted by eqn. 6. That is, while the equation predicts an increase in efficiency as k' decreases, the observed behavior is that efficiency increases as k' increases. In general, for the IC column examined herein, the effect of injection mass on efficiency is decreased as analyte retention increases (and the absolute efficiency increases as retention increases) although no simple correlation between capacity factor and efficiency can be generated from the current data base. Current research is focusing on the establishment of the experimental and theoretical nature of this relationship. However, one can use the current data base to generate an empirical expression defining the relationship between capacity factor, efficiency and injection mass. The resulting empirical expression takes the form:

$$1/N = 1/N_0 + (C/k')(W_x/W_s) \tag{7}$$

where C is a constant.

Figs. 2–4 document the fit of the efficiency/injection mass/capacity factor data which exists for three IC columns; the correlation obtained between eqn. 7 and the observed data (three solutes per column, multiple injection masses) is typified by $r^2 > 0.98$ and represents adequate agreement between the actual and predicted behavior. Finally, it is interesting to note that the linear relationship between injection mass and efficiency holds true even at sample loadings approaching the mass detection

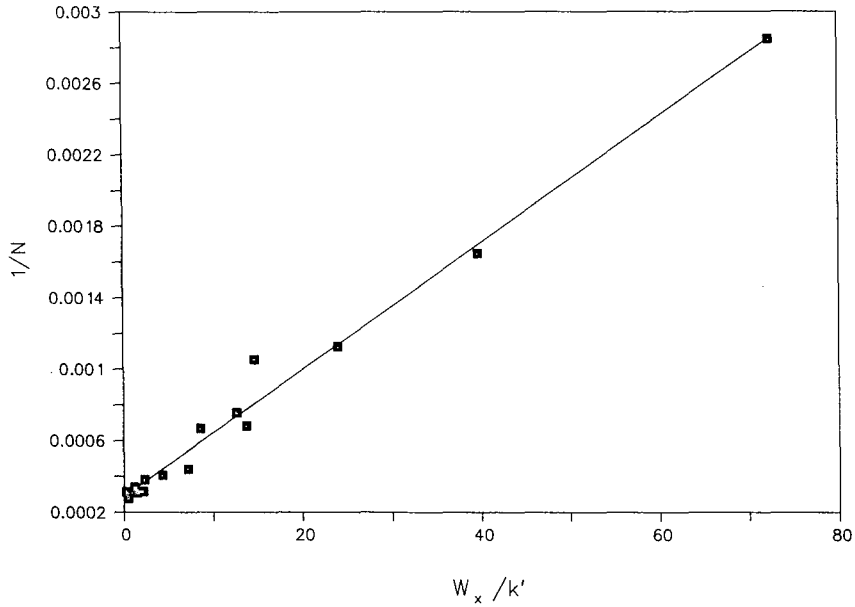

Fig. 2. Relationship between efficiency, injection mass and analyte capacity factor. Column, Wescan 269-013, same mobile phase as in Fig. 1. The data represents three solutes (chloride, nitrate and sulfate), injected over the mass range of 0.1–6 μg per analyte and representing a capacity factor range of 1.9–9.5. r^2 for the fit of this data to eqn. 7 (represented by the solid line) is 0.986.

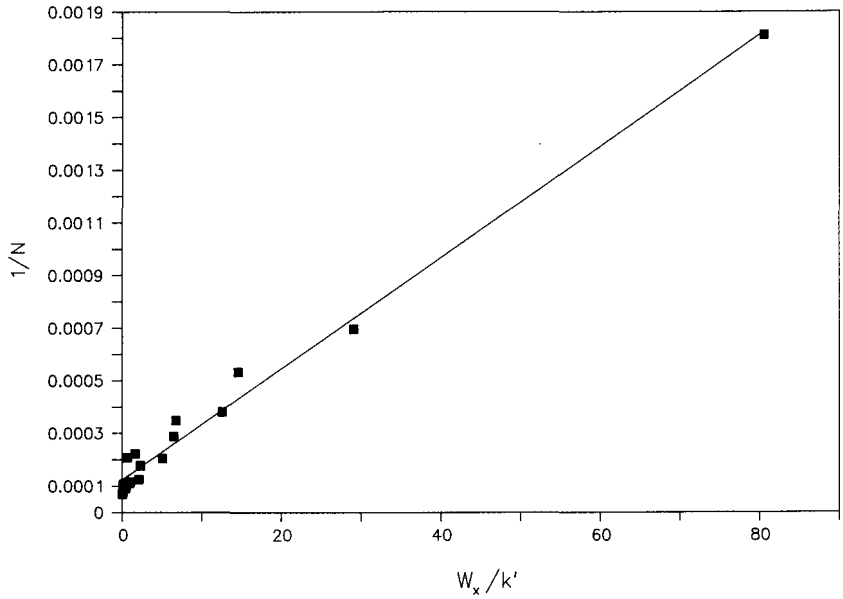

Fig. 3. Relationship between efficiency, injection mass and analyte capacity factor. Column, Dionex AS-5A; mobile phase, 1 m*M* KHP, pH 6; flow-rate, 1 ml/min. The data represents three solutes (chloride, nitrate and sulfate), injected over the mass range of 0.02–3 μg per analyte and representing a capacity factor range of 0.9–9.3. r^2 for the fit of this data to eqn. 7 (represented by the solid line) is 0.986.

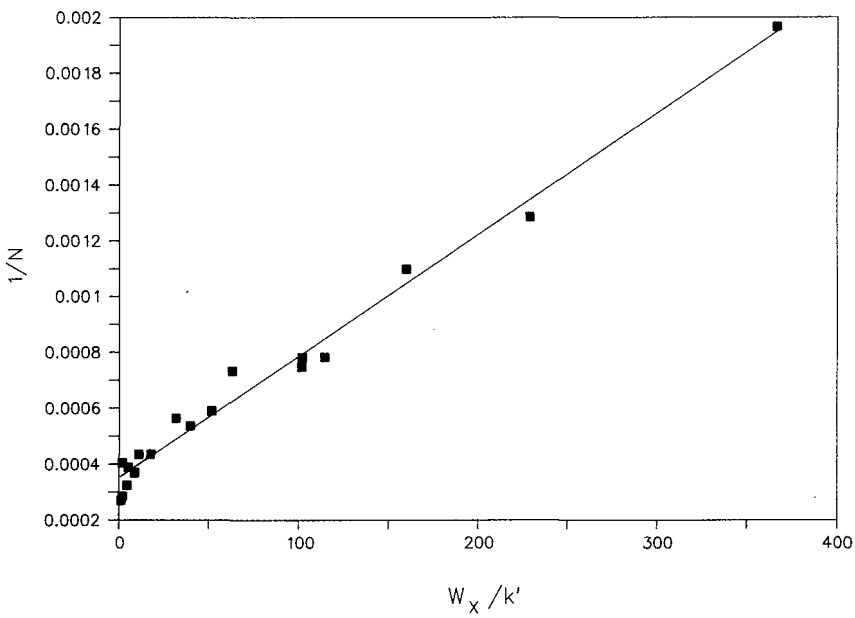

Fig. 4. Relationship between efficiency, injection mass and solute capacity factor. Column, Vydac 301TP; mobile phase, 2 m*M* KHP, pH 6; flow-rate, 1 ml/min. The data represents three solutes (chloride, nitrate and sulfate), injected over the mass range of 0.1–10 μg and representing a capacity factor range of 0.6–2.1. r^2 for the fit of this data to eqn. 7 (represented by the solid line) is 0.984.

limit for the technique (especially true for the 0.02-μg injection used in the evaluation of the AS-5A column).

The effect of injection mass on efficiency at various flow-rates was examined for the AS-5A column and is illustrated in Fig. 5. Essentially the shape of the reduced parameter plot, relating efficiency with linear velocity, is not influenced by injection mass and the magnitude of enhanced efficiency obtained when lower sample loadings are used is not flow-rate dependant. The implication of Figs. 1–5 is clear, efficiency can be maximized by decreasing the sample load, independent of other operating conditions, even to the point of approaching the method's quantitation limit.

Effect of mobile phase composition

The influence of three perturbations of mobile phase composition on efficiency was examined in this study; the effect of increasing the eluting ion concentration (ionic strength) at constant pH, the effect of changing pH (and thus eluent ion charge) at constant ionic strength, and the effect of adding an organic modifier (methanol) to the mobile phase. Considering the first of these, the effect of changing mobile phase ionic strength at constant pH on column efficiency is both column and analyte specific. For example, in Figs. 6–8, one observes that for the 269–013 (silica based) column the shape of the reduced parameter plot is essentially unaffected by changing phthalate concentration in the mobile phase. However, efficiency improves as the concentration of the eluting ion increases. The magnitude of the increase decreases with increasing solute retention (capacity factor) and thus is largest for chloride and smallest for sulfate. However, as shown in Fig. 9, while the shape of the reduced parameter plot for the IonPak A column is again unaffected by the concentration of the eluting

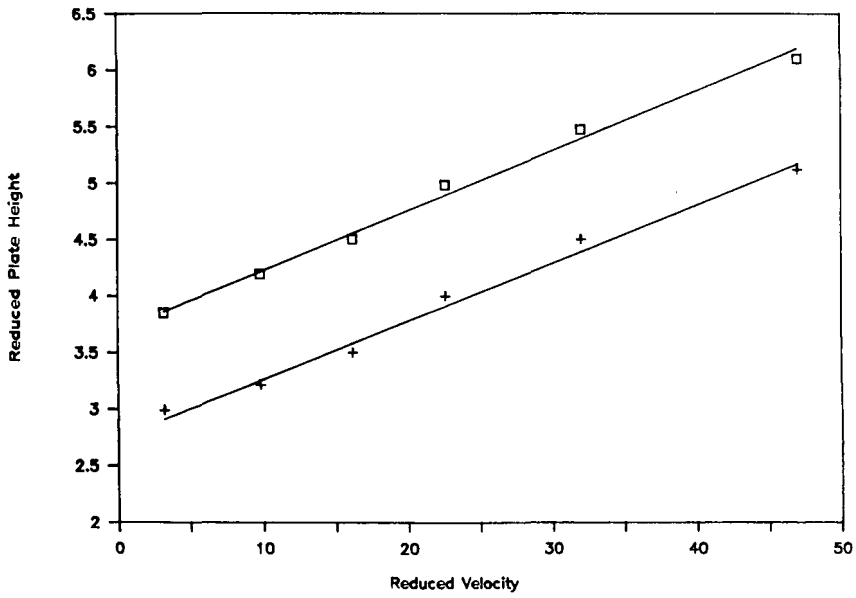

Fig. 5. Effect of injection mass on the reduced parameter plot. Column, Dionex AS-5A; mobile phase, 1 mM KHP, pH 6. □ = 100 ppm; + = 20 ppm.

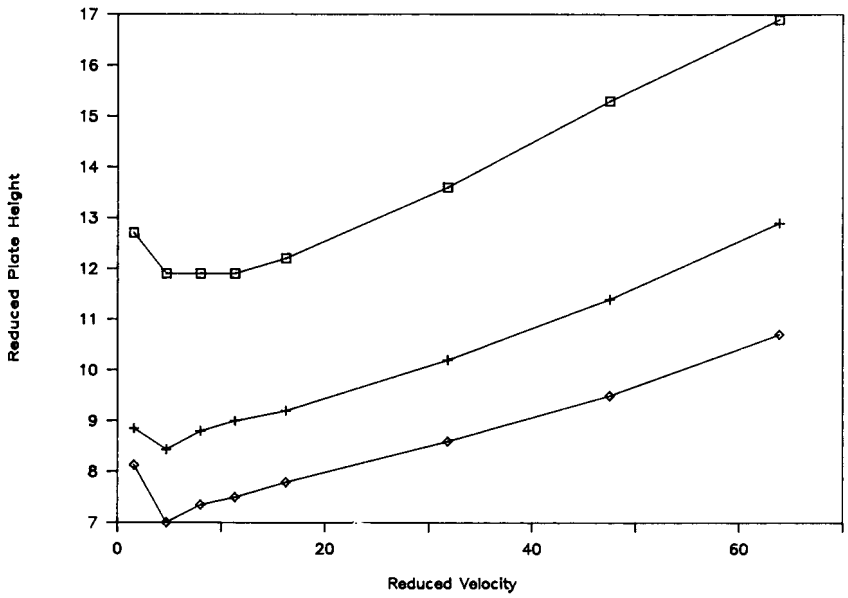

Fig. 6. Effect of mobile phase ionic strength on column efficiency. Concentrations of phthalate ion: □ = 1 mM; + = 2 mM; ◇ = 3 mM. Column, Wescan 269-013; analyte, chloride; injection mass, 1 μg; mobile phase pH = 6.

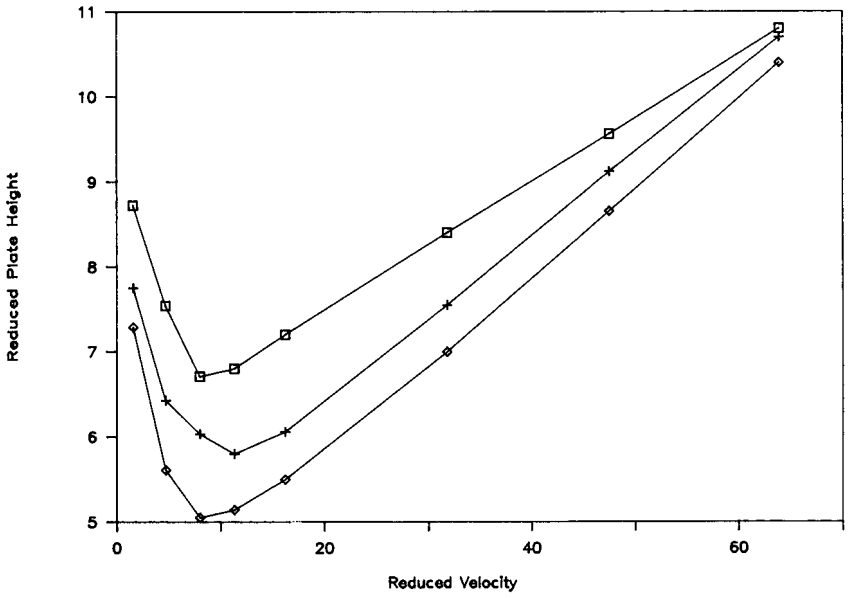

Fig. 7. Effect of mobile phase ionic strength on column efficiency. Concentrations of phthalate ion as in Fig. 6. Same conditions as in Fig. 6; analyte, nitrate.

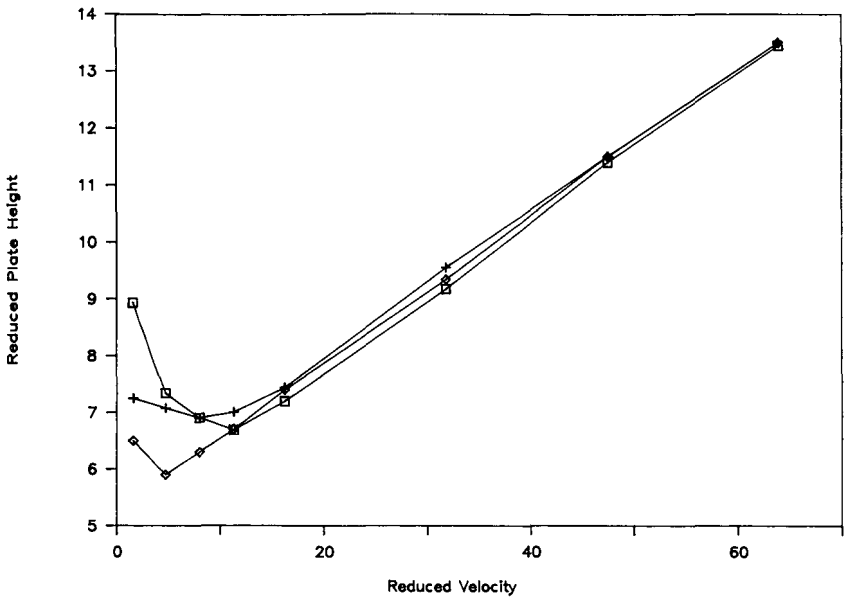

Fig. 8. Effect of mobile phase ionic strength on column efficiency. Concentrations of phthalate ion as in Fig. 6. Same conditions as in Fig. 6; analyte, sulfate.

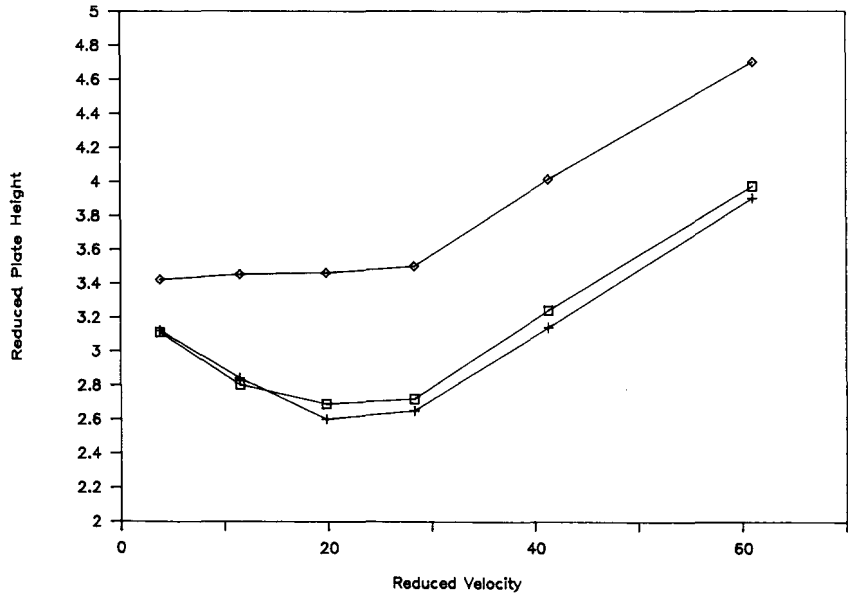

Fig. 9. Effect of mobile phase ionic strength on column efficiency. Concentrations of phthalate ion as in Fig. 6. Same conditions as in Fig. 6; column, Waters Ionpak A.

ion, the most efficient separation is achieved with the mobile phase with the lowest ionic strength (in which the solutes have the largest capacity factor). A similar relationship is observed to occur in the 269-031 column as well (Fig. 10). The behavior exhibited by the latter two columns is consistant with eqn. 7 is terms of the relationship predicted between efficiency and capacity factor. These data serve to illustrate that the mobile phase ionic strength, which impacts the physico-chemical nature of the mobile and stationary phases as well as the equilibrium thermodynamics and reaction kinetics controlling the interaction between the two, has an influence on separation efficiency which is dictated essentially by the nature of the test system and cannot readily be generalized.

In an attempt to evaluate the effect of charge (identity) of eluent ion on efficiency, mobile phase pH and total salt content were manipulated to produce mobile phases in which the total ionic strength was similar but eluent ion speciation was different. Thus the mobile phases used in this portion of the study (1 m*M* total salt at pH 6 and 2.5 m*M* total salt at pH 4.1) have virtually identical ionic strengths but the former is dominated by divalent phthalate ions while the latter is dominated by the singly charged species. Specifically, the phthalate speciation in these two mobile phases, assuming phthalate dissociation constant of 3.1 and 5.4^{10}, are: 2.5 m*M* total salt, pH 4.1; 0.24 m*M* undissociated, 2.18 m*M* monovalent and 0.13 m*M* divalent; 1 m*M* total salt, pH 6.0; 0.01 m*M* undissociated, 0.19 m*M* monovalent and 0.80 m*M* divalent. These mobile phases were used with the PRP-X100 column and the resultant efficiencies were evaluated at a variety of flow-rates. While the selectivity of the column was not influenced by the mobile phase difference (selectivity versus chloride of 1.7 and 5.1 for nitrate and sulfate for both conditions), the pH 4.1 mobile phase was

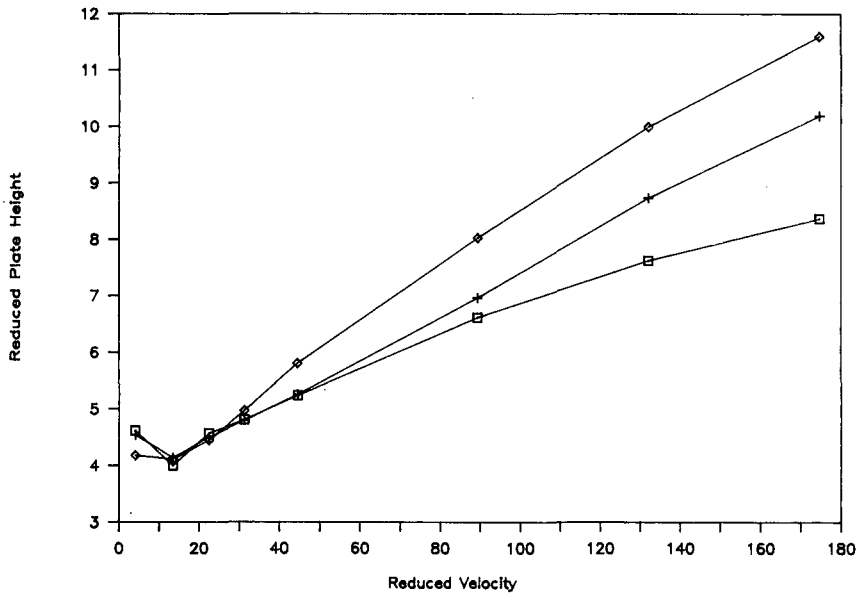

Fig. 10. Effect of mobile phase ionic strength on column efficiency. Concentrations of phthalate ion as in Fig. 6. Same conditions as in Fig. 6; column, Wescan 269-013.

actually "stronger" in terms of producing smaller capacity factors or all three analytes (1.8 *versus* 2.3, 3.2 *versus* 3.8 and 9.5 *versus* 11.3 for chloride, nitrate and sulfate, respectively). However, as shown in Figs. 11 and 12, the pH 6 mobile phase improved efficiency in two ways. At the flow-rates examined, the absolute efficiency was better with the pH 6 mobile phase; additionally, this mobile phase decreases the magnitude of the flow-rate influence on efficiency at higher flow-rates. Clearly the mobile phase speciation influences mass transfer properties which essentially mediate the efficiency at higher flow-rates. Again this behavior is consistant with the capacity factor–efficiency relationship expresed in eqn. 7.

The addition of an organic modifier to an IC mobile phase has been used to impact the performance characteristics of inorganic and organic analyte separations[7,11–13], although the exact mechanism of influence is unclear. In this study, the influence of 0–10% methanol on the chromatographic performance of the silica based stationary phases (301TP and 269–013) was examined. As is shown in Table II, the performance of the 269–013 (which was typical for the 301TP as well) was only minimally impacted by the presence of up to 10% (by volume) organic modifier in the mobile phase.

Effect of temperature

Historically, an increase in column temperature is generally expected to improve column efficiency in ion-exchange separations[14,15]. However, it is fair to say that most stationary phases used in modern IC are significantly different from those for which such generalizations were valid. While reports of the influence of column

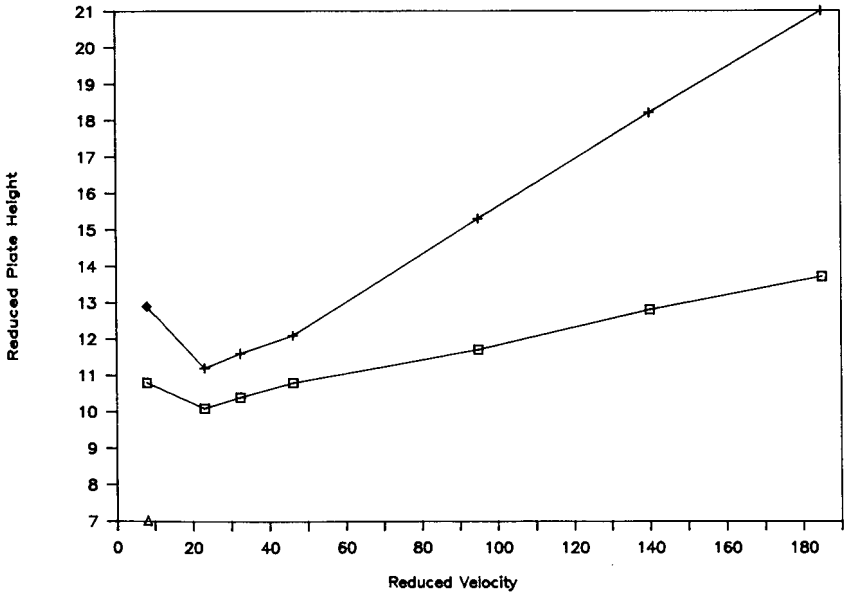

Fig. 11. Effect of mobile phase speciation (at constant ionic strength) on column efficiency. Column, Hamilton PRP-X100; sample size, 1 μg; analyte, chloride. Mobile phases used were (□) 1 m*M* total phthalate at pH 6 and (+) 2.5 m*M* total phthalate at pH 4.1.

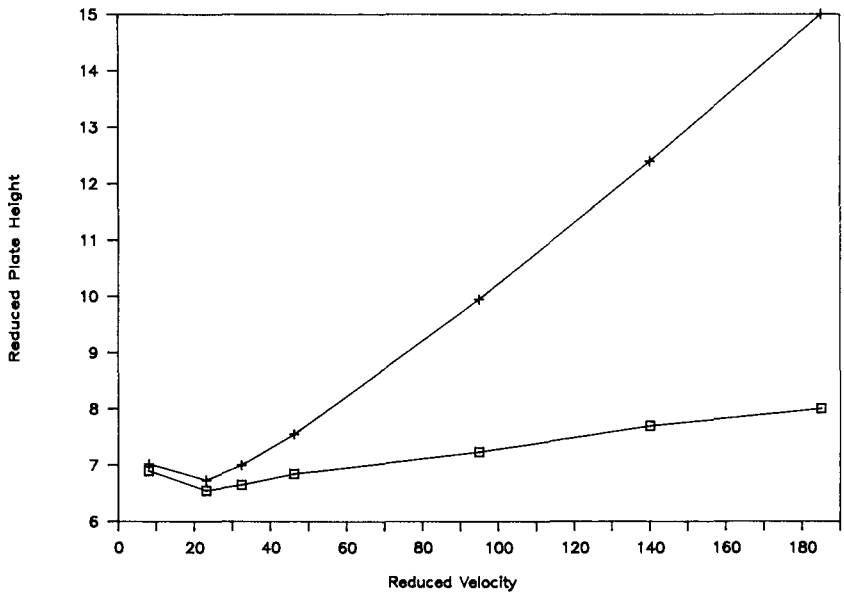

Fig. 12. Effect of mobile phase speciation (at constant ionic strength) on column efficiency. Same conditions and key to symbols as in Fig. 11; analyte, sulfate.

temperature on retention times (and resolution) in IC appear in the literature (for example, see refs. 16 and 17), a full plot of efficiency *versus* linear velocity was not determined as a function of temperature. In this study, the effect of temperature on the reduced parameter plot for the PRP-X100 column was examined. Column temperature was accurately determined by measuring the temperature of the mobile phase entering and leaving the column (which in all cases was equivalent within experimental precision). As shown in Figs. 13 and 14, the nature of the temperature influence itself is impacted by the reduced linear velocity. At higher reduced velocities (flow-rates of 0.5ml/min or greater) efficiency is improved at elevated temperature. The magnitude of the improvement is impacted by the flow-rate (improvement is

TABLE II

EFFECT OF METHANOL ON COLUMN PERFORMANCE

Column, 269-013. Mobile phase, 2 m*M* KHP (pH 6) with varying amounts of methanol (%, v/v). Injection size: 1 μg of each analyte.

Methanol (%)	*Chloride*		*Nitrate*		*Sulfate*		*Resolution*	
	k'	*N*	*k'*	*N*	*k'*	*N*	Cl^-/NO_3^-	NO_3^-/SO_4^{2-}
0	1.18	2153	2.04	2835	4.01	2271	4.03	5.99
3	1.22	2270	2.10	3011	4.17	2400	4.10	6.22
7	1.22	2106	2.14	2750	4.31	2251	4.15	6.23
10	1.20	2103	2.07	2913	4.16	2296	4.05	6.26

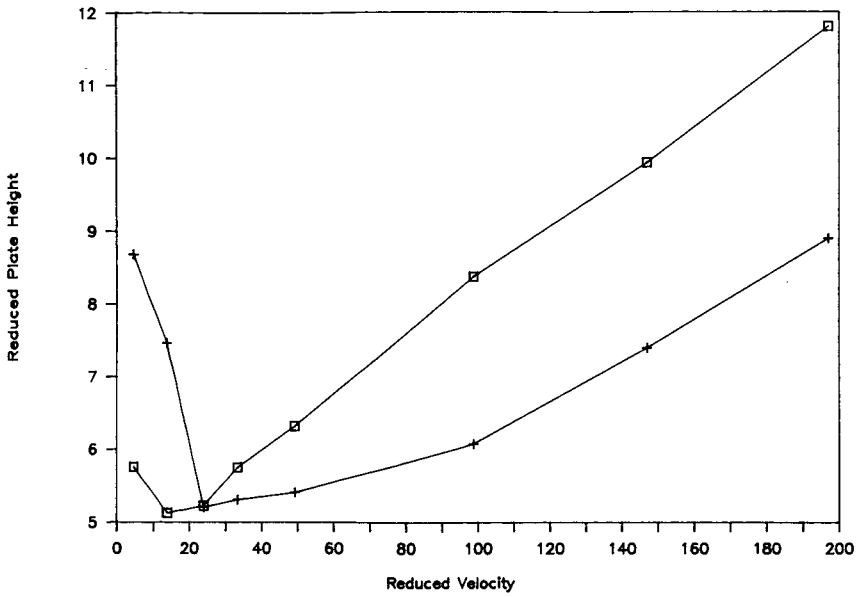

Fig. 13. Effect of column temperature on effiency. Column, Hamilton PRP-X100; mobile phase, 1 m*M* KHP, pH = 6; injection mass, 0.5 μl per analyte; analyte, chloride. □ = 25°C; + = 55°C.

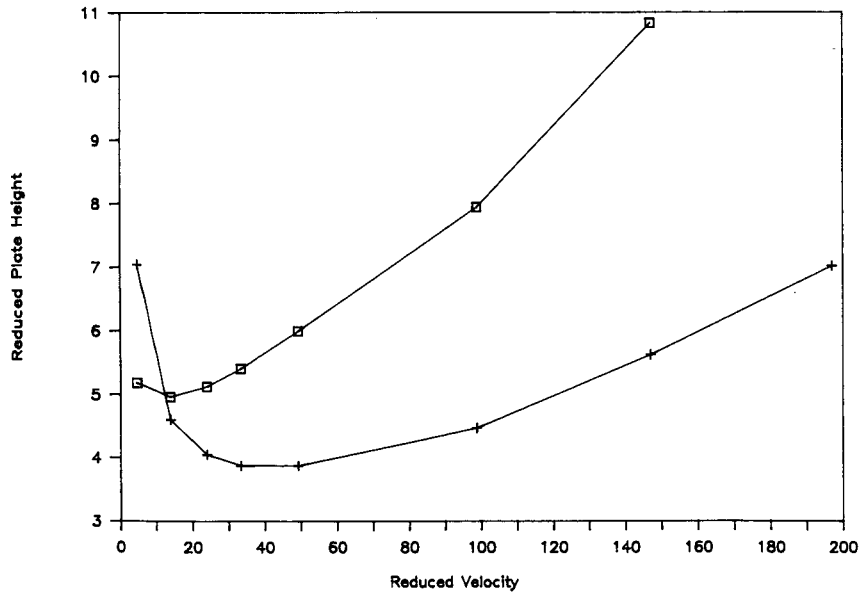

Fig. 14. Effect of column temperature on efficiency. Same conditions as in Fig. 13; analyte, sulfate. Key to symbols as in Fig. 13.

more pronounced at higher flow-rate) and by the capacity factor of the analyte (improvement is more pronounced as capacity factor increases). At low reduced linear velocities, however, an increase in column temperature produces a corresponding decrease in efficiency. This type of relationship between linear velocity and column temperature has been predicted for modern reversed phase stationary phases[18]. It is noted in passing that while the retention of chloride is immune to changing column temperature, nitrate retention is decreased with increasing temperature while sulfate retention exhibited the opposite trend. This observation is consistent with suggestions made elsewhere in the literature that the retention mechanism for nitrate in ion exchange columns is somewhat different than that for other inorganic ions[12].

CONCLUSIONS

The operational efficiency of stationary phases used in modern ion chromatography is greatly influenced by the operating conditions. For all columns studied, efficiency is improved, independent of operating flow-rate, as sample injection mass is decreased, even if the solute concentration is well below the column overload limit and approaches the mass sensitivity of the method. The chemical nature of the mobile phase impacts the efficiency both in terms of the absolute concentration of the eluting ion (ionic strength) and the absolute speciation of a multi-protic eluent. The influence of mobile phase composition on efficiency is generally stationary phases dependent although in general greater efficiencies are achieved when the net charge of the eluting ion is increased. The performance of silica-based stationary phases is independent of methanol concentration in the mobile phase at concentration up to 10% when inorganic species are separated. Increasing the column temperature improves efficiency at higher linear velocities and decreases efficiency at lower linear velocities in accord with theoretical expectations if proper thermal control is used to avoid the generation of thermal gradients in the column.

REFERENCES

1 D. R. Jenke, *J. Liq. Chromatogr.*, in press.
2 H. Poppe and J. C. Kraak, *J. Chromatogr.*, 282 (1983) 399–412.
3 S. McCown, D. Southern, B. E. Morrison and D. Garteiz, *J. Chromatogr.*, 352 (1986) 483–492.
4 L. R. Snyder and J. J. Kirkland, *Introduction to Modern Liquid Chromatography*, Wiley, New York, 1979, p. 223.
5 J. V. H. Schadel and G. Guiochon, *J. Chromatogr.*, 457 (1988) 1–12.
6 K. D. Bartle, in R. M. Smith (Editor), *Supercritical Fluid Chromatography*, Royal Society of Chemistry, London, 1988, p. 4.
7 P. R. Haddad, P. E. Jackson and A. L. Heckenberg, *J. Chromatogr.*, 346 (1985) 139–148.
8 D. R. Jenke and G. K. Pagenkopf, *J. Chromatogr. Sci.*, 22 (1984) 231–233.
9 L. R. Snyder, G. B. Cox and P. E. Antle, *Chromatographia*, 24 (1987) 82–96.
10 G. K. Pagenkopf, *Introduction to Water Chemistry*, Marcel Dekker, New York, 1978, p. 246.
11 R. C. Buechele and D. J. Reuther, *J. Chromatogr.*, 240 (1982) 502–507.
12 D. Jenke, *J. Chromatogr. Sci.*, 24 (1986) 352–355.
13 R. W. Slingsby and C. A. Pohl, *J. Chromatogr.*, 458 (1989) 241–253.
14 Cs. G. Horváth, B. A. Preiss and S. R. Lipsky, *Anal Chem.* 39 (1967) 1422–1428.
15 P. R. Brown, *J. Chromatogr.*, 52 (1970) 257–272.
16 J. Weiss, *Handbook of Iron Chromatography*, Dionex, Sunnyvale, CA, 1986, pp. 51–52.
17 N. E. Fortier and J. S. Fritz, *Talanta*, 34 (1987) 415–418.
18 P. V. Warren, Jr. and B. A. Bidlingmeyer, *Anal. Chem.*, 60 (1988) 2821–2824.

Journal of Chromatography, 479 (1989) 401–409
Elsevier Science Publishers B.V., Amsterdam — Printed in The Netherlands

CHROM. 21 737

LOW-CAPACITY QUATERNARY PHOSPHONIUM RESINS FOR ANION CHROMATOGRAPHY

LINDA M. WARTH, RICHARD S. COOPER and JAMES S. FRITZ*
Ames Laboratory and Department of Chemistry, Iowa State University, Ames, IA 50011 (U.S.A.)
(First received November 14th, 1988; revised manuscript received July 5th, 1989)

SUMMARY

Trimethylammonium, tributylammonium and tributylphosphonium anion-exchange resins were synthesized and used for single-column ion chromatography. The three resins were prepared using a 7–12-μm polystyrene–divinylbenzene resin and are all of a similar, low capacity. The selectivity of these resins for mono- and divalent anions was evaluated and unique anion separations are presented.

INTRODUCTION

Since the introduction of suppressed ion chromatography (SIC) in 1975[1] and single-column ion chromatography (SCIC) in 1979[2], several types of ion exchangers have been used to separate anions. The original work in SIC by Small and Stevens[3] used agglomerated, pellicular resins of a low exchange capacity. Chemically-bonded polymeric resins of an even lower capacity were used by Gjerde *et al.*[2] in SCIC. More recently, statically- or dynamically-coated resins have become popular in anion chromatography, largely because of ease of column preparation[4–6].

Most stationary phases used in anion chromatography are "strong-base" quaternary ammonium resins. The resins most often used are referred to as Type I (benzyltrimethylammonium cation) and Type II (one methyl group replaced by a hydroxyethyl group) resins. A few other types of strong-base resins have also been used in anion chromatography. For example, Barron and Fritz[7,8] synthesized a series of quaternary ammonium resins with varying R group lengths that were used to study the effect of functional group structure on anion selectivity.

Although quaternary ammonium resins have been used extensively as stationary phases[9–11], quaternary phosphonium resins have also been synthesized[12,13]. Most recent work shows that quaternary phosphonium resins have been used extensively as phase-transfer catalysts[14,15]. In many cases, the quaternary phosphonium phase-transfer catalysts were more active catalytically than the analogous quaternary ammonium catalysts[16–18].

To our knowledge, low-capacity quaternary phosphonium ion-exchange resins have never been used in single-column ion chromatography.

There are two major differences (possible advantages) of a tributylphosphoni-

0021-9673/89/$03.50

um (TBP) resin compared with a tributylammonium (TBA) resin: (1) TBP is more reactive than TBA and resins of higher exchange capacity can be prepared, (2) the TBP resin has a considerably higher affinity for nitrate, compared to sulfate, than the TBA resin. This property is being used in other work on the selective removal of nitrate from water supplies. The goal of this work is to synthesize a quaternary phosphonium resin of a low capacity which is suitable for anion chromatography. The preparation, performance, and selectivity of this resin in anion chromatography are then evaluated and compared to that of two different quaternary ammonium ion-exchange resins.

EXPERIMENTAL

Materials and equipment

The 7–12-μm, spherical polystyrene–divinylbenzene resin (PS–DVB) was obtained by courtesy of Dr. Douglas Gjerde at Benson Co. (Reno, NV, U.S.A.). The 25% trimethylamine (in methanol) and tributylamine were obtained from Aldrich (Milwaukee, WI, U.S.A.). The tributylphosphine was obtained from Aldrich or Sigma (St. Louis, MO, U.S.A.). The paraformaldehyde and concentrated hydrochloric acid used for the chloromethylation reactions were obtained from Mallinckrodt (Paris, KT, U.S.A.). The solvents used for rinsing resin were of reagent grade and were obtained from a number of sources. All reagents were used as received.

Ion chromatography was carried out on one of two instruments, both built from similar components. An LKB 2150 high-performance liquid chromatography (HPLC) pump (Pharmacia LKB Biotechnology, Piscataway, NJ, U.S.A.) or a Milton Roy Mini-pump manufactured by Laboratory Data Control (Riviera Beach, FL, U.S.A.) equipped with a high-pressure pulse dampener provided eluent flow. Rheodyne (Berkeley, CA, U.S.A.) Model 7010 injection valves fitted with 50-μl sample loops were used for sample introduction. The resins were packed in glass-lined stainless-steel columns (250 × 2.0 mm I.D.) that were obtained from Scientific Glass Engineering (Austin, TX, U.S.A.). An Eldex (Menlo Park, CA, U.S.A.) column heater or home-made insulation was used to insulate the column and prevent baseline drift. Detectors used were Model 213A conductivity detectors manufactured by Wescan Instruments (Santa Clara, CA, U.S.A.). Strip-chart recorders manufactured by Curken Scientific (Danbury, CT, U.S.A.) were used to record chromatograms.

Procedures

Chemically-bonded resins were prepared using a two-step procedure. First, a formaldehyde–hydrochloric acid procedure[19] was used to chloromethylate the resin. Standard conditions for the chloromethylation reactions employed 1.0 g of resin and 2.2 *M* paraformaldehyde in 25-ml of 10 or 12 *M* hydrochloric acid at room temperature. Then, 40 ml of a 2.0 *M* or greater solution of trimethylamine (TMA), tributylamine (TBA) or tributylphosphine (TBP) in methanol or 1,2-dichloropropane (1,2-DCP) was reacted with the chloromethylated resin at 60–70°C for at least 24 h to obtain quaternary ammonium or phosphonium resins. The amination and phosphination procedures are similar to those in previously-published works[18,19].

The control quaternization experiment was performed by first chloromethylating 1.0 g of resin using 2.2 *M* paraformaldehyde in 12 *M* hydrochloric acid for 18.5

min. The chloromethylated batch of resin was then divided into equal parts and aminated or phosphinated using exactly 2 *M* concentrations of the reagent in 40 ml of either methanol or 1,2-DCP. After amination, the resin was filtered and washed thoroughly with 2.0 *M* hydrochloric acid, water, 2-propanol, water and methanol. The functionalized resin was then air dried.

The strong-base ion-exchange capacities of the resins were determined by rinsing a weighed portion of resin with methanol, water, 0.5 *M* potassium nitrate and then again with water to remove any excess nitrate. The resin was then transferred to a gravity column and the bound nitrate was eluted with 0.005 *M* potassium sulfate. The collected nitrate was then determined spectrophotometrically at 225 nm.

All solutions were made up in distilled, deionized water and were prepared from reagent grade salts. Eluents were prepared by dissolving the acid in distilled, deionized water and, if necessary, adjusting the pH by adding sodium hydroxide. The eluents were then filtered through a 0.2-μm membrane filter after which a vacuum was applied while stirring to remove dissolved gases.

Columns were packed using an upward packing, stirred slurry technique with 40% ethylene glycol and 1% sodium chloride in water as the packing solvent. The packing pressure was approximately 4500 p.s.i. The instrument used to pack the columns was a Shandon HPLC packing pump (Phenomenex, Rancho Palos Verdes, CA, U.S.A.).

RESULTS AND DISCUSSION

Preparation of resins

The purpose of this study was to evaluate and compare the selectivity and performance of low-capacity quaternary phosphonium and ammonium resins in anion chromatography. Three types of resins were prepared; the structures are shown in Fig. 1. All factors other than the structure of the functional group were held constant. For example, the resins were all prepared from the same resin lot and were synthesized to obtain similar exchange capacities so that identical elution conditions could be used.

The anion-exchange resins were prepared by chloromethylating a cross-linked polystyrene resin, followed by reaction with a tertiary amine (TMA or TBA) or a tertiary phosphine (TBP). It became apparent immediately that the reactivities of the

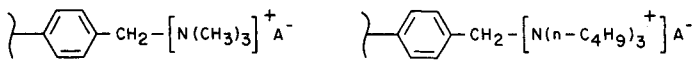

TMA resin TBA resin

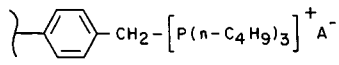

TBP resin

Fig. 1. Structures of the three resins synthesized and compared chromatographically: trimethylammonium resin (TMA), tributylammonium resin (TBA) and tributylphosphonium resin (TBP).

TABLE I

PREPARATION OF CHROMATOGRAPHIC RESINS

Reaction conditions are listed in the Experimental section.

Resin	*Designation*	*Chloromethylation time (min)*	*HCl (M)*	*Amination solvent*	*Capacity (μequiv./g)*
Trimethylammonium	TMA	2, 2.6, 2.5[a]	10	Methanol	90.2
Tributylammonium	TBA	125	12	Methanol	93.3
Tributylphosphonium	TBP	18.5	12	1,2-DCP	96.9

[a] Three separate chloromethylation and amination reactions were used to obtain a total TMA capacity of 90.2 μequiv./g.

TMA, TBA and TBP were greatly different. The following exchange capacities were obtained after performing a control experiment and reacting portions of the same chlormethylated resin with an amine or phosphine at 60–70°C for 24 h: TMA, 219.1 μequiv./g; TBA, 53.1 μequiv./g; TBP, 93.5 μequiv./g.

It was possible, however, to prepare resins of almost the same exchange capacity by varying the extent of chloromethylation. The major synthetic conditions and properties of the quaternary ammonium and phosphonium resins used in this study are summarized in Table I. Note that the times used for chloromethylation were varied considerably to compensate for the differences in reactivity of the amines and phosphine.

Evaluation of resin selectivity

Although the exchange capacities of the three resins in Table I are similar, there is a considerable difference in the amounts of unreacted chloromethyl groups. The

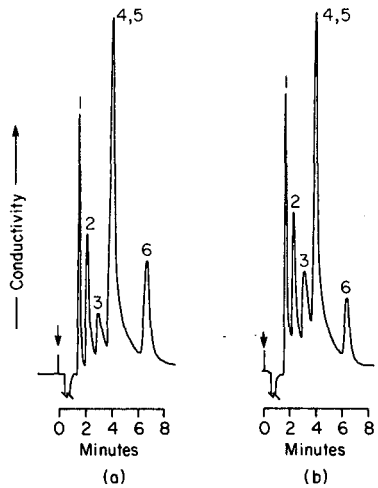

Fig. 2. Separation on TMA resins of (1) chloride, (2) nitrite, (3) bromide, (4) sulfate, (5) nitrate and (6) thiosulfate using 1 m*M* sodium phthalate at pH 6.5 as the eluent at a flow-rate of 0.75 ml/min. Anion concentrations were 6–50 ppm each. (a) TMA resin with a capacity of 70.1 μequiv./g. (b) TMA resin with a capacity of 70.1 μequiv./g and 121 μequiv./g excess chloromethyl groups.

presence of excess chloromethyl groups has been noted previously[20], but the effect of these groups on anion selectivity has not been studied.

Fig. 2 shows chromatograms of identical sample mixtures obtained on the same batch of TMA resin. The separation shown in Fig. 2a was obtained with a resin that was first chloromethylated and then aminated using TMA to obtain an exchange capacity of 70.1 μequiv./g. This column was then unpacked, chloromethylated again, repacked and tested. Fig. 2b shows a separation using the TMA resin (70.1 μequiv./g with excess chloromethyl groups. Identical eluent conditions and sample mixtures were used in both cases. A portion of the resin was again aminated with TMA and a capacity of 191 μequiv./g was obtained. Because of the similarity of these chromatograms, it can be concluded that the presence of excess chloromethyl groups (at a level of 121 μequiv./g) on an anion-exchange resin has virtually no effect on the selectivity of the anions tested in this study.

Columns were packed with TMA, TBA and TBP resins and retention times for a number of anions were measured using identical elution conditions for each column. Relative retention times were then calculated by dividing the adjusted retention time of each anion by the adjusted retention time of chloride. This corrects for the small differences in resin capacity and for any other slight differences in elution conditions.

The relative retention times of various anions are given in Table II using two different eluents. Many of the anions tested show very little change in relative retention on the three columns. However, large polarizable anions, such as bromide, nitrate and iodide, show higher relative retention times on TBA compared to TMA and still higher relative retention times on the TBP column. Chlorate shows almost the same retention times on the quaternary ammonium columns but a distinctly higher relative retention time on the quaternary phosphonium column.

The effect of larger R groups in quaternary ammonium resins on the retention of poorly hydrated anions like bromide, nitrate and iodide has been noted previously[7]. This effect has been attributed to stronger ion pairing that results from disruption of the water structure by these anions and from a tightening of the water structure surrounding the ion pair caused by the larger R groups. These effects appear to be enhanced further by going from a quaternary ammonium to a quaternary phosphonium resin. The phosphonium group is larger and more hydrophobic than the ammonium exchange site. This causes a greater tightening of the water structure around the ion pair and results in longer relative retention times for ions like bromide, nitrate and iodide.

Eluent pH

Chromatograms of a number of anions were compared on TBA and TBP resin columns using 1.5 m*M* sodium phthalate at several pH values. Results for a few of the anions are shown in Figs. 3 and 4. At higher eluent pH values the relative retention times of divalent anions decrease, as expected, because the eluent is present primarily as the 2− anion. However, the relative retention times of monovalent anions increase as the eluent pH becomes higher. This effect is especially pronounced for nitrate and chlorate.

The longer retention of anions such as nitrate and chlorate at higher eluent pH values is rather puzzling, because a 2− eluent anion should elute monovalent sample

TABLE II

SELECTIVITY DATA FOR QUATERNARY AMMONIUM AND PHOSPHONIUM ION-EXCHANGE RESINS

Conditions: the TMA column is a trimethylammonium resin with a capacity of 90.2 μequiv./g. The TBA column is a tributylammonium resin with a capacity of 93.3. μequiv./g. The TBP column is a tributylphosphonium resin with a capacity of 96.9 μequiv./g. All flow-rates were 0.75 ml/min and detection was by conductivity.

Anion	$t'_R/t'_{R,chloride}$					
	30 mM nicotinic acid			*2.2 mM sodium phthalate, pH 6.0*		
	TMA column	*TBA column*	*TBP column*	*TMA column*	*TBA column*	*TBP column*
Acetate	–	–	–	–	0.73	0.67
Glycolate	0.22		0.20	–	–	–
Lactate	0.30	0.25	0.25	–	–	–
Formate	0.34	0.33	0.29	–	–	–
Fluoride	0.39	0.35	0.32	–	–	0.50
Dihydrogenphosphate	0.46	0.44	0.43	0.63	0.71	0.62
Iodate	0.50	0.47	0.44	–	–	0.49
Azide	0.54	0.49	0.50	–	–	–
Methylsulfonate	0.95	0.89	0.86	0.95	0.98	0.94
Propionate	0.96	0.42	0.46	–	–	–
Chloride	1.00	1.00	1.00	1.00	1.00	1.00
Bromate	1.51	1.22	1.26	1.25	1.15	1.22
Ethylsulfonate	1.61	1.18	1.20	1.49	1.33	1.35
Nitrite	1.33	1.34	1.46	1.49	1.59	1.60
Bromide	2.38	2.65	3.02	1.91	2.30	2.69
Malonate	–	–	–	2.09	2.72	2.53
Sulfate	–	–	–	2.09	2.42	2.32
Nitrate	3.08	4.53	5.20	2.49	3.68	4.31
Thiosulfate	–	–	–	3.57	3.77	3.66
Chlorate	–	–	–	4.32	4.34	5.28
Propylsulfonate	–	–	–	4.92	3.20	3.38
Iodide	–	–	–	9.60	17.88	29.08
t'_R for Cl^- (min)	6.95	12.39	11.63	0.85	1.11	1.19

anions more quickly than a 1− eluent anion. One possible explanation is that more phthalate is adsorbed on the resin surface at pH 4.5 than at pH 6.5[21]. This adsorbed phthalate could partially relax the water structure surrounding the exchange site and lessen the effects of water-induced ion pairing on nitrate and chlorate. At pH 6.5, much less phthalate is adsorbed and the stronger water-induced ion pairing results in longer retention times for anions like nitrate and chlorate.

Chromatographic separations

Fig. 5 shows chromatograms comparing separations of several inorganic anions on all three columns. The eluent used was 1.5 m*M* sodium phthalate (pH 6.5) operated at a flow-rate of 0.75 ml/min. Using these conditions, the TBP separation shows much greater resolution of the peaks separated. This results primarily from the

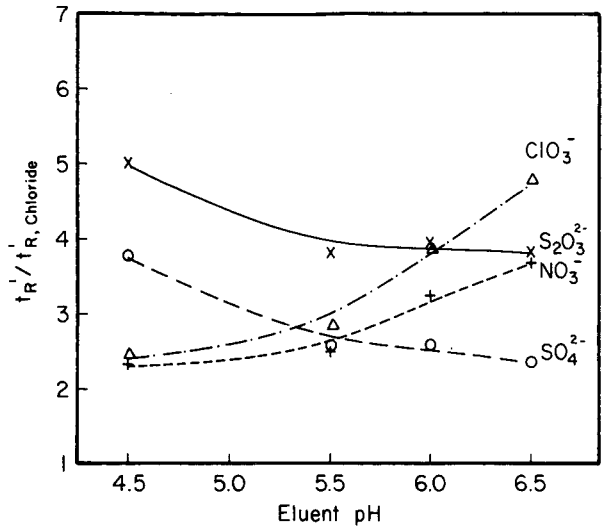

Fig. 3. Relative retentions *versus* eluent pH using the TBA column (93.3 μequiv./g) and a 1.5 m*M* sodium phthalate eluent. Detection was by conductivity.

greater retention of the monovalent bromide and nitrate anions obtained on TBP column.

Figs. 6 and 7 shows additional examples of separations obtained with the TBP column. Fig. 6 shows a separation of chloride and several divalent anions (sulfate, oxalate, tungstate, thiosulfate and chromate). Conductivity detection is used and the

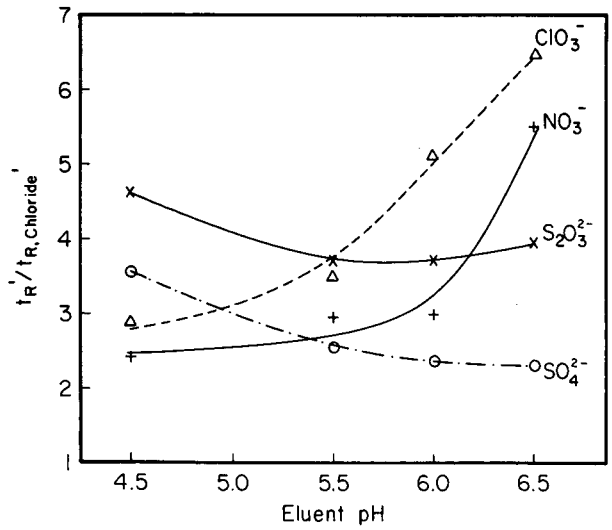

Fig. 4. Relative retentions *versus* eluent pH using the TBP column (96.9 μequiv./g) and a 1.5 m*M* sodium phthalate eluent. Detection was by conductivity.

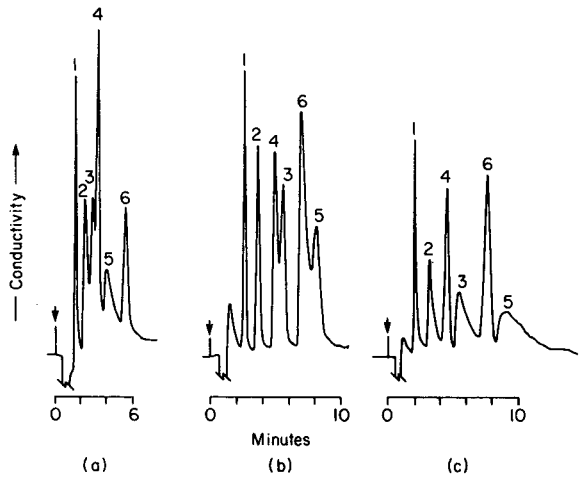

Fig. 5. Separation of common inorganic anions on TMA (a), TBA (b) and TBP (c) columns. Resin capacities are 90.2, 93.3 and 96.9 μequiv./g, respectively. The eluent was 1.5 m*M* sodium phthalate (pH 6.5) at a flow-rate of 0.75 ml/min. Detection was by conductivity. Anions are (1) chloride, (2) nitrite, (3) bromide, (4) sulfate, (5) nitrate and (6) thiosulfate at concentration levels of 6–30 ppm each anion.

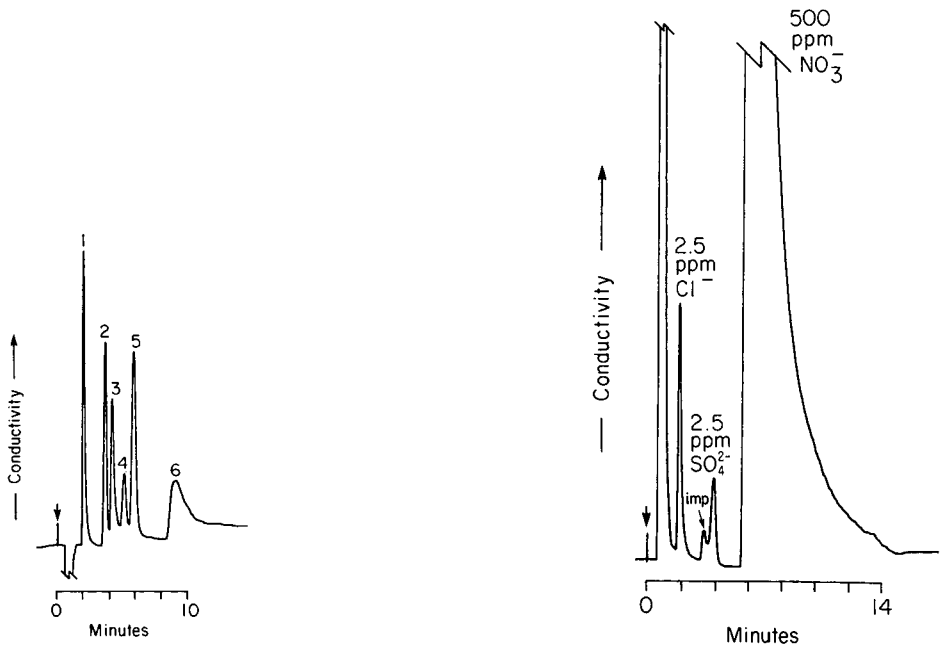

Fig. 6. Separation of chloride and late-eluting anions on the TBP column (96.9 μequiv./g). The eluent was 2.2 m*M* sodium phthalate (pH 6.5) at a flow-rate of 0.75 ml/min. Detection was by conductivity. Anions are (1) 6 ppm chloride, (2) 7.5 ppm sulfate, (3) 10 ppm oxalate, (4) 20 ppm tungstate, (5) 12.5 ppm thiosulfate and (6) 40 ppm chromate

Fig. 7. Separation of low levels of chloride and sulfate in the presence of large amounts of nitrate using the TBP column (96.9 μequiv./g). Separation conditions are listed in Fig. 7.

eluent is 2.2 m*M* sodium phthalate at pH 6.5. The higher capacity of this column and high pH of this eluent allow chloride and the divalent anions that are normally late-eluting to be separated in just 10 min.

Fig. 7 shows a separation of low levels of chloride (2.5 ppm) and sulfate (2.5 ppm) in the presence of a 200-fold excess of nitrate. The eluent used is again 2.2 m*M* sodium phthalate at pH 6.5. Because the TBP column is very selective for nitrate, the determination of low levels of other early-eluting anions is possible. With most columns, this determination would not be possible because the nitrate would elute too early in the chromatogram. A useful application for this type of determination is in the analysis of nitric acid digests.

ACKNOWLEDGEMENTS

The authors gratefully acknowledge Rohm & Haas of Philadelphia for supporting this research, and Dr. John O. Naples for helpful discussions. We also thank Mr. Earl Smith (Iowa State University, Ames, IA, U.S.A.) for technical assistance and Dr. Douglas Gjerde of Benson Co. (Reno, NV, U.S.A.) for supplying the 7–12-μm, spherical polystyrene–divinylbenzene used in this work. This research was performed at the Ames Laboratory, which is operated for the U.S. Department of Energy at Iowa State University.

REFERENCES

1 H. Small, T. S. Stevens and W. C. Bauman, *Anal. Chem.*, 47 (1975) 1801.
2 D. T. Gjerde, J. S. Fritz and G. Schmuckler, *J. Chromatogr.*, 295 (1979) 509.
3 H. Small and T. Stevens, *U.S. Pat.*, 4 101 460 (1975).
4 D. L. DuVal and J. S. Fritz, *J. Chromatogr.*, 295 (1984) 89.
5 R. M. Cassidy and S. Elchuk, *Anal. Chem.*, 54 (1982) 1631.
6 B. B. Wheals, *J. Chromatogr.*, 402 (1987) 115.
7 R. E. Barron and J. S. Fritz, *J. Chromatogr.*, 284 (1984) 13.
8 R. E. Barron and J. S. Fritz, *J. Chromatogr.*, 316 (1984) 201.
9 F. Helfferlich, *Ion Exchange*, McGraw-Hill, New York, 1962, Ch. 3.
10 R. M. Diamond and D. C. Whitney, in J. Marinsky (Editor), *Ion Exchange —A Series of Advances*, Marcel Dekker, New York, 1966, Vol. 2, Ch. 6.
11 T. P. E. Kressman, in C. Calvin and T. R. E. Kressman (Editors), *Ion Exchangers in Organic and Biochemistry*, Interscience, New York, 1957, Ch. 1.
12 N. V. Stamicarbon, *Dutch Pat.*, 75 705 (1954).
13 E. L. McMaster and H. Tolksmith, *U.S. Pat.*, 2 764 561 (1956).
14 M. Tomoi, N. Kori and H. Kakiuchi, *React. Polym.*, 3 (1985) 341.
15 M. Tomoi, E. Ogawa, Y. Hosokawa and H. Kakiuchi, *J. Polym. Sci., Polym. Chem.*, 20 (1982) 3015.
16 M. S. Chiles and P. C. Reeves, *Tetrahedron Lett.*, 36 (1979) 3367.
17 M. S. Chiles, D. D. Jackson and P. C. Reeves, *J. Org. Chem.*, 45 (1980) 2915.
18 M. Tomoi and W. T. Ford, *J. Am. Chem. Soc.*, 103 (1981) 3821.
19 R. E. Barron and J. S. Fritz, *React. Polym.*, 1 (1983) 215.
20 R. E. Barron, *Ph.D. Dissertation*, Iowa State University, Ames, IA, 1983.
21 J. S. Fritz, D. L. DuVal and R. E. Barron, *Anal. Chem.*, 56 (1984) 1177.

Journal of Chromatography, 479 (1989) 410–418
Elsevier Science Publishers B.V., Amsterdam — Printed in The Netherlands

CHROM. 21 722

Note

Capillary gas chromatographic determination of *trans*-3′-hydroxycotinine simultaneously with nicotine and cotinine in urine and blood samples

PETER VONCKEN*, GEORG SCHEPERS and KARL-HEINZ SCHÄFER
INBIFO Institut für biologische Forschung, Fuggerstrasse 3, D-5000 Köln 90 (F.R.G.)
(First received November 6th, 1988; revised manuscript received June 21st, 1989)

Almost three decades ago, McKennis and co-workers isolated hydroxycotinine, a nicotine metabolite, from the urine of dogs[1], rats[2] and humans[3] treated with nicotine or cotinine. Metabolically produced hydroxycotinine, isolated from human urine, was found to be identical with a synthesized product which was thougth to be 3- or 4-hydroxycotinine[4]. The exact structure of the metabolically produced hydroxycotinine isolated from the urine of cotinine-treated monkeys was shown by Dagne and Castagnoli[5] to be *trans*-1-methyl-3-(*R*)-hydroxy-5-(*S*)-3-pyridyl-2-pyrrolidone (*trans*-3′-hydroxycotinine, THOC). Recently, THOC has been identified as a major metabolite of nicotine in the urine of cigarette smokers[6–9].

Only a few chromatographic methods for the determination of THOC in urine or blood have been published[6,10–12]. Three methods used high-performance liquid chromatography (HPLC)[10–12]. Neurath and Pein[6] described a gas chromatographic (GC) method for the determination of THOC in human urine and plasma: after extraction at alkaline pH using dichloromethane, an aliquot of the extract is derivatized with heptafluorobutyric anhydride; after a solvent exchange, the derivative is analyzed by packed column GC by means of electron-capture detection. This method was recently used to investigate the pharmacokinetics of THOC in cigarette smokers[9].

A new GC assay for the determination of THOC without derivatization simultaneously with nicotine and cotinine in urine and blood has been developed.

EXPERIMENTAL

Materials

trans-3′-Hydroxycotinine, N-ethylnornicotine and N-ethylnorcotinine were obtained from the Institut für Biopharmazeutische Mikroanalytik, G. Neurath (Hamburg, F.R.G.). Nicotine (research grade) was supplied by Serva (Heidelberg, F.R.G.), and cotinine (purity >99%) was obtained from Roth (Karlsruhe, F.R.G.). Anhydrous potassium carbonate (purity >99%) was obtained from Aldrich (Steinheim, F.R.G.). The solvent *n*-butyl acetate (Aldrich) was of HPLC grade and dichloromethane (Merck, Darmstadt, F.R.G.) was specified as residue analysis grade.

0021-9673/89/$03.50

Urine and blood samples were obtained from an heavy smoker (approximate daily consumption 50 cigarettes, nicotine delivery in smoke 1 mg per cigarette). The samples were collected at 13:30 p.m. By this time the individual had already smoked 20 cigarettes, the last one 10 min prior to sample collection. Blank samples of urine and plasma were obtained from non-smokers who were not exposed to environmental tobacco smoke for at least 1 week before the samples were taken. All samples were stored at −20°C until used.

Extraction

An 0.5-ml volume of *n*-butyl acetate and 2 ml saturated aqueous potassium carbonate solution were added to 0.5 ml urine in a 5-ml sample tube with a PTFE-sealed screw cap (Macherey-Nagel, Düren, F.R.G.). The extraction solvent *n*-butyl acetate contained the internal standards N-ethylnornicotine (400 μg/l) for nicotine and N-ethylnorcotinine (440 μg/l) for cotinine and THOC. The mixture was shaken for 10 min on a rotary mixer (Cenco, Breda, The Netherlands) at 40 rpm and centrifuged for 5 min at 1000 *g*.

The extraction of 1 ml of plasma or serum was performed using 1 ml dichloromethane and 2 ml saturated aqueous potassium carbonate solution. The extraction solvent dichloromethane contained the internal standards N-ethylnornicotine (250 μg/l) and N-ethylnorcotinine (275 μg/l).

Gas chromatography

Detection was performed using either a nitrogen–phosphorus detector to determine THOC alone in urine or a mass-selective detector for the simultaneous determination of THOC, nicotine and cotinine in urine and blood.

A gas chromatograph (Carlo Erba, 5300 Mega Series) equipped with a nitrogen–phosphorus detector and connected to a laboratory data system (Multichrom; VG Instruments, Wiesbaden, F.R.G.) was used. GC was performed with a fused-silica capillary column (10 m × 0.32 mm) coated with free fatty acid phase (FFAP) (Macherey-Nagel). A 1-μl volume of the *n*-butyl acetate extract was splitlessly injected. The split valve was closed for 0.5 min. The temperature of the injection port and the detector was 350°C. The oven temperature was programmed to increase from 100 to 240°C at a rate of 40°C/min. The temperature was kept at 240°C for 20 min. Helium was used as the carrier gas at a flow-rate of 6.5 ml/min at 240°C. The flow-rates of hydrogen, air and make-up helium were 30, 300 and 40 ml/min, respectively. Under these conditions THOC, nicotine and cotinine had retention times of *ca.* 6.5, 1.3 and 4.4 min, respectively (see Fig. 1). The observed variation in the retention times of cotinine and THOC is due to the steep increase in oven temperature (40°C/min) which could not be completely controlled before the final temperature of 240°C was reached.

For GC–mass spectrometric (MS) analysis a gas chromatograph (Hewlett-Packard, Model 5890) coupled to a computer-controlled mass spectrometer (Hewlett-Packard, Model 5990B) was used. A DB5 fused-silica capillary column (30 m × 0.32 mm; J & W via Carlo Erba, F.R.G.) was directly coupled to the ion source (ionization voltage: 70 eV). A 1-μl volume of the extract was splitlessly injected. The split valve was closed for 0.5 min. The splitless injection port temperature was 280°C. The oven temperature was kept at 100°C for 2.5 min and then raised at 20°C/min to 240°C.

Helium was used as the carrier gas at a flow-rate of 2.4 ml/min at 240°C. Under these conditions the retention times of THOC, nicotine and cotinine were 8.3, 5.1 and 7.8 min, respectively (see Fig. 2).

The mass spectrometer was operated either in the full scan or selected-ion monitoring (SIM) mode. For SIM the following ions were used: nicotine, *m/z* 84, 133 and 161; N-ethylnornicotine, *m/z* 98, 130, 161 and 176; cotinine, *m/z* 98, 118 and 176; N-ethylnorcotinine, *m/z* 112, 118, 146 and 190; THOC *m/z* 106, 135 and 192.

Calibration

Standard solutions of THOC in *n*-butyl acetate were added to blank urine samples in order to obtain five different concentrations ranging from 100 to 3400 μg/l. For each concentration the samples were extracted in duplicate as described and the analysis was performed by GC using nitrogen–phosphorus detection (NPD). Calibration graphs were obtained from linear regressions of the THOC concentrations of the five duplicate extracts *versus* the peak areas.

Standard solutions containing nicotine, cotinine and THOC at five different concentrations and the internal standards at constant concentrations were prepared in *n*-butyl acetate as well as in dichloromethane. In order to obtain calibration samples, blank urine samples were spiked with the *n*-butyl acetate standard solutions and blank plasma samples with the dichloromethane standard solutions. The resulting concentrations ranged from 10 to 1320 μg/l for nicotine, from 10 to 900 μg/l for cotinine and from 20 to 3400 μg/l for THOC. The samples were extracted in duplicate as described and nicotine, cotinine and THOC determined simultaneously in a single GC analysis. Calibration graphs were obtained from the linear regressions of the concentrations of the five duplicate extracts *versus* the peak area ratios.

Recovery

The overall recovery was determined by spiking blank samples with nicotine, cotinine and THOC. The samples were extracted as described without the addition of the internal standards. After separation of the organic layer, the internal standard solution was added yielding equal internal standard concentrations as mentioned in the extraction procedure. The recoveries were calculated by comparing the peak area ratios of the samples with that of the non-extracted standard solution.

RESULTS

The THOC determination in urine by capillary GC with NPD was performed using the external standard method. The linear regression analysis obtained from five different concentrations in duplicate *versus* the peak areas yielded a correlation coefficient r^2 of 0.999 for THOC.

Chromatograms of blank and spiked urine samples from a non-smoker and the chromatogram of a urine sample from a heavy smoker are presented in Fig. 1. As indicated in the chromatogram of the smoker's urine, not only THOC but also nicotine and cotinine are present in the same extract. This led to a modification of the method to enable the determination of THOC simultaneously with nicotine and cotinine. The modifications involved changes of the chromatographic conditions as well as the use of a mass-selective detector in the SIM mode and internal standards. The

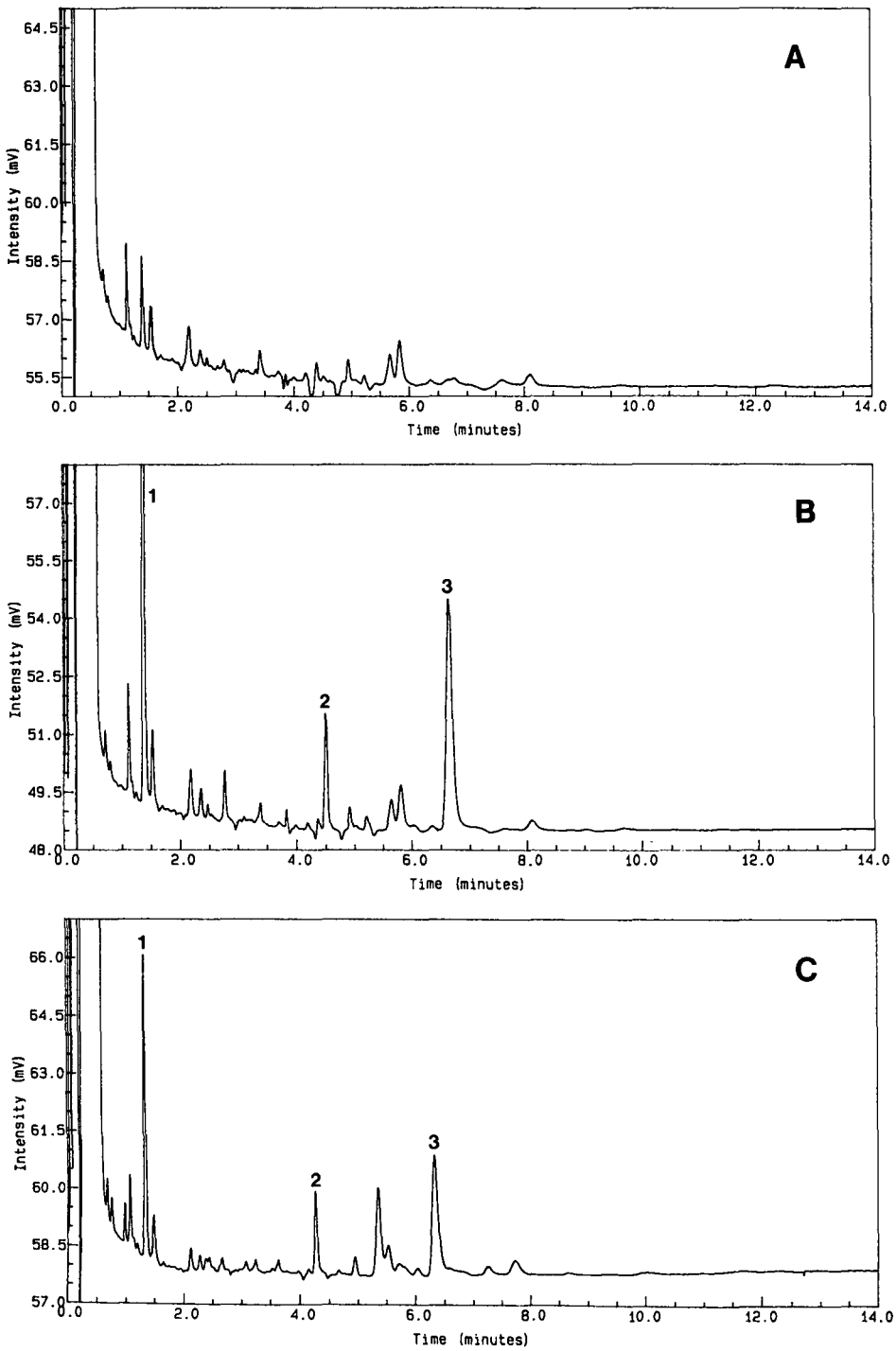

Fig. 1. Capillary gas chromatograms: blank and spiked urine samples from a non-smoker (A,B); urine sample from a heavy smoker (C). Nitrogen–phosphorus detection. Peaks: 1 = nicotine; 2 = cotinine; 3 = *trans*-3′-hydroxycotinine.

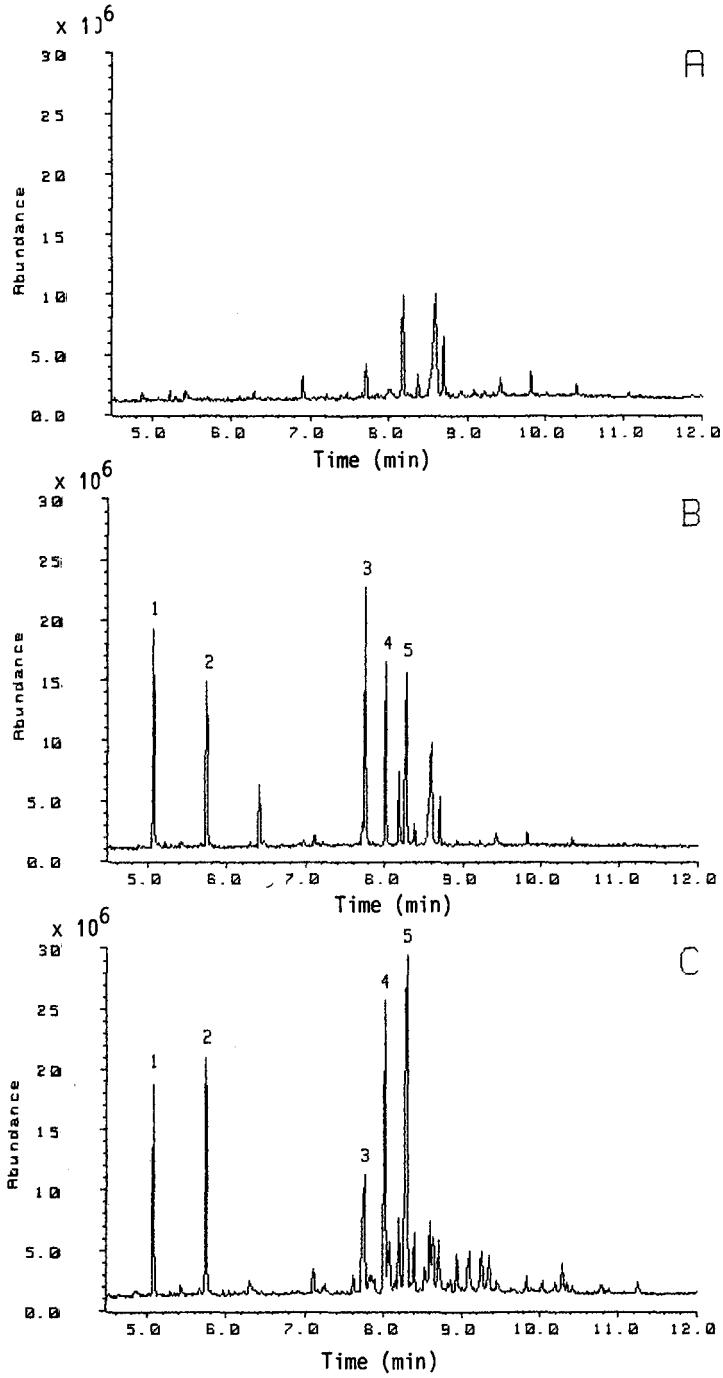

Fig. 2. Capillary gas chromatograms (MS, full scan): blank and spiked urine samples from a non-smoker (A,B); urine sample from a heavy smoker (C). Peaks: 1 = nicotine; 2 = N-ethylnornicotine; 3 = cotinine; 4 = N-ethylnorcotinine; 5 = *trans*-3′-hydroxycotinine.

linear regression analysis obtained from the five different concentrations of the three substances in blank urine, and all in duplicate, *versus* the peak area ratios yielded correlation coefficients, r^2, of 1.000 for THOC, 0.999 for nicotine and 1.000 for cotinine.

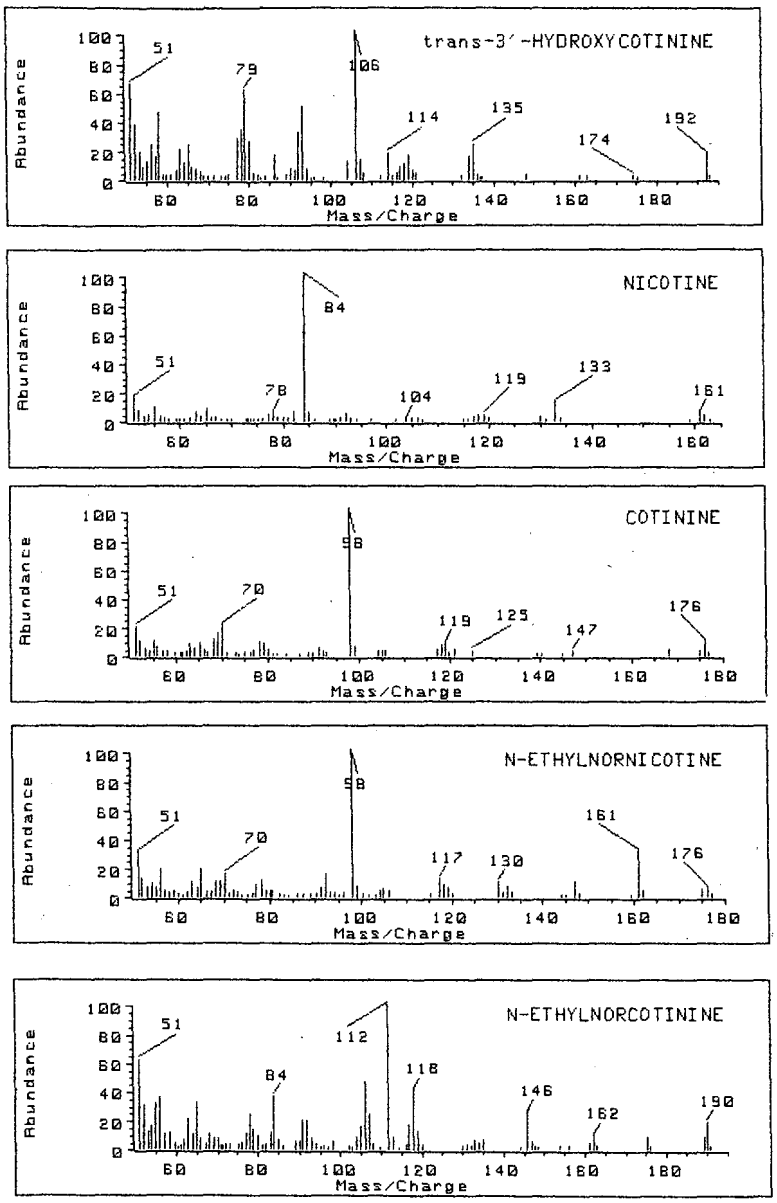

Fig. 3. Electron-impact mass spectra of *trans*-3'-hydroxycotinine, nicotine and cotinine, and of the internal standards N-ethylnornicotine and N-ethylnorcotinine. Mass spectra were obtained from the gas chromatogram of a urine sample from a heavy smoker (see Fig. 2).

An example of the method's application was the determination of nicotine and its aforementioned metabolites in the urine from an heavy smoker. The total ion current (TIC) chromatograms of blank and spiked urine samples from a non-smoker and the chromatogram of an urine sample of an heavy smoker are presented in Fig. 2. The concentrations of THOC, nicotine and cotinine were sufficiently high to operate the instrument in the full scan mode in order to identify the substances. The mass spectra of the three substances as well as those of the internal standards were obtained from the TIC chromatogram of the smoker's urine sample (see Fig. 3). They were identical with those obtained from the TIC chromatogram of a standard solution of the pure reference substances. A check of the peak purity did not indicate the presence of coeluting urinary compounds. The THOC, nicotine and cotinine concentrations in the smoker's urine were determined by GC–MS (SIM) after a ten-fold dilution of the sample in water (see Table I). The method has also been successfully used to determine THOC in urine from rats and hamsters.

Another application was the determination of the concentrations of THOC, nicotine and cotinine in the blood of a heavy smoker (see Table I). *n*-Butyl acetate, which was well suited for the extraction of THOC from urine samples, yielded poor recoveries when used to extract THOC from plasma or serum samples. Therefore, dichloromethane was used for such samples.

The linear regression analysis obtained from five different concentrations of the three substances in blank plasma *versus* the peak area ratios yielded correlation coefficients, r^2, of 0.985 for THOC, 0.999 for nicotine and 0.997 for cotinine. The SIM chromatograms of blank and spiked plasma samples from a non-smoker and the chromatogram of a plasma sample of a heavy smoker are presented in Fig. 4. The determinations performed on the plasma and serum obtained from the same blood sample of a heavy smoker yielded almost the same concentrations of THOC, nicotine and cotinine.

For urine samples, the overall recovery was 82% for THOC, 86% for nicotine and 81% for cotinine. To calculate the detection limits, blank samples were spiked with decreasing concentrations of the three compounds. When using NPD the limit of detection for THOC was 50 μg/l at a signal-to-noise ratio of *ca.* 10:1. With MS/SIM the limits of detection were 10 μg/l for THOC and cotinine, and 2 μg/l for nicotine at signal-to-noise ratios of *ca.* 3:1.

For blood samples the overall recovery was 49% for THOC, 77% for nicotine and 69% for cotinine. The limit of detection (MS/SIM) was 50 μg/l for THOC, 3 μg/l for nicotine and 10 μg/l for cotinine at signal-to-noise ratios of *ca.* 3:1.

TABLE I

CONCENTRATIONS OF NICOTINE, COTININE AND *trans*-3′-HYDROXYCOTININE (THOC) IN URINE AND PLASMA FROM A HEAVY SMOKER

Sample	*Concentration (μg/l)*		
	Nicotine	*Cotinine*	*THOC*
Urine	5000	2700	22 400
Plasma	8.7	194	209

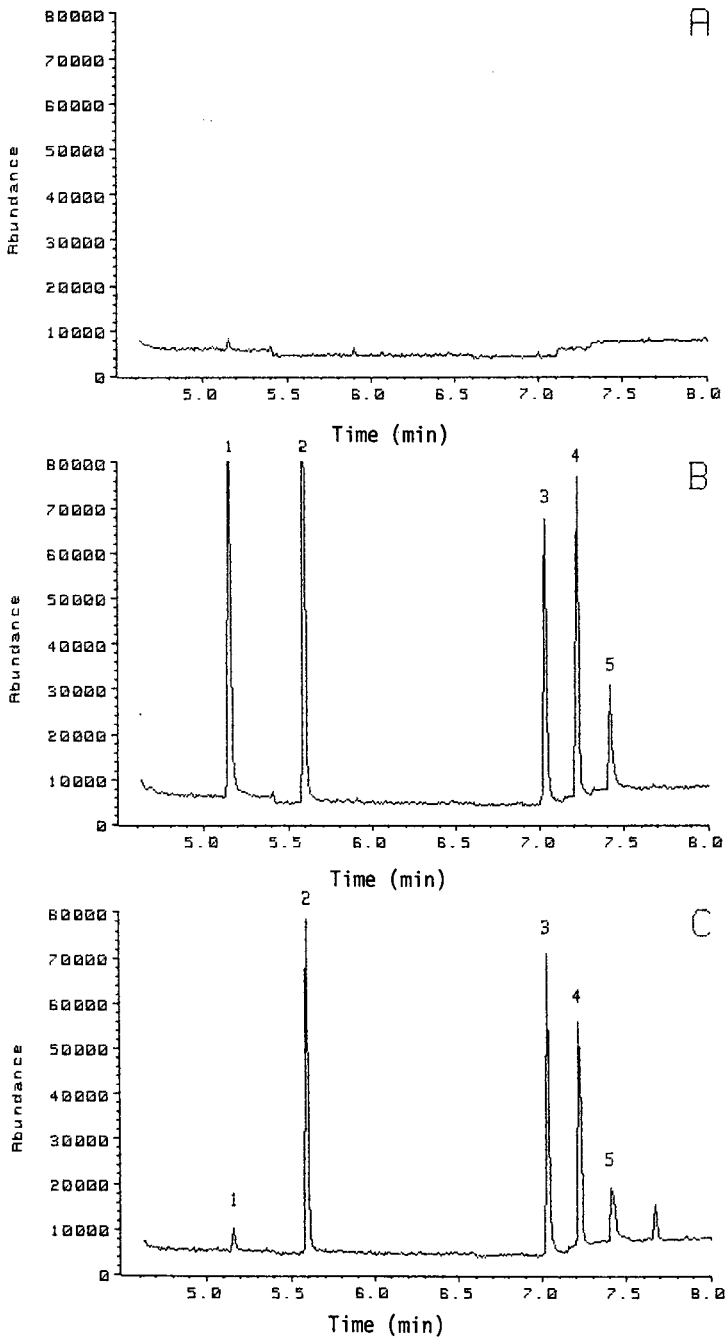

Fig. 4. Capillary gas chromatograms (MS, SIM): blank and spiked plasma samples from a non-smoker (A,B); plasma sample from a heavy smoker (C). Peaks: 1 = nicotine; 2 = N-ethylnornicotine; 3 = cotinine; 4 = N-ethylnorcotinine; 5 = *trans*-3′-hydroxycotinine.

The intra-assay coefficient of variation indicating the precision of the GC–MS method for urine samples was 7.3% for THOC at 280 μg/l, 4.0% for nicotine at 200 μg/l and 1.3% for cotinine at 550 μg/l. The intra-assay coefficient of variation indicating the accuracy of the method was 6.0% for THOC, 1.1% for nicotine and 0.7% for cotinine at the same concentrations as those used to calculate the precision. For blood samples, only the precision was checked. It was 3.0% for THOC at 200 μg/l, 9.5% for nicotine at 10 μg/l and 2.3% for cotinine at 200 μg/l.

The method described is simple and quick to perform. The main advantages are that only one extraction step is required and there is no need for derivatization and solvent exchange. The determination of THOC in urine using NPD was performed because an MS detector is not available in every laboratory. It has been demonstrated that nicotine and two of its major metabolites, cotinine and THOC, can be determined simultaneously from a single urine or blood extract in one GC analysis when using the MS detector.

REFERENCES

1 H. McKennis, L. B. Turnball, E. R. Bowman and E. Wada, *J. Am. Chem. Soc.*, 81 (1959) 3951.
2 H. McKennis, L. B. Turnball, S. L. Schwartz, E. Tamaki and E. R. Bowman, *J. Biol. Chem.*, 237 (1962) 541.
3 E. R. Bowman and H. McKennis, *J. Pharmacol. Exp. Ther.*, 135 (1962) 306.
4 H. McKennis, L. B. Turnball, E. R. Bowman and E. Tamaki, *J. Org. Chem.*, 28 (1963) 383.
5 E. Dagne and N. Castagnoli, *J. Med. Chem.*, 15 (1972) 356.
6 G. B. Neurath and F. G. Pein, *J. Chromatogr.*, 415 (1987) 400.
7 G. B. Neurath, M. Dünger, D. Orth and F. G. Pein, *Int. Arch. Occup. Environ. Health*, 59 (1987) 199.
8 P. Jacob, N. L. Benowitz and A. T. Shulgin, *Pharmacol. Biochem. Behav.*, 30 (1988) 249.
9 G. Scherer, L. Jarczyk, W.-D. Heller, A. Biber, G. B. Neurath and F. Adlkofer, *Klin. Wochenschr.*, 66 (1988) 5.
10 K. C. Cundy and P. A. Crooks, *Xenobiotica*, 17 (1987) 785.
11 G. A. Kyerematen, L. H. Taylor, J. D. deBethizy and E. S. Vesell, *J. Chromatogr.*, 419 (1987) 191.
12 S. O'Doharty, A. Revans, C. L. Smith and M. Cooke, *J. High Resolut. Chromatogr. Chromatogr. Commun.*, 11 (1988) 723.

Journal of Chromatography, 479 (1989) 419–423
Elsevier Science Publishers B.V., Amsterdam — Printed in The Netherlands

CHROM. 21 779

Note

Separation of the enantiomers of N-protected α-amino acids as anilide and 3,5-dimethylanilide derivatives

WILLIAM H. PIRKLE* and JOHN E. McCUNE
School of Chemical Sciences, University of Illinois, Box 44, Roger Adams Laboratory, 1209 West California Street, Urbana, IL 61801 (U.S.A.)
(Received June 13th, 1989)

Accelerated interest in synthetic peptides has led to an increased demand for a method to detect and quantitate minor amounts of enantiomeric impurity in the N-protected amino acids used to prepare these peptides[1–3]. Especially important is the question of the enantiomeric purity of these N-protected amino acids *after* activation of the C-terminal carboxyl group with peptide coupling reagents. Coupling of the carboxyl activated N-protected amino acid with a chiral reagent may lead to chromatographically separable diastereomers. However, it may be difficult to obtain (and verify the purity of) chiral reagents of 100% enantiomeric purity. Since, in these situations, one is normally looking for rather low levels of enantiomeric impurities, the determination of enantiomeric purity by the direct separation of enantiomers is inherently less prone to error than is the determination of the ratio of diastereomeric derivatives.

The enantiomers of chiral acids are frequently separated by high-performance liquid chromatography as amide derivatives on chiral stationary phases (CSPs). The enantiomers of anilide-type derivatives are consistently separable upon one or more of the π-acidic CSPs developed in these laboratories[4,5]. The separation of the enantiomers of anilide and 3,5-dimethylanilide derivatives of representative N-protected α-amino acids upon several commercially available π-acidic CSPs is discussed herein. The analytes were chromatographed on both covalently and ionically bonded CSPs (Fig. 1), derived from (*R*)-N-(3,5-dinitrobenzoyl)phenylglycine, (CSPs **1** and **2**) and (*S*)-N-(3,5-dinitrobenzoyl)leucine (CSPs **3** and **4**), using a mobile phase of 2-propanol in hexane, and, in the case of the covalent CSPs, also with methanol–water. While this paper focuses on the separation of enantiomers, such separations will

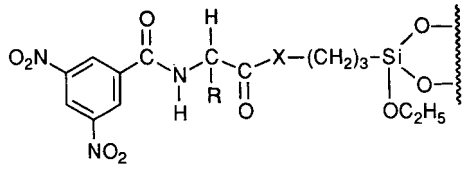

CSP	R	X
1	C_6H_5	NH
2	C_6H_5	$O^{-+}NH_3$
3	iso-C_4H_9	NH
4	iso-C_4H_9	$O^{-+}NH_3$

Fig. 1. CSPs derived from (*R*)-N-(3,5-dinitrobenzoyl)phenylglycine and (*S*)-N-(3,5-dinitrobenzoyl)leucine.

0021-9673/89/$03.50

clearly facilitate the study of the extent of racemization of N-protected amino acids activated with peptide coupling reagents.

EXPERIMENTAL

Chromatography was performed with an Anspec-Bischoff model 2200 isocratic HPLC pump, a Rheodyne Model 7125 injector with a 20-μl sample loop and a Milton Roy-LDC UV Monitor D® fixed-wavelength detector (254 nm). The chromatographic columns, 250 × 4.6 mm I.D. packed with modified 5-μm silica were obtained from Regis. The analog output from the detector was amplified by an external amplifier and converted to a digital signal by a MetraByte Crom-1 A/D® board, controlled by Labtech Acquire® software, installed in an IBM XT® personal computer. The data were analyzed by custom software written and compiled in Microsoft QuickBASIC®.

Generalized derivatization

The N-protected α-amino acids were formed by standard peptide synthesis methods[6].

Anilide derivatives were formed by allowing equal molar quantities of N-protected α-amino acid, aniline (or 3,5-dimethylaniline) and dicyclohexyl carbodiimide (DCC) to react in dichloromethane for 1 h followed by removal (filtration) of insoluble dicyclohexylurea (DCU). Residual DCU is present in the samples; however, DCU has little absorbance at 254 nm and does not interfere with the chromatographic analysis. In most cases the residual DCU prevented accurate determination of the melting points of the analytes. However ^{1}H NMR and mass spectral data are in accord with the assigned structures of the derivatives.

RESULTS AND DISCUSSION

Several α-amino acids (alanine, valine, leucine and phenylalanine) were N-protected with the benzyloxycarbonyl (CBZ), *tert.*-butyloxycarbonyl (BOC) and 9-fluorenylmethyloxycarbonyl (FMOC) protecting groups. These N-protected α-amino acids were subsequently derivatized with aniline and 3,5-dimethylaniline through the agency of DCC to give the corresponding anilides.

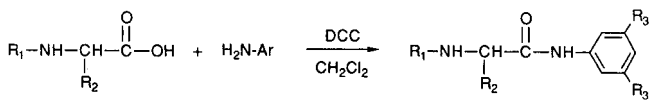

1 2 3

Chromatographic data for the normal-phase separation of the enantiomers of these α-amino acid derivatives on CSPs **1** and **3** are presented in Table I and for CSPs **2** and **4** in Table II. Reversed-phase chromatographic data on CSPs **1** and **3** are shown in Table III. All of the α-amino acid anilides chromatographed are separable on each CSP using 2-propanol in hexane as the mobile phase. The chromatographic separation factor, α, for the 3,5-dimethylanilides is larger than for the anilides in all cases. CSP **3** affords resolution suitable for accurate integration of the peaks of the

TABLE I

NORMAL-PHASE SEPARATION OF THE ANILIDE AND 3,5-DIMETHYLANILIDE DERIVATIVES OF N-PROTECTED α-AMINO ACIDS ON (*R*)-CSP **1** AND (*S*)-CSP **3**

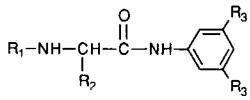

α = Chromatographic separation factor; R_s = r = resolution; k'_1 = capacity factor for the first eluted enantiomer using 2-propanol–hexane (5:95, v/v) as the mobile phase; flow-rate 2 ml/min.

Compound	R_1	R_2	R_3	*CSP 1*			*CSP 3*		
				α	R_s	k'_1	α	R_s	k'_1
3a	FMOC	CH_3	CH_3	1.49	2.78	18.53	2.35	4.36	13.85
3b	FMOC	CH_3	H	1.44	2.44	17.98	2.12	3.72	14.97
3c	FMOC	iso-C_3H_7	CH_3	1.66[a]	3.55	8.50	2.45[b]	3.97	6.97
3d	FMOC	iso-C_3H_7	H	1.50[a]	2.86	8.47	2.03[b]	3.57	7.35
3e	FMOC	iso-C_4H_9	CH_3	1.70	3.97	8.60	3.19	5.44	6.55
3f	FMOC	iso-C_4H_9	H	1.57	3.42	8.59	2.80	4.94	6.94
3g	FMOC	C_6H_5CO	CH_3	1.83	3.95	19.35	2.23	3.69	15.84
3h	FMOC	C_6H_5CO	H	1.68	3.64	18.12	1.99	3.40	16.38
3i	BOC	CH_3	CH_3	1.34	2.23	3.64	1.61	2.70	3.74
3j	BOC	CH_3	H	1.28	1.87	3.25	1.47	2.32	3.46
3k	BOC	iso-C_3H_7	CH_3	1.48	2.88	1.59	1.75	2.84	1.74
3l	BOC	iso-C_3H_7	H	1.38	2.27	1.55	1.59	2.37	1.77
3m	BOC	iso-C_4H_9	CH_3	1.52[a]	3.11	1.75	2.18[b]	3.90	1.87
3n	BOC	iso-C_4H_9	H	1.43	2.82	1.67	1.98	3.90	1.85
3o	BOC	C_6H_5CO	CH_3	1.56	3.51	3.86	1.62	2.58	4.40
3p	BOC	C_6H_5CO	H	1.48	3.30	3.62	1.55	2.54	4.27
3q	CBZ	CH_3	CH_3	1.37	2.53	14.25	2.14	4.49	14.73
3r	CBZ	CH_3	H	1.33	2.27	12.52	1.94	3.86	13.42
3s	CBZ	iso-C_3H_7	CH_3	1.55	3.46	6.26	2.13	4.22	6.51
3t	CBZ	iso-C_3H_7	H	1.44	3.00	5.96	1.88	3.82	7.02
3u	CBZ	iso-C_4H_9	CH_3	1.62	3.81	6.60	2.81	5.71	6.66
3v	CBZ	iso-C_4H_9	H	1.52	3.51	6.19	2.52	5.52	6.56
3w	CBZ	C_6H_5CO	CH_3	1.57	3.45	14.17	1.83	3.12	17.38
3x	CBZ	C_6H_5CO	H	1.53	3.21	13.65	1.66	2.82	17.79

[a] The (*R*)-enantiomer is most retained.
[b] The (*S*)-enantiomer is most retained.

enantiomers for all derivatives using 2-propanol in hexane and for all but the BOC derivatives using the reverse mobile phase. In all cases surveyed, the homochiral diasteromeric adsorbate (*R,R* or *S,S*) is the more stable. That is, the absolute configuration of the most retained enantiomer is the same as that of the CSP. While an explicit statement of the mechanism of chiral recognition must await further study, preliminary data suggests that a face to face approach of the analyte and CSP occurs as a consequence of π–π and dipole stacking interactions. The more stable of the diastereomeric adsorbates is the one having the bulky substituents on the stereogenic centers of the CSP and analyte external to the stack[7].

TABLE II

NORMAL-PHASE SEPARATION OF THE ANILIDE AND 3,5-DIMETHYLANILIDE DERIVATIVES OF N-PROTECTED α-AMINO ACIDS ON (*R*)-CSP **2** AND (*S*)-CSP **4**

For structural formula and symbol definitions, see Table I

Compound	*CSP 2*			*CSP 4*		
	α	*R*	k'_1	α	R_s	k'_1
3a	1.64	2.79	3.85	2.52	4.87	2.43
3b	1.49	2.25	4.39	2.26	4.61	2.77
3c	1.51[a]	2.49	1.44	2.10[b]	3.87	0.90
3d	1.32[a]	1.84	1.74	1.81[b]	3.33	1.13
3e	1.41	2.29	1.41	2.26	4.75	0.92
3f	1.26	1.60	1.75	2.01	4.31	1.14
3g	1.61	2.98	3.00	2.23	4.30	1.77
3h	1.45	2.46	3.52	1.99	3.92	2.20
3i	1.38	1.87	0.97	2.11	3.91	0.75
3j	1.29	1.69	1.09	1.91	3.61	0.84
3k	1.35	1.47	0.34	1.87	2.56	0.26
3l	1.21	1.01	0.43	1.66	2.23	0.34
3m	1.25[a]	1.05	0.35	1.94[b]	2.86	0.28
3n	1.18	1.20	0.42	1.78	2.73	0.35
3o	1.38	1.96	0.79	1.91	3.19	0.59
3p	1.29	1.66	0.93	1.77	3.36	0.73
3q	1.59	2.81	3.40	2.55	5.19	2.51
3r	1.46	2.39	3.72	2.35	4.74	2.80
3s	1.51	2.37	1.18	2.26	4.43	0.89
3t	1.33	1.82	1.40	1.97	3.80	1.06
3u	1.37	2.08	1.15	2.47	4.73	0.91
3v	1.26	1.59	1.38	2.22	4.36	1.12
3w	1.51	2.66	2.58	2.39	4.05	1.87
3x	1.39	2.32	2.94	2.17	4.05	2.28

[a] The (*R*)-enantiomer is most retained.
[b] The (*S*)-enantiomer is most retained.

CONCLUSION

The enantiomers of the 3,5-dimethylanilide and anilide derivatives of N-protected α-amino acids are readily separated on both covalently and ionically bonded α-acidic CSPs derived from phenylglycine and leucine. Proper selection of CSP and mobile phase will afford resolution sufficient for quantitation of enantiomeric excesses by integration for all analytes discussed. While the data presented herein is by no means an exhaustive survey of all α-amino acids of potential interest, the methods discussed should be readily extended to other N-protected α-amino acids. The wide spread availibility, chromatographic efficiency and the ability to use both normal and reversed phase eluents make the CSPs discussed especially attractive for these analyses.

TABLE III

REVERSED-PHASE SEPARATION OF THE ANILIDE AND 3,5-DIMETHYLANILIDE DERIVATIVES OF N-PROTECTED α-AMINO ACIDS ON (*R*)-CSP **1** AND (*S*)-CSP **3**

For structural formula and symbol definitions, see Table I, except k_1' = capacity factor for the first eluted enantiomer using water–methanol (10:90) as the mobile phase; flow-rate 2 ml/min.

Compound	*CSP 1*			*CSP 3*		
	α	*R*	k_1'	α	R_s	k_1'
3a	1.35	3.89	3.01	1.69	5.67	1.67
3b	1.19	2.25	2.14	1.42	3.43	1.15
3c	1.40[a]	4.26	2.72	1.70[b]	5.74	1.52
3d	1.22[a]	2.42	2.05	1.39[b]	3.13	1.14
3e	1.41	4.29	2.82	1.90	7.01	1.66
3f	1.23	2.61	2.12	1.55	4.35	1.18
3g	1.53	5.90	3.94	1.70	6.18	2.15
3h	1.31	3.51	2.92	1.43	3.70	1.57
3i	1.13	1.07	0.81	1.30	1.62	0.49
3j	1.00	0.00	0.68	1.19	≈0.00	0.33
3k	1.17	1.35	0.76	1.34	1.77	0.46
3l	1.08	≈0.00	0.62	1.18	0.72	0.34
3m	1.19[a]	1.42	0.80	1.44[b]	2.42	0.50
3n	1.09	≈0.00	0.64	1.26	1.14	0.36
3o	1.27	2.34	1.08	1.36	2.43	0.66
3p	1.14	1.16	0.84	1.21	1.16	0.47
3q	1.22	2.26	1.40	1.57	4.11	0.80
3r	1.12	1.13	1.01	1.34	2.15	0.55
3s	1.28	2.63	1.26	1.61	4.06	0.75
3t	1.16	1.35	0.97	1.34	2.15	0.55
3u	1.30	2.82	1.32	1.80	5.20	0.82
3v	1.16	1.48	1.00	1.51	3.10	0.57
3w	1.39	3.86	1.86	1.59	4.34	1.08
3x	1.22	2.24	1.38	1.35	2.67	0.78

[a] The (*R*)-enantiomer is most retained.
[b] The (*S*)-enantiomer is most retained.

ACKNOWLEDGEMENTS

This work was partially supported by grants from the National Science Foundation and the Eli Lilly Company. Preliminary investigations of these systems were conducted by Daniel S. Reno and Kristal Ball at the University of Illinois.

REFERENCES

1 J. Maibaum and D. H. Rich, *J. Org. Chem.*, 53 (1988) 869.
2 Y. Okamoto, R. Aburatnani, Y. Kaida and K. Hatada, *Chem. Lett.*, (1988) 1125.
3 S. Görög, B. Herényi and M. Löw, *J. Chromatogr.*, 353 (1986) 417.
4 W. H. Pirkle and J. E. McCune, *J. Chromatogr.*, 469 (1989) 67.
5 W. H. Pirkle and J. E. McCune, *J. Chromatogr.*, 471 (1989) 271.
6 M. Bodansky and A. Bodansky, *The Practice of Peptide Synthesis*, Springer, New York, 1984.
7 D. S. Reno, *Ph.D. Thesis*, University of Illinois, Urbana, IL, 1987.

Journal of Chromatography, 479 (1989) 424–429
Elsevier Science Publishers B.V., Amsterdam — Printed in The Netherlands

CHROM. 21 728

Note

Determination of ethirimol, in the presence of some normal soil constituents, by liquid chromatography

F. SÁNCHEZ-RASERO*, T. E. ROMERO and C. G. DIOS
Estación Experimental del Zaidín, C.S.I.C., Profesor Albareda, 1, 18008 Granada (Spain)
(First received April 10th, 1989; revised manuscript received June 22nd, 1989)

Ethirimol is the ISO common name for 5-butyl-2-ethylamino-6-methylpyrimidin-4-ol. It is a systemic fungicide, effective in controlling mildew in cereals and grasses. Its solubility in water is about 200 ppm.

Ethirimol interactions[1], degradation[2] and distribution[3] in soil have already been studied. Nevertheless, it is interesting to know the adsorption–desorption mechanism of this fungicide on kaolinite, montmorillonite and peat in order to be able to predict its behaviour in different soils and in the environment.

Determinations of ethirimol have been done by gas–liquid chromatography (GLC) of a methyl derivative using a nitrogen-selective thermoionic detector[4] but the method is time consuming and not appropriate for measuring in aqueous phases. Ethirimol has also been determined by liquid scintillation counting [1,2] and direct UV analysis[1] but the isotopic technique does not distinguish between entire and degraded molecules and many substances interfere in the direct UV analysis.

A method is presented in this paper that avoids all those inconveniences.

EXPERIMENTAL

Apparatus

An Hewlett-Packard 1090 liquid chromatograph, equipped with a diode array detector and DPU multichannel integrator, as described in a previous paper[5] was used. The column (Hewlett-Packard 799160D-552) was 100 mm × 2.1 mm I.D., stainless steel, packed with ODS-Hypersil (5 μm).

The Millex filters (Millipore, Bedford, MA, U.S.A.) used were Type HV_4, 4 mm, pore size 0.45 μm.

Soil constituents

Kaolinite from Lage (Spain), montmorillonite from Almería (Spain) and peat from Padul (Spain) were used.

Reagents

Methanol, high-performance liquid chromatography (HPLC) quality, was obtained from Panreac (Madrid, Spain). Water was purified with a Milli-Q water purification system. The eluent was methanol–water (80:20). Ethirimol, as an analytical standard of known purity (98.4%), was obtained from ICI (Yalding, U.K.).

0021-9673/89/$03.50

Calibration solutions

First a solution of an ethirimol standard in water was prepared at $7.26 \cdot 10^{-2}$ g/l and four more solutions were prepared by dilution in water at $4.356 \cdot 10^{-2}$, $1.452 \cdot 10^{-2}$, $0.8712 \cdot 10^{-2}$ and $0.2904 \cdot 10^{-2}$ g/l.

Sample solutions

Approximately 1.0 g of the soil constituent was weighed (to the nearest 0.1 mg). A 20-ml volume of an ethirimol solution at a concentration within the range $0.2904 \cdot 10^{-2}$–$7.26 \cdot 10^{-2}$ g/l was added and shaken mechanically for X min (the time necessary for the study on adsorption–desorption). The solution was then centrifuged at 12 062 *g* for 20 min and an aliquot of the supernatant was filtered through a Millex HV_4 filter into a small vial fitted with a cap.

Chromatography

The chromatographic conditions were as follows: flow-rate, 0.2 ml/min; column temperature, 40°C; wavelength readings at 225 ± 2 nm *vs.* 450 ± 25 nm, and simultaneously at 297 ± 2 nm *vs.* 450 ± 25 nm; range, automatic; injection volume, 2 µl; spectra from the peak, upslope, apex and downslope; stop time, 2.1 min.

Calibration graph

The calibration graph, see Fig. 1, was constructed with computer software, by the quadratic method, from triplicate injections of the five calibration solutions. Taking into account the low solubility of ethirimol in water (200 ppm), a wider range of concentrations is not feasible.

Quantitation

Triplicate injections of each sample solution were made and the results directly obtained in $g/l \cdot 10^{-2}$.

RESULTS AND DISCUSSION

The linear calibration graph (Fig. 1) shows that Beer's law is followed at the tested concentrations.

Fig. 2 shows the chromatography of (a) a kaolinite–ethirimol sample, of (b) a

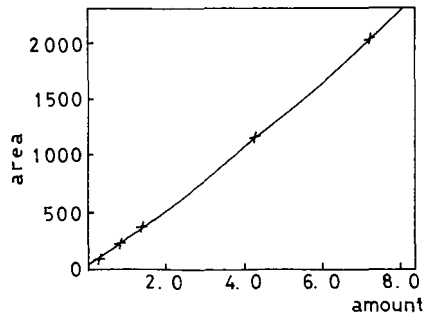

Fig. 1. Calibration graph for ethirimol.

montmorillonite-ethirimol sample and of (c) a peat–ethirimol sample in real time. In the three cases the separation of ethirimol from impurities seems to be adequate, taking into account not only that no peak was observed at the ethirimol retention time when no spiked samples of kaolinite, montmorillonite and peat were chromatographed under the same conditions, but also the purity of the ethirimol peak as will be demonstrated below.

Fig. 3 shows the replots of the previous chromatograms (a), (b) and (c), with special annotation: (d), (e) and (f), where baselines, retention times, tick marks and hatched shadings of integrated areas are shown. This is an adventage of the chromatograph used and reveals just how correct the integration process is. On the other hand, it shows how the information obtained in a chromatographic development can be used for further calculations and/or representations without repeating the chromatographic steps.

Fig. 4, the signal plus spectra plot of the same chromatogram (c, Fig. 1), shows the purity of the chromatographic peak. To do this, the detector performs three scans at three points (times) in every chromatographic peak: prior to, at and after every maximum. These spectrochromatograms are shown separately (1–3) and overlaid (4) (upper left, Fig. 4). If the three spectra are similar, the peak corresponds to a pure substance, in this case, ethirimol. This demonstration of the purity of a chromatographic peak is possible only with the use of a diode array detector. The identical shape of the spectrum for the analytical standard and an unknown sample is a confirmatory test of identity.

The ethirimol spectrum shows a maximum absorbance at 225 nm and another at 297 nm which are the two wavelengths chosen for simultaneous integration. Fig. 5 shows the ratio of the signals obtained at these two wavelenghts *vs.* time for the ethirimol peak shown in chromatogram (c), Fig. 2. The linear relationship is a second demonstration of peak purity and is another advantage of the diode array detector and the multichannel integrator.

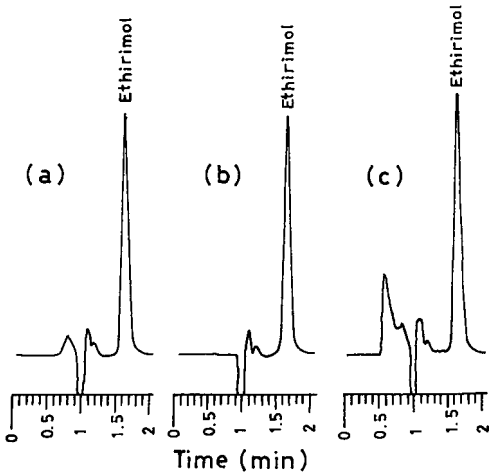

Fig. 2. Chromatography of (a) a kaolinite–ethirimol sample, (b) a montmorillonite–ethirimol sample and (c) a peat–ethirimol sample in real time.

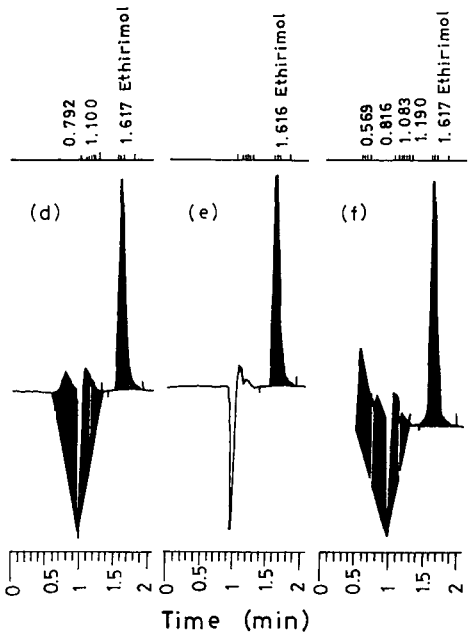

Fig. 3. Replots (d), (e) and (f) of the chromatograms in Fig. 2a, b and c, respectively.

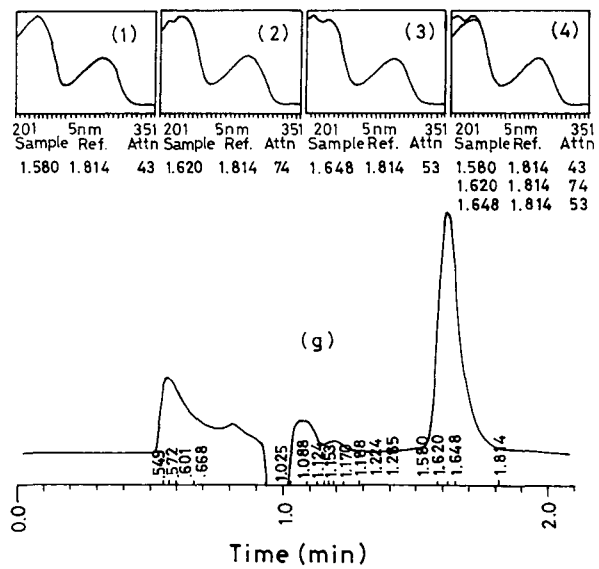

Fig. 4. Signal plus spectra plot of the chromatogram in Fig. 2c. (g) chromatographic signal; (1), (2) and (3) spectrochromatograms of the ethirimol peak, prior to, at and after its absorption maximum; (4) the three previous spectrochromatograms overlaid.

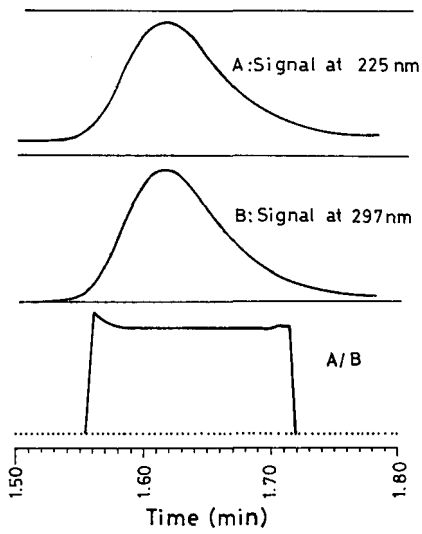

Fig. 5. Ratio of signals in the chromatogram in Fig. 2c between 1.5 and 1.8 min.

The standard addition technique was used to test the ability of the HPLC system to accurately determine added ethirimol in a peat–ethirimol supernatant. Five 2-ml aliquots of a peat–ethirimol supernatant at a concentration of $5.5185 \cdot 10^{-2}$ g/l were added with 0, 1, 2, 3 and 4 ml of an ethirimol solution at a concentration of $11.037 \cdot 10^{-2}$ g/l and 4, 3, 2, 1 and 0 ml of water respectively. The detector response to ethirimol in the presence of coextracted constituents of the peat soil ranged from 97.68 to 104.35% of theoretical. Details are given in Table I. A peat–ethirimol sample was chosen for this experiment because peat extracts are dirtier than those of kaolinite and montmorillonite, as is seen in Fig. 2.

The relative standard deviations for nine repeated injections of two ethirimol samples at $1.96 \cdot 10^{-2}$ and $7.42 \cdot 10^{-2}$ g/l were respectively $S_r = 3.28$ and 0.40.

The detection limit was 0.4 ng of ethirimol, equivalent to 2 μl of a solution at a concentration of $0.02 \cdot 10^{-2}$ g/l.

TABLE I

RECOVERY FOR ETHIRIMOL

C.L. = Confidence limit ($P = 0.05$).

Ethirimol added (ng/2 µl)	*Ethirimol found (ng/2 µl ± C.L.)*	*Response (%)*	S_r[a]
36.79	38.39 ± 2.01	104.35	1.22
73.58	74.55 ± 2.72	101.32	0.85
110.37	110.04 ± 2.49	99.70	0.53
147.16	143.75 ± 2.89	97.68	0.47

[a] Relative standard deviation for three determinations.

The method described is specific, accurate and precise and it presents a detection limit comparable to that of the Edwards method[4] using GLC with nitrogen-selective thermoionic detection. Other advantages of this method, due to the use of a microbore column, a diode array detector and a multichannel integrator are an enormous saving in operating costs, valuable information on the integration process and different tests of the purity or otherwise of every chromatographic peak.

In view of the limited solubility of ethirimol in water, 200 ppm, the concentration range studied, $(0.2904–7.26) \cdot 10^{-2}$ g/l, is the most suitable for adsorption–desorption studies of ethirimol on soil and soil constituents.

ACKNOWLEDGEMENTS

We gratefully acknowledge support for this work from grant PR84-0160-C04-02 from the Comision Asesora de Investigación Cientifica y Técnica (CAICYT). The valuable technical assistance of M^{a}.D. Maroto is gratefully acknowledged.

REFERENCES

1 I. J. Graham-Bryce and J. Coutts, *Proc. 6th Br. Insectic. Fungic. Conf.* (1971) 419.
2 I. R. Hill and D. J. Arnold, *Proc. 7th Br. Insectic. Fungic. Conf.*, (1973) 47.
3 G. F. Collier, I. J. Graham-Brice, B. A. G. Knight and J. Coutts, *Pestic. Sci.*, 10 (1979) 50.
4 M. J. Edwards, in *Analytical Methods for Pesticides and Plant Growth Regulators*, Vol. 8, Academic Press, New York, (1976), p. 291.
5 F. Sánchez-Rasero and A. Peña-Heras, *J. Assoc. Off. Anal. Chem.*, 71 (1988) 1064.

Journal of Chromatography, 479 (1989) 430–436
Elsevier Science Publishers B.V., Amsterdam — Printed in The Netherlands

CHROM. 21 762

Note

Analyse par chromatographie liquide haute performance ultra-rapide de la théophylline et de l'anisate de sodium (ou de potassium) dans différentes préparations pharmaceutiques

J. THOMAS
Laboratoire de chimie, Faculté des Sciences et Techniques, Parc de Grandmont, Tours 37200 (France)
(Reçu le 7 mars 1989: manuscrit modifié reçu le 23 juin 1989)

L'analyse de la théophylline, bronchodilatateur traitant l'asthme[1], peut être réalisée dans divers milieux selon certaines techniques[2]. De très nombreux travaux du domaine biomédical utilisent la chromatographie liquide haute performance (CLHP) pour la doser, ainsi par rapport à la méthode bien connue d'Orcutt *et al.*[3] certaines méthodes innovatrices[4–14] ont été décrites au cours de ces dix dernières années. Plutôt rares sont de telles applications dans le domaine pharmaceutique[15–17], bien que la CLHP soit une technique pouvant être sûre et très rapide convenant alors aux analyses de médicaments réalisées en grandes séries.

Dans cette optique, nous avons eu à doser simultanément la théophylline avec l'anisate de sodium (ou de potassium) dans des formes pharmaceutiques variées et plus ou moins complexes. Une seule méthode[18], du domaine biomédical, décrit l'analyse de ces deux composés. D'une part le temps d'analyse y est trop long: 6 min, et d'autre part elle n'offre pas de garantie de reproductibilité de sélectivité. En effet, le pH est tel que l'acide anisique est partiellement ionisé, or nous avons constaté que de petites erreurs de calibration du pH-mètre entraînent des variations de rétention de ce composé pouvant conduire à l'interférence, voire la coélution, avec la théophylline. Parmi les méthodes originales citées, celles utilisant le partage avec polarités de phases inversées en mode isocratique sont les plus aptes à procurer reproductibilité et gain de temps, or aucune d'elles n'est satisfaisante. En effet, dans certaines[9,10,13,16] le pH utilisé ionise partiellement l'un de nos composés à doser, et le temps d'analyse est en outre trop long. Du point de vue vitesse[19], l'analyse peut être rapide[14,17], à très grande vitesse[6], voire à super vitesse[7]. Mais alors elle utilise un pH qui a l'inconvénient décrit précédemment avec, soit une phase mobile beaucoup trop éluante[14,17] s'accompagnant d'une traînée de pic[17] ou associée à une phase stationnaire trop faiblement sélective[14] vis-à-vis de nos composés, soit un matériel peu courant car spécifique à la micro-CLHP[7]. Si le pH est approprié[11], l'analyse est trop longue. Enfin, la phase mobile peut être trop agressive rendant la méthode[8,12,15] difficilement utilisable en routine, avec en outre un temps d'analyse beaucoup trop long. Nous avons donc été conduits à présenter une nouvelle méthode isocratique ultra-rapide de dosage de la théophylline et de l'anisate dans diverses formes pharmaceutiques avec le souci d'offrir une excellente reproductibilité, de sélectivité notamment, obtenue dans des conditions très douces, excluant toute interférence avec les constituants des matrices, et utilisant du matériel courant.

0021-9673/89/$03.50

PARTIE EXPÉRIMENTALE

Appareillage

Le système comprend: une pompe (Beckman, San Ramon, CA, États-Unis) Modèle 114M, un détecteur UV (Merck, Darmstadt, R.F.A.) Modèle 655 A à longueur d'onde variable et équipé d'une cellule semi-micro de 2,4 μl, un injecteur (Valco, Houston, TX, États-Unis) Modèle C6W avec une boucle à échantillon de 5 μl, et un enregistreur (Kipp & Zonen, Delft, Hollande). La colonne en acier inox de 4 cm × 0,46 cm I.D., est garnie de Spherisorb ODS 2, 3 μm (Phase Separations, Norwalk, CT, États-Unis). En amont de cette colonne est placé un filtre (Rheodyne, Berkeley, CA, États-Unis) dont le fritté a pour porosité 0,5 μm. Les tubes de connexion ont 0,15 mm (0,006 in.) pour diamètre interne et ils ont pour longueur: 4 cm entre l'injecteur et le filtre, 4 cm entre ce dernier et l'entrée de colonne, et 10 cm entre la sortie de colonne et le support de cellule. Le détecteur travaille avec un temps de réponse rapide: 0,35 s pour ne pas perdre l'efficacité[20,21] vis-à-vis du composé le moins retenu.

Solvants, réactifs et éluant

L'eau provient d'un système Milli-Q (Millipore, Bedford, MA, États-Unis). L'acétonitrile (Carlo Erba, Milan, Italie) est de qualité CLHP. Le dihydrogénophosphate de potassium, K_2HPO_4, et l'acide orthophosphorique ont la qualité "pour analyses". L'acide *n*-hexanoique est distillé avant emploi. L'acide anisique (Aldrich, Steinheim, R.F.A.), la théophyllinne et la β-hydroxypropylthéophylline (Sigma, St. Louis, MO, États-Unis) ont été recristallisés avant emploi.

La phase aqueuse tamponnée contenant l'acide *n*-hexanoique 0,006 *M* est préparée juste avant emploi: on mélange l'acide *n*-hexanoique avec une solution aqueuse 0,01 *M* en K_2HPO_4; le pH est ensuite ajusté à 6,60 par addition de H_3PO_4 dilué, et cette phase aqueuse est filtrée à travers une membrane (Millipore) ayant une porosité de 0,45 μm. L'acétonitrile est filtré sur membrane de 0,2 μm par le fabricant.

L'éluant est ajusté à la composition: phase aqueuse précédente–acétonitrile (86:14, v/v). Le dégazage se fait par un énergique barbotage d'hélium avant équilibration du système, puis en continu à un plus faible débit durant l'équilibration et les analyses.

Préparation des échantillons

Tout échantillon est amené à la même composition que celle de la phase mobile de façon à éliminer les artefacts du détecteur[22], et est filtré avant l'injection à travers une membrane de cellulose régénérée (Sartorius, Göttingen, R.F.A.) de porosité 0,2 μm.

Solutions standards

Chaque solution standard est préparée de façon à avoir, pour les constituants à doser, la même composition en poids que celle indiquée pour l'échantillon pratique correspondant.

Echantillons pratiques (Théophylline Bruneau).

Ampoule injectable. Le contenu d'une ampoule est versé dans une fiole jaugée de

1000 ml et l'on complète avec de l'eau pure. On prélève 1 ml que l'on mélange avec: 0,8 ml d'acétonitrile, 16,2 ml de phase aqueuse tamponnée contenant *n*-$C_5H_{11}COOH$, et 2 ml de solution à 0,2 g l^{-1} de β-hydroxypropylthéophylline dans l'acétonitrile. Temps total de préparation (échantillon prêt pour l'injection) t = moins de 2 min.

Suppositoire. Un suppositoire est introduit dans un erlen de 500 ml, puis fondu dans environ 100 ml d'eau pure à 70°C. Après agitation vigoureuse, refroidissement dans la glace et filtration sur Büchner, le filtrat est versé dans une fiole jaugée de 1000 ml (si le suppositoire est pour adultes), et l'on complète avec de l'eau pure. Sur 1 ml de cette solution, on effectue les mêmes opérations que celles décrites avec l'*Ampoule injectable.* t = 7 min, dont 6 min pour l'extraction.

Comprimés dragéifiés (avec et sans butobarbital). Un comprimé dragéifié est écrasé, puis introduit dans un erlen de 250 ml. Après agitation avec de l'eau pure froide, on filtre sur Büchner. Après lavage du filtre, le filtrat est versé dans une fiole jaugée (respectivement de 500 et de 250 ml pour les comprimés sans et avec butobarbital), et on complète avec de l'eau. Avec 1 ml on procède ensuite comme avec l'*Ampoule injectable.* t = 7 min, dont 6 min pour l'extraction.

Sirop. On mesure 10 ml de sirop que l'on introduit dans une fiole jaugée de 500 ml. On complète avec de l'eau pure. On prélève 1 ml et l'on procède comme avec l'*Ampoule injectable.* t = moins de 2 min.

Remarque: tous les prélèvements sont effectués à l'aide d'une batterie de Pipetman permettant, après éventuelle extraction, de préparer très rapidement l'échantillon pour l'injection dans le chromatographe.

RÉSULTATS ET DISCUSSION

Etant très répandue, bon marché, et existant en diverses tailles de granulométrie, la Spherisorb ODS-2 a été choisie comme phase stationnaire.

A pH 6,60 la théophylline (pK_a = 8,8; pK_b = 13,7) est sous forme neutre, tandis que l'acide anisique (pK_a = 4,5) est pratiquement totalement ionisé. Ainsi, à cette valeur de pH nous avons vérifié que de petites erreurs de calibration du pH-mètre n'ont aucune influence sur les rétentions de ces composés, rendant invariante la résolution, R_s, notamment quand on donne à celle-ci des valeurs faibles.

Une phase mobile peu éluante [tampon aqueux, pH 6,60–acétonitrile (93:7)] parcourant une colonne (15 cm de long) remplie de Spherisorb ODS-2, 5 μm, a d'abord été utilisée pour s'assurer qu'aucune interférence n'existe entre les composés à doser, l'étalon et les constituants des matrices des formulations les plus complexes. On a alors observé une traînée de pic (A_e = 4,0) de l'anisate. Il a été montré que sur Spherisorb ODS-2 des interactions silanophiles se produisent avec les solutés basiques[23]. Avec l'ion anisate, l'échange d'ions ne peut intervenir. Quant à l'adsorption par liaison H sur des silanols résiduels acides, elle ne peut être la cause majeure de cette traînée. En effet, dans les mêmes conditions d'analyse une bien moindre traînée de pic (A_s = 2,0) est obtenue avec l'aniline pratiquement à l'état neutre, sensiblement de même encombrement stérique que l'ion anisate et de même basicité (pK_b = 9,5).

L'introduction dans la phase mobile d'acide hexanoique (pK_a = 4,9) essentiellement sous forme ionisée, procure à l'ion anisate une bonne symétrie de pic (A_s = 1,1). En outre, la sélectivité avec la théophylline est augmentée car le temps de réten-

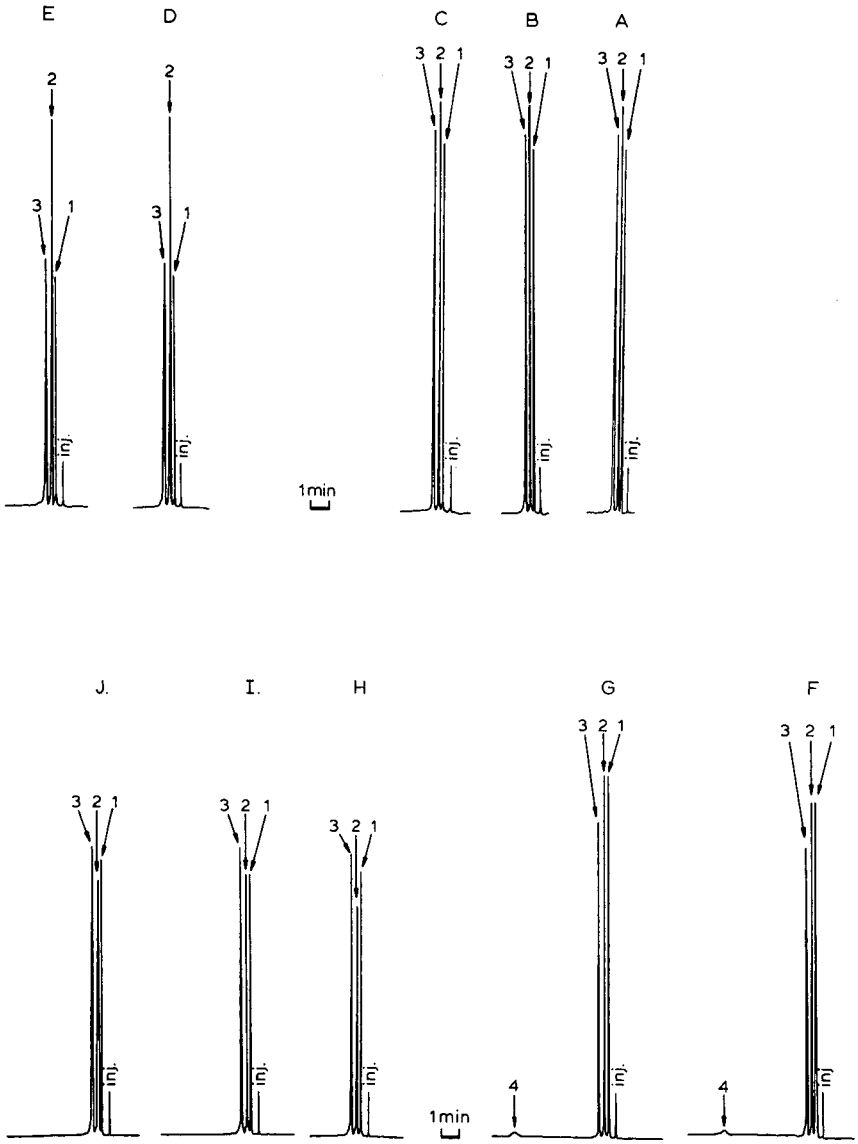

Fig. 1. Chromatogrammes types en CLHP ultra-rapide de solutions standards et d'échantillons pratiques. (A) une solution standard pour les ampoules injectables; (B) un échantillon d'ampoule pour injection par voie intraveineuse ou intramusculaire; (C) un échantillon comme le précédent, mais après 150 injections sur la même colonne; (D) une solution standard pour suppositoires; (E) un échantillon d'extrait de suppositoires pour adulte; (F) une solution standard pour sirop; (G) un échantillon de sirop; (H) une solution standard pour les comprimés dragéifiés; (I) un échantillon d'extrait de comprimé dragéifié; (J) un échantillon d'extrait de comprimé dragéifié contenant du butobarbital. Conditions: colonne, 4 cm × 0,46 cm I.D., remplie de Spherisorb ODS 2 (3 μm); phase mobile, tampon aqueux (pH = 6,60) contenant l'acide *n*-hexanoique (0,006 *M*)–acétonitrile (86:14, v/v); débit 1 ml min^{-1}; pression, 41 bar; détection, A, B et C: 277,5 nm, D et E: 272 nm, F, G, H, I et J: 276 mm; sensibilité, 0,04 u.a.; vitesse de l'enregistreur, 5 nm min^{-1}; température, 20 ± 2°C; pics, 1 = anisate, 2 = théophylline, 3 = β-hydroxypropylthéophylline, 4 = hydroxy-4 benzoate de méthyle.

tion de l'anisate est diminué, devenant très proche du temps "mort". Ce qui nous fait dire qu'en présence de l'ion hexanoate un mécanisme s'apparentant à l'exclusion d'ions[24,25] est susceptible d'intervenir, au moins partiellement.

Notons que cet additif, moyennement hydrophobe, est éliminé facilement de la colonne en fin de manipulation.

Réalisée ensuite sur une colonne de 4 cm de long remplie de particules de 3 μm, la séparation optimisée des composants des différents échantillons contenant l'étalon interne, est représentée sur la Fig. 1.

Sauf pour le sirop, les séparations sont réalisées en moins de 70 s en présence de l'étalon interne. Et comme nous avons, à dessein, sélectionné ce dernier notamment pour sa rétention supérieure à celles des composés à doser, l'analyse est achevée en moins de 50 s si la méthode de l'étalonnage externe est adoptée. Le comprimé contenant le butobarbital est ainsi très vite analysé (Fig. 1J) car, quand bien même ce barbiturique serait extrait, il ne peut être détecté dans nos conditions de travail. Par contre, la séparation complète des composants détectés du sirop (Fig. 1G) nécessite 6 min en raison du caractère hydrophobe de l'hydroxy-4 benzoate de méthyle.

La symétrie des pics est bonne. L'efficacité du système est de l'ordre de 1400 plateaux théoriques vis-à-vis de la théophylline conduisant à une résolution, entre cette dernière et l'anisate, légèrement inférieure à 3. Cela laisse une marge de manoeu-

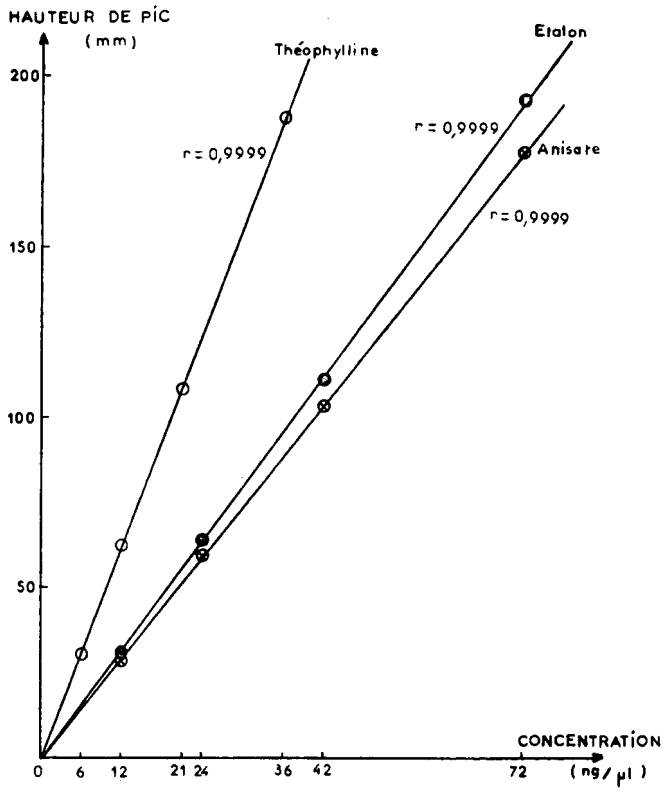

Fig. 2. Linéarité de la réponse du détecteur sur l'ensemble de la gamme des concentrations étudiées.

vre à l'utilisateur de la méthode. En effet, la faible pression (41 bar) d'une part, et la possibilité de diminuer encore R_s sans risque de recouvrement de pic d'autre part, font que l'utilisateur pourra encore gagner en temps d'analyse tout en respectant certaines exigences de résolution.

La Fig. 1C montre la séparation obtenue à partir d'un échantillon d'ampoule injectable, après 150 injections sur la même colonne, dix jours après le début des expériences, seul le fritté d'entrée de colonne ayant été changé. Au terme de cette période de tests, on constate que la résolution reste remarquablement constante. En outre, signalons que cette dernière ne subit pas de variation sensible avec de petits écarts de température autour de la normale.

Pour étudier les variations de hauteurs de pics, nous avons effectué dix injections successives d'un même échantillon issu d'une ampoule injectable. A des niveaux de concentration de 12 ng μl^{-1} pour la théophylline et de 24 ng μl^{-1} pour les autres composés, l'erreur sur la reproductibilité des hauteurs des pics est inférieure à $\pm$ 1,8%, la plus grande erreur affectant l'anisate élué en premier.

Concernant la courbe de réponse du détecteur, la Fig. 2 montre des relations linéaires entre les hauteurs des pics et les concentrations de solutions de théophylline, d'anisate de sodium et de β-hydroxypropylthéophylline, couvrant la gamme de 6–72 ng μl^{-1}.

La précision des résultats est calculée sur cinq échantillons préparés à partir de la même solution aqueuse (dilution à 1 l du contenu d'une ampoule injectable). L'erreur relative obtenue est inférieure à $\pm$ 2%.

CONCLUSION

La méthode décrite, originale et souple, est donc applicable aux formes les plus complexes du médicament. Considérant à la fois les temps très courts, de préparation de l'échantillon, de la séparation, la méthode est cependant particulièrement appropriée pour analyser en grandes séries, avec beaucoup de sûreté, les ampoules injectables.

RÉFÉRENCES

1 T. W. Rall, dans A. Goodman, L. Goodman et A. Gilman, (Rédacteurs), *Pharmacological Basis of Therapeutics*, Macmillan, New York, 6me éd., 1980, Ch. 25, p. 592.
2 W. J. Hurst, R. A. Martin et S. M. Tarka, *Prog. Clin. Biol. Res.*, 158 (1984) 17.
3 J. J. Orcutt, P. P. Kozak, Jr., S. A. Gillman et L. H. Cummins, *Clin. Chem.*, 23 (1977) 599.
4 K. T. Muir, J. H. G. Jonkman, D.-S. Tang, M. Kunitani et S. Riegelman, *J. Chromatogr.*, 221 (1980) 85.
5 P. van Aerde, E. Moerman, R. Van Seeveren et P. Braeckman, *J. Chromatogr.*, 222 (1981) 467.
6 P. M. Kabra et L. J. Marton, *Clin. Chem.*, 28 (1982) 687.
7 D. Dezaro, C. Horn et R. A. Hartwick, *Clin. Chem.*, 29 (1983) 1158.
8 G. Schumann, I. Isberner et M. Oellerich, *Fresenius' Z. Anal. Chem.*, 317 (1984) 677.
9 H. Ong et S. Marleau, *J. Liq. Chromatogr.*, 7 (1984) 779.
10 Y. H. Park, C. Goshorn et O. Hinsvark, *J. Chromatogr.*, 343 (1985) 359.
11 N. Grgurinovich, *J. Chromatogr.*, 380 (1986) 431.
12 J. J. Lauff, *J. Chromatogr.*, 417 (1987) 99.
13 R. Chiou, R. J. Stubbs et W. F. Bayne, *J. Chromatogr.*, 422 (1987) 281.
14 R. Meatherall et D. Ford, *Ther. Drug. Monit.*, 10 (1988) 101.
15 H. S. I. Tan, P. C. Booncong et S. L. Fine, *J. Pharm. Sci.*, 70 (1981) 783.

16 T.-M. Chen et L: Chafetz, *J. Pharm. Sci.*, 70 (1981) 804.
17 S. E. Roberts et M. F. Delaney, *J. Chromatogr.*, 242 (1982) 364.
18 A.-M. Brisson, D. Barthes et J.-B. Fourtillan, *Bull. Soc. Pharm. Bordeaux*, 117 (1978) 115.
19 J. C. Gfeller, R. Haas, J. M. Troendlé et F. Erni, *J. Chromatogr.*, 294 (1984) 247.
20 J. L. DiCesare, M. W. Dong et L. S. Ettre, *Chromatographia*, 14 (1981) 257.
21 *Supelco Technical Note, HPLC Bulletin 819*, Supelco, Bellefonte, PA, 1985, p. 4.
22 D. A. Jowett, *Clin. Chem.*, 27 (1981) 1785.
23 E. Bayer et A. Paulus, *J. Chromatogr.*, 400 (1987) 1.
24 R. Rosset, M. Caude et A. Tardy, *Manuel pratique de chromatographie en phase liquide*, Masson, Paris, 2^{me} éd., 1982, p. 192.
25 B. K. Glód, A. Piasecki et J. Stafiej, *J. Chromatogr.*, 457 (1988) 43.

Journal of Chromatography, 479 (1989) 437–440
Elsevier Science Publishers B.V., Amsterdam — Printed in The Netherlands

CHROM. 21 768

Note

Performing high salt concentration gradient elution ion-exchange separations using thermospray mass spectrometry

FONG-FU HSU and WILLIAM R. SHERMAN*
Department of Psychiatry, Washington University School of Medicine, St. Louis, MO 63110 (U.S.A.)
(First received April 24th, 1989; revised manucript received July 12th, 1989)

Thermospray liquid chromatography (LC)–mass spectrometry (thermospray) can be performed by vaporizing the liquid chromatograph effluent with a resistance-heated capillary vaporizer within the mass spectrometer[1]. The greatest sensitivity is obtained when the capillary is heated to a temperature such that complete vaporization of the LC effluent occurs at a temperature at the capillary exit that produces neither unvaporized droplets nor a superheated dry vapor[1]. In gradient elution ion-exchange separations with thermospray analysis the ionic strength is changed with volatile salts such as ammonium formate or ammonium acetate. As an example of interest to us, in ion-exchange separations of inositol phosphates the salt concentration has to be raised to 0.8 *M* to elute the most highly phosphorylated member of this group of compounds, inositol hexaphosphate. However, an ammonium acetate concentration of 0.8 *M* causes frequent clogging of the vaporizer reducing its useful life and interrupting analyses. A simple way to avoid that problem is to add, postcolumn, a gradient in the reverse sense of that of the eluting gradient, enabling the thermospray process to be performed with an isocratic salt solution of half the concentration of the eluting buffer. This has the additional benefit of increased stability of the thermospray process and of the resulting ion intensities by not having to program the vaporizer temperature.

EXPERIMENTAL

Two methods have been used to generate a gradient that is the reverse of the separation gradient. In both cases the high-pressure separation pumping system consisted of a pair of Shimadzu Model LC-6A pumps with gradient controller (Shimadzu, Kyoto, Japan). The counter-gradient was developed in two ways: (1) using two sets of HPLC pumps, each with a gradient programmer, and (2) generating the reverse gradient with a two-reservoir low-pressure gradient mixer that supplies a single high-performance LC pump. In both cases the mixing tee used was a Valco (Houston, TX, U.S.A.) 1/16-in. tee.

Method 1 (Fig. 1)

Two Waters Model M-6000A HPLC pumps (Fig. 1, pumps 3 and 4) and Model 660 gradient forming programmer (Waters, Milford, MA, U.S.A.) were used

0021-9673/89/$03.50

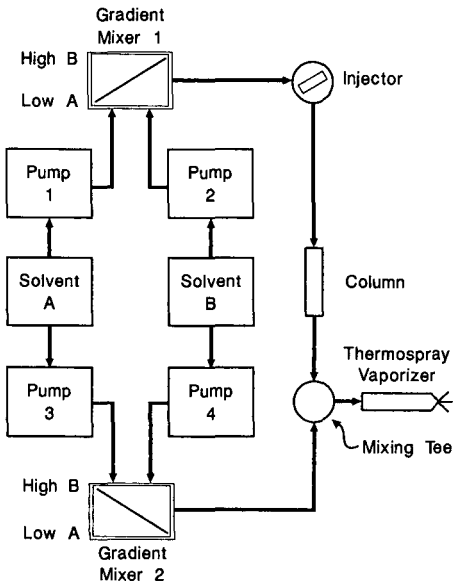

Fig. 1. Diagram of the pumping arrangement for isocratic thermospray mass spectrometry with a high ionic strength gradient elution separation.

drawing eluent from the same reservoirs that supplied the separation gradient, however, generating the gradient from high to low concentration and matched in time and volume with the separation gradient.

Method 2

The arrangement differs from that of Fig. 1 in that the counter gradient was developed at ambient pressure and supplied to a single Waters M-6000A pump. The linear gradient was supplied by a 100-ml concentric cylinder linear gradient former (Pace Model PGM-1; Isolab, Akron, OH, U.S.A.). The counter-gradient volume and the pumping rate were matched with that of the separation gradient.

Inositol phosphate mixture

A mixture of *myo*-inositol monophosphates (IP_1s) and polyphosphates (IP_2s, IP_3s, etc.) was prepared by dissolving 6.5 g of sodium phytate ($Na_{12}IP_6$) (Sigma, St. Louis, MO, U.S.A.) in 75 ml of water, adjusting the pH to 9.2 with glacial acetic acid and heating under reflux for 48 h. The mixture was found, by high-voltage paper electrophoresis[2], to contain all of the IP_ns except IP_6. A small amount of $InsP_6$ was added to give a mixture of all of the $InsP_n$s.

Separation of the myo-*inositol phosphate mixture*

Separations were carried out on either of two resin-based anion-exchange columns; Mono-Q, 50 mm × 5 mm (Pharmacia LKB, Piscataway, NJ, U.S.A.) or Shodex DEAE-825, 75 mm × 8 mm (Showa Denko, New York, NY, U.S.A.). In each case the separation gradient was from 0.1 *M* to 0.8 *M* aqueous ammonium formate with a flow-rate of 0.8 ml/min.

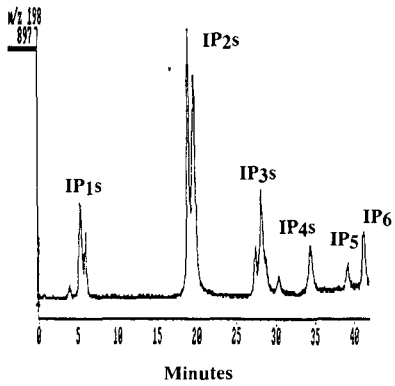

Fig. 2. Separation of inositol phosphates (IP_1s = *myo*-inositol monophosphates, IP_2s the bisphosphates, etc.) with a linear gradient of ammonium acetate from 0.1 *M* (at zero time) to 0.8 *M* (at 40 min) and thermospray LC–mass spectrometric detection. The separation was monitored by following *m/z* 198, *i.e.*, $[MNH_4]^+$ of unphosphorylated *myo*-inositol that is produced from each of the inositol phosphates during the thermospray process.

RESULTS

The separation of the inositol phosphate mixture on the mono-Q column is shown in Fig. 2. The counter-gradient in this case was provided by method 1. The thermospray process results in the hydrolysis of phosphomonoesters, thus the only positive ion of significant intensity seen in the thermospray mass spectrum of any of the IPs is *m/z* 198, *i.e.*, ammoniated inositol; $[MNH_4]^+$ (ref. 3). Since the rates of hydrolysis of the different species differ, the amount of inositol produced decreases with increasing degrees of phosphorylation and the ion intensity is thus not proportional to the inositol polyphosphate concentration. The several peaks in the elution regions noted in Fig. 2 (*e.g.*, IP_1s, IP_2s, etc.) are reproducible. The extent to which they are due to phosphate positional isomers of *myo*-inositol, or to inositol with different numbers of phosphate moieties, has not yet been determined. With the system used, the thermospray mass spectrometry for the entire process takes place in 0.4 *M* ammonium formate, a concentration that results in no vaporizer clogging.

The advantages of method 1 are flexibility: both linear and exponential gradients can be accommodated, only limited by the capabilities of the two programmers; the total volume of eluent is readily set by the pumping rate; the end point of a run remains 0.4 *M* without operator attention. Method 2, while inexpensive, constrains one to linear gradients (or to matching the shapes of exponential volume-dilution gradients) and the volume of eluent for a separation must be known in advance. In the latter case the operator must terminate the introduction of effluent to the instrument otherwise, at the point where the volume-dilution system empties its reservoirs, the solvent entering the mass spectrometer becomes the high-concentration eluent. An alternative not tested by us is to use two low-pressure gradient formers each supplying a single high-performance LC pump.

ACKNOWLEDGEMENT

This research was supported by the following grants from the National Institutes of Health: NS-05159, AM-20579 and RR-00954.

REFERENCES

1 M. L. Vestal and G. J. Fergusson, *Anal. Chem.*, 57 (1985) 2373.
2 U. B. Seiffert and B. W. Agranoff, *Biochim. Biophys. Acta*, 98 (1965) 574.
3 F.-F. Hsu, H. D. Goldman and W. R. Sherman, *Proc. 36th ASMS Conf. on Mass Spectrometry and Allied Topics, San Francisco, CA, June 5–10, 1988*, p. 1053.

Journal of Chromatography, 479 (1989) 441–444
Elsevier Science Publishers B.V., Amsterdam — Printed in The Netherlands

CHROM. 21 769

Note

Separation of phenols and their glucuronide and sulfate conjugates by anion-exchange liquid chromatography

F. REBER BROWN and WILLIAM M. DRAPER*
California Public Health Foundation, Hazardous Materials Laboratory, 2151 Berkeley Way, Berkeley, CA 94704 (U.S.A.)
(First received March 14th, 1989; revised manuscript received June 7th, 1989)

Improved methods are needed for both separation and detection of polar, foreign compound metabolites in biological tissues and fluids. The most important mammalian conjugation reactions involve attachment of glucuronide and sulfate moieties, with glucuronidation predominating[1,2]. Accordingly, our method development efforts have been focused on these two conjugate classes.

Gas chromatography (GC) and GC–mass spectrometry (MS) have been used to measure glucuronides, but isolation and derivatization are necessary[3]. Sulfate conjugates are generally hydrolized by acid or enzymatically, followed by analysis of the non-polar hydrolysis product[3]. The use of high-performance liquid chromatography (HPLC) offers the potential for the direct determination of sulfate and glucuronide conjugates with little or no sample preparation.

Various HPLC methods for these compounds have been published, most of these based on ion-pair reversed-phase chromatographic systems[4–10]. In each of these reports, the authors separated either a single phenol and its glucuronide and sulfate, or the sulfate or glucuronide conjugates of several different phenols. In contrast, the present paper describes the simultaneous separation of three phenols and their respective glucuronide and sulfate conjugates using a strong anion-exchange chromatographic column and an ammonium formate buffer, an application that has not previously been reported.

EXPERIMENTAL

Chemicals

Phenyl-β-D-glucuronide, 1-naphthyl-β-D-glucuronide, 4-nitrophenyl-β-D-glucuronide, and 1-naphthyl sulfate potassium salt were purchased from Sigma (St. Louis, MO, U.S.A.). Phenyl sulfate potassium salt was purchased from TCI American (Portland, OR, U.S.A.). 4-Nitrophenyl sulfate was prepared in our laboratory as potassium salts using a modification of the procedure of Burkhardt and Lapworth[11] as described elsewhere[12]. The commercial and synthetic compounds were confirmed by negative fast atom bombardment MS and high-field proton nuclear magnetic resonance spectroscopy[12].

Standards were prepared in either distilled, deionized water or pesticide grade methanol (EM Science, Cherry Hill, NJ, U.S.A.). The mobile phase consisted of

0021-9673/89/$03.50

pesticide grade acetonitrile (EM Science) and aqueous ammonium formate buffer. The ammonium formate buffer was prepared by adjusting the pH of a 0.05 *M* formic acid solution to 4.5 with concentrated ammonia (J. T. Baker, Phillipsburg, NJ, U.S.A.). The formic acid was 96% and was obtained from Merck (Rahway, NJ, U.S.A.).

C.A. registry numbers. Phenol: [108-95-2]; phenyl sulfate potassium salt: [1733-88-6]; phenyl glucuronide: [17685-05-1]; 4-nitrophenol: [100-02-7]; 4-nitrophenyl sulfate potassium salt: [6217-68-1]; 4-nitrophenyl glucuronide: [10344-94-2]; 1-naphthol: [90-15-3]; 1-naphthyl sulfate potassium salt: [6295-74-5]; 1-naphthyl glucuronide: [17238-47-0].

HPLC system

The chromatographic system consisted of an Isco Model 2300 HPLC pump and an Isco V^4 variable-wavelength absorbance detector (Lincoln, NE, U.S.A.). A Valco C6W injection valve (Houston, TX, U.S.A.) with a 10-μl sample loop was used for sample introduction. The chromatograms were recorded on a Spectra-Physics (San Jose, CA, U.S.A.) Model 4290 digital integrator. The separations were carried out on a Supelco (Bellefonte, PA, U.S.A.) 25 cm × 4.6 mm 5-μm LC-SAX column.

Experimental procedure

A mixed standard solution containing nine target compounds, each at approximately 100 ng/μl was used. The compounds were phenol, phenyl glucuronide, phenyl sulfate potassium salt, 4-nitrophenol, 4-nitrophenyl glucuronide, 4-nitrophenyl sulfate potassium salt, 1-naphthol, 1-naphthyl glucuronide and 1-naphthyl sulfate potassium salt. Serial dilutions were made of the stock solution to give solutions of approximately 50, 25, 12, and 6 ng/μl of each component. The mixtures were chromatographed isocratically with a mobile phase of buffer–acetonitrile (3:2, v/v) at a total flow-rate of 1.5 ml/min. Compounds were detected by absorbance at 254 nm and identified by retention time. Calibration curves were constructed by plotting peak area *vs.* concentration.

TABLE I

CAPACITY FACTORS AND EFFICIENCY OF LC-SAX COLUMN

Compound	*Retention time (min)*	*Capacity factor*	*Number of theoretical plates*
Void volume	2.36	–	–
Phenol	2.78	0.18	4300
4-Nitrophenol	3.14	0.33	5500
1-Naphthol	3.48	0.48	6700
Phenyl glucuronide	5.37	1.28	7100
4-Nitrophenyl glucuronide	5.79	1.45	8300
1-Naphthyl glucuronide	7.15	2.03	5600
Phenyl sulfate	11.0	3.68	17 000
4-Nitrophenyl sulfate	13.4	4.68	16 100
1-Naphthyl sulfate	19.5	7.26	12 000

RESULTS AND DISCUSSION

The retention times, capacity factors and numbers of theoretical plates for each compound are shown in Table I, and a typical chromatogram is shown in Fig. 1. Complete separation is achieved within 25 min. The calibration curves for the nine compounds are all linear, with correlation coefficients of 0.996 or greater. Limits of detection based on peak heights three times the peak-to-peak baseline noise range from 9 ng for phenol to 270 ng for phenyl sulfate.

The LC–UV procedure described may be readily adapted to HPLC–MS. A commonly used interface for HPLC–MS is the thermospray (TSP) interface, which uses a volatile buffer, generally ammonium acetate or ammonium formate, to effect ionization[13]. The mobile phase used with the SAX column would therefore be compatible with HPLC–TSP–MS. Particle beam interfaces do not require an ionizing buffer, and could therefore use ion pairing reagents[13]. However, such reagents contaminate the interface and the mass spectrometer source[14]. This SAX method is therefore also well suited to particle beam LC–MS. While ammonium formate was used in this work, we found that ammonium acetate gives very similar results[14].

While the LC-SAX column gave very efficient and reproducible separations, it was very sensitive to storage conditions. Column performance was maintained by rinsing the column at the end of the day with about 45–60 ml of a phosphate solution, prepared by adding concentrated phosphoric acid to a 0.05 *M* solution of K_2HPO_4 to

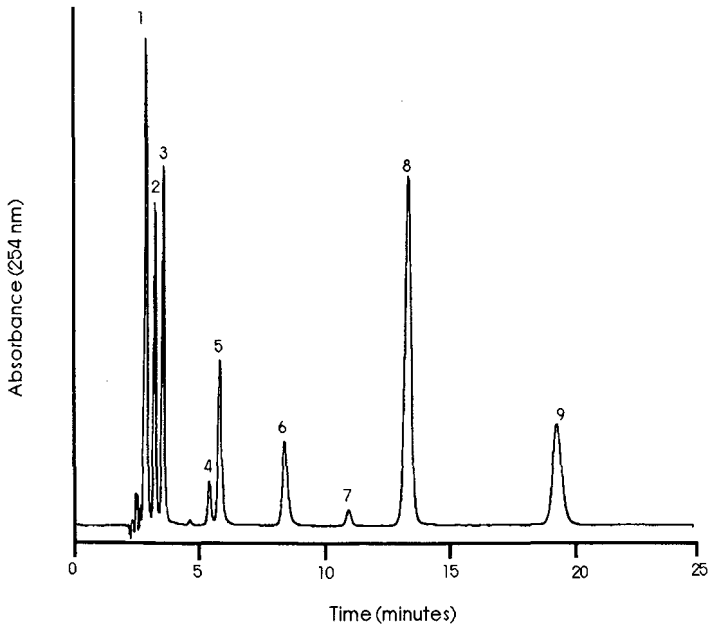

Fig. 1. Sample chromatogram of 100 ng/μl standard. Peaks: 1 = phenol; 2 = 4-nitrophenol; 3 = 1-naphthol; 4 = phenyl glucuronide; 5 = 4-nitrophenyl glucuronide; 6 = 1-naphthyl glucuronide; 7 = phenyl sulfate potassium salt; 8 = 4-nitrophenyl sulfate potassium salt; 9 = 1-naphthyl sulfate potassium salt.

a pH of 2.5. Failure to store the column in the phosphate solution would result in a severe decrease in retention time, especially for the sulfates. The original chromatographic characteristics of the column could be restored by storage in the phosphate solution for one to two days.

ACKNOWLEDGEMENTS

This work was carried out at the California Department of Health Services Hazardous Materials Laboratory, and was funded by Superfund Project No. ES 04705 from the National Institute of Environmental Health Sciences of the National Institutes of Health.

REFERENCES

1 G. J. Dutton (Editor), *Glucuronic Acid: Free and Combined,* Academic Press, New York, 1966.
2 C. D. Klaassen, M. O. Amdur and J. Doull (Editors), *Toxicology: The Basic Science of Poisons,* Macmillan, New York, 1986.
3 D. D. Kaufman, G. G. Still, G. D. Paulson and S. K. Bandal, *Bound and Conjugated Pesticide Residues (ACS Symposium Series)*, American Chemical Society, Washington, DC, 1976.
4 M. Ogata and Y. Yamasaki, *Int. Arch. Occup. Environ. Health,* 44 (1979) 177–181.
5 M. A. Ragan and M. D. Mackinnon, *J. Chromatogr.,* 178 (1979) 505–513.
6 A. Karakaya and D. E. Carter, *J. Chromatogr.,* 195 (1980) 431–434.
7 P.-O. Lagerström, *J. Chromatogr.,* 250 (1982) 43–54.
8 J. C. Rhodes and J. B. Houston, *Xenobiotica,* 11 (1981) 63–70.
9 G. Diamond and A. J. Quebbemann, *J. Chromatogr.,* 177 (1979) 368–371.
10 M. M. Krahn, D. W. Brown, T. K. Collier, A. J. Friedman, R. G. Jenkins and D. C. Mallins, *Chromatogr. Newsl.,* 8 (1980) 29–31.
11 G. N. Burckhardt and A. Lapworth, *J. Chem. Soc.,* (1926) 684.
12 W. M. Draper, F. R. Brown, R. Bethem and M. J. Miille, *Biomed. Environ. Mass Spectrom.,* 18 (1989) 767–774.
13 T. R. Covey, E. D. Lee, A. P. Bruins and J. D. Henion, *Anal. Chem.,* 58 (1986) 1451A-1461A.
14 F. R. Brown and W. M. Draper, unpublished results.

Journal of Chromatography, 479 (1989) 445–451
Elsevier Science Publishers B.V., Amsterdam — Printed in The Netherlands

CHROM. 21 730

Note

Florisil® sorbent sampling and ion chromatographic determination of airborne aliphatic carboxylic acids

P. SIMON*, F. BRAND and C. LEMACON
Institut National de Recherche et de Sécurité, BP 27, 54501 Vandoeuvre Cedex (France)
(Received April 27th, 1989)

Aliphatic monocarboxylic acids are industrial chemicals with a wide variety of applications. They are used in the preparation of polymers, resins, dyestuffs, in the manufacture of various esters for solvent purposes, in the food industry, in cosmetics and as chemical intermediates[1].

The prominent physiological consequence of exposure to carboxylic acid functions is the primary irritation of eyes, skin or mucous membranes, short-chain acids (formic, acetic, propionic acids) being also responsible for burns[2], and occupational standards have been set to limit the exposure to aliphatic acids.

Various methods are available for the sampling and analysis of airborne carboxylic acids[3–5]. The oldest and usual sampling method involves the bubbling of the air sample through an absorber solution[3,4,6–8], which makes individual monitoring awkward; consequently, chemisorption methods have been developed and samplers consist of solid sorbents[5,9–12]. These sampling methods are generally associated with gas chromatography[9,13] and liquid chromatography[10–12], with which a chemical derivatization step may be employed to lower the detection limit. However, there are few sampling and analytical methods which are applicable to the aliphatic carboxylic acid family, and the current procedures have the disadvantage of employing liquid traps[6–8] or an additional derivatization step[13,14].

The aim of this work was to examined whether Florisil® is a general solid sorbent sampler for aliphatic carboxylic acids and can be used in conjunction with an easy and rapid method for the analysis of formic, acetic, propionic, monochloroacetic, acrylic and methacrylic acids. We have selected high-performance ion-exclusion chromatography with conductimetric detection as a relevant analytical method.

MATERIALS AND METHODS

Reagents

Benzoic, sulphuric and aliphatic carboxylic acids of analytical grade were obtained from Merck. Water for high-performance liquid chromatography (HPLC) was purified by passage through a Millipore Milli-Q water treatment system. Acetonitrile of chromatographic grade was obtained from Merck.

0021-9673/89/$03.50

Preparation of the sampling tubes

The sampling tubes, made of Pyrex (50 mm × 6 mm I.D.), were packed with about 0.8 g of Florisil (OSI 30–60 mesh) held between two glass-wool plugs.

Standard and generation system

Acids were dissolved in acetonitrile and further diluted in order to form a series of four dilutions (Table I). A 10-μl aliquot of each acid solution was injected in a Dynamic U-tube system. The dynamic U-tube system developed previously[15] to determine breakthrough and recovery consisted of a U-shaped tube as a flow chamber and sample container. One side arm was used as the air inlet, the other held the absorption tube and was connected to the pump. The U-tube assembly was immersed in a thermostated water-bath. Air was pumped through the Florisil tube at a flow-rate of 1 l/min. Relative humidities of 35, 65 and 100% were obtained by drawing air through saturated salt solutions.

TABLE I

RECOVERY OF ACIDS FROM FLORISIL

Acid	*Std. solutions (g/l)*	*% Recovery*[a]	
		av.[b]	*S.D.*[c]
Formic acid	90.2	98.7	0.5
	45.1	100	1.2
	22.5	100	0.8
	4.5	97.7	1.7
Acetic acid	254.4	99	0.8
	127.2	101	1
	63.6	100	1.5
	12.7	100	1.5
Monochloroacetic acid	51.9	100	0
	25.9	100.5	1
	12.9	100.7	1
	2.6	98.7	1.5
Propionic acid	290	99.2	1
	148.5	101	0.8
	74.2	101.5	1.7
	14.8	96.5	2.9
Acrylic acid	378	99	1.4
	189	100.5	1
	94.6	97.5	2.6
	18.9	98.7	1.5
Methacrylic acid	852.4	97.7	1.9
	426.2	100.5	1
	213.1	97.2	2
	42.6	99.7	0.5

[a] Recovery for 10 μl of acid standard solution placed in the Florisil tube.
[b] Average of four determinations.
[c] Standard deviation.

Desorption of samples

The sorbent was transferred to glass vials with PTFE-lined screwcaps and 5 ml of water were added. The mixture was then mechanically shaken for 10 min, and 10 μl of 1 *N* sulphuric acid was added prior to injection into the chromatographic system.

Apparatus

A Waters Associates Model 590 chromatographic pump, a 20-μl sample loop (Rheodyne Model 7125) and a conductivity detector (Perkin-Elmer LC-21 or Waters 430) were employed. An integrator (Hitachi D-2000) and a recorder (Sefram) were used to convert the peaks into quantitative data.

Column

The Aminex HPX 87 H organic acid analysis column (300 mm × 7.8 mm) was obtained from Bio-Rad (France) and contains an 8% cross-linked cation-exchange resin (H^+) consisting of totally porous 10-μm particles.

Chromatographic analysis

Samples free of particulate matter were injected directly into the chromatographic system. The eluent, $2.5 \cdot 10^{-4}$ *M* sulphuric or benzoic acid, was pumped at a flow-rate of 0.8 ml/min through the cationic resin column. The retention times were compared with those of known standards, and the method of peak-height measurement with an external standard was used for qualitative and quantitative assessment, respectively.

RESULTS AND DISCUSSION

Solid sorbents have previously been used to sample carboxylic acids in air, but they varied from one technique and test compound to another[3,5,9–12,14]. The Florisil sorbent used in this work was applied to six carboxylic acids. A static method was used to evaluate the adsorption–desorption efficiency of each acid at increasing levels (Table I). The standard solutions were directly injected into the Florisil tube and air was pumped through the tube at about 1 l/min for 60 min. For each acid, the amounts collected were in the concentration range of 0.52–85.2 mg/m^3.

The sampling efficiency was investigated by generating the test atmospheres in the dynamic U-tube system. The results are summarized in Table II. In any case, the U-tube was rinsed with the extracting solution after sampling, and the washing liquid was analyzed to ascertain the transfer of the carboxylic acid in the collection tube.

For a vapour concentration equal to twice the ACGIH standard level[a], no breakthrough of any of the compounds occurred when 120 l of air conditioned to 100% relative humidity were sampled. A 0.8-g amount of Florisil was quite sufficient to collect the totality of each acid. During preliminary experiments, silica gel (Merck Kieselgel 60, 30–70 mesh) was tested; the use of this support is not recommended for

[a] American Conference of Governmental Industrial Hygienists: Treshold Limit Values and Biological Exposure Indices for 1988–1989. Time-weighted average values: formic acid, 9 mg/m^3; acetic acid, 25 mg/m^3; propionic acid, 30 mg/m^3; acrylic acid, 30 mg/m^3; methacrylic acid, 70 mg/m^3.

TABLE II

COLLECTION AND RECOVERY OF ACIDS USING THE DYNAMIC U-TUBE SYSTEM

Acids	*Std. solutions (g/l)*	*% Recovery*[a]	
		av.[b]	*S.D.*[c]
Formic acid	90.2	94.8	1.9
	45.1	94.8	4
	22.5	92.6	3.1
	4.5	97	2.1
Acetic acid	254.4	91.8	4.3
	127.2	94.6	2
	63.6	90.5	3.6
	12.7	101	4.7
Monochloroacetic acid	50	92.2	1.7
	22.4	98	1.7
	12.5	93	4.4
	2.5	94.3	2.6
Propionic acid	297	92.8	4
	148.5	97.3	1.8
	74.2	95.3	6.5
	14.8	94.3	2.6
Acrylic acid	378	96	3.8
	189	97.8	1.5
	94.6	99	1.1
	18.9	94	2.5
Methacrylic acid	852	99	1.8
	426	97.6	1
	213.1	100	1.5
	42.6	93	2.8

[a] Recovery for 10 μl of acid standard solution placed in the U-tube system.
[b] Average of six determinations.
[c] Standard deviation.

formic and acetic acids, as a breakthrough of these compounds appeared for a vapour concentration equal to the ACGIH standard level when 60 l of air at 65% relative humidity were sampled.

The stability of trapped samples was studied for vapour concentrations equal to half and a tenth of the ACGIH standard level for each acid; storing in the dark at 4°C for 9 and 21 days did not significantly hinder the recovery.

In order to prevent the polymerization of acrylic acid, Vincent and Guient[9] recommended the use of silica gel treated with *p*-methoxyphenol. During the assessment of the applicability of Florisil to acrylic and methacrylic acids, no decomposition of these monomeric substances was observed with the untreated sorbent. It should be noted, however, that the acids used in this evaluation contained 200 ppm of *p*-methoxyphenol.

Ion-exclusion chromatography (IEC) associated with conductivity or sometimes UV detection is commonly used for the separation and determination of car-

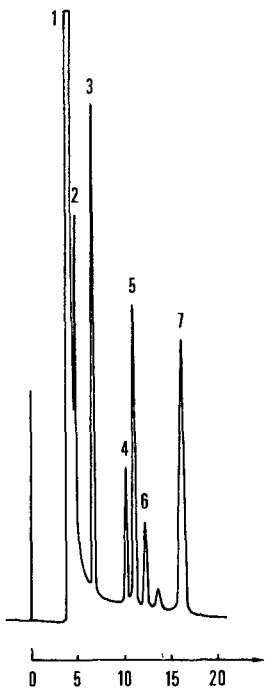

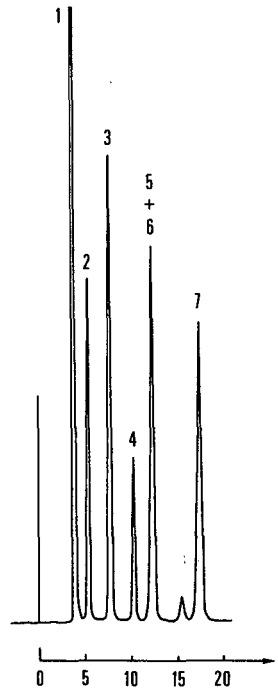

Fig. 1. Separation of acids on the Aminex HPX 87 H column with a $2.5 \cdot 10^{-4}$ *M* benzoic acid mobile phase; flow-rate 0.8 ml/min; conductivity 20 μS full scale. Peaks: 1 = sulphuric acid; 2 = monochloroacetic acid (400 ng); 3 = formic acid (360 ng); 4 = acetic acid (1000 ng); 5 = acrylic acid (2000 ng); 6 = propionic acid (1200 ng); 7 = methacrylic acid (4000 ng).

Fig. 2. Separation of acids on the Aminex HPX 87 H column with a $2.5 \cdot 10^{-4}$ *M* sulphuric acid mobile phase; flow-rate 0.8 ml/min; conductivity 20 μS full scale. Peaks as in Fig. 1.

boxylic acids[6–8,10,12,16–18]. According to Tanaka and Fritz[16,17], high-performance separation of the six carboxylic acids can be obtained by using a strongly acidic cation-exchange resin (H^+) with diluted aqueous solutions of sulphuric or benzoic acid as the eluents. Such eluents have a much lower background conductance than the strongly acidic eluents commonly used and permit a more sensitive detection of the sample acids.

In the present work we used the method of Tanaka and Fritz; a satisfactory separation of the six acids studied was obtained with an aqueous solution of benzoic acid ($2.5 \cdot 10^{-4}$ *M*) or sulphuric acid ($2.5 \cdot 10^{-4}$ M) as the eluent (Figs. 1 and 2). With benzoic acid, a weak resolution between sulphuric and monochloroacetic acids was obtained, but separation of acrylic and propionic acids was achieved with $R_s > 1.25$. Conversely, with sulphuric acid as the eluent, sulphuric and monochloroacetic acids were separated while acrylic and propionic acids had the same retention time.

The detection limits (signal/noise ratio > 3) were approximately 0.2, 0.3, 3, 5, 2 and 5 μg/ml for monochloroacetic, formic, acetic, propionic, acrylic and methacrylic

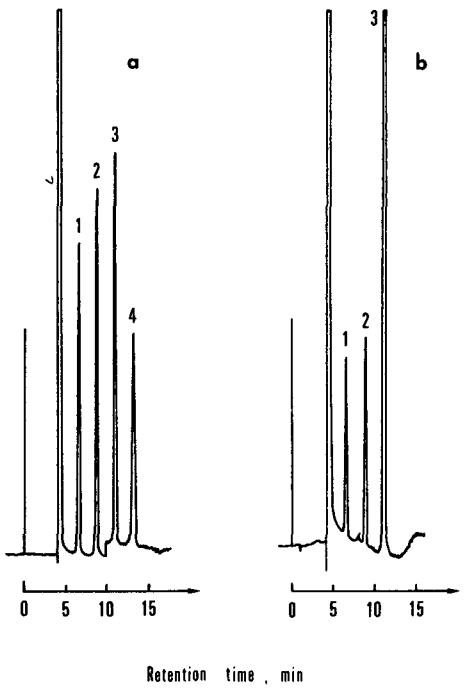

Fig. 3. Ion-exclusion chromatograms of standard acid and acid vapours from the air of a pickling workshop with a $2.5 \cdot 10^{-4}$ *M* sulphuric acid mobile phase; flow-rate 0.8 ml/min; conductivity 5 μS (0–10 min), 2 μS full scale (10 min). (a) Acid standard. Peaks: 1 = monochloroacetic acid (100 ng); 2 = formic acid (180 ng); 3 = acetic acid (500 ng); 4 = propionic acid (600 ng). (b) Air sample (96 l). Peaks: 1 = monochloroacetic acid (0.02 mg/m^3); 2 = formic acid (0.05 mg/m^3); 3 = acetic acid (0.47 mg/m^3).

acids corresponding to concentrations of 0.1, 0.15, 1.5, 2.5, 1 and 2.5 mg/m^3 in an air sample of 10 l, respectively.

The method has been successfully used to measure low levels of airborne aliphatic carboxylic acids in a metal sheet pickling workshop; Fig. 3b shows a liquid chromatogram of acids from this source. Monochloroacetic, acetic and formic acids were detected at the respective levels of 0.02, 0.47 and 0.05 mg/m^3 in the air sample (96 l pumped). Dichloromethane present in the atmosphere (63 mg/m^3) did not interfere with the determination of acids. One possible disadvantage of this sampling method in an industrial environment is the positive interference from acyl chlorides. Acyl chlorides are hydrolysed in humid air to carboxylic and hydrochloric acids on solid sorbents and in solution. Therefore, the sampling method may overestimate the carboxylic acid level.

The Florisil sorbent seems to be a well adapted support for the sampling of many aliphatic carboxylic acids. This solid adsorbent is compatible with ion-exclusion analysis, which is not liable to known interferences except from acyl chlorides. The method is rapid, easy and appears suitable for the determination of aliphatic carboxylic acids at ppm (v/v) or ppb levels, such as those found in industrial emissions.

ACKNOWLEDGEMENTS

The authors thank J. De Ceaurriz for his critical advice on the manuscript and the secretarial work of D. Francois and C. Bertrand is appreciated.

REFERENCES

1 Kirk-Othmer, *Encyclopedia of Chemical Technology*, Vol. 4, Wiley-Interscience, New York and London, 3rd ed., 1978, pp. 814–845.
2 *Patty's Industrial Hygiene and Technology*, Vol. 2C, Wiley-Interscience, New York and London, 3rd ed., 1982, pp. 4901–4987.
3 *Osha Analytical Methods Manual*, Vol. 1, OSHA Analytical Laboratory, Salt Lake City, UT, Method 28 (1981); Vol. 2, Methods ID-112 and ID-118 (1984).
4 *Niosh Manual of Analytical Methods*, Vol. 5, U.S. Government Printing Office, Washington, DC, 2nd ed., 1979, Method S 173.
5 *Niosh Manual of Analytical Methods*, Vol. 1, U.S. Government Printing Office, Washington, DC, 3rd edn., 1984, Method 1603.
6 T. Yasuoka, J. Takano, S. Mitsuzawa, H. Saitoh and K. Oikawa, *Bunseki Kagaku*, 32 (1983) 580–584.
7 C. Anselme, J. Manem, A. Bruchet and M. Caillet, *Tech. Sci. Munic. Eau.*, 80 (1985) 141–148.
8 S. Tanaka, M. Guchi, K. Yamanaka, T. Yamada, N. Nakao and Y. Hashimoto, *Bunseki Kagaku*, 36 (1987) 12–17.
9 W. J. Vincent and V. Guient, Jr., *Am. Ind. Hyg. Assoc. J.*, 43 (1982) 499–504.
10 R. E. Pauls and G. J. Weight, *J. Chromatogr.*, 254 (1983) 171–177.
11 S. Vainiotalo, P. Pfäffli and A. Zitting, *J. Chromatogr.*, 258 (1983) 207–211.
12 D. W. Mason, H. K. Dillon and R. A. Glaser, *Am. Ind. Hyg. Assoc. J.*, 47 (1986) 14–21.
13 K. Kawamura and J. R. Kaplan, *Anal. Chem.*, 56 (1984) 1616–1620.
14 K. Kawamura, L. L. Ng and J. R. Kaplan, *Environ. Sci. Technol.*, 19 (1985) 1082–1086.
15 L. W. Severs, R. G. Melcher and M. J. Kocsis, *Am. Ind. Hyg. Assoc. J.*, 39 (1978) 321–326.
16 K. Tanaka and J. S. Fritz, *J. Chromatogr.*, 361 (1986) 151–160.
17 K. Tanaka and J. S. Fritz, *J. Chromatogr.*, 409 (1987) 271–279.
18 K. Kihara, S. Rokushika and H. Hatano, *J. Chromatogr.*, 410 (1987) 103–110.

Journal of Chromatography, 479 (1989) 452–458
Elsevier Science Publishers B.V., Amsterdam — Printed in The Netherlands

CHROM. 21 725

Note

Simultaneous determination of monoethanolamine and glycine betaine in plants

HORST MÜLLER* and HANS ECKERT
Forschungszentrum für Bodenfruchtbarkeit Müncheberg, Bereich Jena, Naumburgerstrasse 98a, 6909 Jena 9 (G.D.R.)
(First received February 6th, 1989; revised manuscript received June 20th, 1989)

The association of monethanolamine (EA) and glycine betaine (GB) with drought resistance of plants requires the determination of these compounds in any study of stress physiology and of the alleviation of stress by bioregulators.

Methods used for the determination of EA and GB include thin-layer chromatography (TLC)[1–3], gas chromatography (GC)[4–7] and high-performance liquid chromatography (HPLC)[8–11]. In addition, GB was determined spectrometrically as its reineckate[12], periodide[13] or by means of an enzymatic method[15] in biological material.

Comparatively little is known about the quantitation of EA in plant material. Reissmann *et al.*[5] suggested a GC procedure for barley grains, but this method is laborious and needs a time-consuming derivatization step.

Since none of these methods allows a simultaneous determination of EA and GB and meets all requirements concerning specificity, sensitivity and rapidity, we developed a simple ion-exchange chromatography–TLC procedure which is especially suitable for a simultaneous determination of EA and GB in routine analysis.

MATERIALS AND METHODS

Plant material

Barley plants (*Hordeum vulgare* L., cv. Salome) were grown in Mitscherlich pots under well watered and drought stressed conditions as described previously[16].

Chemicals and radiochemicals

EA, reagent grade, was obtained from VEB Laborchemie (Apolda, G.D.R.). GB, reagent grade, and Dowex resins were obtained from Serva (Heidelberg, F.R.G.). All other chemicals used in extraction, purification and quantification were of reagent grade quality.

[1-^{14}C]EA used as the internal standard was from Isocommerz (Dresden, G.D.R.). [$^{14}CH_3$]GB was synthesized from [$^{14}CH_3$]choline (Isocommerz) according to Lintzel and Fomin[17]. Both labelled compounds were purified by the analytical procedure described below and their purity confirmed by comigration with authentic standard compounds in TLC and checked by means of a TLC scanner Berthold II. Radiochemical impurities were $\leqslant 0.5\%$.

0021-9673/89/$03.50

Extraction and precleaning

Fresh plant material (main shoots and tillers, respectively) was immediately homogenized with 200 ml methanol–chloroform–water (70:20:10, v/v/v) after harvesting. To this mixture a standard amount of [^{14}C]EA (43.40 kBq/μmol, 1.43 μg) and [^{14}C]GB (20.19 kBq/μmol, 4.10 μg) were added to each sample[a]. These samples were kept at room temperature in the dark for more than 24 h. Then, the solution was filtered and the residue reextracted with additional solvent until chlorophyll removal was complete. The pooled extracts were shaken with one-third volume of water. After separation the aqueous phase was evaporated to 10 ml under vacuum and for precleaning passed through a column of the strong cation exchanger Dowex 50W-X8(H^+) 8 ml in the case of 25 g fresh plant matter. After washing with water, EA and GB were eluted with 1 *M* ammonia.

Separation of EA from GB

After concentration of the 1 *M* ammonia eluate (to about 10 ml) it was passed through two columns (8 ml each) coupled in series and containing the strong anion-exchange resin Dowex 2-X8(OH^-) and the weak cation-exchange resin Dowex CCR-2(H^+), respectively. The effluent, including water for washing, contained GB and was evaporated to dryness and for quantification redissolved in 2 ml 80% methanol[a]. EA retained on the weak cation exchanger was eluted with 1 *M* ammonia. After removing the ammonia by concentrating to 10 ml under vacuum, 1 ml 1 *M* HCl was added and the solution evaporated to dryness. The residue was redissolved in 1 ml methanol for quantification.

Quantification of EA and GB

Determination of EA and GB was performed by TLC using precoated silica gel plates (Silufol, Prague, Czechoslovakia) without prior activation. Aliquots of the prepared solutions (1 μl in the case of GB and 2 μl in the case of EA) were applied to the plates. The developing solvent systems were: EA methanol–25% aqueous ammonia (8:2, v/v); GB methanol–25% aqueous ammonia–water (7:2:1, v/v). Plates were developed one-dimensionally at room temperature over a distance of 8 cm in a saturated chamber. After drying the plates at 110°C for 5 min, EA spots were visualized by spraying with 0.2% ninhydrin in ethanol and heating again at 110°C for 3 min (R_F = 0.3, limit of detection 10 ng). Visualization of GB was carried out by treating the developed and dried plates with hydrogen chloride vapour, removing surplus HCl at 110°C for 10 min and spraying with 0.05% aqueous methyl orange. GB showed deep red spots on a yellow background (R_F = 0.5, limit of detection 0.3 μg). Quantification of both compounds was performed by means of a scanning densitometer (FZB Müncheberg, Bereich Jena, G.D.R.). The calibration graph for each plate was obtained by spotting in 50-ng steps for EA and in 0.5-μg steps for GB. The response of the scanning densitometer was linear in the range 0–250 ng for EA (r = 0.9995, wavelength 570 nm) and 0–4 μg for GB (r = 0.991, wavelength 550 nm).

---

[a] In order to economize on reagents and ion exchangers it is possible to miniaturize the method up to 0.5 g plant fresh matter. However, from a plant physiological viewpoint, a representative sample size must be guaranteed. That means that the sample size can be miniaturized only if the plant material is sufficiently homogenized before extraction, *e.g.* freeze-dried and ground.

Isotope dilution analysis

After spotting on the TLC plate, 50-μl aliquots (in triplicate) of each sample were immediately taken for scintillation counting (Liquid Scintillation Counter Rackbeta 1219; LKB, Sweden) in a dioxane-based scintillator with the scintillators 2,5-diphenyloxazole (PPO) and 1,4-bis(5-phenyloxazolyl-2)benzene (POPOP) and quench correction with an external standard. Knowing the specific radioactivities of the authentic ^{14}C-labelled compounds added and of the EA and GB recovered, the endogenous levels of EA and GB can be calculated.

RESULTS AND DISCUSSION

As a result of its unique charge properties (a permanent positive charge on the quaternary ammonium group with a carboxyl group of low pK_a), GB is not retained on either strong anion or weak cation-exchange resin[6]. This allows an excellent separation from the cationic EA as well as from impurities by an exchanger system arranged in series (see Fig. 1). By means of the strong anionic resin [Dowex 2-X8(OH^-)] all anions were removed, especially amino acids which disturb the subsequent quantification, and on the other hand all cations were retained on the weak cation resin [Dowex CCR-2(H^+)]. The effluent of this column combination contains GB, whereas EA is retained on the weak cation exchanger. After separating the columns EA can be eluted with ammonia.

A precondition for a good separation and quantification is a precleaning step involving filtration of the crude extract through a column of a strong cation exchanger [Dowex 50W-X8(H^+)]. This resin suppresses the ionization of the carboxyl group of GB and retains GB as well as EA, whereas uncharged compounds and anions were removed by the effluent. In addition, this precleaning prevents an overcharge of the anion resin in the subsequent separation step, in particular when the sample size exceeds 0.5 g plant dry matter. After washing the column with water, EA and GB can be eluted with ammonia (see Fig. 1).

The separation efficiency achieved by the column combination together with the preceding purification step is shown in Table I. The results demonstrate that artefacts are not produced during the analytical procedure and that there is no overlap between EA and GB. However, the recovery data show that there are some losses of EA, which can be explained by the volatility of the basic EA during the evaporation of the ammonia eluate. Therefore, the analytical procedure was generally performed with an internal standard. We used the ^{14}C-labelled compounds of EA and GB, allowing quantification by an isotope dilution procedure. The good separation of EA and GB (see Table I) enables the addition of both compounds before starting the extraction procedure. Because of the high specific radioactivity of [^{14}C]EA and [^{14}C]GB used, the amount added was less than 1% of the EA and GB content found in the plant tissue (Table IV). The low radioactivity of about 1 kBq per sample does not require any special radiohygienic precautions, taking into account the low volatility of EA.

Even if the purity of the EA and GB fractions allows the derivatization and quantification by GC, it was found that TLC offers a more rapid and simpler method giving well reproducible results with an high sensitivity. For GB we developed a sensitive detection method because the usual Dragendorff reagent[18] was too insensi-

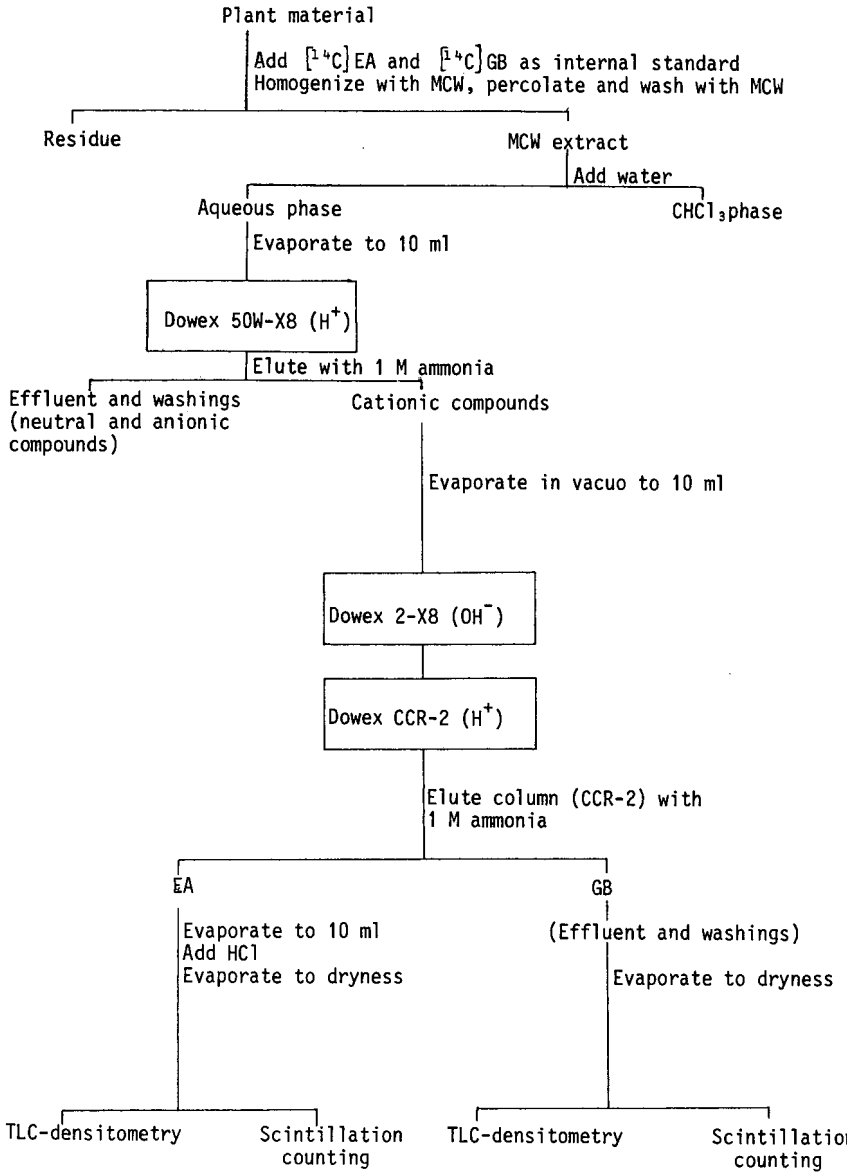

Fig. 1. Analytical procedure for determination of EA and GB in barley shoots. MCW = Methanol–chloroform–water (70:20:10, v/v/v).

tive (limit of detection $\approx$ 10 μg). With regard to the acidity of the GB hydrochloride, visualization with a methyl orange reagent proved to be suitable and allows a detection limit of 0.3 μg. EA was detected with the sensitive ninhydrin reagent[19] (detection limit 10 ng). The accuracy of the method was tested by analysing prepared mixtures of EA and GB (Table II). Good recoveries with low standard deviations were obtained. When the method was applied to prepared extracts of spring barley (previously ana-

TABLE I

SEPARATION EFFICIENCY OF THE ION-EXCHANGE PROCEDURE TESTED AFTER ADDITION OF [^{14}C]EA OR [^{14}C]GB TO 15 g PLANT FRESH MATTER (n = 3)

Analytical fraction	*[^{14}C]EA (0.5 mg, 59.8 kBq) = 100*	*[^{14}C]GB (15 mg, 64.9 kBq) = 100*
Radioactivity found (% of ^{14}C added):		
Extraction residue[a]	0.3	0.2
Chloroform phase[a]	0.6	0.2
Aqueous phase	98.2	98.7
Effluent (Dowex 50W-X8)	0.1	0.4
Eluate (1M ammonia)	96.8	97.6
GB fraction (effluent Dowex 2-X8/ Dowex CCR-2)	0.0	96.3
EA fraction (eluate Dowex CCR-2)	85.4[b]	0.6
Recovery ± S.D.	85.4 ± 4.9	96.9 ± 3.8

[a] After combustion in the Oxymat IN 4101.
[b] Losses of EA resulted from evaporation of the ammonia eluate.

lysed by GC[5,7]) to which definite amounts of EA and GB had been added, good recoveries were obtained too (Table III). Moreover, the standard deviations in Table II and III show that the precision of the method is satisfactory.

The identity of EA and GB found in the extract was confirmed by GC after derivatizing the hydrochlorides. Although GC represents an alternative to TLC, the method is too laborious for routine analysis and does not provide a decisive improvement in sensitivity. GB was derivatized according to Ranfft and Gerstl[7] and EA

TABLE II

RECOVERY OF EA AND GB FROM SYNTHETIC MIXTURES

Mixture	*Concentration (ng µl^{-1})*		*Recovery (%)*	*S.D. (%)*
	Original	*Found*[a]		
(1) EA	25.0	25.8	103.2	2.9
GB	509	528	103.7	3.4
(2) EA	54.0	55.3	102.4	2.6
GB	1021	1016	99.5	1.6
(3) EA	78.2	77.5	99.1	1.8
GB	1492	1522	98.0	2.4
(4) EA	108.7	110.0	101.2	1.9
GB	2012	1996	100.8	2.1
(5) EA	129.4	133.1	102.9	3.1
GB	2586	2534	102.0	1.9
Mean recovery ± S.D.: EA, 101.8 ± 1.6%; GB, 100.8 ± 2.2%				

[a] Mean of four replicates.

TABLE III

RECOVERY OF EA AND GB ADDED TO EXTRACTS OF MAIN SHOOTS OF BARLEY AFTER ION-EXCHANGE CHROMATOGRAPHY

Mixture	*Concentration (ng μl^{-1})*			*Recovery (%)*	*S.D. (%)*
	Original[a]	*Added*	*Found*[b]		
(1) EA	68.1	0	65.3	95.9	4.1
GB	1440.0	0	1492	103.6	6.5
(2) EA	68.1	10	82.1	105.1	5.0
GB	1440.0	600	2178	106.8	6.0
(3) EA	68.1	20	91.9	104.3	3.2
GB	1440.0	900	2306	98.5	1.6
(4) EA	68.1	30	103.4	105.4	5.7
GB	1440.0	1200	2531	95.9	3.5
(5) EA	68.1	40	112.4	104.0	6.4
GB	1440.0	1500	2910	99.0	3.0
Mean recovery ± S.D.: EA, 102.9 ± 3.9%; GB, 100.8 ± 4.2%					

[a] Previously analysed by GC
[b] Mean of six analyses.

according to the method of Reissmann *et al.*[5]. The determination was performed with a gas chromatograph GCHF 18.3-4 (VEB Chromatron Berlin) on a glass column (1 m × 3 mm I.D., 3% SE-30 on Gas-Chrom Q, 100–120 mesh) by means of flame ionization detection (FID). The oven temperature was 120 (GB) or 100°C (EA) and the retention times 2.03 (GB) or 2.3 min (EA). Since EA and GB found in the plant material were eluted at retention times which correspond to those of authentic standard compounds and since moreover the concentrations determined by TLC can be confirmed by GC, the identity of the extracted EA and GB was considered to be established.

It should be noted that at least trigonelline and stachydrine cannot be separated from GB by the ion-exchange procedure or the TLC system used. However, preliminary checks with a multiple TLC development or changes of developing systems which allow a clear separation of the three betaines showed that trigonelline and stachydrine were absent or present only in traces in well watered and drought stressed barley plants, respectively. Likewise, it was not possible to separate basic amino acids, *e.g.*, arginine and lysine from the EA fraction by the ion-exchange procedure. However, applying the TLC system methanol–ammonia a clear separation was achievable. Any addition of water to this system deteriorates the separation and can lead to a misinterpretation of the EA content.

The advantages of the procedure described consist in the possibility of a simultaneous determination of both compounds and above all in the specific and sensitive detection as well as in the rapidity and simple applicability.

The procedure outlined above was used to determine the levels of endogenous EA and GB in well watered and drought stressed barley plants at the end of the shooting stage (Table IV). The results show that the GB content significantly increased under stress, whereas no change in the EA content was found. The GB levels

TABLE IV

CONTENTS OF EA AND GB IN MAIN SHOOTS AND TILLERS OF WELL WATERED AND DROUGHT STRESSED BARLEY PLANTS (μmol g^{-1} DRY MATTER)

Plant organ	*Water status*[a]	*Dry matter (g)*	*GB*[b]	*EA*[b]
Main shoots	+	1.59	34.4	2.9
	−	1.34	62.7[c]	2.6
Tillers	+	2.64	46.6	3.2
	−	1.77[c]	56.7[c]	3.7

[a] + Well watered; − drought stressed.
[b] Mean of four analyses.
[c] P = 5% significance between + and −

corresponded well with the results of other authors[20,21]. For EA, quantitative results in plant material have not been reported in the literature. Since, however, the extraction efficiency was high with about 90% (verified by feeding experiments with ^{14}C-labelled EA and GB, respectively) and no hydrolysis of phosphatidylethanolamine was detected (experiments with L-α-kephaline, dipalmitolyl), the EA levels found seem to be reliable.

ACKNOWLEDGEMENTS

We thank Prof. Dr. G. Schilling from the Martin-Luther-University (Halle, G.D.R.) and Prof. Dr. H.-R. Schütte from the Institute of Plant Biochemistry (Halle, G.D.R.) for comments on the manuscript.

REFERENCES

1 R. Roser and P. H. Tocci, *J. Chromatogr.*, 72 (1972) 207.
2 S. P. Sristava and V. K. Dua, *Anal. Chem.*, 279 (1976) 367.
3 R. Storey and R. G. Wyn Jones, *Phytochemistry*, 16 (1977) 447.
4 P. Cancalon and J. K. Klingman, *J. Chromatogr. Sci.*, 10 (1972) 253.
5 P. Reissmann, H. Eckert and G. Eckert, *Nahrung*, 30 (1986) 679.
6 W. D. Hitz and A. D. Hanson, *Phytochemistry*, 19 (1980) 2371.
7 K. Ranfft and G. Gerstl, *Anal. Chem.*, 276 (1975) 51.
8 N. Seiler, B. Knödgen and F. Eisenbeiss, *J. Chromatogr.*, 145 (1978) 29.
9 C. W. Ford, *J. Sci. Food Agric.*, 35 (1984) 881.
10 J. Gorham, *J. Chromatogr.*, 287 (1984) 345.
11 J. Gorham, *J. Chromatogr.*, 361 (1986) 301.
12 B. Cromwell and S. D. Rennie, *Biochem. J.*, 55 (1953) 189.
13 S. R. Grattan and C. M. Grieve, *Plant Soil*, 85 (1985) 3.
14 G. P. Jones, B. P. Naidu, R. K. Starr and L. G. Paleg, *Aust. J. Plant Physiol.*, 13 (1986) 649.
15 J. J. Martin and J. D. Finkelstein, *Anal. Biochem.*, 111 (1981) 72.
16 H. Eckert, P. Reissmann and H. Bergmann, *Biochem. Physiol. Pflanzen*, 183 (1988) 15.
17 W. Lintzel and S. Fomin, *Biochem. Z.*, 238 (1931) 438.
18 R. M. C. Dawson, D. C. Elliot, W. H. Elliot and K. M. Jones, *Data for Biochemical Research*, Clarendon Press, Oxford, 1968, pp. 518–528.
19 R. A. Fahmy, A. Niederwieser, G. Pataki and M. Brenner, *Helv. Chim. Acta*, 44 (1961) 2022.
20 J. A. R. Ladyman, W. D. Hitz and A. D. Hanson, *Planta*, 150 (1980) 191.
21 R. G. Wyn Jones and R. Storey, *Aust. J. Plant Physiol.*, 5 (1978) 801.

Journal of Chromatography, 479 (1989) 459–463
Elsevier Science Publishers B.V., Amsterdam — Printed in The Netherlands

CHROM. 21 721

Note

Photodecomposition of Moclobemide on a silica gel thin-layer chromatographic plate

S. NAKAI, T. KOBAYASHI and T. EZAWA*

Department of Drug Metabolism & Product Development, Nippon Roche Research Center, 200 Kajiwara, Kamakura, Kanagawa Pref., 247 (Japan)

(First received February 28th, 1989; revised manuscript received June 5th, 1989)

Moclobemide [*p*-chloro-N-(2-morpholinoethyl)benzamide] (MBD), a monoamine oxidase (MAO) inhibitor, is an antidepressant and has also recently been developed as a nootropic drug.

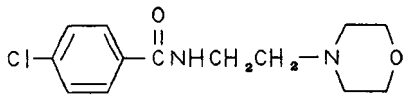

During our thin-layer chromatographic (TLC) study of MBD an unknown spot was occasionally detected on a silica gel plate by UV irradiation (254 nm) or by spraying with 4,4′-tetramethyldiaminodiphenylmethane (TDM) reagent after chlorination. We needed to find out why this spot had appeared; therefore, we began to study the stability of the sample solution, possible contamination, the quality of the TLC plate and the influence of light or air on the sample.

In the presence of diffuse daylight, MBD adsorbed on the silica gel of the TLC plate was found to give an unknown spot, which was later determined to be a photodecomposition product of MBD. The production of an artifact or photodegradation of MBD during TLC has not been investigated before. However, photochemical reactions of compounds adsorbed on silica gel have been reported for Vitamin K_3[1], 3-alkyl-1-phenyltriazine[2], stilbene[3], dipyridamol[4] and pyrazolidine-3,5-diones[5].

The aim of the present study was to investigate the cause of the decomposition of MBD and to identify its decomposition products in order to develop adequate TLC conditions for MBD. In this paper, an high-performance liquid chromatographic (HPLC) method to identify photodegradation products of MBD is also described.

EXPERIMENTAL

Materials and reagents

Moclobemide and its N-oxide derivative were from F. Hoffmann-La Roche (Basle, Switzerland). All reagents were of analytical grade. All materials and reagents were used without further purification.

0021-9673/89/$03.50

Chromatographic procedures

Silica gel 60 F_{254} pre-coated plates (E. Merck, F.R.G.) were used for TLC. The plates were developed with chloroform–methanol–water (13:6:1, v/v/v; system I) or ethyl acetate–ethanol–28% ammonia (8:2:1, v/v/v; system II).

In addition to normal-phase TLC, reversed-phase TLC was performed by using a $KC_{18}F$ precoated plate (Whatman, U.K.) with a mobile phase methanol–water (3:2, v/v). All plates were air dried, and the spots were detected by irradiation with short-wavelength ultraviolet light (254 nm). Our HPLC system consisted of a Model CCPD pump and a Model UV-8000 detector set at 235 nm (Tosoh, Japan) and a 7125 injector (Rheodyne, U.S.A.), and the following chromatographic systems were employed: (A) an ODS-80 column (15 cm x 4.6 mm I.D.) (Tosoh) with methanol–water (3:2, v/v) as the eluent at a flow-rate of 0.8 ml/min for preparative HPLC. (B) an Inertsil-ODS column (15 cm × 4.6 mm I.D.) (Gasukuro Kogyo, Japan) with acetonitrile–0.1% triethylamine solution adjusted to pH 6.0 with 50% phosphoric acid (1:3, v/v) as the eluent at a flow-rate of 1.2 ml/min for identification of unknown compounds.

Procedure for photodegradation of moclobemide on the TLC plate

The plates with 100 μg of MBD were exposed for several hours to various sources of light by using a fademeter (Model CF-20S; Shimadzu, Japan) with a wavelength below 275 nm, a near-UV lamp (FL20S.BI; Toshiba, Japan) with a spectral distribution between 290 and 390 nm, an ordinary white fluorescent lamp (400–700 nm) and diffuse daylight or a UV lamp (254 nm). Each plate was developed with solvent system I in order to confirm whether degradation had occurred.

Separation and purification

A 1-ml volume of 10% (w/v) MBD in methanol was streaked on the silica gel TLC plate. The plate was exposed to diffuse daylight for 3 h and then developed using solvent system I. A narrow band at R_F 0.37 from four plates was scraped off, and the silica was extracted with 25 ml of methanol. After centrifugation at *ca.* 1600 *g*, the residual silica was reextracted with methanol. The pooled methanol extracts were filtered by using a membrane filter (0.25 μm, hydrophobic; Toyo Roshi, Japan) and then evaporated to dryness under reduced pressure. The residue was dissolved in 300 μl of methanol and the solution was subjected to our HPLC system A. Samples corresponding to the predominant peak with a retention time of about 4.4 min were collected. About 0.4 mg of material were obtained after drying the pooled fractions.

Structural elucidation

NMR spectra were recorded with a 400-MHz Model GX-270 spectrometer (JEOL, Japan). Low- and high-resolution mass spectra were taken by direct injection of the sample with a Model DX-300 spectrometer (JEOL).

RESULTS AND DISCUSSION

MBD has been reported to be stable against heat, humidity and light[6]; however, during our TLC study of this compound, an unknown spot was occasionally detected by UV irradiation (254 nm) or by spraying with TDM reagent after chlo-

rination. In order to explain the cause of this phenomenon, the stability of the sample solution, possible contamination, the quality of the TLC plate and the effect of light or air on MBD were investigated.

Among the various sources of light described in the procedure for photodegradation section, the carbon arc fademeter and diffuse daylight gave the unknown spot in the TLC chromatogram. Thus we thought light, especially with wavelength below 275 nm, was the main factor in the decomposition of MBD. The photodecomposition was dependent on the difference in light sources, though the same lot of TLC plate was used.

An unknown spot was also detected when MBD was applied to a silica gel plate without the fluorescent additive (silica gel 60, precoated, Merck) or a plate previously developed with methanol and dried, under diffuse daylight which had passed through glass window-panes.

We confirmed no decomposition of MBD by spotting and developing a chromatogram in the dark, indicating that photolysis plays a decisive role.

These findings mean that the quality of the silica gel plate is not responsible for the decomposition of MBD, in contrast with the case reported by Macek[7].

Upon exposure to the carbon arc fademeter, no decomposition of MBD was observed when dissolved in methanol, acetonitrile and chloroform which is said to be sensitive to light, while the formation of the N-oxide derivative was more or less detected for the MBD in dichloromethane, dichloroethane, acetone and dioxane solutions.

No photodecomposition of MBD was found in the solid state, in which the particle size is about 14 μm, when exposed to direct rays from the sun on the roof of our laboratory.

In addition, during experimentation, the photodecomposition of MBD on a

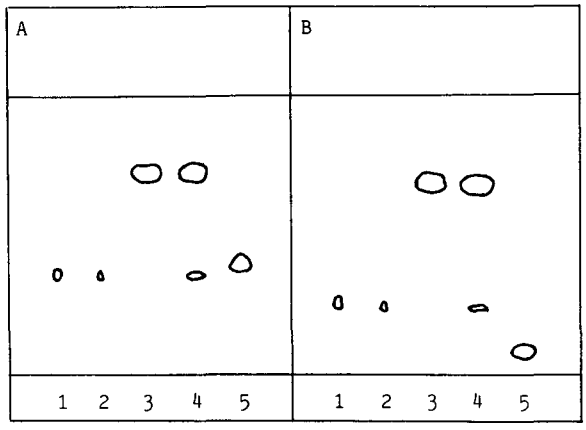

Fig. 1. Separation of the sample and standards on a silica gel TLC plate. (A) Solvent system, chloroform–methanol–water (13:6:1); (B) solvent system, ethyl acetate–ethanol–28% ammonia (8:2:1). Spots: 1 = isolated decomposition product (*ca.* 4 μg); 2 = authentic N-oxide of MBD (2 μg); 3 = MBD (100 μg); 4 = exposed MBD (100 μg); 5 = *p*-chlorobenzoic acid (10 μg). Samples 1, 2, 3 and 5 were applied to the plate after spotting MBD and exposure to diffuse daylight passing through a glass window-pane for 3 h. Detection: irradiation with UV light (254 nm).

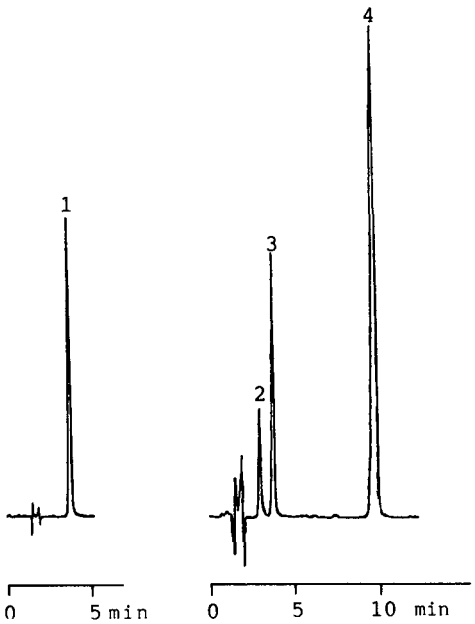

Fig. 2. Chromatograms of the isolated photodecomposition product (A) and a mixture of standards (B). Peaks: 1 = isolated photodecomposition product; 2 = *p*-chlorobenzoic acid; 3 = authentic N-oxide of MBD; 4 = MBD. Conditions: column, 150 mm × 4.6 mm I.D. Inertsil-ODS (5 μm); mobile phase, acetonitrile–0.1% triethylamine solution adjusted to pH 6.0 with phosphoric acid (1:3, v/v); flow-rate 1.2 ml/min; room temperature; UV detection at 235 nm.

TLC plate proved to be irreproducible, possibly because it was influenced by the day-to-day differences in the amount of diffuse daylight that reached the plate.

The structure of the compound isolated was identified by subjecting it to low- and high-resolution mass spectroscopy as well as to 400-MHz NMR analysis. The molecular weight of the sample was shown to be 284 by low-resolution mass spectroscopy, and the elemental composition of the molecular fragment ion was found to be $C_{13}H_{17}ClN_2O_3$ by high-resolution mass spectrometry. Our results show that the degradation product contains one more oxygen atom compared with MBD. Proton NMR spectra for MBD and its decomposition product in C^2HCl_3 showed that the chemical shifts of protons in the morpholine moiety of the decomposition product are different from those of MBD, indicating that an N-oxide had been formed. The structural assignments for the decomposition product were confirmed by comparing it to an authentic N-oxide of MBD.

Furthermore, the decomposition product isolated was chromatographed together with an authentic N-oxide of MBD by TLC solvent systems I and II as well as by HPLC system B. As shown in Figs. 1 and 2, the chromatographic behaviour of the decomposition product was identical with that of the synthetic N-oxide of MBD. *p*-Chlorobenzoic acid, the main degradation product of MBD, can also be separated by TLC and HPLC (Figs. 1 and 2). Accordingly, these analytical conditions can be used to monitor the stability of MBD.

The reported decomposition by photooxidation occurs when MBD is adsorbed

on the silica gel of the TLC plate and exposed to light with a wavelength of less than 275 nm. As described previously[8] the reaction is thought to result from the excitation of silica by UV light, and then the oxygen excited by the silica reacts with MBD:

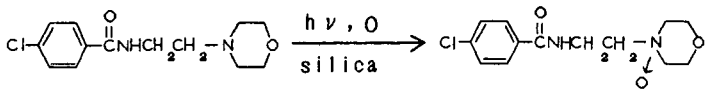

This assumption is probably supported by the fact that a remarkable decrease in the formation of N-oxide was observed when MBD was spotted on an ODS TLC plate and exposed to diffuse daylight. However, different degradation products from N-oxide were produced on the ODS plate. The chemical structure of the new degradation products is now under investigation. Since the decomposition product of MBD is an artifact formed by the interaction of light and MBD on the silica gel TLC plate, samples should be applied promptly and protected from intens diffuse daylight during the TLC procedure.

ACKNOWLEDGEMENTS

We are grateful to Mr. N. Nakayama and Ms. Y. Kodama (Nippon Roche Research Center) for recording the NMR and mass spectra.

REFERENCES

1 H. Weibin and E. T. Storm, *J. Am. Chem. Soc.*, 90 (1968) 7296.
2 M. Kawanishi, I. Otani and H. Nozaki, *Tetrahedron Lett.*, 53 (1968) 5575.
3 L. D. Weis, T. R. Evans and P. A. Leermakers, *J. Am. Chem. Soc.*, 90 (1968) 6109.
4 K. Kigasawa, H. Shimizu, S. Hayashida and K. Ohkubo, *Yakugaku Zasshi*, 104 (1984) 1191.
5 M. Takács, P. Kertész, E. Wiener and J. Reisch, *Arch. Pharm, (Weinheim Ger.)*, 318 (1985) 824.
6 F. Hoffmann-La Roche, Basle, unpublished results, 1987.
7 K. Macek, *J. Chromatogr.*, 33 (1968) 337.
8 Y. Fujita, in I. Yasumori (Editor), *Shin Jikken Kagaku Kouza*, Vol. 16, Maruzen, Tokyo, 1978, pp. 513–523.

Author Index

Errata

J. Chromatogr., 469 (1989) 383–389
p. 385, Table I, 13th anion should read "$S_2O_3^{2-}$".
p. 386, 11th line, "Na_2SO" should read "Na_2SO_4".
p. 387, 11th line, reference number 16 should be inserted.

Vol. 479 (2)

journal of chromatography news section

AWARD

KURT GROB MEMORIAL PRIZE

During the 10th International Symposium on Capillary Chromatography, held in Riva del Garda, Italy, May 23–25, 1989, the Kurt Grob Memorial Prize was awarded for the first time to Dr. T. Reiher (Berlin) and Dr. T. Welsch (Leipzig), "for their contribution to the production of inert glass capillary columns by high temperature silylation".

The late Professor Kurt Grob was one of the great pioneers in the art, as well as in the science, of capillary gas chromatography and in its application to tobacco smoke analysis and the investigation of trace components in water. His fundamental work on column technology and the preparation of glass capillaries was seminal for further work on the industrial preparation methods of fused silica columns.

In 1976, at a national chromatography symposium, Thomas Welsch presented for the first time the high temperature silylation of glass capillaries with hexamethyldisilazane at 300°C. One year later this method was described by Welsch, Engewald and Klaucke in the January issue of *Chromatographia* under the title: "Zur Desaktivierung von Glaskapillaren mittels Silanisierung". Today it is evident that this short, three-page manuscript described the method that later, applied to de-ionised and dehydrated glass surfaces by Professor Kurt Grob, proved to be the technological basis on which the whole field of gas chromatography on inert, temperature stable columns, as we know it today, is based and which sounded the knell of the use of glass capillaries with an active salt layer under the stationary phase. This paper can well be described as one of the milestones in the history of capillary gas chromatography.

Dr. T. Reiher's work was published in 1987, as a two page note in the March issue of the *Journal of High Resolution Chromatography,* entitled: "A contribution to high temperature silylation". The note describes the mechanism by which new silanol groups are formed via the substitution of functional groups of the silylating agent, especially phenyl groups, by traces of water during high temperature silylation. This, from various points of view, is of fundamental importance. It explains the relationship, which until then had not been discovered, between the type of support and the chemical nature of the silylating agent, as well as the choice of the silylation temperature on the one hand, and the role of the secondary silanols, which are formed during the high temperature silylation, on the other. Their correct application permits a targeted optimisation of present preparative methods and presents a lucid interpretation of the previously inexplicable phenomenon, that the support still had active silanols, even after high temperature silylation, able to react with suitable terminal groups of the stationary phases. The theory proposed by Reiher thus bridged an existing gap in the theory of the technology of high temperature gas chromatography.

ANNOUNCEMENTS OF MEETINGS

11th INTERNATIONAL SYMPOSIUM ON BIOMEDICAL APPLICATIONS OF CHROMATOGRAPHY AND ELECTROPHORESIS, TALLINN, U.S.S.R., APRIL 24–28, 1990

The 11th International Symposium on Biomedical Applications of Chromatography and Electrophoresis will be organized in Tallinn (Estonia) by the Scientific Council on Chromatography of the Academy of Sciences of the U.S.S.R. in cooperation with the Chromatography and Electrophoresis Section of the Czechoslovak Chemical Society and the Chromatography Group of the Society for Clinical Chemistry and Laboratory Diagnostics of the German Democratic Republic and Estonian Academy of Sciences.

All aspects of the theory and applications of chromatography and electrophoresis in biochemistry and medicine will be discussed. Special emphasis will be given to: applications of chromatography and electrophoresis in clinical diagnostics; analysis of drugs; drug monitoring and pharmacokinetic studies; sample preparation; chiral separations; new separation methods and instrumentation.

The programme will comprise lectures (invited plenary lectures and selected original contributions), posters and discussions. English is the symposium language. Authors desiring to present papers should submit a 150–250 word abstract by December 5th, 1989. The Scientific Committee will recommend a limited number of papers for publishing in a symposium issue of the *Journal of Chromatography, Biomedical Applications*. The recommended manuscripts will be, however, subjected to routine refereeing procedures.

The symposium fee is expected to be US$180 for active participants (board and lodging included).

For further details or registration contact: Dr. Ljudmila Kolomiets, Scientific Council on Chromatography, Institute of Physical Chemistry, Leninskii prospect 31, 117915 Moscow, U.S.S.R. Tel.: (095) 2320065; telex: 411029 pesum su.

1st INTERNATIONAL SYMPOSIUM ON APPLICATIONS OF HPLC IN ENZYME CHEMISTRY, VERONA, ITALY, SEPTEMBER 18–21, 1990

An International Symposium on Applications of HPLC in Enzyme Chemistry will be held at the Institutes of Legal Medicine and of Clinical Chemistry, University of Verona, Verona, Italy from September 18 to 21, 1990.

This symposium, organized by the University of Verona, will focus on four areas. These are: (1) the development of assays for individual enzymes, (2) the analysis of restriction enzyme cleavage products, (3) the assay of activities in multienzyme complexes, and (4) the development and use of enzymatic reactors in HPLC.

The selection of invited speakers will reflect this focus. In addition to the invited plenary lectures, the program will consist of oral presentations and posters. Both a technical exhibition of international suppliers and social events are planned. The proceedings (oral and poster presentations) will be published in the *Journal of Chromatography*. The symposium language will be English.

The members of the Scientific Committee include: Prof. E.F. Rossomando (Farmington), Chairman, Dr. A.M. Krstulović (Paris), Co-Chairman, Prof. E.G.E. Jahngen (Lowell), Prof. K. Macek (Prague), Prof. M. Marigo (Verona), Prof. T. Nagatsu (Nagoya) and Prof. P.-A. Pernemalm (Sweden), Prof. G. Piemonte (Verona) and Dr. F. Tagliaro (Verona). The members of the Organizing Committee are: Prof. M. Marigo (Verona), Prof. G. Piemonte (Verona) and Dr. F. Tagliaro (Verona) and Dr. E. Trabetti (Verona).

The deadline for preliminary registration and submission of the titles of communications is January 15, 1989. The final data for receipt of abstracts is May 15, 1990. Abstracts should be sent to Prof. E.F. Rossomando, Department of Biostructure and Function, University of Connecticut Health Center, Farmington, CT 06032, U.S.A. Tel.: (203) 679-2421; Fax: (203) 679-2518.

Preliminary program and registration forms will be available in March 1990. The deadline for advance registration will be May 15, 1990. Requests for registration materials and abstract forms should be sent to: Dr. Elisabetta Trabetti, Istituto di Medicina Legale, Università di Verona, Policlinico di Borgo Roma, 37134 Verona, Italy, telephone +39 45 504073, fax: +39 45 58212.

PUBLICATION SCHEDULE FOR 1989

Journal of Chromatography and Journal of Chromatography, Biomedical Applications

MONTH	J	F	M	A	M	J	J	A	S	
Journal of Chromatography	461 462 463/1	463/2 464/1	464/2 465/1 465/2	466 467/1 467/2	468 469 470/1 470/2	471 472/1 472/2 473/1	473/2 474/1 474/2 475	476 477/1 477/2	478/1 478/2 479/1	The publication schedule for further issues will be published later
Bibliography Section		486/1		486/2		486/3		486/4		
Biomedical Applications	487/1	487/2	488/1 488/2	489/1 489/2	490/1 490/2	491/1	491/2	492 493/1	493/2 494	495

INFORMATION FOR AUTHORS

(Detailed *Instructions to Authors* were published in Vol. 478, pp. 453–456. A free reprint can be obtained by application to the publisher, Elsevier Science Publishers B.V., P.O. Box 330, 1000 AH Amsterdam, The Netherlands.)

Types of Contributions. The following types of papers are published in the *Journal of Chromatography* and the section on *Biomedical Applications*: Regular research papers (Full-length papers), Notes, Review articles and Letters to the Editor. Notes are usually descriptions of short investigations and reflect the same quality of research as Full-length papers, but should preferably not exceed six printed pages. Letters to the Editor can comment on (parts of) previously published articles, or they can report minor technical improvements of previously published procedures; they should preferably not exceed two printed pages. For review articles, see inside front cover under Submission of Papers.

Submission. Every paper must be accompanied by a letter from the senior author, stating that he is submitting the paper for publication in the *Journal of Chromatography*. Please do not send a letter signed by the director of the institute or the professor unless he is one of the authors.

Manuscripts. Manuscripts should be typed in double spacing on consecutively numbered pages of uniform size. The manuscript should be preceded by a sheet of manuscript paper carrying the title of the paper and the name and full postal address of the person to whom the proofs are to be sent. Authors of papers in French or German are requested to supply an English translation of the title of the paper. As a rule, papers should be divided into sections, headed by a caption (*e.g.*, Summary, Introduction, Experimental, Results, Discussion, etc.). All illustrations, photographs, tables, etc., should be on separate sheets.

Introduction. Every paper must have a concise introduction mentioning what has been done before on the topic described, and stating clearly what is new in the paper now submitted.

Summary. Full-length papers and Review articles should have a summary of 50–100 words which clearly and briefly indicates what is new, different and significant. In the case of French or German articles an additional summary in English, headed by an English translation of the title, should also be provided. (Notes and Letters to the Editor are published without a summary.)

Illustrations. The figures should be submitted in a form suitable for reproduction, drawn in Indian ink on drawing or tracing paper. Each illustration should have a legend, all the *legends* being typed (with double spacing) together on a *separate sheet*. If structures are given in the text, the original drawings should be supplied. Coloured illustrations are reproduced at the author's expense, the cost being determined by the number of pages and by the number of colours needed. The written permission of the author and publisher must be obtained for the use of any figure already published. Its source must be indicated in the legend.

References. References should be numbered in the order in which they are cited in the text, and listed in numerical sequence on a separate sheet at the end of the article. Please check a recent issue for the layout of the reference list. Abbreviations for the titles of journals should follow the system used by *Chemical Abstracts*. Articles not yet published should be given as "in press" (journal should be specified), "submitted for publication" (journal should be specified), "in preparation" or "personal communication".

Dispatch. Before sending the manuscript to the Editor please check that the envelope contains three copies of the paper complete with references, legends and figures. One of the sets of figures must be the originals suitable for direct reproduction. Please also ensure that permission to publish has been obtained from your institute.

Proofs. One set of proofs will be sent to the author to be carefully checked for printer's errors. Corrections must be restricted to instances in which the proof is at variance with the manuscript. "Extra corrections" will be inserted at the author's expense.

Reprints. Fifty reprints of Full-length papers, Notes and Letters to the Editor will be supplied free of charge. Additional reprints can be ordered by the authors. An order form containing price quotations will be sent to the authors together with the proofs of their article.

Advertisements. Advertisement rates are available from the publisher on request. The Editors of the journal accept no responsibility for the contents of the advertisements.

How to succeed in SFC without overspending

There are two practical alternatives to spending $30,000 to $50,000 for a supercritical fluid chromatograph, and both use Isco lab-proven syringe pumps.

1 Adapt your GC for SFC with programmable fluid delivery. An Isco SFC-500 pump with PC-based controller gives you pulseless flow, menu-driven software for pressure and density gradients, and unlimited method storage on computer disks. It installs as a "front end" on practically any GC, using the existing column oven and detector(s). And it offers a uniquely flexible way to apply SFC methodology to your difficult GC separations.

2 Order a complete Isco packed column SFC system with absorbance detection. Programmable fluid delivery and 1 mm columns with 3 µm packings can give you over 1,000,000 plates/m. The 190-to-750 nm variable detector has ultrafast response and flow cells down to 0.12 µl to let you see your peaks the way the column resolves them.

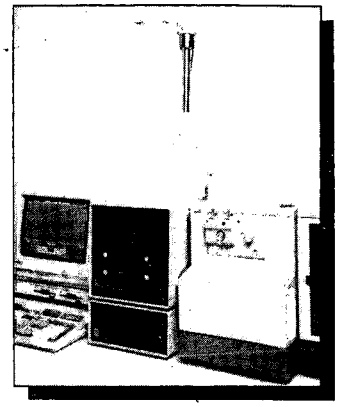

Find out how affordable your SFC success story can be. Contact your Isco distributor today for more information.

Isco, Inc.
P.O. Box 5347
Lincoln, Nebraska 68505

ISCO

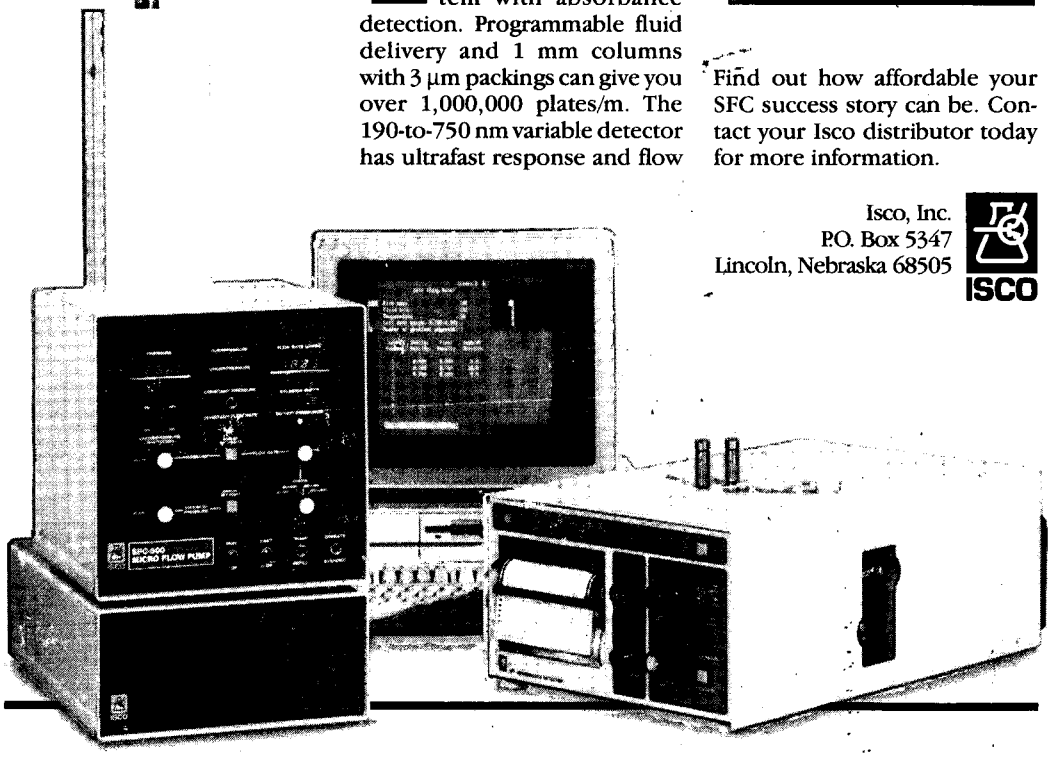

Distributors • **The Netherlands:** Beun-de Ronde B.V. Abcoude 02946-3119 • **Hungary:** Lasis Handelsges. mbH Wien 82 01 83 • **Spain:** Iberlabo, s.a. Madrid 01 251 14 91 • **W. Germany:** Colora Messtechnik GmbH Lorch, Württ. 07172 1830 • **France:** Ets. Roucaire, S.A. Velizy (1) 39 46 96 33 • **Italy:** Gio. de Vita e C. s.r.l. Roma 4950611 • **U.K.:** Life Science Laboratories, Ltd, Luton (0582) 597676 • **Norway:** Dipl. Ing. Houm A.S. Oslo 02 15 92 50 • **Switzerland:** IG Instrumenten-Gesellschaft AG Zurich 01 4613311 • **Belgium:** SA HVL NV Bruxelles (02) 720 48 30 • **Denmark:** Mikrolab Aarhus A/S Højbjerg 06-29 61 11 • **Austria:** Neuber Gesellschaft mbH Wien 42 62 35 •